ASSESSING ECOSYSTEM RESPONSE TO NATURAL AND ANTHROPOGENIC DISTURBANCES USING AN ECO-HYDROLOGICAL MODEL

A Dissertation
Presented to
The Academic Faculty

By

Alex G. Abdelnour

In Partial Fulfillment
Of the Requirements for the Degree
Doctor of Philosophy in Civil Engineering

Georgia Institute of Technology

December 2011

ASSESSING ECOSYSTEM RESPONSE TO NATURAL AND ANTHROPOGENIC DISTURBANCES USING AN ECO-HYDROLOGICAL MODEL

Approved by:

Dr. Marc Stieglitz, Advisor
School of Civil and Environmental Engineering
Georgia Institute of Technology

Dr. Thorsten Stoesser
School of Civil and Environmental Engineering
Georgia Institute of Technology

Dr. Mustafa Aral
School of Civil and Environmental Engineering
Georgia Institute of Technology

Dr. Ellery Ingall
School of Earth and Atmospheric Sciences
Georgia Institute of Technology

Dr. Terry Sturm
School of Civil and Environmental Engineering
Georgia Institute of Technology

Dr. Robert McKane
Western Ecology Division
US Environmental Protection Agency

Date Approved: September 21, 2011

To my daughter Sophia Olivia Abdelnour

ACKNOWLEDGEMENTS

I am most grateful to my family, whose moral support and emphatic encouragement made the completion of this work possible. I would like to thank my father Gabriel, my mother Laure, my sister Nayla as well as my wife Rana for their continual support and love during the last few years.

I would like to express my sincere thanks and appreciation to my advisor and mentor Dr Marc Stieglitz for believing in me and always providing me with the necessary guidance and support throughout these years.

I am also deeply grateful to Dr Robert McKane for his continuous guidance, teaching, insightful discussion and helpful comments. This research would not have been possible without his mentorship.

I also would like to thank my committee members Dr Mustafa Aral, Dr Thorsten Stoesser, Dr Terry Sturm, and Dr Ellery Ingall for their valuable comments and suggestions.

Finally, I would like to thank my lab mates and friends Sopan Patil, Yiwei Cheng and Dr Feifei Pan for their professional support, friendship, and collaboration.

CONTRIBUTION OF AUTHORS

Several authors contributed towards this PhD Dissertation. Dr Marc Stieglitz and Dr Robert McKane provided endless edits and comments to improve the manuscript. Dr Feifei Pan developed the initial version of the hydrological component of VELMA. Yiwei Cheng developed the snow-blowing model that has been incorporated into the model.

Sopan Patil provided the bias correction analysis for the future climate data mapping into the H.J. Andrews station (Appendix C; Chapter 6).

TABLE OF CONTENTS

PAGE

ACKNOWLEDGEMENTS....iv

LIST OF TABLES....x

LIST OF FIGURES.... xi

SUMMARY....xvi

CHAPTER 1: INTRODUCTION....1
1.1. Research Motivation....1
1.2. Scope of the Study....2
1.3. Thesis Organization....2
1.4. References……....4

CHAPTER 2: BACKGROUND AND LITERATURE REVIEW....7
2.1. Introduction....7
2.2. Forest Harvest Impact on Catchment Hydrology and Biogeochemistry....8
2.3. Variability in the Ecosystem Response to Forest Harvest....9
2.4. Climate Change Impact on Catchment Hydrology and Biogeochemistry....10
2.5. Limitation of Experimental Studies....12
2.6. Eco-Hydrological Models....13
2.7. Limitations of Existing Eco-hydrological Models....14
2.8. References....15

CHAPTER 3: CATCHMENT HYDROLOGICAL RESPONSES TO FOREST HARVEST AMOUNT AND SPATIAL PATTERN....25
3.1. Abstract....25
3.2. Introduction....26
3.3. Site Description....28
3.4. The Eco-Hydrological Model....31
3.5. Simulation Methods....32
3.5.1.Data....32
3.5.2.Calibration Simulations....33
3.6. Simulations Results....34
3.6.1. Pre-Harvest Hydrological Dynamics (1969-1974)....34
3.6.2. Post-Harvest Hydrological Dynamics (1975-2008)....35
3.6.3. Harvest Sensitivity Simulations and Results....40
3.6.3.1. Harvest Location....40
3.6.3.2. Harvest Amount....41
3.7. Discussion....48
3.8. Conclusion....52

3.9. Appendix....52
3.9.1. Appendix A: Hydrological Model Description....52
3.9.1.1. Soil Column Framework....53
3.9.1.1.1. Vertical Water Drainage....55
3.9.1.1.2. Precipitation, Rain, Snow and Snowmelt....56
3.9.1.1.3. Surface Soil Infiltration....56
3.9.1.1.4. Evapotranspiration....57
3.9.1.1.5. Watershed Framework....58
3.9.1.2. Lateral Subsurface Runoff....59
3.9.1.3. Surface Runoff....59
3.9.1.4. Total Runoff....60
3.9.2. Appendix B: Evapotranspiration Recovery Function Description....60
3.9.2.1. Background....60
3.9.2.2. Evapotranspiration Recovery Function....61
3.10. Acknowledgments....64
3.11. References....64

CHAPTER 4: EFFECTS OF FIRE AND HARVEST ON CARBON AND NITROGEN DYNAMICS IN A PACIFIC NORTHWEST FOREST CATCHMENT....72
4.1. Abstract....72
4.2. Introduction....73
4.3. Site Description....76
4.4. The Eco-Hydrological Model Description....78
4.5. Simulation Methods....80
4.5.1. Data....80
4.5.2. Simulation Scenarios....81
4.6.Simulation Results and Discussion....84
4.6.1. Post-fire “build-up” of Ecosystem C and N Stocks (1525-1968)....84
4.6.1.1. Post-Fire Plant Biomass and SOC (1525-1968)....84
4.6.1.2. Post-Fire Dissolved C and N losses (1525-1968)....85
4.6.1.3. Post-Fire Gaseous C and N losses (1525-1968)....86
4.6.1.4. Post-Fire NPP and NEP (1525-1968)....86
4.6.2. Old-Growth Biogeochemical Dynamics (1969-1974)....88
4.6.3. Post-Harvest Biogeochemical Dynamics (1975-2008)....90
4.6.3.1. Post-Clearcut Plant Biomass and SOC (1975-2008)....90
4.6.3.2. Post-Clearcut Dissolved C and N losses (1975-2008)....92
4.6.3.3. Post-Clearcut Gaseous C and N losses (1975-2008)....94
4.6.3.4. Post-Clearcut NPP and NEP (1975-2008)....95
4.7. Conclusion....96
4.8. Appendix A: Model Description....99
4.8.1. Soil Column Framework....100
4.8.1.1. The Soil Temperature Model....102
4.8.1.2. The Plant-Soil Model....103
4.8.1.3. Atmospheric Nitrogen Deposition....105
4.8.1.3.1. Michealis Menton Functions....105
4.8.1.3.2. Plant Mortality....106

4.8.1.3.3. Plant Uptake....106
4.8.1.3.4. Water Stress Function....107
4.8.1.3.5. Biomass Root Fraction....107
4.8.1.3.6. Vertical Transport of Nutrients....107
4.8.1.3.7. Soil Organic Carbon Decomposition....108
4.8.1.3.8. Nitrification Rate....109
4.8.1.3.9. Denitrification Rate....110
4.8.2. Watershed Framework....112
4.8.2.1. Lateral Transport of Nutrients....112
4.9. Acknowledgments....113
4.10. References....113

CHAPTER 5: CATCHMENT BIOGEOCHEMICAL RESPONSES TO FOREST HARVEST AMOUNT AND SPATIAL PATTERN....124
5.1. Abstract....124
5.2. Introduction....125
5.3. Site Description....127
5.4. The Eco-Hydrological Model....130
5.5. Simulation Methods....133
5.5.1. Data....133
5.5.2. Model Spatial Structure....134
5.5.3. Model Simulations....134
5.5.3.1. Harvest Location Scenarios (1975-2008)....135
5.5.3.2. Harvest Amount Scenarios (1975-2008)....136
5.5.3.3. Old-growth Control Scenario (1975-2008)....137
5.6. Results and Discussion....138
5.6.1. Whole-Catchment Clearcut Simulation....139
5.6.2. Harvest Location Simulations....140
5.6.3. Harvest Amount....144
5.7. Conclusion....151
5.8. Acknowledgments....152
5.9. References....152

CHAPTER 6: CLIMATE CHANGE IMPACT ON CATCHMENT HYDROLOGICAL AND BIOGEOCHEMICAL PROCESSES....160
6.1. Abstract....161
6.2. Introduction....161
6.3. Site Description....163
6.4. Model Description....165
6.5. Climate Forcing and Validation Data Description....169
6.5.1. Climate Forcing Data....169
6.5.2. Climate Projection Data (2009-2100)....170
6.5.3. Model Calibration-Validation Data....174
6.6. Simulation Methods....174
6.6.1. Calibration Simulation (1994-1998)....174
6.6.2. Model Validation Simulation (1999-2008)....175

6.6.3. Climate Change Simulations (2009-2100).....177
6.7. Simulation Results.....178
6.6.1. Catchment Hydrological Response to Climate Change.....178
6.6.2. Catchment Biogeochemical Response to Climate Change.....182
6.8. Discussion.....187
6.9. Conclusion.....190
6.10. Acknowledgments.....191
6.11. Appendix A: Model Parameters and Calibration Values.....191
6.12. Appendix B: Future Meteorological Data Selection.....193
6.13. Appendix C: Mapping Future Climate Data to CS2MET.....194
6.14. Appendix D: Spatial Distribution of Temperature and Precipitation.....196
6.15. Appendix E: Stand Age Map.....198
6.16. References.....199

CHAPTER 7: CONCLUSIONS AND FUTURE RESEARCH.....212
7.1. Conclusions.....212
7.2. Future Research.....215

CURRICULUM VITAE.....218

LIST OF TABLES

Table 3.1: Daily, monthly and annual streamflow modeling performance for: a) the pre-harvest period (1969-1974), and b) the post-harvest period (1975-2008) 36

Table 3.B.1: Model parameters values used to simulate the hydrologic processes of WS10 in the H.J. Andrews Experimental Forest.....63

Table 4.1: Comparison of the post-fire simulation results, for the period 1960-1968, when the ecosystem is considered in steady state (i.e. old-growth condition) against observed old-growth values at other Pacific Northwest Forest.....83

Table 4.2: Comparison of simulation results from the old-growth simulation against observed values at WS10 and other old-growth Pacific Northwest Forests.....90

Table 4.3: Streamflow and nutrient losses modeling skills for the post-harvest period (1975-2008) (Observed daily streamflow from 1975 to 2008; Observed tri-weekly NH_4 ($mgNm^{-2}yr^{-1}$), NO_3 ($mgNm^{-2}yr^{-1}$), and DON ($mgNm^{-2}yr^{-1}$) losses from 1979 to 2007; Observed tri-weekly DOC ($mgCm^{-2}yr^{-1}$) losses from 2001 to 2007) 94

Table 4.B.1: Model parameter values used to simulate the biogeochemical processes of watershed 10 in the H.J. Andrews Experimental Forest.....113

Table 6.1: Daily, monthly and annual streamflow modeling performance for: a) the calibration period (1992-1998), and b) the validation period (1999-2008) 176

Table 6.2: Comparison between the validation simulation results (i.e. 40% old-growth, 20% mature, 40% post-clearcut between the age of 5 and 25 year-old) and the observed Pacific Northwest mature/old-growth ecosystem average values.....177

Table 6.A.1: Hydrological Model Parameters and Calibration Values. 192

Table 6.A.2: Soil Temperature and Plant-Soil Model Parameters and Calibration Values.....192

LIST OF FIGURES

Figure 3.1: The study site is the watershed 10 (WS10) of the H.J. Andrews Experimental Forest located in the western Cascade Range of Oregon.....29

Figure 3.2: Simulated mean soil water degree of saturation in layer 1, 2, 3 and 4 of the soil column for the pre-clearcut period of January 1, 1969 to December 31, 1974.....35

Figure 3.3: Observed and simulated daily streamflow for the pre-clearcut period of January 1, 1969 to December 31, 1974.....35

Figure 3.4: Observed and simulated daily streamflow for the pre-clearcut period of January 1, 1975 to December 31, 1979.....36

Figure 3.5: Simulated seasonal and annual absolute changes in streamflow for the post-clearcut period of 1975 to 2008.....38

Figure 3.6: Simulated seasonal and annual relative changes in streamflow for the post-clearcut period of 1975 to 2008.....38

Figure 3.7: Spatial pattern of forest harvest. Twenty scenarios of 20% clearcut area each were simulated. The location of the 20% clearcut area varied from an all-ridge location (scenario A) to an all-valley location (Scenario T) 40

Figure 3.8: Absolute and relative increase in annual streamflow for a 20% clearcut as a function of the average flow path distance in meters between the harvest area and the nearest stream channel. The solid black line is the fitted linear trendline.....41

Figure 3.9: Harvest amount scenarios. Selected examples of fifty clearcut scenarios ranging from 0% to 100% with a ~2% increment in harvest area were simulated (1) from ridge to valley, and (2) from valley to ridge, to assess the impact of increasing harvest area on catchment hydrological response.....42

Figure 3.10: Simulated absolute change in annual streamflow as a function of harvest area. Forest clearcut was simulated from ridge to valley with an increment of 2% in harvest area.....43

Figure 3.11: Simulated absolute changes in catchment annual evapotranspiration as a function of harvest area. Forest clearcut was simulated from ridge to valley with an increment of 2% in harvest area.....43

Figure 3.12: Simulated absolute change in annual streamflow as a function of harvest area. Forest clearcut was simulated from valley to ridge with an increment of 2% in harvest area.....44

Figure 3.13: Simulated absolute changes in catchment annual evapotranspiration as a function of harvest area. Forest clearcut was simulated from valley to ridge with an increment of 2% in harvest area.....45

Figure 3.14: Simulated absolute and relative increase in average annual streamflow (Q), and average annual evapotranspiration (ET) as a function of harvest area, over the first five years after clearcut.....46

Figure 3.15: Simulated absolute and relative increase in monthly streamflow as a function of harvest area, in the 1-5 years after clearcut (1975-1979).....47

Figure 3.16: Comparison of the simulated increase in annual streamflow in WS10 (red dots) with observed increase in annual streamflow for 95 catchments in the US [Stednick, 1996] (Green line), and for the Pacific Northwest (Stednick data) (Orange line) as a function of the percent of catchment harvested.....49

Figure 3.A.1: Conceptual catchment modeling framework using multi-layered soil columns 53

Figure 3.A.2: The soil column framework consists of 4-layer soil column, a standing water layer, and a snow layer. DTB is the soil column depth to bedrock. z_i, Ks_i, ϕ_i, and s_i, are the thickness, the saturated hydraulic conductivity, the soil porosity, and the soil water storage of layer i, respectively.....54

Figure 3.B.1: Changes in net primary production (NPP) of temperate forests (red dots are individual forest stands sampled throughout the world; dashed black line is a 10-year moving average) [Luyssaert et al., 2008], and NPP of boles for Pacific Northwest coniferous forests (black circles and solid black line) as a function of stand age (i.e. time after stand-replacing disturbance) [Acker et al., 2002] 61

Figure 4.1: The study site is the watershed 10 (WS10) of the H. J. Andrew Experimental Forest located in the western Cascade Range of Oregon. The red dots represent the locations of the stream gages. The black triangles represent the locations of the meteorological stations.....76

Figure 4.2: Schematics of the historical events that shaped the landscape in WS10: a natural stand-replacing fire that occurred in 1525 A.D. [Wright et al., 2002] and a 100% man-made clearcut in 1975. The three periods of interest are: a) the post-fire recovery period from 1525 to 1968, b) the old-growth period (1969-1974) chosen at the end of the post fire recovery period where temperature and precipitation data are available to drive the model, and c) the post-harvest period from 1975 to 2008 81

Figure 4.3: Simulated biomass (red-line) and soil organic carbon (blue-line) recovery after the 1525 A.D. stand-replacing fire. The black-dots are the observed [Janisch and Harmon, 2002] accumulation of bole biomass (multiplied by 1.3 to get total plant biomass) for a 500-year chronosequence of 36 Pseudotsuga-Tsuga dominated forest stands in southwestern Washington State.....85

Figure 4.4: Simulated net primary production (red-line), net ecosystem production (blue-line) and soil heterotrophic respiration (green dashed line) recovery after the 1525 A.D. stand-replacing fire.....87

Figure 4.5: Comparison between the simulated post-fire 10-year moving average of ecosystem net primary production NPP (blue-line) and the observed (1) NPP of temperate forests (red dots are individual forest stands sampled throughout the world; dashed red line is a 10-year moving average) [Luyssaert et al., 2008], and (2) NPP of boles for Pacific Northwest coniferous forests (black dots and solid black line) as a function of stand age (i.e. time after stand-replacing disturbance) [Acker et al., 2002] 88

Figure 4.6: Simulated recovery of plant biomass ($kgCm^{-2}$; red-line), soil organic carbon ($kgCm^{-2}$; blue-line), net primary production ($gCm^{-2}yr^{-1}$; black-dashed line), net ecosystem production ($gCm^{-2}yr^{-1}$; black-line), and soil heterotrophic respiration ($gCm^{-2}yr^{-1}$; green-line) after a 100% clearcut in 1975.....91

Figure 4.7: Simulated (red-dots) versus observed (black-dots) nitrate NO_3 ($mgNm^{-2}$), ammonium NH_4 ($mgNm^{-2}$), DON ($mgNm^{-2}$), and DOC losses ($mgCm^{-2}$) to the stream after the 1975 clearcut of watershed 10 in the H.J. Andrews. The simulated values are averages over the same time interval as the observed values.....93

Figure 4.A.1: Conceptual catchment modeling framework using multi-layered soil columns.....99

Figure 4.A.2: The soil column hydrological framework consists of 4-layer soil column, a standing water layer, and a snow layer.....100

Figure 4.A.3: The soil column biogeochemical framework simulates ecosystem carbon storage and the cycling of carbon and nitrogen between a plant biomass layer and a 4-layer soil column.....101

Figure 5.1: The study site is the watershed 10 (WS10) of the H. J. Andrew Experimental Forest located in the western Cascade Range of Oregon. The red dots represent the locations of the stream gages. The black triangles represent the locations of the meteorological stations. 129

Figure 5.2: Conceptual catchment modeling framework using multi-layered soil columns.....130

Figure 5.3: The soil column hydrological framework consists of 4-layer soil column, a standing water layer, and a snow layer.....131

Figure 5.4: The soil column biogeochemical framework simulates ecosystem carbon storage and the cycling of carbon and nitrogen between a plant biomass layer and a 4-layer soil column.....132

Figure 5.5: Spatial pattern of forest harvest. Twenty scenarios of 20% clearcut area each were simulated. The location of the 20% clearcut area varied from an all-ridge location (scenario A) to an all-valley location (Scenario T) 136

Figure 5.6: Harvest amount scenarios. Selected examples of fifty clearcut scenarios ranging from 0% to 100% with a ~2% increment in harvest area were simulated (1) from ridge to valley, and (2) from valley to ridge, to assess the impact of increasing harvest area, irrespective of location, on catchment hydrological response.....137

Figure 5.7: Absolute annual changes in heterotrophic, denitrification, ammonium, nitrate, DON, and DOC losses for a 20% clearcut as a function of the average flow path distance in meters between the harvest area and the nearest stream channel.....142

Figure 5.8: The absolute change (compared to old-growth values) in simulated annual ammonium losses to the stream with respect to harvest area for the a) ridge-to-valley and b) valley-to-ridge set of scenarios.....145

Figure 5.9: The absolute change (compared to old-growth values) in simulated annual nitrate NO_3 losses to the stream with respect to harvest area for the a) ridge-to-valley and b) valley-to-ridge set of scenarios.....146

Figure 5.10: The absolute change (compared to old-growth values) in simulated annual DON losses, DOC losses, N_2-N_2O emission and R_h with respect to harvest area for the ridge-to-valley set of scenarios.....147

Figure 5.11: The absolute change (compared to old-growth values) in simulated annual DON losses, DOC losses, N_2-N_2O emission, and R_h with respect to harvest area for the valley-to-ridge set of scenarios.....148

Figure 5.12: The average absolute change (compared to old-growth values) in simulated annual DON losses, DOC losses, N_2-N_2O emission, and R_h with respect to harvest amount, over the first five years after clearcut (1975-1980) for (1) the valley-to-ridge scenarios, and (2) for the ridge-to-valley scenarios.....150

Figure 6.1: The study site is the 64 km^2 H. J. Andrew Experimental Forest located in the western Cascade Range of Oregon. The black triangles represent the locations of the meteorological stations. CS2MET is the meteorological station used in this study.....164

Figure 6.2: The soil column hydrological framework consists of 4-layer soil column, a standing water layer, and a snow layer.....166

Figure 6.3: The soil column biogeochemical framework simulates ecosystem carbon storage and the cycling of carbon and nitrogen between a plant biomass layer and a 4-layer soil column.....168

Figure 6.4: Conceptual catchment modeling framework using multi-layered soil columns.....169

Figure 6.5: Absolute and relative changes in average annual and seasonal temperature for the periods 2010-2029, 2030-2049, 2050-2069, and 2070-2089.....172

Figure 6.6: Absolute and relative changes in average annual and seasonal precipitation for the periods 2010-2029, 2030-2049, 2050-2069, and 2070-2089.....173

Figure 6.7: Simulated and observed stream discharge for the validation period of 1999 to 2008.....176

Figure 6.8: Simulated daily changes in historical and future basin average snow water equivalent (mm). The projected 2010-2029 (blue line), 2030-2049 (purple line), 2050-2069 (green line), 2070-2089 (red line) daily changes in snow water equivalent correspond to the average value of the upper, lower, and middle of the road climate change scenarios.....179

Figure 6.9: Absolute and relative changes in average seasonal precipitation (orange), streamflow (blue), evapotranspiration (red), soil moisture (green), maximum snow water equivalent depth (gray) and average snow water equivalent depth (brown) for the periods 2010-2029, 2030-2049, 2050-2069, and 2070-2089. 180

Figure 6.10: Absolute and relative changes in average annual precipitation (orange), streamflow (blue), evapotranspiration (red), soil moisture (green), maximum snow water equivalent depth (gray) and average snow water equivalent depth (brown) for the periods 2010-2029, 2030-2049, 2050-2069, and 2070-2089.....181

Figure 6.11: Simulated historical and future monthly changes in net primary production (NPP; sub-plot a), soil heterotrophic respiration (Rh; sub-plot b), and net ecosystem production (NEP; sub-plot c). The projected 2010-2029 (blue line), 2030-2049 (purple line), 2050-2069 (green line), 2070-2089 (red line) monthly correspond to the average value of the upper, lower, and middle of the road climate change scenarios.....183

Figure 6.12: Absolute and relative changes in average annual ammonium NH_4 losses (red; $mgNm^{-2}yr^{-1}$), nitrate NO_3 losses (orange; $mgNm^{-2}yr^{-1}$), DON losses (green; $mgNm^{-2}yr^{-1}$), nitrification rates (purple; $gNm^{-2}yr^{-1}$), and denitrification rates (yellow; $mgNm^{-2}yr^{-1}$) for the periods 2010-2029, 2030-2049, 2050-2069, and 2070-2089.....185

Figure 6.13: Absolute and relative changes in average annual DOC losses (brown; $mgCm^{-2}yr^{-1}$), soil heterotrophic respiration (blue; $gCm^{-2}yr^{-1}$), net primary production (light purple; $gCm^{-2}yr^{-1}$), and net ecosystem production (gay; $gCm^{-2}yr^{-1}$) for the periods 2010-2029, 2030-2049, 2050-2069, and 2070-2089.....185

Figure 6.D.14: Spatial maps at 30m resolution of annual average air temperature and precipitation developed for the HJA using the PRISM model.....197

Figure 6.E.15: The 1988 land cover map for the H.J. Andrews Experimental forest....199

SUMMARY

The impact of natural and anthropogenic disturbances on catchment hydrological and biogeochemical dynamics are difficult or impossible to capture through experimentation or observation alone. Process-based simulation models can address this need by providing a framework for synthesizing and analyzing data describing catchment responses to climate, harvest, fire, and other disturbances. When properly constrained, models allow a self-consistent representation and analysis of process-level interactions within catchments, as well as the ability to isolate and make inferences about the contribution of specific processes to observed responses. Models can also extend a data set by allowing behavior of unmeasured system components to be inferred. However, existing models are either too simple to capture important process-level hydrological and biogeochemical controls on ecosystem responses to disturbance, or are too computationally expensive to simulate the local dynamics over large watershed areas, or require a high level of expertise to implement.

To this end, a spatially distributed, physically based, eco-hydrological model (VELMA: Visualizing Ecosystems for Land Management Assessments) that is both computationally efficient and relatively easy to implement was collaboratively developed. The model simulates changes in soil water infiltration and redistribution, evapotranspiration, surface and subsurface runoff, carbon and nitrogen cycling in plants and soils, and the transport of dissolved forms of carbon and nitrogen from the terrestrial landscape to streams. VELMA is designed to simulate the integrated responses of vegetation, soil, and water resources to multiple forcing variables, e.g., changes in climate, land-use and land cover. It is intended to be broadly applicable to a variety of ecosystems (forest, grassland, agricultural, tundra, etc.) and to provide a computationally efficient means for scaling up ecohydrological responses across multiple spatial and temporal scales – hillslopes to basins, and days to centuries.

The first part of the study focuses on exploring catchment hydrological responses to forest harvest amount and spatial pattern. VELMA was applied to a small Pacific Northwest Long Term Ecological Research catchment to elucidate how hillslope and

catchment scale processes control stream discharge. The study site is watershed 10 of the H.J Andrews Experimental Forest, a 10-hectare forested catchment in which the former 450 year-old stand of Douglas-fir and Western hemlock was clearcut in 1975. The climate is relatively mild with wet winters and dry summers. Mean annual precipitation and air temperature is 2300mm and 8.5°C, respectively. Simulated and observed daily streamflow are in good agreement for both the pre-harvest (1969-1974) and post-harvest (1975-2008) periods (Nash-Sutcliffe Efficiency = 0.807 and 0.819, respectively). One hundred scenarios, where harvest amounts ranged from 2% to 100%, irrespective of location were conducted. Results show that (1) for the extreme case of a 100% clearcut, stream discharge increased by 28% or 340mm but returned to pre-clearcut levels within 50 years, (2) fall increases in streamflow were large in absolute terms, whereas summer increases were large in relative terms, and (3) annual streamflow increased linearly at a rate of 3.5 mm/year for each percent of catchment harvested. Thereafter, to assess the impact of harvest location on stream discharge, twenty harvest scenarios were simulated, where harvest amount (20%) was fixed and harvest location varied. Results show that the streamflow response is strongly sensitive to harvest distance from the stream channel. Specifically, a 20% clearcut area in the uplands near the catchment divide resulted in an average annual streamflow increase of 53mm, whereas a 20% clearcut near the stream channel resulted in an average annual streamflow increase of 92mm.

The second part of the study focuses on exploring the impact of fire and harvest on carbon and nitrogen dynamics. VELMA was applied to a small Pacific Northwest Long Term Ecological Research catchment (WS10), where two significant disturbance events have shaped the life history of vegetation growth: The first was a stand-replacing fire in *circa* 1525 A.D. The second was a clearcut harvest in 1975. VELMA was used to reconstruct, analyze and draw insights into the response of Pacific Northwest catchments and specifically Douglas-fir dominated catchments to natural and anthropogenic disturbances. Observed ecological and hydro-biogeochemical data from WS10 in combination with published chronosequence data from Pacific Northwest forest ecosystems were used to calibrate and test the modeled response to fire and harvest. Model parameters were first calibrated to simulate the post-fire build-up of ecosystem carbon and nitrogen stocks from the 1525 fire to 1969, and then used to simulate the

biogeochemical response of an old-growth (1969-1974) and recently clearcut (1975-2008) forest. Simulated and observed daily nitrate, ammonium, DON and DOC losses are in good agreement for the post-harvest period of 1975 to 2007 (Correlation Coefficient = 0.46, 0.7, 0.83, and 0.92 respectively). Results show that (1) losses of dissolved nutrients in an old-growth forest are generally low and occur primarily as DON and DOC, 2) NO_3 losses to the stream are poorly correlated to streamflow, whereas NH_4, DON and DOC losses are strongly correlated to streamflow, (3) carbon and nitrogen losses from the terrestrial system to the stream and atmosphere increased immediately after clearcut as a result of reduced N uptake from plants, high soil organic carbon decomposition, and increase in water availability. These results also suggest that VELMA can be used as a tool to provide process-level insights into the impact of disturbances on catchment C and N dynamics–details that would be difficult or impossible to capture through experimentation or observation alone.

The third part of the study focuses on exploring catchment biogeochemical responses to forest harvest amount and spatial pattern. VELMA was applied to the same small Pacific Northwest Long Term Ecological Research (LTER) catchment (WS10), to elucidate how hillslope and catchment-scale processes control soil carbon and nitrogen dynamics in response to clearcut. VELMA was previously calibrated and validated at capturing post-fire and post-harvest hydrological and biogeochemical dynamics in WS10. One hundred scenarios, where harvest amounts ranged from 2% to 100%, irrespective of location were conducted. Main conclusions are that (1) annual ammonium (NH_4) and nitrate (NO_3) losses increased with increasing harvest amount, (2) average annual NH_4 and NO_3 losses to the stream increased exponentially for a buffer zone of less than 60% of the catchment area, and reached 0.08 $gNm^{-2}yr^{-1}$ and 0.9 $gNm^{-2}yr^{-1}$, respectively for a 100% clearcut, and (3) average annual dissolved organic nitrogen (DON) and carbon (DOC) losses, N_2 and N_2O emissions, and soil heterotrophic respiration increased linearly (correlation coefficient R^2=0.95, 0.98, 0.88, and 0.96, respectively) at a rate of 0.2 $mgNm^{-2}yr^{-1}$, 4.9 $mgCm^{-2}yr^{-1}$, 7.9 $mgNm^{-2}yr^{-1}$, and 1.3 $gCm^{-2}yr^{-1}$, respectively for each 1% of catchment area harvested. Finally, to assess the impact of harvest location on biogeochemical fluxes, twenty harvest scenarios were simulated, where harvest amount (20%) was fixed and harvest location varied. These simulations show that nutrient losses

are strongly sensitive to harvest distance from the stream channel. Specifically, NH_4 and NO_3 losses to the stream increased exponentially with decreasing distance from the stream channel, DON and DOC losses, N_2 and N_2O emissions increased linearly at rate of 0.03 $mgNm^{-2}yr^{-1}$, 0.32 $mgCm^{-2}yr^{-1}$, and 0.1 $mgNm^{-2}yr^{-1}$, respectively, with decreasing distance from the stream channel, and soil heterotrophic respiration decreased linearly at a rate of 0.13 $mgCm^{-2}yr^{-1}$ with decreasing distance to the stream channel. Moreover, these results suggest that VELMA can help inform land managers and policymakers interested in exploring the impact of alternative land-use scenarios on nitrogen and carbon losses to surface waters and to the atmosphere. An important aspect of such assessments is VELMA's capability for simulating the effectiveness of riparian buffers in reducing stream nutrient loads.

In the final part of the study, VELMA was used to simulate the impact of future climate change on catchment hydrology and carbon and nitrogen dynamics. VELMA was applied to an intensely studied watershed in the Pacific Northwest: the H.J. Andrews 64 km^2 Experimental Forest. The goal was to provide process level insight into the impact of climate change on ecosystem processes at high spatial resolution relevant to formulating management decision. Daily projected temperature and precipitation from an upper bound (IPSLCM4_A2), lower bound (GISS_ER_B1) and middle of the road (ECHAM5_A2) climate change scenarios were used to force the model. The projected daily temperature and precipitation were spatially interpolated across the H.J. Andrews watershed using a climate analysis model PRISM that includes for the effects of elevation, forest canopy, cloudiness, topographic shading, orographic lifting, and temperature inversion on temperature and precipitation. Simulation results suggest that the combined effects of warmer and wetter winters as well as drier and hotter summers will result in lower winter snow accumulation, earlier spring snowmelt, higher winter streamflow, and lower summer streamflow and soil moisture. Moreover, simulation results suggest that climate will impact ecosystem carbon and nitrogen dynamics. Specifically, warmer winter and spring enhance soil microbial activity and biomass growth, which results in higher gaseous carbon and nitrogen fluxes and higher dissolved organic carbon and nitrogen losses to the stream, but lower dissolved inorganic carbon and nitrogen losses to the stream and lower amount of carbon sequestration. This

analysis provide decision makers and resource managers with critical information on the potential extend of impact climate change will have on forest carbon and nitrogen dynamics, site productivity and water quality and quantity.

CHAPTER 1

INTRODUCTION

1.1. Research Motivation

Forests in the United States cover about 33 percent of the land area [*Smith et al.*, 2004; *Trends*, 2001] and are responsible for 80% of the fresh water supply [*Sedell et al.*, 2000]. More than 40 percent of all municipalities and about 180 million people depend on fresh water from forests [*Thompson*, 2006]. Forested ecosystems experienced a surge in environmental stressors such as timber production, land conversion for agriculture, fire, and climate warming [*Agee*, 1994; *Agee*, 1996; *Mote et al.*, 1999; *Mote*, 2003; *Mote et al.*, 2003; *Stednick*, 2008]. As a result, concerns over the effects of these stressors on streamwater quantity and quality, future site productivity, sediment transport, aquatic habitat, and aquatic organism populations emerged [*Bormann et al.*, 1968; *Brown and Krygier*, 1970; *Hibbert*, 1966; *Likens et al.*, 1970; *Rishel et al.*, 1982; *Rothacher*, 1970; *Swank and Crossley*, 1988; *Swank et al.*, 2001; *Swanston and Swanson*, 1976]. Land managers and policy makers are currently faced with the difficult task of establishing rules and regulations that would help meet streamwater quantity and quality demands. Until recently, water managers have relied on scientific results from experimental studies to assess the impact of forest disturbances on ecosystem services [*Barten et al.,* 2008]. However, experimental studies are usually expensive, require a long time commitment, are often site-specific, and cannot be used alone to quantify the contribution of specific processes to observed hydrological and biogeochemical responses [*Alila and Beckers*, 2001; *Stednick*, 2008; *Ward*, 1971]. As a result, land managers have started to request process-based simulation models that can address their need by providing a whole-system synthesis of disparate data sets (soils, vegetation, climate, etc.) and by analyzing underlying process-level controls on catchment hydrological and biogeochemical responses to disturbance. These models have to be properly constrained, physically based, computationally efficient and relatively easy to implement with adequate physical processes to simulate the interacting impact of climate, hydrology and ecology.

1.2. Scope of the Study

The objective of this study is to develop an ecohydrological model (VELMA: Visualizing Ecosystems for Land Management Assessments) that simulates changes in soil water infiltration and redistribution, evapotranspiration, surface and subsurface runoff, carbon and nitrogen cycling in plants and soils, and the transport of dissolved forms of carbon and nitrogen from the terrestrial landscape to streams. This model is aimed to provide policy makers and land managers with an accessible, computationally efficient, and relatively easy to implement tool for analyzing the effects of changes in climate, land-use, and land cover on watershed processes at scales relevant to formulating management decisions. VELMA is applied to a Pacific Northwest Long Term Ecological Research catchment to explore the impact of fire, clearcut, harvest amount and spatial pattern, as well as climate change, on water quality and quantity. The following research questions are addressed in this study:

- How does forest harvest location within a watershed affect streamflow, evapotranspiration, soil moisture, nutrient fluxes, and biogeochemical processes?
- How does forest harvest amount affect hydrological and biogeochemical processes?
- Is there threshold behavior in the catchment hydrological and biogeochemical response to increasing harvest amount?
- How feedbacks among the cycles of C, N and water regulate ecosystem responses to natural and man-made disturbances?
- What is the impact of climate change on forest hydrological and biogeochemical processes?

1.3. Thesis Organization

The first part of the study focuses on the hydrological response of a catchment to clearcut. Specifically, the hydrological component of VELMA is applied to a small highly studied catchment in the Pacific Northwest, in order to explore the impact of harvest amount and spatial pattern on catchment soil moisture, evapotranspiration and stream discharge. First, VELMA is calibrated and validated at capturing steady-state pre-

clearcut hydrological conditions as well as post-clearcut hydrological conditions in WS10. Then one hundred scenarios, where harvest amounts ranged from 2% to 100%, irrespective of location, were conducted to explore the impact of increasing harvest amount on streamflow, evapotranspiration and soil moisture, and to test for hydrological threshold. Thereafter, to assess the impact of harvest location on stream discharge, twenty harvest scenarios were simulated, where harvest amount (20%) was fixed and harvest location varied.

The second part of the study focuses on the biogeochemical response of Pacific Northwest forests to natural and man-made disturbances. Specifically, VELMA is applied to a small intensively studied catchment (WS10), where two significant disturbance events have shaped the life history of vegetation growth. The first was a stand-replacing fire in *circa* 1525. The second was a clearcut harvest in 1975. Observed ecological and hydro-biogeochemical data from this site in combination with published chronosequence data from Pacific Northwest forest ecosystems were used to calibrate and test the modeled response to fire and harvest. Model parameters were first calibrated to simulate the post-fire build-up of ecosystem carbon and nitrogen stocks from the 1525 fire to 1969, and then used to simulate the biogeochemical response of an old-growth (1969-1974) and recently clearcut (1975-2008) forest.

The third part of the study focuses on catchment biogeochemical responses to forest harvest amount and spatial pattern. VELMA was applied to a small Pacific Northwest Long Term Ecological Research (LTER) catchment (WS10), to elucidate how hillslope and catchment-scale processes control soil carbon (C) and (N) dynamics in response to clearcut. VELMA was previously calibrated and validated at capturing post-fire and post-harvest hydrological and biogeochemical dynamics in WS10 (Part 2). Thereafter, a number of harvest amount (one hundred scenarios ranging from 0% to 100%) and harvest location scenarios are conducted to explore (1) the impact of increasing harvest amount on biogeochemical fluxes, (2) the existence of biogeochemical thresholds, and (3) the impact of harvest location on biogeochemical fluxes.

The final part of the study focuses on the impact of future climate change on catchment hydrology and C and N dynamics. VELMA is applied to a Long-term

Ecological Research site, the H.J. Andrews 64 km^2 Experimental Forest (HJA), in the Pacific Northwest. The goal is to provide process level insight into the impact of climate change on ecosystem processes at high spatial resolution relevant to formulating management decision. Daily projected temperature and precipitation from an upper bound (IPSLCM4_A2), lower bound (GISS_ER_B1) and middle of the road (ECHAM5_A2) climate change scenarios are used to force the model. The projected daily temperature and precipitation are spatially interpolated across the H.J. Andrews watershed using a climate analysis model PRISM that includes for the effects of elevation, forest canopy, cloudiness, topographic shading, orographic lifting, and temperature inversion on temperature and precipitation. Climate change impacts on seasonal and annual streamflow, soil moisture, evapotranspiration, snowdepth, plant biomass, dissolved C and N losses from the terrestrial system to the stream and to the atmosphere, as well as site productivity are explored.

The thesis is organized such as the introduction is provided in chapter 1. The background and literature review is provided in chapter 2. The first part of the study is presented in chapter 3. A thorough description of the hydrological component of VELMA is provided in Appendix A of chapter 3. The second part of the study is presented in chapter 4. A thorough description of the biogeochemical and soil temperature component of VELMA is provided in Appendix A of chapter 4. The third and the final part of the study are provided in chapter 5 and 6, respectively. Finally, Chapter 7 concludes the thesis by summarizing the overall results, highlighting significant aspects of the study and listing the further improvement possibilities as informed by this research study.

1.4. References

Agee, J. (1994), Fire and weather disturbances in terrestrial ecosystems of the eastern Cascades. US Forest Service, *Pacific Northwest Research Station. General Technical Report PNW-GTR-320*.

Agee, J. K. (1996), *Fire ecology of Pacific Northwest forests*, Island Pr.

Alila, Y., and J. Beckers (2001), Using numerical modelling to address hydrologic forest management issues in British Columbia, *Hydrological Processes*, *15*(18), 3371-3387.

Barten, K., A. Jone, and L. Achterman (2008), Hydrologic Effects of a Changing Forest Landscape. Committee on Hydrologic Impacts of Forest Management, *Water Science and Technology Board. The National Academies Press: Washington, DC*.

Bormann, F., G. Likens, D. Fisher, and R. Pierce (1968), Nutrient loss accelerated by clear-cutting of a forest ecosystem, *Science*, *159*(3817), 882.

Bosch, J., and K. Von Gadow (1990), Regulating afforestation for water conservation in South Africa, *South African Forestry Journal*, *153*(1), 41-54.

Brown, G. W., and J. T. Krygier (1970), Effects of clear-cutting on stream temperature, *Water Resources Research*, *6*(4), 1133-1139, doi:1110.1029/WR1006i1004p01133.

Hibbert, A. (1966), Forest treatment effects on water yield, in *Proceedings of a National Science Foundation advanced science seminar, International symposium on forest hydrology. Pergamon Press, USA*, edited by W.E. Sopper and H.W. Lull, pp. 527-543, Pergamon Press, New York,.

Likens, G., F. Bormann, N. Johnson, D. Fisher, and R. Pierce (1970), Effects of forest cutting and herbicide treatment on nutrient budgets in the Hubbard Brook watershed-ecosystem, *Ecological Monographs*, *40*(1), 23-47.

Mote, P. (2003), Trends in snow water equivalent in the Pacific Northwest and their climatic causes, *Geophysical Research Letters*, *30*(12), 1601.

Mote, P., D. Canning, D. Fluharty, R. Francis, J. Franklin, A. Hamlet, M. Hershman, M. Holmberg, K. Ideker, and W. Keeton (1999), Impacts of climate variability and change, *Pacific Northwest. National Atmospheric and Oceanic Administration, Office of Global Programs, and JISAO/SMA Climate Impacts Group, Seattle, WA*.

Mote, P. W. (2003), Trends in snow water equivalent in the Pacific Northwest and their climatic causes, *Geophysical Research Letters*, *30*(12), 1601.

Mote, P. W., E. A. Parson, A. F. Hamlet, W. S. Keeton, D. Lettenmaier, N. Mantua, E. L. Miles, D. W. Peterson, D. L. Peterson, and R. Slaughter (2003), Preparing for climatic change: the water, salmon, and forests of the Pacific Northwest, *Climatic Change*, *61*(1), 45-88.

Rishel, G., J. Lynch, and E. Corbett (1982), Seasonal stream temperature changes following forest harvesting, *Journal of Environmental Quality*, *11*(1), 112.

Rothacher, J. (1970), Increases in water yield following clear-cut logging in the Pacific Northwest, *Water Resources Research*, *6*(2), 653-658, doi:610.1029/WR1006i1002p00653.

Sedell, J., M. Sharpe, D. Dravnieks, M. Copenhagen, and M. Furniss (2000), Water and the Forest Service, *FS-660. Washington, DC: USDA Forest Service, Washington Office*, *40*.

Smith, W., P. Miles, J. Vissage, and S. Pugh (2004), Forest resources of the United States, 2002, *Gen. Tech. Rep. NC-241. St. Paul, MN: US Department of Agriculture, Forest Service, North Central Research Station*, *137*.

Stednick, J. D. (2008), *Hydrological and biological responses to forest practices: the Alsea Watershed study*, illustrated ed., Springer.

Swank, W., and D. Crossley (1988), Introduction and site description, *Forest Hydrology and Ecology at Coweeta. Ecological Studies*, *66*.

Swank, W., J. Vose, and K. Elliott (2001), Long-term hydrologic and water quality responses following commercial clearcutting of mixed hardwoods on a southern Appalachian catchment, *Forest Ecology and Management*, *143*(1-3), 163-178.

Swanston, D., and F. Swanson (1976), Timber harvesting, mass erosion, and steepland forest geomorphology in the Pacific Northwest, *Geomorphology and Engineering, pp.199-221, Coates, ed. Dowden, Hutchinson, and Ross, Inc., Stroudsburg, Pa*.

Thompson, J. (2006), Society's choices: land use changes, forest fragmentation, and conservation, *Notes*.

Trends, H. (2001), US Forest Facts and Historical Trends, *FS-696. Washington, DC: USDA Forest Service*, 18.

Ward, R. (1971), Small Experimental Watersheds: an Appraisal of Concepts and Research Developments. University of Hull, Hull Printers Ltd.: Hull, UK.

CHAPTER 2

BACKGROUND AND LITERATURE REVIEW

2.1. Introduction

Forest management practices such as timber production were a dominant feature of forests across the Pacific Northwest as a result of increasing demands for natural resources [*Stednick*, 2008]. Typical practices in early 20th century included dispersed patch clearcutting, broadcast burning, and artificial regeneration [*Grant et al*., 2008]. All of which had adverse effects on ecosystem health, wildlife preservation, salmonid resources and water quality and quantity [*Binkley and Brown*, 1993; *Winkler et al.,* 2009; *Lehmkuhl and Ruggiero*, 1991; *Stednick*, 2008]. However, changes in social values and in technology as well as an increasing scientific understanding of ecosystem responses have fueled the debate over timber production and preservation of natural ecosystems [*Swanson and Franklin*, 1992]. As a result, research has been increasingly focused on minimizing the potential impact of forest management practices on biodiversity and sustainability of forested systems [*Duan*, 1996]. Early research relied on field studies of paired basin watershed to test the impact of experimental clearcut on watershed processes. These experimental studies provided land managers and policymakers with the general principles that govern watershed ecohydrological response to disturbances. However, due to changing environments, site-specific characteristics, land ownership and forest regulations, forest ecohydrological research has to move from principle to prediction [*Barten et al.*, 2008]. Prediction is needed to test the impact of unmeasured processes such as climate change, land-use scenarios, future forest harvest, fire, and insect outbreak, amongst others, on watershed hydrological and ecological processes. Prediction is becoming possible due to the technological advancement in computing power. As a result, more researchers are relying on computer models ranging from simple lumped hydrological models to physically based spatially distributed ecohydrological models, to test the impact of forest natural and anthropogenic disturbances on ecosystem productivity, wildlife, stream health and water quality and

quantity [e.g. *Tague and Band* 2000; *Tague and Band* 2004; *Wigmosta et al.*, 1994; *Waichler et al.,* 2005; *Krysanova et al.*, 1998; *Arheimer et al.,* 2005; *Aber et al.,* 2002].

2.2. Forest Harvest Impact on Catchment Hydrology and Biogeochemistry

Forest harvest impact on watershed hydrological and biogeochemical processes has been extensively addressed through field experiments across the U.S. in places such as the H.J. Andrews, the Hubbard Brook, and the Coweeta experimental forests [*Berris and Harr*, 1987; *Bormann and Likens*, 1979a; b; *Bormann et al.*, 1968; *Bormann et al.*, 1974; *Harr*, 1976; *Harr and McCorison*, 1979; *Harr et al.*, 1979; *Likens et al.*, 1978; *Likens et al.*, 1970; *Sollins et al.*, 1981; *Webster et al.*, 1992]. Paired-basin experiments have been conducted to identify vegetation removal effects on streamflow [*Hicks et al.*, 1991; *Jones and Post*, 2004; *Matheussen et al.*, 2000; *Stednick*, 1996], peakflow [*Beschta et al*., 2000; *Golding*, 1987; *Grant et al*., 2008; *Harr and McCorison*, 1979; *Jones*, 2000; *Jones and Grant*, 1996], summer lowflow [*Hicks et al.*, 1991; *Keppeler and Ziemer*, 1990; *Rothacher*, 1965], carbon (C) and nitrogen (N) dynamics, and nutrient export to the stream [*Aust and Blinn*, 2004; *Sollins and McCorison*, 1981a; *Sollins et al.*, 1981; *Vitousek and Reiners*, 1975; *Vitousek et al.*, 1979]. A number of generalizations concerning the effects of harvest on streamflow and C and N dynamics have emerged from analyses of paired-catchment studies: (a) Removal of forest cover has been found to: (1) increase water yield [*Bosch and Hewlett*, 1982; *Rothacher*, 1970; *Sahin and Hall*, 1996], peak streamflow [*Harr and McCorison*, 1979; *Jones*, 2000; *Jones and Grant*, 1996], and soil water saturation [*Londo et al.*, 1999], (2) reduce canopy interception and evapotranspiration [*Moore et al*., 2004; *Moore and Wondzell*, 2005], (3) expose the snow surface to greater winds and solar radiation, which results in earlier snowmelt and higher snowmelt rates [*Berris and Harr*, 1987; *Winkler et al*., 2005], (4) increase nitrogen export to the stream through a decrease in plant N uptake and an increase in microbial nitrification [*Bormann et al.*, 1968; *Fredriksen*, 1975; *Likens et al.*, 1970; *Vitousek et al.*, 1979], (5) increase greenhouse gas emissions [*Harmon et al.*, 1990] and soil microbial activity [*Bormann et al*., 1968; *Grant et al*., 2007; *Potter et al*., 2001], and (6) reduce carbon and nitrogen pools as well as forest productivity [*Grigal*, 2000; *Johnson and Henderson*, 1995; *Ryan et al.*, 1997; *Sollins and McCorison*, 1981; *Sollins et al.*, 1981];

(b) Forest regrowth has been found to: (1) reduce the initial increase in water yield and nutrient export to the stream [*Cairns and Lajtha*, 2005; *Vitousek and Reiners*, 1975], (2) increase evapotranspiration and nutrient uptake [*Jones*, 2000; *Sollins and McCorison*, 1981; *Vitousek and Reiners*, 1975], and (3) result in summer flow deficits during the growing season of young vigorous forest [*Jones and Post*, 2004; *Moore et al*., 2004; *Perry*, 2008]; and (c) The initial response to harvest and the subsequent recovery of streamflow, forest productivity, nutrient pools, and nutrient losses are highly variable and difficult to predict [*Binkley and Brown*, 1993; *Bosch and Hewlett*, 1982; *Stednick*, 1996; *Vitousek et al.*, 1979].

2.3. Variability in the Ecosystem Response to Forest Harvest

The factors that control the variability in hydrological and biogeochemical response to harvest include harvest amount, harvest location, vegetation type, and climatic/hydrologic regimes, amongst others. For example, *Stednick's* [1996] meta-analysis of 95 paired-catchment studies highlighted major differences in the response of annual streamflow to harvest across 8 climate regions within the United States. At the two extremes, catchments in the Rockies and the Pacific Coast yielded 9 and 50 mm more streamflow annually for every 10% increase in harvest area, respectively. *Stednick's* [1996] analysis also showed a large unexplained variability in the relationship between harvest amount and annual water yield within each of the 8 climate regions. However, it was unclear in this analysis how harvest location within a watershed, as opposed to harvest amount, impacted stream response. *Stednick* [1996] argues that part of the streamflow response variability to forest harvest might be caused by the physical location of harvest within the watershed.

Vitousek et al., [1979] analyzed 19 experimental studies to explore the quantitative and temporal dynamics of nutrient losses after forest harvest. *Vitousek et al.,* [1979] found that the extent of nitrogen losses following forest harvest varies tremendously from site to site and can be in part explained in terms of site characteristics. *Binkley and Brown* [1993] analyzed the effects of harvesting on streamwater concentrations of nitrate from 31 experimental studies in the US and Canada, and found that post-harvest streamwater nitrate concentrations were usually higher in the east of continental U.S.

compared to the center and west of the country. The variability in the forest biogeochemical response was also apparent within a region. For example, after a 100% clearcut, streamwater nitrate concentration increased by 0.075 $mgL^{-1}yr^{-1}$ (3-fold), 0.159 $mgL^{-1}yr^{-1}$ (53-fold), and 0.46 $mgL^{-1}yr^{-1}$ (11-fold) in Coyote Creek (OR), High Ridge (OR) and UBC Research Forest (BC), respectively and decreased by 0.05 $mgL^{-1}yr^{-1}$ (29%) in Bitterroot (MT). *Binkley and Brown* [1993] reported that a 33% clearcut in Fraser Colorado resulted in an average annual increase of 0.054 $mgL^{-1}yr^{-1}$ (9-fold), whereas an 88% clearcut in Alsea Oregon resulted in no increases in annual streamwater nitrate concentration. Thus, it was unclear how harvest location might have influenced nutrient fluxes due to partial clearcut.

2.4. Climate Change Impact on Catchment Hydrology and Biogeochemistry

Over the course of the 20th century, the Pacific Northwest experienced an increase in annual temperature and precipitation of 0.8°C and 13%, respectively [*Mote*, 2003]. Specifically, the largest warming rates occurred in the winter and spring whereas the largest increase in precipitation occurred in the winter [*Cayan et al*., 2001; *Folland et al*., 2001; *Mote*, 2003; *Regonda et al*., 2005]. As a result, the ecohydrological regime of the region changed [*Mote et al*., 1999]. These changes included earlier spring snowmelt [*Regonda et al.*, 2005], reduced summer streamflow [*Stewart et al.*, 2005], reduced snow accumulation depth [*Knowles et al.,* 2006; *Mote et al.,* 2005; *Mote et al.,* 2003], reduced low elevation snowfall [*Groisman et al.*, 2004; *Knowles et al.*, 2006], increased forest productivity [*Boisvenue and Running*, 2006], and increasing nutrient losses to the stream [*Mote et al*., 2003]. Such changes in water quantity and quality in the Pacific Northwest will be further impacted and altered with continuing climate warming in the 21th century. Based on the 2007 Intergovernmental Panel on Climate Change (IPCC) Fourth Assessment Report (AR4), the Pacific Northwest could face a projected average increase in temperature of 3°C (1.6 to 9.4°C), and a projected average increase in annual precipitation of approximately 2% (-10 to +20%) by 2100 [*Mote and Salathe,* 2010]. In addition to changes in annual values of temperature and precipitation, the seasonality of climate is also expected to change. Most climate models project an enhanced seasonal cycle with warmer and drier (20-40% reduction in precipitation) summers, and wetter

falls and winters. Climate change will also impact the temporal distribution of precipitation with a considerable increase in extreme precipitation events [*Mote and Salathe*, 2009; *Salathe et al*., 2009].

To date, there has been a number of impact modeling studies that explored the projected future regional changes in water quantity due to climate warming in the Pacific Northwest [e.g. *Christensen and Lettenmaier*, 2007; *Christensen et al.,* 2004; *Mote and Salathe,* 2010; *Payne et al.,* 2004; *Van Rheenen et al.,* 2004]. These climate change impact studies indicate: (1) an increase in annual streamflow as a result of higher winter and fall season precipitation [*Elsner et al.*, 2010; *Maurer and Duffy*, 2005; *Miles et al.*, 2000], (2) an increase in winter runoff as more precipitation is projected to fall as rain rather than snow [*Chang and Jung*, 2010; *Elsner et al.*, 2010; *Graves and Chang*, 2007; *Loukas et al.*, 2002], (3) a decrease in spring and summer streamflow as a result of higher evapotranspiration, lower winter snowpack, earlier snowmelt and lower warm season precipitation [*Lettenmaier et al.*, 1999; *Leung and Wigmosta*, 1999; *Mastin et al.*, 2008], (4) an increase in annual evapotranspiration due to higher temperatures in the winter, spring and fall [*Spittlehouse*, 2007; *Spittlehouse and Stewart*, 2003] 4) a decrease in summer soil moisture [*Elsner et al.*, 2010; *Hamlet and Lettenmaier*, 1999], 6) a reduction in snowpack accumulation as a result of the shift in winter precipitation from snow to rain [*Casola et al.,* 2009; *Graves and Chang,* 2007; *Minder,* 2010; *Tague et al.,* 2008], and 7) an earlier generation of snowmelt runoff [*Elsner et al.*, 2010; *Pike et al.*, 2008; *Stewart et al.*, 2005]. Instead, fewer studies have modeled the impact of climate change on water quality and ecosystem processes in the Pacific Northwest. Nevertheless, a number of generalizations have emerged from existing climate change impact analysis performed in Europe, Alaska, California and eastern U.S. amongst others. Specifically, these studies found that, irrespective of location, a projected increase in cool and warm seasons air temperatures result in: (1) a longer growing season as a result of higher spring and fall temperatures [*Feng and Hu*, 2004; *Sebestyen et al.*, 2009], (2) higher microbial decomposition in the winter due to higher temperature and soil moisture content [*Boisvenue and Running*, 2006; *Clair and Ehrman*, 1996; *McClain et al.*, 1998], (3) higher nutrient concentration in the stream as a result of higher microbial decomposition [*Arheimer et al.*, 2005; *Baron et al.*, 2009; *Chang et al.*, 2001], (4) a reduction of the total

carbon storage in the soil [*Franklin*, 1992; *McClain et al.*, 1998], (5) an increase in ecosystem growth rates [*Boisvenue and Running,* 2006; *Spittlehouse and Stewart.,* 2003], and (6) an increase in ecosystem net primary production due to the effects of higher temperature on soil nitrogen mineralization [*Boisvenue and Running,* 2006; *Melillo.,* 1993; *Sun et al.,* 2000; *Tague et al.,* 2009].

2.5. Limitations of Experimental Studies

Experimental paired watershed studies began in the early 20th century as a result of increasing concern of the impact of land-use and specifically forest harvest on water quality and quantity, salmonid resources and ecosystem health. Paired basin studies were generally intended to explore the impact of forest harvest, roads, and fire on streamflow, peak flow, summer low flow, nutrient dynamics, nutrient losses to the stream, and stream health, amongst others. Paired basin studies are mainly completed over small areas and consist of comparing the hydrological/biogeochemical metrics of a treated and untreated watersheds [*Grant et al*., 2008]. The treated and untreated watersheds are usually in close proximity and are selected based on their similar properties such as soil type, soil texture, vegetation cover, topography, climate and hydrological dynamics [*Brooks et al.*, 1991; *Brooks et al.*, 1991]. First, a pre-disturbance period is usually needed to develop a statistical relationship between the hydrographs/stream chemistries of these two watersheds. Then, the difference in the hydrological/biogeochemical response between the treated and the untreated watershed is interpreted as the disturbance effect.

Paired basin experiments have been and will still be extensively used by researchers and land-managers to test the impact of disturbances on catchment hydrological, biogeochemical, and ecological processes. However, paired basin experiments have some major limitations. For example, (1) the statistical relationship between the treated and the untreated watersheds might change with time due to different successional rate of change in vegetation or the occurrence of natural disaster such as fire and insect outbreak [*Bosch and Hewlett*, 1982], (2) experimental studies of forest harvest alone is problematic as a result of the associated road building, slash burning, and soil compaction, amongst others [*Whitehead and Robinson*, 1993], (3) experimental paired basin studies do not distinguish between harvest location and amount and are usually

limited to one treatment experiment per watershed [*Stednick*, 1996], (4) the local climate variability in temperature and precipitation between the treated and untreated watershed might lead to differences in the hydrograph [*Monteith et al.*, 2006], (5) experimental studies are usually expensive and require a long time commitment to get a statistical significant pre- and post-treatment period of data [*Ackermann*, 1966], (6) the inherent accuracy errors associated with measuring instruments [*Grant et al*., 2008], and (7) the impossibility to explore the impact of climate change on catchment processes. Therefore, while carefully designed paired-catchment experiments and statistical analyses can provide strong circumstantial evidence for process-level controls, they cannot be used alone to quantify the contribution of specific treatments and future conditions on ecosystem hydro-biogeochemical processes.

2.6. Eco-hydrological Models

Process-based ecohydrological models can address this need by providing a whole-system synthesis of disparate data sets (soils, vegetation, climate, etc.) and by analyzing underlying process-level controls on catchment hydrological and biogeochemical responses to disturbances. Properly constrained models allow a self-consistent representation and analysis of process-level interactions within catchments, as well as the ability to isolate and make inferences about the contribution of specific processes to observed responses. Models can also extend a data set by providing a framework for exploring conditions that would be too difficult or costly to implement in practice, and by allowing behavior of unmeasured system components to be inferred. Similarly, models can be used to isolate the effect of a 'target' treatment factor from the effects of other factors that may be unavoidably altered within a single treatment [*McKane et al.*, 1997]. These properties are apparent in various modeling studies of the effects of disturbances on catchment hydrological and biogeochemical processes. For example: (1) *Tague and Band* [2000] used the RHESSys ecohydrological model to isolate the effects of harvest and roads on streamflow; (2) *Waichler et al.,* [2005] applied the DHSVM (Dynamic Hydrology Soil Vegetation Model [*Wigmosta et al.*, 1994]) hydrological model to 3 watersheds in the H.J. Andrews Experimental Forest to quantify the effects of forest harvest, without roads, on streamflow, peakflow, and water balance; (3) *Whitaker et al.,*

[2002] used the DHSVM hydrological model to evaluate peak flow sensitivity to clearcut in different elevation bands in a snow-dominated catchment in British Columbia, (4) *Sayama and McDonnell* [2009] used the OHDIS-KWMSS [*Tachikawa et al.*, 2004] hydrological model to infer the age and upland source areas of water contributing to streamflow, (5) *Aber et al.,* [2002] applied the PnET-CN model [*Aber et al*., 1997] on watershed 6 of the Hubbard Brook Experimental Forest, to test the individual and combined effects of climate variability, changes in atmospheric chemistry, and physical and biotic disturbances on DIN loss rate, (6) *Arheimer et al.,* [2005] used the HBV-N model [*Arheimer and Brandt*, 1998] to explore the impact of climate change on nitrogen leaching, water discharge, and nitrogen retention in a catchment in southern Sweden, (7) *Marshall and Randhir* [2008] used the SWAT model (Soil and Water Assessment Tool [*Arnold et al.*, 1998]) to assess the impact of climate change on water quantity and quality at a regional scale in the Connecticut River Watershed of New England, (8) *Krysanova and Haberlandt* [2002] used the SWIM ecohydrological model (Soil and Water Integrated Model [*Krysanova et al.*, 1998]) to study the impact of various fertilization schemes on nitrogen leaching from arable land in large river basins, and (9) *Stieglitz et al.,* [2006] used a simple plant soil model PSM to analyze climate change impact on terrestrial carbon and nitrogen dynamics in arctic Alaska. Thus, models such as these can provide a detailed process-based understanding of experimental responses that would be impossible with the data alone. Moreover, simulation models offer an effective tool to complement field research and to examine the integrated responses of vegetation, soil, and water resources to interacting stressors.

2.7. Limitations of Existing Eco-hydrological Models

Existing process-based models have some disadvantages. Many models either do not simulate the interaction between hydrological and ecological processes or are too simple to simulate process-level controls of interest. For example: (1) PSM [*Stieglitz et al.*, 2006], and MEL (Multiple Element Limitation Model [*Rastetter et al.*, 1997]) are biogeochemical models that simulate C and N dynamics in soil and plant, but do not simulate the interactions of C and N with hydrological processes, (2) DHSVM [*Wigmosta et al.*, 1994] and VIC (Variable Infiltration Capacity [*Wood et al.*, 1992]) do not simulate

biogeochemical processes and are pure hydrological models, and (3) PnET-CN [*Aber et al*., 1997] is a simple lumped parameter model of monthly carbon, nitrogen and water balance. Others are semi-distributed ecohydrological models that lack the details to simulate plot level disturbances such as upland clearcut and hillslope riparian processes (e.g. SWIM [*Krysanova et al.*, 1998], SWAT [*Arnold et al.*, 1998]). Last, some models simulate the interaction of hydrology and ecology, but are so complex that they require calibration and forcing data that are often unavailable (e.g. leaf area index, solar radiation, wind speed, relative humidity amongst others), are too computationally expensive to simulate large watersheds and landscapes, or require a high level of expertise to implement. Moreover, for a variety of reasons, most current modeling frameworks have been limited to the research community [*Beckers et al.*, 2009]. Therefore, there is a need for a balanced approach; specifically an accessible (i.e. open source) spatially distributed ecohydrological model that is both computationally efficient and relatively easy to implement for analyzing the effects of changes in climate, land-use, and land cover on watershed processes at scales relevant to both researchers and policy makers.

2.8. References

Aber, J., S. Ollinger, C. Driscoll, G. Likens, R. Holmes, R. Freuder, and C. Goodale (2002), Inorganic Nitrogen Losses from a Forested Ecosystem in Responseto Physical, Chemical, Biotic, and Climatic Perturbations, *Ecosystems*, *5*(7), 648-658.

Aber, J. D., S. V. Ollinger, and C. T. Driscoll (1997), Modeling nitrogen saturation in forest ecosystems in response to land use and atmospheric deposition, *Ecological Modelling*, *101*(1), 61-78.

Ackermann, W. S. (1966), Guidelines for Research on the Hydrology of Small Watersheds. Office of Water Resources, US Dept. of Interior, Washington DC, 26 pp.

Arheimer, B., and M. Brandt (1998), Modelling nitrogen transport and retention in the catchments of southern Sweden, *Ambio (Sweden)*.

Arheimer, B., J. Andreasson, S. Fogelberg, H. Johnsson, C. B. Pers, and K. Persson (2005), Climate change impact on water quality: model results from southern Sweden, *Ambio*, 559-566.

Arnold, J. G., R. Srinivasan, R. S. Muttiah, and J. Williams (1998), Large Area Hydrologic Modeling and Assessment Part I: Model Development, *JAWRA Journal of the American Water Resources Association*, *34*(1), 73-89.

Aust, W. M., and C. R. Blinn (2004), Forestry best management practices for timber harvesting and site preparation in the eastern United States: an overview of water quality and productivity research during the past 20 years (1982-2002), *Water, Air, & Soil Pollution: Focus*, *4*(1), 5-36.

Baron, J. S., T. M. Schmidt, and M. D. Hartman (2009), Climate induced changes in high elevation stream nitrate dynamics, *Global Change Biology*, *15*(7), 1777-1789.

Barten, K., A. Jone, and L. Achterman (2008), Hydrologic Effects of a Changing Forest Landscape. Committee on Hydrologic Impacts of Forest Management, *Water Science and Technology Board. The National Academies Press: Washington, DC*.

Beckers, J., B. Smerdon, T. Redding, A. Anderson, R. Pike, and A. T. Werner (2009), Hydrologic Models for Forest Management Applications: Part 1: Model Selection, *Watershed Management Bulletin*, *13*(1), 35-44.

Berris, S. N., and R. D. Harr (1987), Comparative snow accumulation and melt during rainfall in forested and clear-cut plots in the western Cascades of Oregon, *Water Resources Research*, *23*(1), 135-142, doi:110.1029/WR1023i1001p00135.

Beschta, R., M. Pyles, A. Skaugset, and C. Surfleet (2000), Peakflow responses to forest practices in the western Cascades of Oregon, USA, *Journal of Hydrology*, *233*(1-4), 102-120.

Binkley, D., and T. Brown (1993), Forest practices as nonpoint sources of pollution in North America, *Water Resources Bulletin*, *29*(5), 729-740.

Boisvenue, C. L., and S. W. Running (2006), Impacts of climate change on natural forest productivity and evidence since the middle of the 20th century, *Global Change Biology*, *12*(5), 862-882.

Bormann, F., and G. Likens (1979a), Pattern and process in a forested ecosystem, edited, Springer-Verlag, New York.

Bormann, F., and G. Likens (1979b), Catastrophic disturbance and the steady state in northern hardwood forests, *American Scientist*, *67*, 660-669.

Bormann, F., G. Likens, D. Fisher, and R. Pierce (1968), Nutrient loss accelerated by clear-cutting of a forest ecosystem, *Science*, *159*(3817), 882.

Bormann, F., G. Likens, T. Siccama, R. Pierce, and J. Eaton (1974), The export of nutrients and recovery of stable conditions following deforestation at Hubbard Brook, *Ecological Monographs*, *44*(3), 255-277.

Bosch, J., and J. Hewlett (1982), A review of catchment experiments to determine the effect of vegetation changes on water yield and evapotranspiration, *Journal of Hydrology*, *55*(1-4), 3-23.

Brooks, K., P. Folliott, H. Gregersen, and J. Thames (1991), Hydrology and the Management of Watersheds: The Economics of Watershed Practices and

Management. 6ta. Ed. Iowa, edited, United States Of. America, Iowa State University Press.

Brooks, R. P., E. D. Bellis, C. S. Keener, M. J. Croonquist, and D. Arnold (1991), A methodology for biological monitoring of cumulative impacts on wetland, stream, and riparian components of watersheds.

Cairns, M., and K. Lajtha (2005), Effects of succession on nitrogen export in the west-central Cascades, Oregon, *Ecosystems*, *8*(5), 583-601.

Casola, J. H., L. Cuo, B. Livneh, D. P. Lettenmaier, M. T. Stoelinga, P. W. Mote, and J. M. Wallace (2009), Assessing the Impacts of Global Warming on Snowpack in the Washington Cascades, *Journal of Climate*, *22*(10), 2758-2772.

Cayan, D. R., S. A. Kammerdiener, M. D. Dettinger, J. M. Caprio, and D. H. Peterson (2001), Changes in the onset of spring in the western United States, *BULLETIN-AMERICAN METEOROLOGICAL SOCIETY*, *82*(3), 399-416.

Chang, H., and I. W. Jung (2010), Spatial and temporal changes in runoff caused by climate change in a complex large river basin in Oregon, *Journal of Hydrology*, *388*(3-4), 186-207.

Chang, H., B. M. Evans, and D. R. Easterling (2001), The Effects of Climate Change on Streamflow and Nutrient Loading *JAWRA Journal of the American Water Resources Association*, *37*(4), 973-985.

Christensen, N., and D. Lettenmaier (2007), A multimodel ensemble approach to assessment of climate change impacts on the hydrology and water resources of the Colorado River Basin, *Hydrology and Earth System Sciences*, *11*(4), 1417-1434.

Christensen, N. S., A. W. Wood, N. Voisin, D. P. Lettenmaier, and R. N. Palmer (2004), The effects of climate change on the hydrology and water resources of the Colorado River basin, *Climatic Change*, *62*(1), 337-363.

Clair, T. A., and J. M. Ehrman (1996), Variations in discharge and dissolved organic carbon and nitrogen export from terrestrial basins with changes in climate: a neural network approach, *Limnology and Oceanography*, 921-927.

Duan, J. (1996), A coupled hydrologic-geomorphic model for evaluating effects of vegetation change on watersheds: Ph.D. Dissertation, Oregon State University, Corvallis, OR, 133p.

Elsner, M. M., L. Cuo, N. Voisin, J. S. Deems, A. F. Hamlet, J. A. Vano, K. E. B. Mickelson, S. Y. Lee, and D. P. Lettenmaier (2010), Implications of 21st century climate change for the hydrology of Washington State, *Climatic Change*, *102*(1), 225-260.

Feng, S., and Q. Hu (2004), Changes in agro-meteorological indicators in the contiguous United States: 1951 to 2000, *Theoretical and Applied Climatology*, *78*(4), 247-264.

Folland, C., T. Karl, R. Christy, R. Clarke, G. Gruza, J. Jouzel, M. Mann, J. Oerlermans, M. Salinger, and S. Wang (2001), Climate change 2001: the scientific basis,

Contribution of Working Group I to the IPCC Third Assessment Report, Cambridge University Press, Cambridge, 99-181.

Franklin, J. (1992), New Forestry Principles From Ecosystem Analysis of Pacific Northwest Forests 1,2 *Ecological Applications*, *2*(3), 262-214.

Fredriksen, R. (1975), Nitrogen, phosphorus and particulate matter budgets of five coniferous forest ecosystems in the western Cascades Range, Oregon, Doctoral thesis, 71 pp, Oregon State University, Corvallis.

Golding, D. L. (1987), Changes in streamflow peaks following timber harvest of a coastal British Columbia watershed, paper presented at Forest Hydrology and Watershed Management, IAHS, Vancouver.

Grant, G., S. Lewis, F. Swanson, J. Cissel, and J. McDonnell (2008), Effects of forest practices on peak flows and consequent channel response: a state-of-science report for western Oregon and Washington, *General Technical Report. PNW-GTR-760. Portland, OR: USDA Forest Service, Pacific Northwest Research Station*, *76*.

Grant, R., T. Black, E. Humphreys, and K. Morgenstern (2007), Changes in net ecosystem productivity with forest age following clearcutting of a coastal Douglas-fir forest: testing a mathematical model with eddy covariance measurements along a forest chronosequence, *Tree Physiology*, *27*(1), 115.

Graves, D., and H. Chang (2007), Hydrologic impacts of climate change in the Upper Clackamas River Basin, Oregon, USA, *Climate Research*, *33*(2), 143-158.

Grigal, D. (2000), Effects of extensive forest management on soil productivity, *Forest Ecology and Management*, *138*(1-3), 167-185.

Groisman, P. Y., R. W. Knight, T. R. Karl, D. R. Easterling, B. Sun, and J. H. Lawrimore (2004), Contemporary changes of the hydrological cycle over the contiguous United States: Trends derived from in situ observations, *Journal of Hydrometeorology*, *5*(1), 64-85.

Hamlet, A. F., and D. P. Lettenmaier (1999), Effects of Climate Change on Hydrology and Water Resources in the Columbia River Basin, *JAWRA Journal of the American Water Resources Association*, *35*(6), 1597-1623.

Harmon, M. E., W. K. Ferrell, and J. F. Franklin (1990), Effects on carbon storage of conversion of old-growth forests to young forests, *Science*, *247*(4943), 699-701.

Harr, R. (1976), Forest practices and streamflow in western Oregon, *Gen. Tech. Report PNW-GTR-049. Portland, OR: US Department of Agriculture, Forest Service, Pacific Northwest Research Station. 23 p.*

Harr, R., and F. M. McCorison (1979), Initial effects of clearcut logging on size and timing of peak flows in a small watershed in western Oregon, *Water Resources Research*, *15*(1), 90-94, doi:10.1029/WR1015i1001p00090.

Harr, R., R. Fredriksen, and J. Rothacher (1979), Changes in streamflow following timber harvest in southwestern Oregon, *Research Paper PNW-RP-249. Portland,*

OR: U.S. Department of Agriculture, Forest Service, Pacific Northwest Research Station, 22.

Hicks, B., R. Beschta, and R. Harr (1991), Long-term changes in streamflow following logging in western Oregon and associated fisheries implications, *Water Resources Bulletin*, *27*(2), 217-226.

Johnson, D., and P. Henderson (1995), Effects of forest management and elevated carbon dioxide on soil carbon storage, *Soil management and the greenhouse effects*, 137-145.

Jones, J. A. (2000), Hydrologic processes and peak discharge response to forest removal, regrowth, and roads in 10 small experimental basins, western Cascades, Oregon, *Water Resources Research*, *36*(9), 2621-2642, doi:2610.1029/2000WR900105.

Jones, J. A., and G. E. Grant (1996), Peak flow responses to clear-cutting and roads in small and large basins, western Cascades, Oregon, *Water Resources Research*, *32*(4), 959-974.

Jones, J. A., and D. A. Post (2004), Seasonal and successional streamflow response to forest cutting and regrowth in the northwest and eastern United States, *Water Resources Research*, *40*(5), W05203, doi:05210.01029/02003WR002952.

Keppeler, E. T., and R. R. Ziemer (1990), Logging effects on streamflow: water yield and summer low flows at Caspar Creek in northwestern California, *Water Resources Research*, *26*(7), 1669-1679.

Knowles, N., M. D. Dettinger, and D. R. Cayan (2006), Trends in snowfall versus rainfall in the western United States, *Journal of Climate*, *19*(18), 4545-4559.

Krysanova, V., and U. Haberlandt (2002), Assessment of nitrogen leaching from arable land in large river basins:: Part I. Simulation experiments using a process-based model, *Ecological Modelling*, *150*(3), 255-275.

Krysanova, V., D. I. Muller-Wohlfeil, and A. Becker (1998), Development and test of a spatially distributed hydrological/water quality model for mesoscale watersheds, *Ecological Modelling*, *106*(2-3), 261-289.

Lehmkuhl, J. F., and L. F. Ruggiero (1991), Forest fragmentation in the Pacific Northwest and its potential effects on wildlife, *LF Ruggiero, KB Aubry, AB Carey, and MF Huff. Wildlife and vegetation of unmanaged Douglas-fir forests. US Forest Service, Pacific Research Station, General Technical Report PNW-GTR-285*, 35-46.

Lettenmaier, D. P., A. W. Wood, R. N. Palmer, E. F. Wood, and E. Z. Stakhiv (1999), Water resources implications of global warming: A US regional perspective, *Climatic Change*, *43*(3), 537-579.

Leung, L. R., and M. S. Wigmosta (1999), Potential Climate Change Impacts on Mountain Watersheds in the Pacific Northwest, *JAWRA Journal of the American Water Resources Association*, *35*(6), 1463-1471.

Likens, G., F. Bormann, R. Pierce, and W. Reiners (1978), Recovery of a deforested ecosystem, *Science*, *199*(4328), 492-496.

Likens, G., F. Bormann, N. Johnson, D. Fisher, and R. Pierce (1970), Effects of forest cutting and herbicide treatment on nutrient budgets in the Hubbard Brook watershed-ecosystem, *Ecological Monographs*, *40*(1), 23-47.

Londo, A., M. Messina, and S. Schoenholtz (1999), Forest harvesting effects on soil temperature, moisture, and respiration in a bottomland hardwood forest, *Soil Science Society of America Journal*, *63*(3), 637.

Loukas, A., L. Vasiliades, and N. R. Dalezios (2002), Climatic impacts on the runoff generation processes in British Columbia, Canada, *Hydrology and Earth System Sciences*, *6*(2), 211-228.

Marshall, E., and T. Randhir (2008), Effect of climate change on watershed system: a regional analysis, *Climatic Change*, *89*(3), 263-280.

Mastin, M. C., U. S. B. o. Reclamation, and G. Survey (2008), *Effects of potential future warming on runoff in the Yakima River Basin, Washington*, US Dept. of the Interior, US Geological Survey.

Matheussen, B., R. Kirschbaum, I. Goodman, G. O'Donnell, and D. Lettenmaier (2000), Effects of land cover change on streamflow in the interior Columbia River Basin (USA and Canada), *Hydrological Processes*, *14*(5), 867-885.

Maurer, E. P., and P. B. Duffy (2005), Uncertainty in projections of streamflow changes due to climate change in California, *Geophysical Research Letters*, *32*(3), L03704.

McClain, M. E., R. E. Bilby, and F. J. Triska (1998), Nutrient cycles and responses to disturbance, *River ecology and management: lessons from the Pacific coastal ecoregion*, 347-372.

McKane, R., E. Rastetter, G. Shaver, K. Nadelhoffer, A. Giblin, J. Laundre, and F. Chapin III (1997), Climatic effects on tundra carbon storage inferred from experimental data and a model, *Ecology*, *78*(4), 1170-1187.

Melillo, J. M., A. D. McGuire, D. W. Kicklighter, B. Moore, C. J. Vorosmarty, and A. L. Schloss (1993), Global climate change and terrestrial net primary production, *Nature*, *363*(6426), 234-240.

Miles, E. L., A. K. Snover, A. F. Hamlet, B. Callahan, and D. Fluharty (2000), Pacific Northwest Regional Assessment: The Impacts of Climate Variability and Climate Change on the Water Resources of the Columbia River Basin, *JAWRA Journal of the American Water Resources Association*, *36*(2), 399-420.

Minder, J. R. (2010), The sensitivity of mountain snowpack accumulation to climate warming, *Journal of Climate*, *23*(10), 2634-2650.

Monteith, S., J. Buttle, P. Hazlett, F. Beall, R. Semkin, and D. Jeffries (2006), Paired basin comparison of hydrological response in harvested and undisturbed hardwood forests during snowmelt in central Ontario: I. Streamflow, groundwater and flowpath behaviour, *Hydrological Processes*, *20*(5), 1095-1116.

Moore, G., B. Bond, J. Jones, N. Phillips, and F. Meinzer (2004), Structural and compositional controls on transpiration in 40-and 450-year-old riparian forests in western Oregon, USA, *Tree Physiology*, *24*(5), 481.

Moore, R., and S. Wondzell (2005), Physical Hydrology in the Pacific Northwest and the Effects of Forest HarvestingñA Review, *Journal of the American Water Resources Association*, *41*, 753-784.

Mote, P. (2003), Trends in snow water equivalent in the Pacific Northwest and their climatic causes, *Geophysical Research Letters*, *30*(12), 1601.

Mote, P., and E. Salathe (2009), Future Climate in the Pacific Northwest, Chapter 1 in: Littell, JS, MM Elsner, LC Whitely Binder, and AK Snover, *The Washington Climate Change Impacts Assessment: Evaluating Washingtonís Future in a Changing Climate*.

Mote, P., D. Canning, D. Fluharty, R. Francis, J. Franklin, A. Hamlet, M. Hershman, M. Holmberg, K. Ideker, and W. Keeton (1999), Impacts of climate variability and change, *Pacific Northwest. National Atmospheric and Oceanic Administration, Office of Global Programs, and JISAO/SMA Climate Impacts Group, Seattle, WA*.

Mote, P. W., and E. P. Salathe (2010), Future climate in the Pacific Northwest, *Climatic Change*, *102*(1), 29-50.

Mote, P. W., A. F. Hamlet, M. P. Clark, and D. P. Lettenmaier (2005), Declining mountain snowpack in western North America, *Bulletin of the American Meteorological Society*, *86*(1), 39-44.

Mote, P. W., E. A. Parson, A. F. Hamlet, W. S. Keeton, D. Lettenmaier, N. Mantua, E. L. Miles, D. W. Peterson, D. L. Peterson, and R. Slaughter (2003), Preparing for climatic change: the water, salmon, and forests of the Pacific Northwest, *Climatic Change*, *61*(1), 45-88.

Payne, J. T., A. W. Wood, A. F. Hamlet, R. N. Palmer, and D. P. Lettenmaier (2004), Mitigating the effects of climate change on the water resources of the Columbia River basin, *Climatic Change*, *62*(1), 233-256.

Perry, T. D. (2008), Do vigorous young forests reduce streamflow? Results from up to 54 years of streamflow records in eight paired-watershed experiments in the HJ Andrews and South Umpqua Experimental Forests, Master's thesis, 152 pp, Oregon State University, Corvallis.

Pike, R., D. Spittlehouse, K. Bennett, V. Egginton, P. Tschaplinski, T. Murdock, and A. Werner (2008), Climate change and watershed hydrology: part iñrecent and projected changes in British Columbia, *Streamline Watershed Management Bulletin*, *11*(2), 1-8.

Potter, C., E. Davidson, D. Nepstad, and C. Carvalho (2001), Ecosystem modeling and dynamic effects of deforestation on trace gas fluxes in Amazon tropical forests, *Forest Ecology and Management*, *152*(1-3), 97-117.

Rastetter, E. B., G. I. Ågren, and G. R. Shaver (1997), Responses of N-limited ecosystems to increased CO2: a balanced-nutrition, coupled-element-cycles model, *Ecological Applications*, *7*(2), 444-460.

Regonda, S. K., B. Rajagopalan, M. Clark, and J. Pitlick (2005), Seasonal cycle shifts in hydroclimatology over the western United States, *Journal of Climate*, *18*(2), 372-384.

Rothacher, J. (1965), Streamflow from small watersheds on the western slope of the Cascade Range of Oregon, *Water Resources Research*, *1*, 125-134, doi:110.1029/WR1001i1001p00125.

Rothacher, J. (1970), Increases in water yield following clear-cut logging in the Pacific Northwest, *Water Resources Research*, *6*(2), 653-658, doi:610.1029/WR1006i1002p00653.

Ryan, M., D. Binkley, and J. H. Fownes (1997), Age-related decline in forest productivity: pattern and process, *Advances in ecological research*, *27*, 213-262.

Sahin, V., and M. Hall (1996), The effects of afforestation and deforestation on water yields, *Journal of Hydrology*, *178*(1-4), 293-309.

Salathe Jr, E., Y. Zhang, L. Leung, and Y. Qian (2009), Regional climate model projections for the State of Washington. Washington climate change impacts assessment: evaluating Washington's future in a changing climate, *press system to accommodate increased rainfall resulting from climate change. J Environ Plan and Manag*, *46*(5), 755-770.

Sayama, T., and J. McDonnell (2009), A new time-space accounting scheme to predict stream water residence time and hydrograph source components at the watershed scale, *Water Resources Research*, *45*, W07401, doi:07410.01029/02008WR007549.

Sebestyen, S. D., E. W. Boyer, and J. B. Shanley (2009), Responses of stream nitrate and DOC loadings to hydrological forcing and climate change in an upland forest of the northeastern United States, *Journal of Geophysical Research*, *114*(G2), G02002.

Sollins, P., and F. M. McCorison (1981), Nitrogen and carbon solution chemistry of an old-growth coniferous forest watershed before and after cutting, *Water Resources Research*, *17*(5), 1409–1418, doi:1410.1029/WR1017i1005p01409. .

Sollins, P., K. Cromack Jr, F. Mc Corison, R. Waring, and R. Harr (1981), Changes in nitrogen cycling at an old-growth Douglas-fir site after disturbance, *Journal of Environmental Quality*, *10*(1), 37.

Spittlehouse, D. (2007), Climate change, impacts and adaptation scenarios, *BC Ministry of Forests and Range, Victoria, BC URL:* http://www. *for. gov. bc. ca/hts/Future_Fore sts/Scenarios. pdf*.

Spittlehouse, D. L., and R. B. Stewart (2003), Adaptation to climate change in forest management, *BC Journal of Ecosystems and Management*, *4*(1), 1-11.

Stednick, J. (1996), Monitoring the effects of timber harvest on annual water yield, *Journal of Hydrology*, *176*(1-4), 79-95.

Stednick, J. (2008), Long-term Water Quality Changes Following Timber Harvesting, *ECOLOGICAL STUDIES*, *199*, 157.

Stednick, J. D. (2008), *Hydrological and biological responses to forest practices: the Alsea watershed study*, Springer Verlag.

Stewart, I., D. Cayan, and M. Dettinger (2005), Changes towards earlier streamflow timing across North America, *Journal of Climate*, *18*, 1136-1155.

Stieglitz, M., R. B. McKane, and C. A. Klausmeier (2006), A simple model for analyzing climatic effects on terrestrial carbon and nitrogen dynamics: An arctic case study, *Global biogeochemical cycles*, *20*(3), GB3016.

Sun, G., D. M. Amatya, S. G. McNulty, R. W. Skaggs, and J. H. Hughes (2000), Climate Change Impacts on the Hydrology and Productivity of a Pine Plantation *JAWRA Journal of the American Water Resources Association*, *36*(2), 367-374.

Swanson, F. J., and J. F. Franklin (1992), New forestry principles from ecosystem analysis of Pacific Northwest forests, *Ecological Applications*, *2*(3), 262-274.

Tachikawa, Y., G. Nagatani, and K. Takara (2004), Development of stage discharge relationship equation incorporating saturated-unsaturated flow mechanism, *Annual Journal of Hydraulic Engineering, Japan. Society of Civil Engineers*, *48*, 7-12.

Tague, C., and L. Band (2000), Simulating the impact of road construction and forest harvesting on hydrologic response, *Earth Surface Processes and Landforms*, *26*(2), 135-151.

Tague, C., and L. Band (2004), RHESSys: Regional Hydro-Ecologic Simulation System-An object-oriented approach to spatially distributed modeling of carbon, water, and nutrient cycling, *Earth Interactions*, *8*, 1-42.

Tague, C., L. Seaby, and A. Hope (2009), Modeling the eco-hydrologic response of a Mediterranean type ecosystem to the combined impacts of projected climate change and altered fire frequencies, *Climatic Change*, *93*(1), 137-155.

Tague, C., G. Grant, M. Farrell, J. Choate, and A. Jefferson (2008), Deep groundwater mediates streamflow response to climate warming in the Oregon Cascades, *Climatic Change*, *86*(1), 189-210.

Van Rheenen, N., A. Wood, R. Palmer, and D. Lettenmaier (2004), Potential implications of PCM climate change scenarios for California hydrology and water resources, *Climatic Change*, *62*, 257-281.

Vitousek, P., and W. Reiners (1975), Ecosystem succession and nutrient retention: a hypothesis, *BioScience*, *25*(6), 376-381.

Vitousek, P., J. Gosz, C. Grier, J. Melillo, W. Reiners, and R. Todd (1979), Nitrate losses from disturbed ecosystems, *Science*, *204*(4392), 469-474.

Waichler, S. R., B. C. Wemple, and M. S. Wigmosta (2005), Simulation of water balance and forest treatment effects at the HJ Andrews Experimental Forest, *Hydrological Processes*, *19*(16), 3177-3199.

Webster, J., S. Golladay, E. Benfield, J. Meyer, W. Swank, and J. Wallace (1992), Catchment disturbance and stream response: an overview of stream research at Coweeta Hydrologic Laboratory, *The conservation and management of rivers. John Wiley and Sons, Chichester, UK*, 231ñ253.

Whitaker, A., Y. Alila, J. Beckers, and D. Toews (2002), Evaluating peak flow sensitivity to clear-cutting in different elevation bands of a snowmelt-dominated mountainous catchment, *Water Resources Research*, *38*(9), 1172, doi:1110.1029/2001WR000514.

Whitehead, P., and M. Robinson (1993), Experimental basin studies--an international and historical perspective of forest impacts, *Journal of Hydrology*, *145*(3-4), 217-230.

Wigmosta, M. S., L. W. Vail, and D. P. Lettenmaier (1994), A distributed hydrology-vegetation model for complex terrain, *Water Resources Research*, *30*(6), 1665-1680, doi:1610.1029/1694WR00436.

Winkler, R., D. Spittlehouse, and D. Golding (2005), Measured differences in snow accumulation and melt among clearcut, juvenile, and mature forests in southern British Columbia, *Hydrological Processes*, *19*(1), 51-62.

Winkler, R. D., R.D. Moore, T. Redding, D. Spittlehouse, B. Smerdon, and D. Carlyle-Moses. (2010), Chapter 7 - The effects of forest disturbance on hydrologic processes and watershed response In: R.G. Pike, T.E. Redding, R.D. Moore, R.D. Winkler and K.D. Bladon (editors) 2010. Compendium of forest hydrology and geomorphology in British Columbia. B.C. Min. For. Range, For. Sci. Prog., Victoria, B.C. and FORREX Forum for Research and Extension in Natural Resources, Kamloops, B.C. Land Manag. Handb. 66. pp. 179-212., B.C. Ministry of Forests and Range Research Branch, Victoria, B.C. and FORREX Forest Research Extension Partnership, Kamloops.

Wood, E. F., D. P. Lettenmaier, and V. G. Zartarian (1992), A land-surface hydrology parameterization with subgrid variability for general circulation models, *Journal of Geophysical Research*, *97*(D3), 2717-2728.

CHAPTER 3

CATCHMENT HYDROLOGICAL RESPONSES TO FOREST HARVEST AMOUNT AND SPATIAL PATTERN

Alex Abdelnour[1], Marc Stieglitz[1,2], Feifei Pan[1,3], Robert McKane[4]
Accepted in Water Resources Research-Paper: 2010WR010165R

[1] Department of Civil and Environmental Engineering, Georgia Institute of Technology, Atlanta, GA, USA.
[2]School of Earth Atmospheric Sciences, Georgia Institute of Technology, Atlanta, GA, USA.
[3]Department of Geography, University of North Texas, Denton, TX, USA.
[4]US Environmental Protection Agency, Corvallis, OR, USA.

3.1. Abstract

Forest harvest effects on streamflow generation have been well described experimentally, but a clear understanding of process-level hydrological controls can be difficult to ascertain from data alone. We apply a new model, Visualizing Ecosystems for Land Management Assessments (VELMA), to elucidate how hillslope and catchment-scale processes control stream discharge in a small Pacific Northwest catchment. VELMA is a spatially distributed ecohydrology model that links hydrological and biogeochemical processes within watersheds. The study site is WS10 of the H.J Andrews LTER, a 10-ha forested catchment clearcut in 1975. Simulated and observed daily streamflow are in good agreement for both the pre- (1969-1974) and post-harvest (1975-2008) periods (Nash-Sutcliffe Efficiency = 0.807 and 0.819, respectively). One hundred scenarios, where harvest amounts ranged from 2% to 100% were conducted. Results show that (1) for the case of a 100% clearcut, stream discharge initially increased by ~29% or 345mm but returned to pre-clearcut levels within 50 years, and (2) annual streamflow increased at a near linear rate of 3.5mm/year for each percent of catchment harvested, irrespective of location. Thereafter, to assess the impact of harvest location on stream discharge, twenty harvest scenarios were simulated, where harvest amount was fixed at 20% but harvest location varied. Results show that the streamflow response is strongly sensitive to harvest distance from the stream channel. Specifically, a 20% clearcut area near the catchment divide resulted in an average annual streamflow increase of 53mm, whereas a 20% clearcut near the stream resulted in an average annual streamflow increase of 92mm.

3.2. Introduction

Forest harvest effects on streamflow dynamics have been well described experimentally [*Beschta et al.,* 2000; *Bowling et al.,* 2000] . For example, results from paired-catchment studies have shown that: (1) removal of forest cover increases water yield [*Hibbert*, 1966; *Keppeler and Ziemer*, 1990; *Rothacher*, 1970] and peak streamflow [*Golding*, 1987; *Harr and McCorison*, 1979; *Jones*, 2000; *Jones and Grant*, 1996] by decreasing evapotranspiration [*Bosch and Hewlett*, 1982]; (2) regrowth after harvest decreases water yield [*Jones*, 2000; *Jones and Post*, 2004; *Sahin and Hall*, 1996]; and (3) the initial response to harvest and the subsequent recovery of annual, peak, and low flows are highly variable and difficult to predict [e.g. *Bosch and Hewlett*, 1982; *Hibbert*, 1966; *Jones and Post*, 2004; *Stednick*, 1996].

The factors that control the variability in streamflow response to harvest include harvest amount, vegetation type, and climatic/hydrologic regimes. Stednick's [1996] meta-analysis of 95 paired-catchment studies highlighted major differences in the response of annual streamflow to harvest across 8 climate regions within the United States. At the two extremes, catchments in the Rockies and the Pacific Coast yielded 9 and 50mm more streamflow annually for every 10% increase in harvest area, respectively (below 15 and 25 percent clearcut, respectively, there was no discernable increase in streamflow for either region). Moreover, Stednick's [1996] analysis showed a large variability in the relationship between harvest amount and annual water yield within each of the 8 climate regions. For example, the increase in annual water yield following a 100% clearcut in Rocky mountain watersheds ranged from 0mm to over 350mm. It was also unclear how harvest location within a watershed, as opposed to harvest amount, impacted stream response [*Stednick*, 1996].

Analyses that have focused on ecohydrological controls have provided important insights into the variability of streamflow responses to harvest. *Jones* [2000] and *Jones and Post* [2004] analyzed paired coniferous forest catchments in the Pacific Northwest and northeastern United States and found that the magnitude, seasonality, and duration of streamflow responses to forest harvest and regrowth were consistent with fundamental water balance concepts in hydrology. Specifically, *Jones* [2000] found that peak

discharge in 10 experimental watersheds in the western Cascade range of Oregon increased by as much as 50% for a 100% clearcut, by as much as 30% for a 50% clearcut, and by as much as 20% for a 25% clearcut. *Jones and Post* [2004] examined the seasonality of streamflow to forest clearcut and found that the relative increase in streamflow is highest during warm and dry seasons when evapotranspiration is high, and the absolute increase in streamflow is largest in moist seasons when evapotranspiration is low. Nonetheless, although carefully designed paired-catchment experiments and statistical analyses can provide strong circumstantial evidence for process-level controls, they cannot be used alone to quantify the contribution of specific processes to observed streamflow responses.

Process-based simulation models can address this need by providing a framework for synthesizing data describing catchment responses to climate, harvest and other disturbances. When properly constrained, models allow a self-consistent representation and analysis of process-level interactions within catchments, as well as the ability to isolate the contribution of specific processes to observed responses. Models can also extend a data set by allowing behavior of unmeasured system components to be examined. Similarly, models can be used to isolate the effect of a 'target' treatment factor from the effects of other factors that may be unavoidably altered within a single treatment [*McKane et al.*, 1997]. These properties are apparent in various modeling analyses of experimental data for paired-catchment studies in the Pacific Northwest. For example, *Tague and Band* [2000] used the RHESSys ecohydrological model to isolate the effects of harvest and roads on streamflow. *Waichler et al.,* [2005] applied the DHSVM hydrological model (Dynamic Hydrology Soil Vegetation Model [*Wigmosta et al.*, 1994]) to 3 watersheds in the H.J. Andrews Experimental Forest in order to quantify the effects of forest harvest, without roads, on streamflow, peakflow, and water balance. *Whitaker et al.,* [2002] used the DHSVM hydrological model to evaluate peak flow sensitivity to clearcut at various elevation bands in a snow-dominated catchment in British Columbia. *Sayama and McDonnell* [2009] used the OHDIS-KWMSS [*Tachikawa et al.*, 2004] hydrological model to infer the age and upland source areas of water contributing to streamflow. Thus, models such as these can provide a more detailed and process-based understanding of experimental responses that would be

impossible with the data alone.

However, existing process-based models have some disadvantages. Many models are too simple to simulate process-level controls of interest – e.g., interactions among hydrological and ecological processes. At the other extreme, some models are so complex that they require calibration and forcing data that are often unavailable. Finally, some models are too computationally expensive to simulate large watersheds and landscapes, and require a high level of expertise to implement. Moreover, for a variety of reasons, most current modeling frameworks have been limited to the research community [*Beckers et al.*, 2009]. Therefore, we contend that there is a need for a balanced approach; specifically, an accessible, spatially distributed, ecohydrological model that is both computationally efficient and relatively easy to implement for analyzing the effects of changes in climate, land use, and land cover, on watershed processes at scales relevant to formulating management decisions.

We present a relatively simple ecohydrological model that aims to address both scientific and decision making needs. We apply this model to a small experimental catchment in the Pacific Northwest to investigate the ecohydrological controls on: (1) the effects of clearcut on stream discharge, soil moisture, and evapotranspiration, (2) the relation between harvest amount and catchment hydrological response, (3) the sensitivity of streamflow to harvest location, and (4) threshold behavior in the catchment hydrological response.

A description of the study area and history is provided in section 3.3. An overview of the ecohydrological model VELMA (Visualizing Ecosystems for Land Management Assessment) is provided in section 3.4. Simulation method and model calibration are described in section 3.5. Simulations results are described in section 3.6. Discussion and conclusion are presented in section 3.7 and 3.8, respectively.

3.3. Site Description

Watershed 10 (WS10) of the H.J. Andrews Experimental Forest (HJA) is a small 10.2 hectares catchment located in the western-central Cascade Mountains of Oregon, at latitude 44°15′N, longitude 122°20′W (Figure 3.1). WS10 has been the site of intensive

research and manipulation by the U.S. forest Service since the 1960's, mainly designed to study the effects of logging on hydrology, sediment transport, and nutrient loss [*Dyrness*, 1973; *Fredriksen*, 1975; *Harmon et al.*, 1990; *Harr and McCorison*, 1979; *Jones and Grant*, 1996; *Rothacher*, 1965; *Sollins and McCorison*, 1981; *Sollins et al.*, 1981].

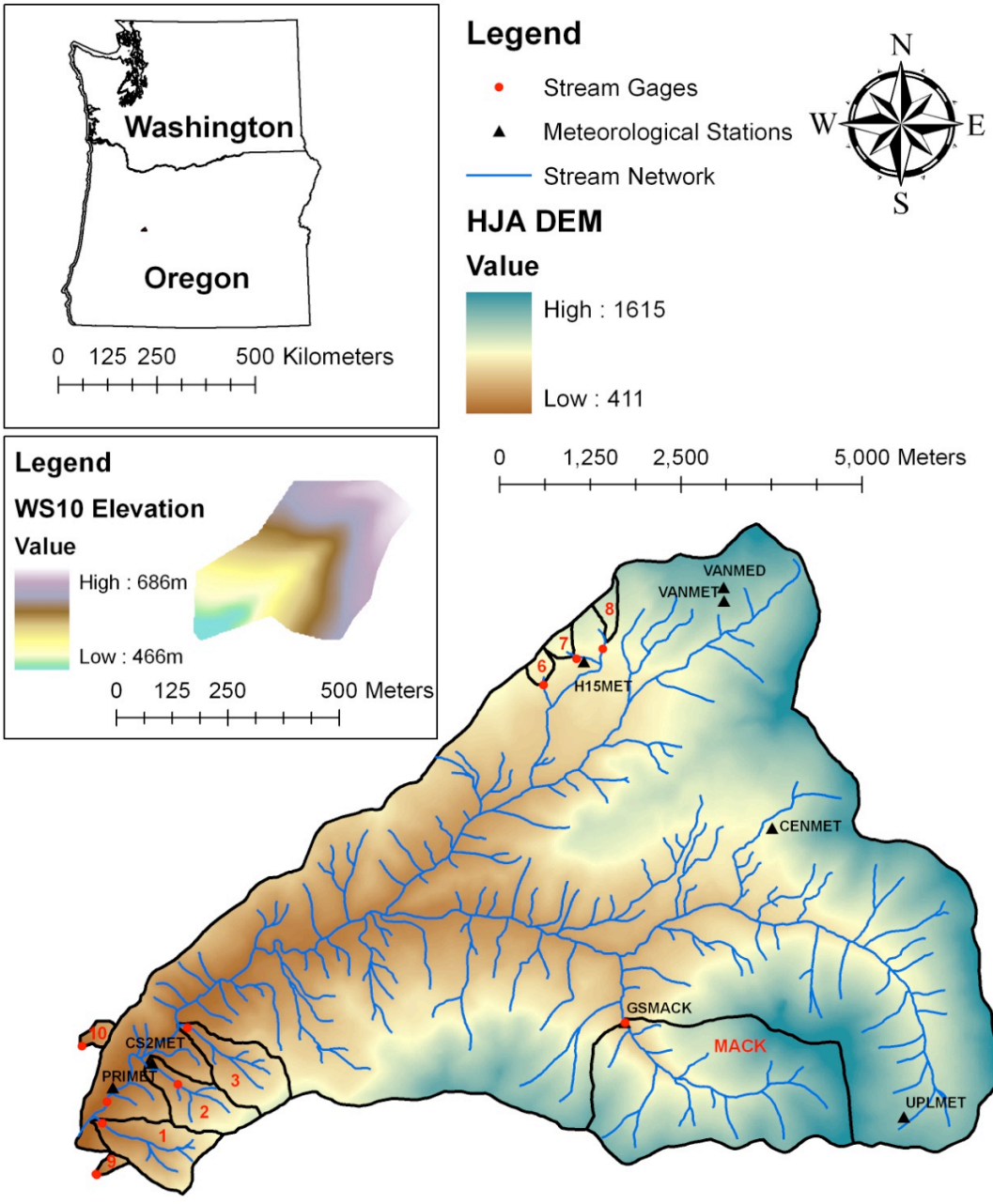

Figure 3.1: *The study site is the watershed 10 (WS10) of the H.J. Andrews Experimental Forest located in the western Cascade Range of Oregon.*

Basin elevation ranges from 430m at the stream gauging station to 700m at the southeastern ridgeline. Near stream and side slope gradients are approximately 24° and 25° to 50°, respectively [*Grier and Logan*, 1977; *Sollins et al.*, 1981]. The climate is relatively mild with wet winters and dry summers [*Grier and Logan*, 1977]. Mean annual temperature is 8.5°C. Daily temperature extremes vary from 39°C in the summer to -20°C in the winter [*Sollins and McCorison*, 1981]. Mean annual precipitation is 2300mm and falls primarily as rain between October and April [*Jones and Grant*, 1996]. Total rainfall during June-September averages 200mm. Snow rarely persists longer than a couple of weeks and usually melts within 1 to 2 days [*Harr and McCorison*, 1979; *Harr et al.*, 1982; *Jones*, 2000]. Average annual streamflow is 1600mm, which is approximately 70% of annual precipitation.

Soils are of the Frissel series, classified as Typic Dystrochrepts with fine loamy to loamy-skeletal texture [*Sollins et al.*, 1981; *Vanderbilt et al.*, 2003] that are generally deep and well drained [*Grier and Logan*, 1977]. These soils quickly transmit subsurface water to the stream. Subsurface flow is a dominant component of the downslope water movement and is characterized by a strong preferential flow along the soil-bedrock interface [*Van Verseveld et al.*, 2008]. Overland flow rarely occurs [*Harr and McCorison*, 1979].

Prior to the 1975 100% clearcut, WS10 was a 400 to 500 year-old forest dominated by Douglas-fir (*Pseudotsuga menziesii*), western hemlock (*Tsuga heterophylla*), and western red cedar (*Thuja plicata*) [*Grier and Logan*, 1977] reaching up to ~ 60m in height. Rooting depths rarely exceed 100 cm [*Santantonio et al.*, 1977]. Species such as the vine maple (*Acer circinatum*), Pacific rhododendron (*Rhododendron maximum*), and chinkapin (*Castanopsis chrysophylla*) regenerated during the spring after logging. Forest regrowth in WS10 was rapid, initially by small trees and shrubs that survived logging, and soon after by planted seedlings of Douglas-fir [*Gholz et al.*, 1985]. The dominant vegetation of WS10 today is a ~ 35 year-old mixed Douglas-fir and western hemlock stand.

3.4. The Eco-Hydrological Model

A spatially distributed ecohydrological model, Visualizing Ecosystems for Land Management Assessment (VELMA) has been developed to simulate changes in soil water infiltration and redistribution, evapotranspiration, surface and subsurface runoff, carbon (C) and nitrogen (N) cycling in plants and soils, and the transport of dissolved forms of carbon and nitrogen from the terrestrial landscape to streams. VELMA is designed to simulate the integrated responses of vegetation, soil, and water resources to multiple forcing variables, e.g., changes in climate, land use and land cover. It is intended to be broadly applicable to a variety of ecosystems (forest, grassland, agricultural, tundra, etc.) and to provide a computationally efficient means for scaling up ecohydrological responses across multiple spatial and temporal scales – hillslopes to basins, and days to centuries.

VELMA uses a distributed soil column framework to simulate the movement of water, heat, and nutrients (NH_4, NO_3, DON, DOC) within the soil, between the soil and the vegetation, and between the soil surface and vegetation to the atmosphere. The soil column model consists of three coupled sub-models: (1) a *hydrological model* that simulates vertical and lateral movement of water within soil, losses of water from soil and vegetation to the atmosphere, and the growth and ablation of the seasonal snowpack, (2) a *soil temperature model* that simulates daily soil layer temperatures from surface air temperature and snow depth and, (3) a *plant-soil model* that simulates C and N dynamics. [Note: for the purposes of this paper, we describe only the hydrologic aspects of the model]. Each soil column consists of *n* soil layers. Soil water balance is solved for each layer (Equations 3.1-3.6, Appendix A). We employ a simple logistic function (Equation 3.9, Appendix A) that is based on the degree of saturation to capture the breakthrough characteristics of soil water drainage (Equation 3.7, Appendix A). Evapotranspiration increases exponentially with increasing soil water storage and asymptotically approaches the potential evapotranspiration rate (*PET*) as water storage reaches saturation [*Davies and Allen*, 1973; *Federe*r, 1979; 1982; *Spittlehouse and Black*, 1981] (Equation 3.12, Appendix A). *PET* is estimated using a simple temperature-based method [*Hamon*, 1963] (Equation 3.13, Appendix A). An evapotranspiration recovery function is used to

account for the effects of changes in stand-level transpiration rates during succession, e.g., after fire or harvest (Equation 3.21, Appendix B). Snowmelt is estimated using the degree-day approach [*Rango and Martinec*, 1995] and accounts for the effects of rain on snow [*Harr*, 1981] (Equation 3.10, Appendix A).

The soil column model is placed within a catchment framework to create a spatially distributed model applicable to watersheds and landscapes. Adjacent soil columns interact with each other through the downslope lateral transport of water (Figures 3.A.1 and 3.A.2, Appendix A). Surface and subsurface lateral flow are routed using a multiple flow direction method [*Freeman*, 1991; *Quinn et al.*, 1991]. As with vertical drainage of soil water, lateral subsurface downslope flow is modeled using a simple logistic function multiplied by a factor that accounts for the local slope angle (Equations 3.16, Appendix A). A detailed description of the processes and equations is provided in Appendix A.

3.5. Simulations Methods

3.5.1 Data

The model is forced with daily temperature and precipitation. Daily observed streamflow data is used to calibrate and validate simulated discharge. For simulations presented here, daily meteorological data for the period January 1, 1969 - December 31, 2008 are obtained from the H.J. Andrews LTER PRIMET, CS2MET, and H15MET meteorological stations located around WS10 [*Daly and McKee*, 2011] (see Figure 3.1). Daily observed streamflow measurements at WS10 are available from 1969 to 2008 [*Johnson and Rothacher*, 2009]. A 30-m resolution Digital Elevation Model (DEM) of the H.J. Andrews's watershed 10 [*Valentine and Lienkaemper*, 2005] is used to compute flow direction, delineate watershed boundaries, and generate a channel network. The soil column is divided into 4 layers: a surface layer, intermediate layers, and a deep layer. The average soil column depth to bedrock is taken to be 2m [*Ranken*, 1974]. The dominant soil texture is specified as loam [*Ranken*, 1974]. Porosity, field capacity and wilting point values are obtained accordingly [*Dingman*, 1994].

3.5.2 Calibration Simulations

Model calibration is needed to accurately capture the pre- and post-harvest hydrological dynamics at WS10. This model calibration consists of two simulations: a pre-harvest old-growth simulation for the period 1969-1974 and a post-harvest simulation for the period 1975-2008.

The pre-clearcut old-growth simulation is conducted for the period 1969 to 1974 in order to calibrate model hydrological parameters such as the surface soil hydraulic conductivity (*Ks*), soil layer thicknesses, ET shape factor, and snowmelt parameters (Table 3.B.1). These model parameters are calibrated to (1) reproduce the observed daily streamflow for the period 1969-1974, (2) capture the observed subsurface dynamics in WS10 (i.e. preferential lateral transport of water at the soil-bedrock interface [*Ranken*, 1974; *Van Verseveld et al.*, 2008], and (3) mimic the rapid runoff response to rainfall [*Kirchner*, 2003; *Ranken*, 1974]). Once this pre-clearcut calibration is complete, model hydrological parameters are considered fixed for the post-harvest calibration simulation described below. A detailed description of the catchment hydrological dynamics associated with the pre-harvest calibration simulation is provided in section 3.6.1.

The post-harvest simulation is conducted for the period 1975 to 2008. This post-harvest simulation is used to calibrate those ET recovery function parameters that control post-harvest forest regrowth and recovery in transpiration. The ET recovery function parameters are calibrated to reproduce the observed daily streamflow for the period 1975-2008 (see Appendix B for details on the calibration process). Once this final model calibration is complete, all model parameters are considered fixed for all scenarios simulations that explore the impact of harvest amount and location on catchment hydrological processes (see section 3.6.3). A detailed description of the catchment hydrological dynamic associated with the post-harvest calibration simulation is presented in section 3.6.2. The values of model parameters are provided in Table 3.B.1.

3.6. Simulations Results

3.6.1 Pre-Harvest Hydrological Dynamics (1969-1974)

Averaged over the period 1969-1974, pre-harvest evapotranspiration amounts to ~ 5% (~ 50mm) of winter (December–February) precipitation, ~ 95% (~ 91mm) of summer precipitation (June–August), and 35% of annual precipitation. Daily simulated streamflow peaks in November-March due to high precipitation and low evapotranspiration. The largest storm for the 1969-1974 period produces a peak flow of 64mm/day. Streamflow rapidly declines in spring-summer as temperatures rise and precipitation diminishes. Summer months are characterized by low flow (~ 0.5mm/day), high temperatures (reaching 40°C), and low precipitation (less than 8% of annual precipitation). Surface runoff resulting from infiltration excess is rare (<1%). Subsurface flow generated from the surface soil layer, the intermediate soil layers, and the deep soil layer account for ~ 37%, 32%, and 31% of the annual streamflow, respectively. Soil water content is highest in the winter and lowest in the summer. At the onset of the summer dry period, the surface *soil water degree of saturation* (SD) declines rapidly from a winter average of 50% to a summer average of 18.5% (Figure 3.2). Surface SD is the lowest (6%) in August and highest (52%) in December. The SD in the intermediate soil layers is less responsive to changes in precipitation and temperature and exhibits an average time lag of 32 days compared to the surface SD. The SD for these intermediate soil layers is lowest (53%) in September and highest (82%) in February. The SD for the deep soil layer is near saturation (94 ± 4%) at all times of the year. For this 1969-1974 calibration simulation, the model captures the overall seasonal dynamics of streamflow (Figure 3.3) with a Nash-Sutcliffe coefficient of 0.807 [*Nash and Sutcliffe*, 1970], a correlation coefficient of 0.907, and an index of agreement of 0.839 [*Willmott*, 1981] (Table 3.1a). The model tends to overpredict low flows and underpredict peak flows.

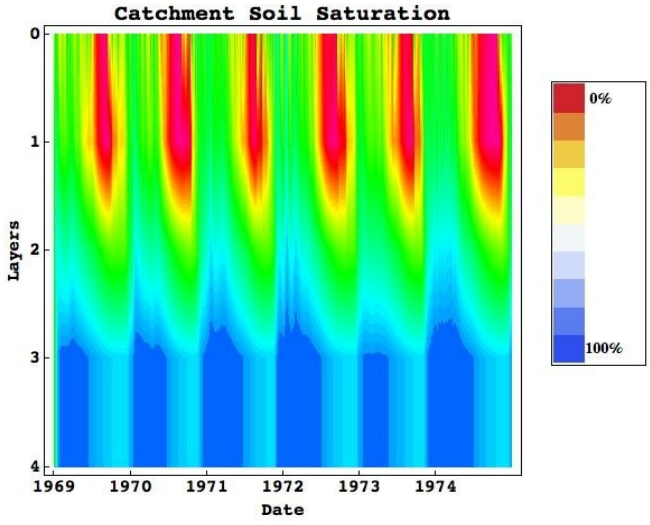

Figure 3.2: *Simulated mean soil water degree of saturation in layer 1, 2, 3 and 4 of the soil column for the pre-clearcut period of January 1, 1969 to December 31, 1974.*

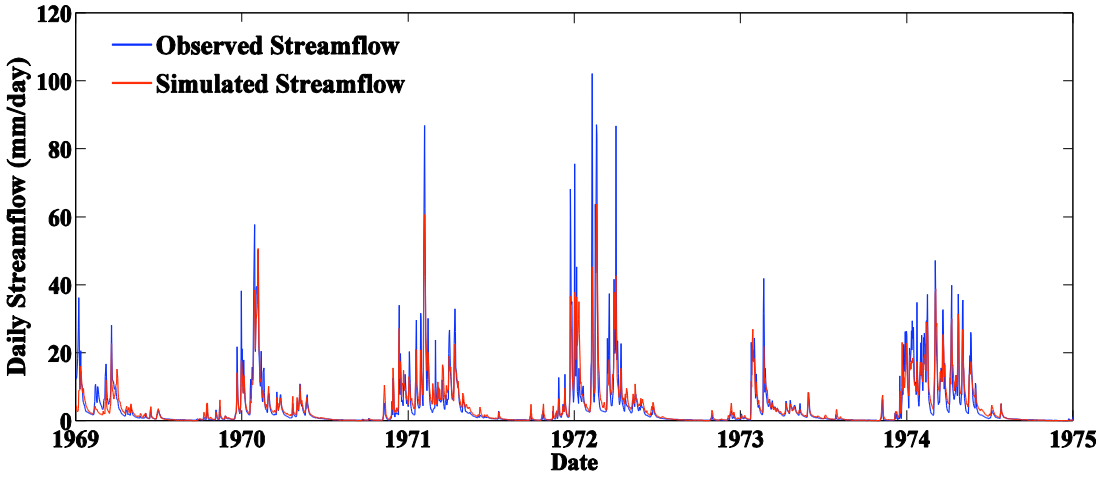

Figure 3.3: *Observed and simulated daily streamflow for the pre-clearcut period of January 1, 1969 to December 31, 1974.*

3.6.2 Post-Harvest Hydrological Dynamics (1975-2008)

To examine post-harvest hydrological dynamics, two simulations are conducted; a control simulation, for the period 1975 to 2008, in which no vegetation is removed, and a post-harvest simulation, also for the period 1975 to 2008, in which vegetation is removed in the spring and summer of 1975. Vegetation removal is simulated by manipulating the ET recovery function to reflect the post-clearcut bulk successional dynamics. The

function controlling changes in transpiration during forest regrowth is described in Appendix B. Briefly, the transpiration rate is set to zero at the onset of the clearcut and increases asymptotically until reaching pre-disturbance values at 50 years. Simulation results are presented at daily, monthly and yearly time scales, in terms of the difference between the post-harvest simulation values and the control simulation values. For the post-harvest period (1975-2008), the model captures the daily dynamics of streamflow in WS10 (Figure 3.4) with a Nash-Sutcliffe coefficient of 0.819, a correlation coefficient of 0.913, and an index of agreement of 0.821. Model performance at the daily, monthly, and yearly time scales in simulating post-harvest streamflow is presented in Table 3.1b.

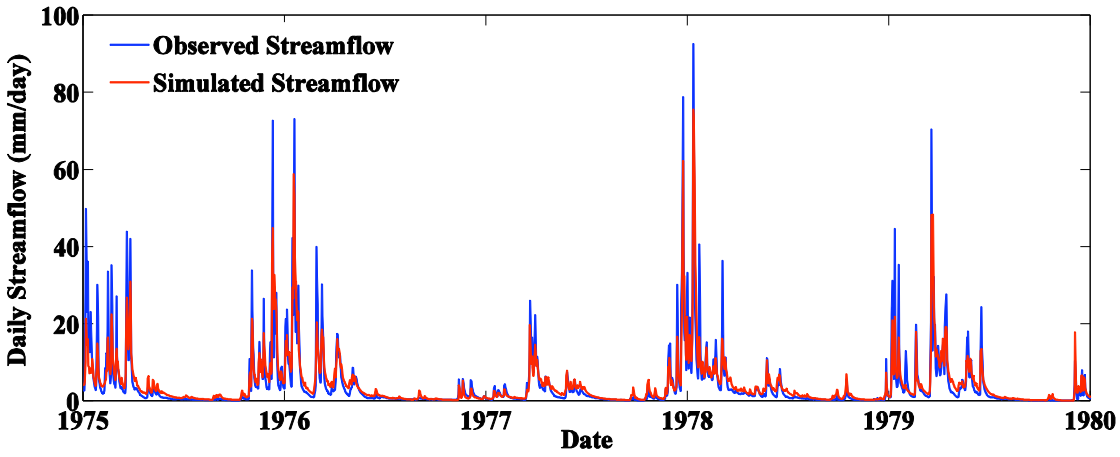

Figure 3.4: *Observed and simulated daily streamflow for the post-clearcut period of January 1, 1975 to December 31, 1979.*

Table 3.1: Daily, monthly and annual streamflow modeling performance for: a) the pre-harvest period (1969-1974), and b) the post-harvest period (1975-2008).

Period	Streamflow Modeling Skills for Daily, Monthly and Yearly Time Period				
	Correlation Coefficient R^2	Nash-Sutcliffe Efficiency E_2	First degree Efficiency E'_1	Baseline adjusted Index of agreement d'_1	Root Mean Square Error RMSE
a- Pre-harvest Period (1969-1974)					
Daily Flow	0.907	0.807	0.694	0.839	3.854
Monthly Flow	0.979	0.955	0.83	0.912	35.04
Annual Flow	0.959	0.771	0.444	0.761	120.854
b- Post-harvest Period (1975-2008)					
Daily Flow	0.913	0.819	0.668	0.821	3.341
Monthly Flow	0.983	0.963	0.831	0.912	27.163
Annual Flow	0.977	0.951	0.786	0.895	87.034

On daily time scales, the 1975-1979 fall and winter daily streamflow are on average 1 to 3 mm higher than control values, whereas spring and summer daily streamflow are on average 0.5 to 1.5mm higher than control values. The maximum daily streamflow surplus of 20mm (relative to control values) occurs in the fall of 1979. The maximum daily summer streamflow surplus is 2mm. These initial (1975-1979) summer daily streamflow surpluses switch to deficits after the year 2000, 25 years after clearcut, due to high transpiration rates (higher than old-growth values) associated with young vigorous forest.

On a seasonal basis, absolute changes in streamflow are consistently largest during the fall and winter wet season. For the period 1975-1979, fall and winter streamflow increase by an average of 142 and 90mm, respectively, whereas summer and spring streamflow increase by an average of 40 and 73mm, respectively (Figure 3.5). By contrast, relative changes in streamflow are largest in the summer averaging 140% for the first five years after harvest and smallest in the winter at approximately 15% (Figure 3.6). Relative increases in fall and spring streamflow are intermediate at 36% and 40%, respectively, for the first five years after harvest (Figure 3.6). By the year 2000, 25 years after harvest, simulated changes in summer and fall streamflow are negative (i.e. lower than control values) as a result of increasing rates of transpiration during forest regrowth (Figure 3.5). As the forest matures, simulated transpiration rates approach pre-harvest levels, such that changes in summer streamflow are similar to control values.

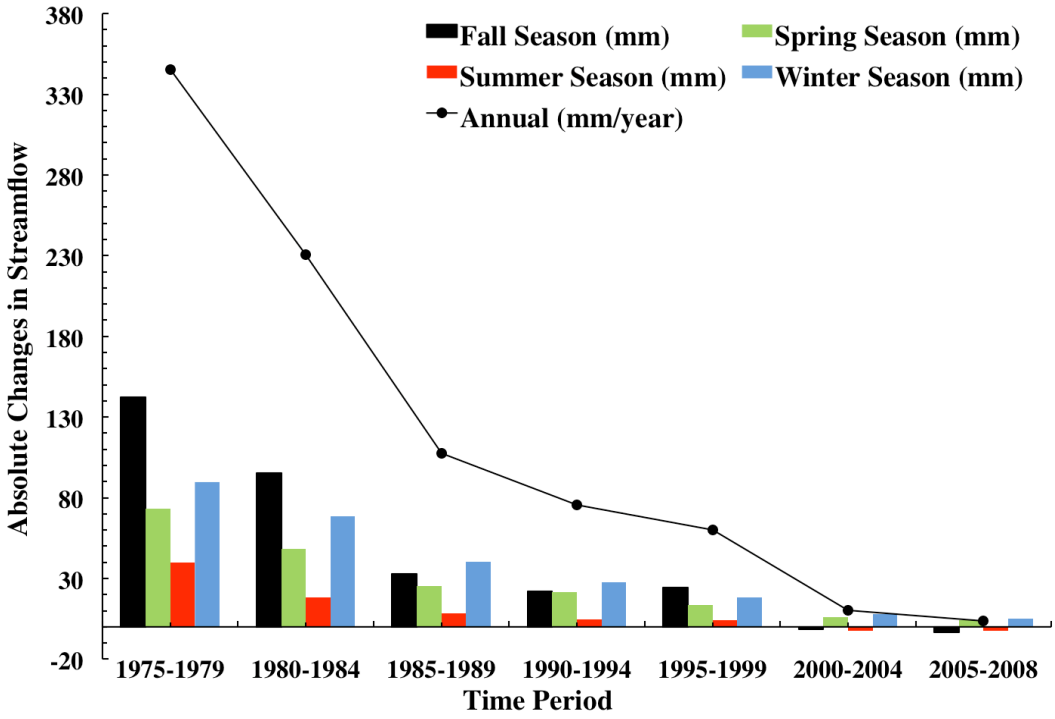

Figure 3.5: *Simulated seasonal and annual absolute changes in streamflow for the post-clearcut period of 1975 to 2008.*

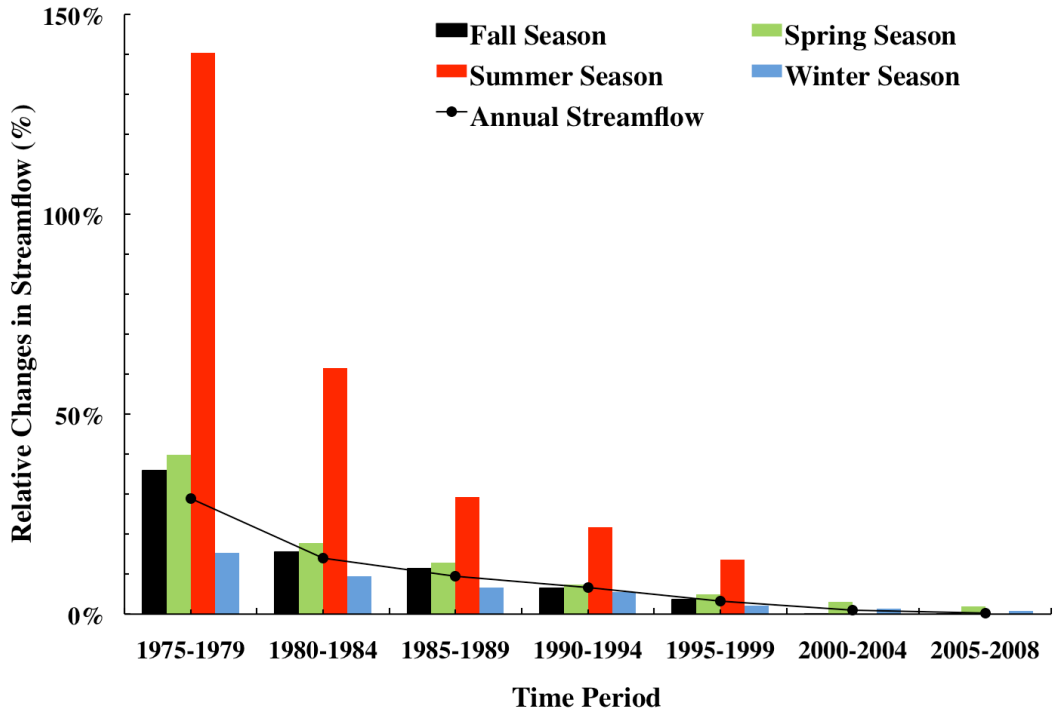

Figure 3.6: *Simulated seasonal and annual relative changes in streamflow for the post-clearcut period of 1975 to 2008.*

For the first five years after disturbance, average seasonal changes in *soil water degree of saturation* (SD) are largest in the summer and fall, with average increases of 18% and 14%, respectively. Winter and spring SD increase by an average of only 5%. Twenty-five years after clearcut, summer and fall SD changes are negative (i.e. less than control values). Negative relative changes in SD develop in June and are most intense (~ -1.5%) in July, August, September and October. By the end of October, negative relative changes in SD are less than 0.6% but last until the end of November.

On an annual scale, simulated annual average evapotranspiration decreases by ~ 43% or 370mm/year for the period 1975-1979. Consequently, average annual streamflow increases by ~ 29% or 345mm/year during the same period. In the first year after disturbance, annual streamflow increases by 326mm. Average increases in annual streamflow peaks two years after clearcut and reaches ~ 500mm as a result of high precipitation and low evapotranspiration demands. Thereafter, changes in annual streamflow decline. Thirty years after disturbance, simulated post-harvest streamflow is approximately equal to simulated control streamflow (Figures 3.5 and 3.6). Simulated deep subsurface flow (i.e. flow at the soil-bedrock interface) is the major contributor to the post-harvest increase in streamflow. Simulated deep subsurface flow increases by an average of 50% after clearcut. By contrast, changes in subsurface flow for surface and intermediate layers are less than 20%. Thirty years after harvest, changes in subsurface flow are within 1% of control values. Simulated annual catchment SD increases by an average of 12% for the period 1975-1980. The largest increase in soil water degree of saturation is in the intermediate layers, with an annual average increase of 15%. By contrast, simulated SD in the soil surface and deep layers increases by 7% and 5%, respectively.

3.6.3 Harvest Scenarios Simulations

Harvest location and amount simulations, described below, are forced with WS10 data for the period 1975-2008.

3.6.3.1 Harvest Location

To assess the impact of harvest location on stream discharge, twenty simulations scenarios are conducted. Each scenario has the harvest amount fixed at 20% of the catchment area. However, harvest location within the watershed varies. The location of each 20% clearcut varies from an all ridge location (Figure 3.7; scenario A) to an all valley location (Figure 3.7; scenario T). Catchment pixels within a 20% clearcut are based on flow accumulation.

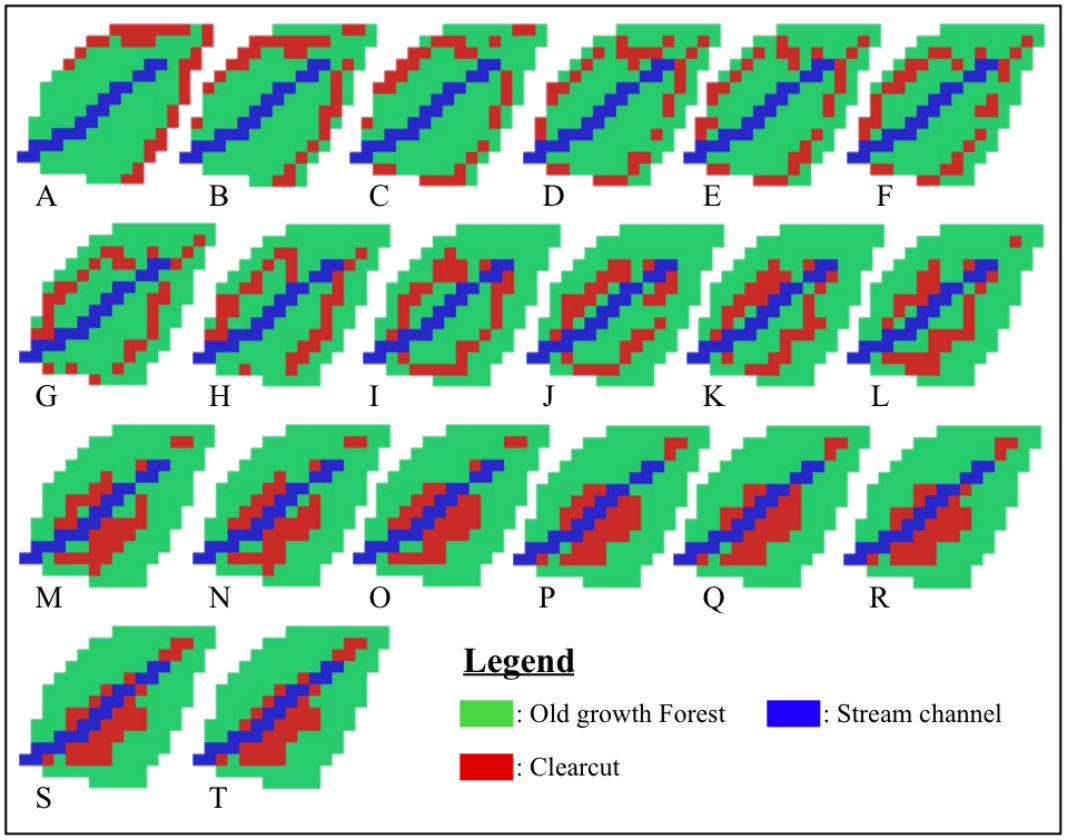

Figure 3.7: *Spatial pattern of forest harvest. Twenty scenarios of 20% clearcut area each were simulated. The location of the 20% clearcut area varied from an all ridge location (scenario A) to an all valley location (Scenario T).*

Simulation results show that forest harvest location is important. A 20% clearcut in the uplands (an average distance of 152m to the nearest stream channel, based on flow direction) results in an average annual streamflow increase of ~ 54mm or 4% over the first five years after clearcut (1975-1979). By contrast, a 20% clearcut in the lowlands (an average distance of 53m from the nearest stream channel, based on flow direction) results in an average annual streamflow increase of ~ 92mm or 8% over the same period. Taken together, these 20 simulations suggest a linear increase in streamflow as the clearcut location shifts from the uplands to the lowlands (Figure 3.8; correlation coefficient R^2=0.97).

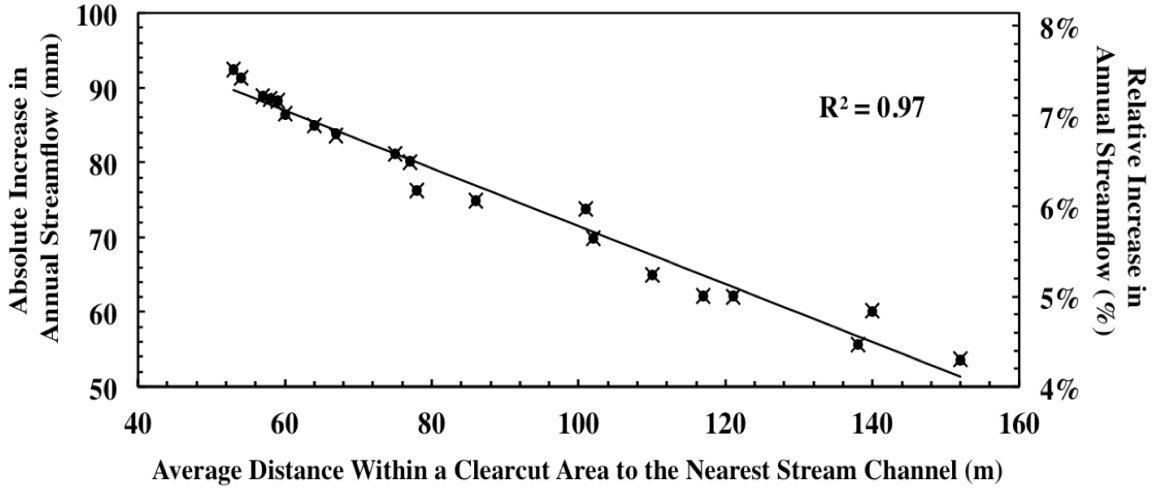

Figure 3.8: *Absolute and relative increase in annual streamflow for a 20% clearcut as a function of the average flow path distance in meters between the harvest area and the nearest stream channel. The solid black line is the fitted linear trendline.*

3.6.3.2 Harvest Amount

To assess the impact of harvest amount on stream discharge, evapotranspiration and soil water degree of saturation, one hundred virtual harvest amount scenarios are simulated. Fifty harvest amount scenarios ranging from 2% to 100%, with an approximate increment of 2% in harvest area, are simulated from ridge to valley (Figure 3.9). Thereafter, fifty harvest amount scenarios ranging from 2% to 100%, with an

approximate increment of 2% in harvest area, are simulated from valley to ridge (Figure 3.9). Catchment pixels for a given clearcut amount are based on flow accumulation.

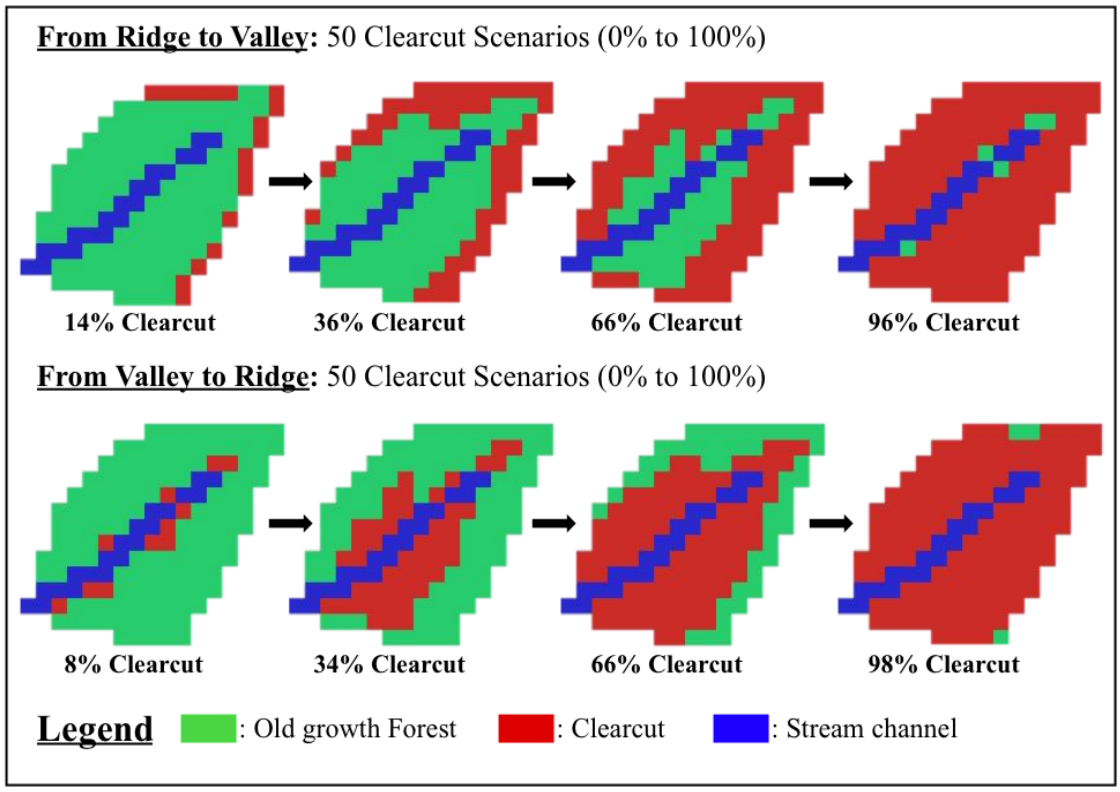

Figure 3.9: *Harvest amount scenarios. Selected examples of fifty clearcut scenarios ranging from 0% to 100% with a ~2% increment in harvest area were simulated (1) from ridge to valley, and (2) from valley to ridge, to assess the impact of increasing harvest area on catchment hydrological response.*

For ridge-to-valley simulations, the relationship between the change in annual streamflow and harvest area is near linear (correlation coefficient R^2=0.97), with a slight convex curvature (Figure 3.10). Specifically, average annual streamflow increases by ~ 2mm for each 1% of catchment area harvested near the ridge, but by ~ 4mm for each 1% of catchment area harvested near the valley. The negative relationship between annual evapotranspiration and harvest area is also near linear (correlation coefficient R^2=0.98), with a slight concave curvature (Figure 3.11). In particular, average annual evapotranspiration decreases by ~ 3mm for each 1% of catchment area harvested near the ridge, but by ~ 4mm for each 1% of catchment area harvested near the valley.

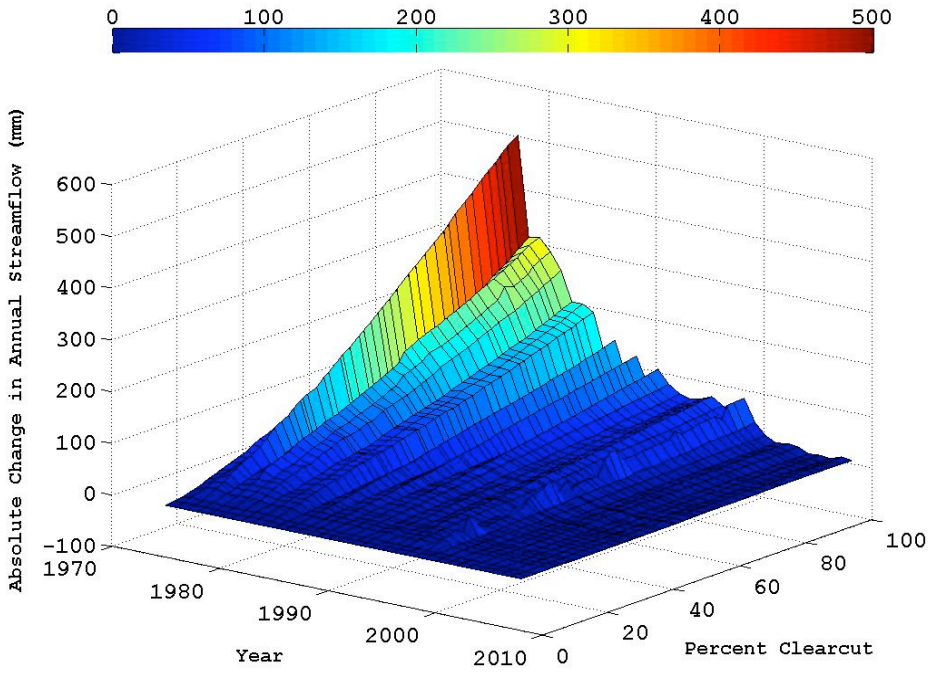

Figure 3.10: *Simulated absolute change in annual streamflow as a function of harvest area. Forest clearcut was simulated from ridge to valley with an increment of 2% in harvest area.*

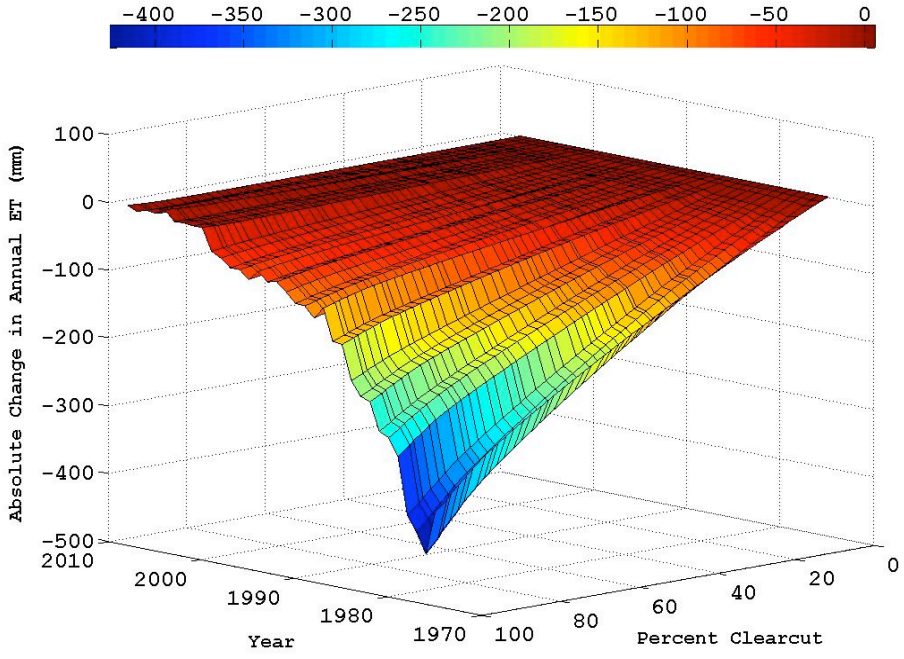

Figure 3.11*: Simulated absolute changes in catchment annual evapotranspiration as a function of harvest area. Forest clearcut was simulated from ridge to valley with an increment of 2% in harvest area.*

For valley-to-ridge simulations, the relationship between the change in annual streamflow and harvest area is near linear (correlation coefficient R^2=0.98), with a slight concave curvature (Figure 3.12). Specifically, average annual streamflow increases by ~ 4mm for each 1% of catchment area harvested near the valley, but by ~ 3mm for each 1% of catchment area harvested near the ridge. The negative relationship between annual evapotranspiration and harvest area is also near linear (correlation coefficient R^2=0.98), with a slight convex curvature (Figure 3.13). In particular, average annual evapotranspiration decreases by ~ 5mm for each 1% of catchment area harvested near the valley, but by ~ 3mm for each 1% of catchment area harvested near the ridge.

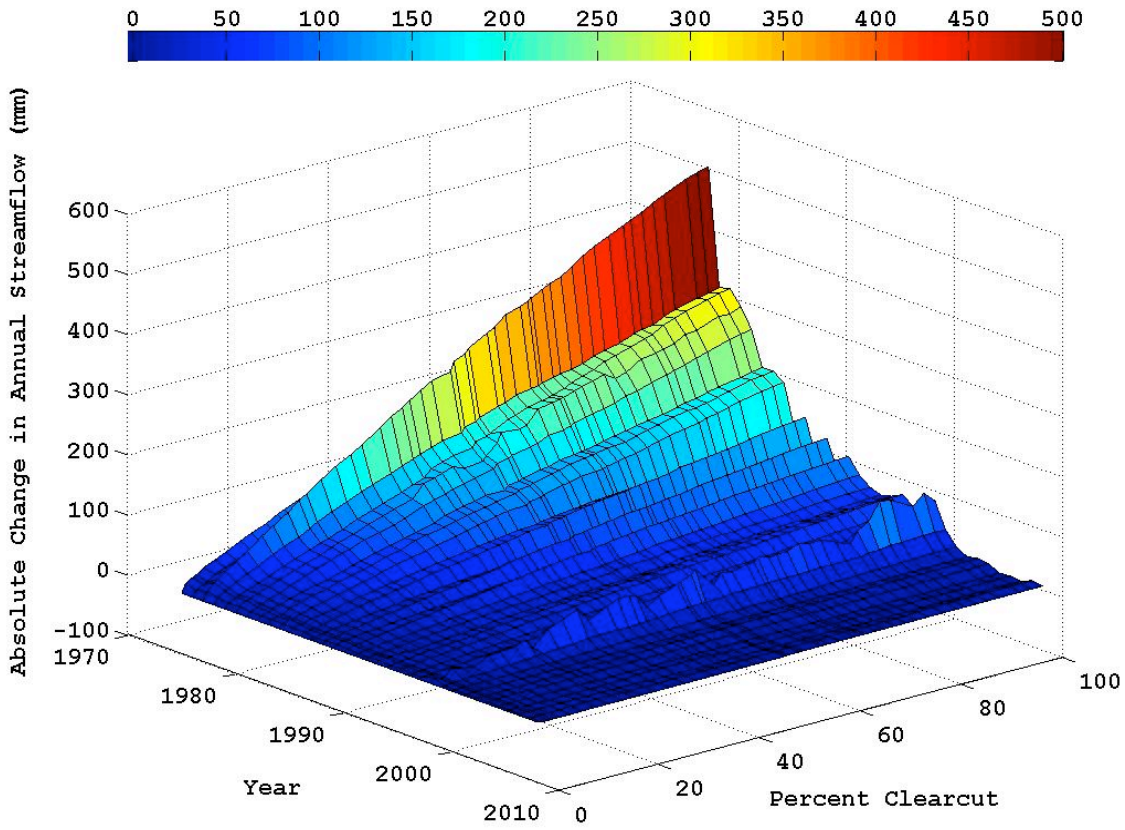

Figure 3.12: *Simulated absolute change in annual streamflow as a function of harvest area. Forest clearcut was simulated from valley to ridge with an increment of 2% in harvest area.*

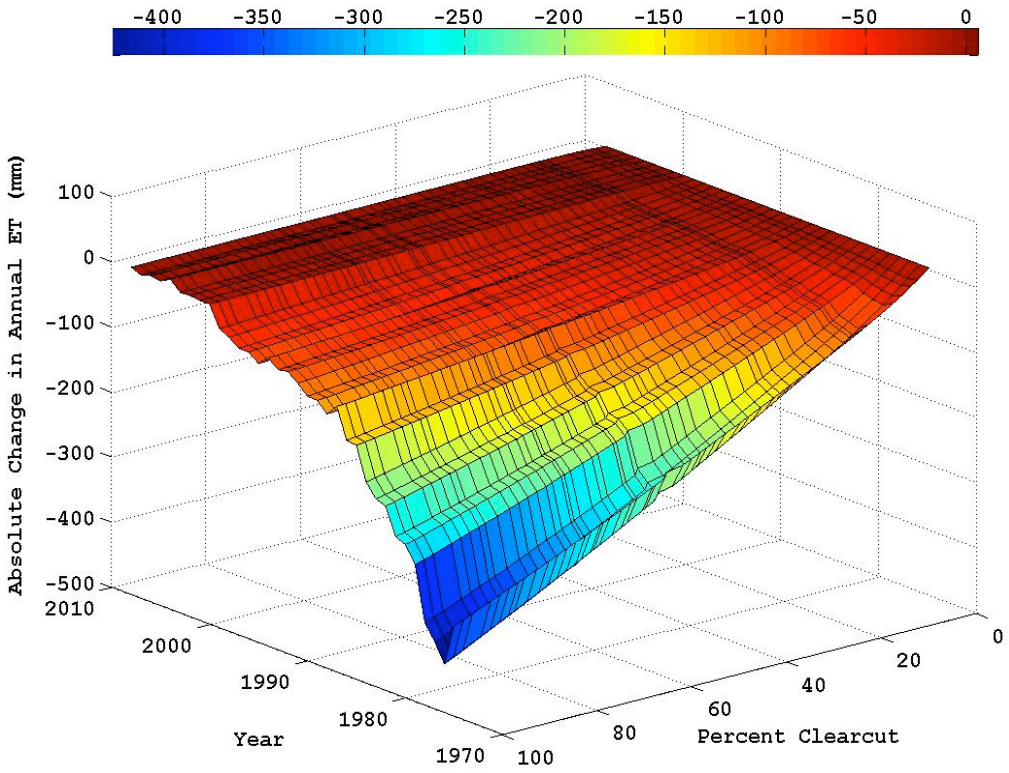

Figure 3.13: *Simulated absolute changes in catchment annual evapotranspiration as a function of harvest area. Forest clearcut was simulated from valley to ridge with an increment of 2% in harvest area.*

While there are some differences between the ridge-to-valley and the valley-to-ridge simulations (Figure 3.14), together they suggest that, irrespective of location (1) annual streamflow increases linearly at a rate of ~ 3.5mm/year for each percentage of catchment harvested, (2) annual evapotranspiration decreases linearly at a rate of ~ 3.6mm/year for each 1% of catchment area harvested, and (3) whole catchment soil water degree of saturation increases linearly at a rate of 1.2% for each 1% of catchment area harvested (not shown). Moreover, there are no apparent hydrologic thresholds that lead to a non-linear streamflow response to increasing harvest amount.

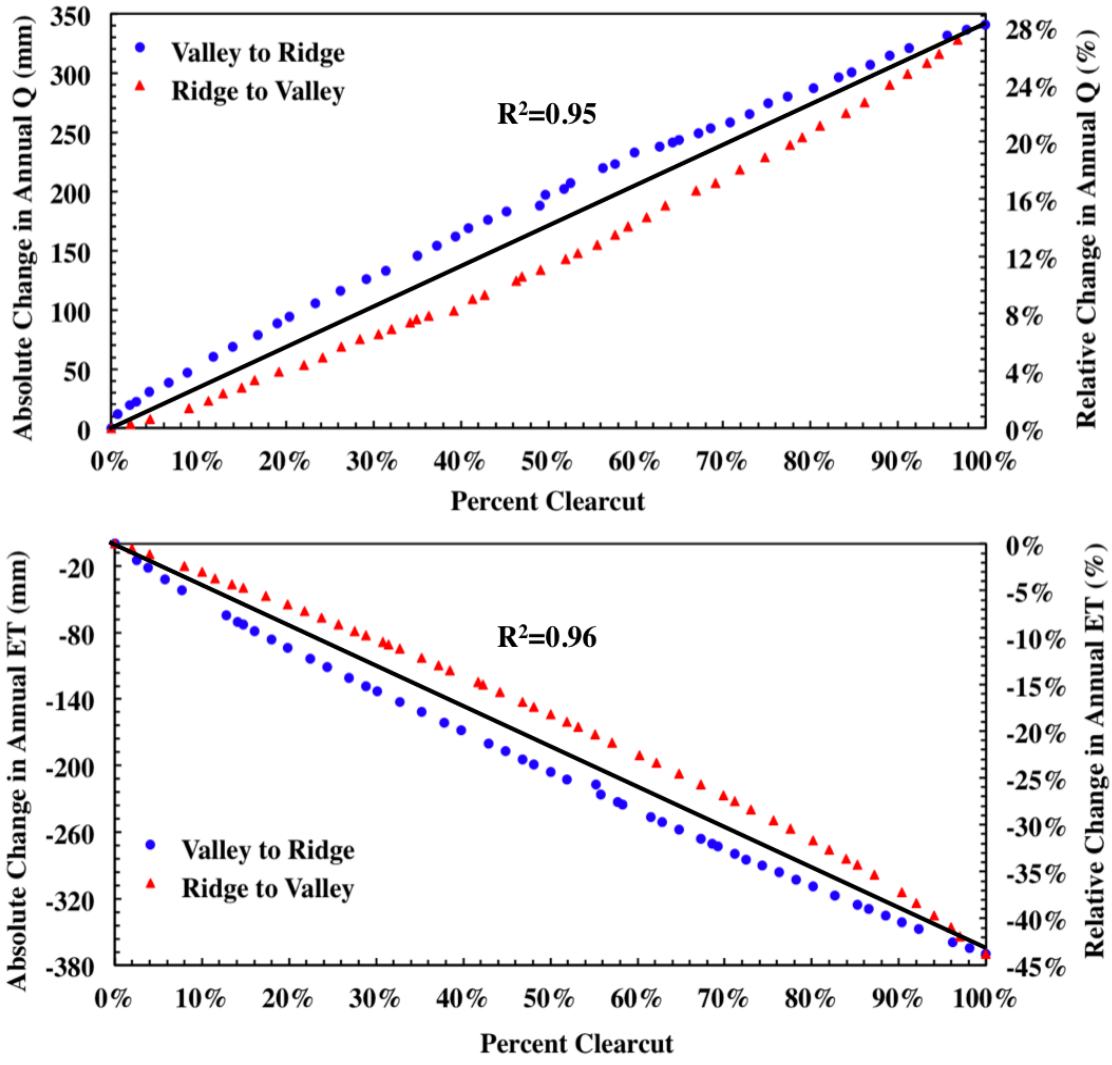

Figure 3.14: *Simulated absolute and relative increase in average annual streamflow (Q), and average annual evapotranspiration (ET) as a function of harvest area, over the first five years after clearcut. The red triangles represent the ridge-to-valley simulations results. The blue dots represent the valley-to-ridge simulations results. The solid black line is the fitted linear trendline.*

Considering all harvest amount scenarios, the absolute changes in streamflow are largest during the fall-winter wet season, whereas the largest relative changes in streamflow are in summer months just after clearcut (Figure 3.11). In the first five years after clearcut, maximum daily increases in streamflow range from 1mm to 20mm for a 2% and 100% harvest scenario, respectively. Changes in soil water degree of saturation are most pronounced in the intermediate layers of the soil column and during the summer

and fall seasons. Thirty years after disturbance, simulated post-harvest streamflow, evapotranspiration, and soil water degree of saturation are approximately equal to simulated control values.

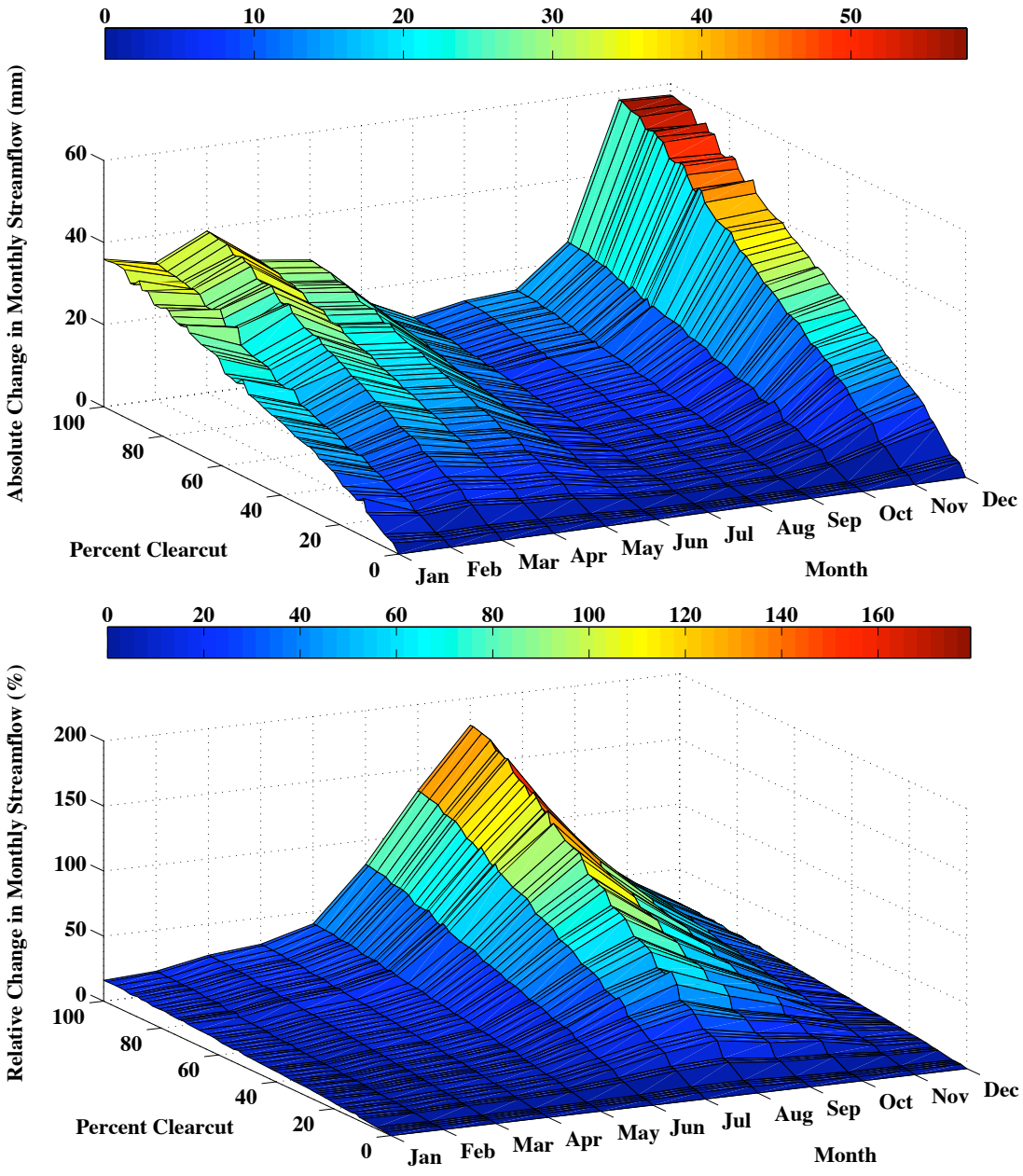

Figure 3.15: *Simulated absolute and relative increase in monthly streamflow as a function of harvest area, in the 1-5 years after clearcut (1975-1979).*

3.7. Discussion

A spatially distributed ecohydrologic model, VELMA, was used to analyze the effects of harvest amount and location on catchment hydrological processes at an intensively studied 10-hectare catchment in the western Oregon Cascades that was clearcut in 1975. Comparison of 40 years of modeled and observed streamflow data show that VELMA captures daily, seasonal, and annual streamflow dynamics for both the pre- (1969-1974) and post-harvest (1975-2008) periods. Multiple simulation scenarios are conducted to explore the effects of harvest amount and location on catchment hydrological response. Results show that (1) for the case of a 100% clearcut, stream discharge initially increases by ~ 29% or 345mm but returns to pre-clearcut levels within 50 years (Figures 3.5 and 3.6), 2) fall increases in streamflow are large in absolute terms, whereas summer increases are large in relative terms (Figure 3.15), (3) annual streamflow increases linearly at a rate of 3.5mm/year for each percent of catchment harvested, irrespective of location (Figure 3.14), (4) the increase in annual streamflow is small (less than 40mm/year) for harvest amounts of less than 10% (Figure 3.14), and (5) streamflow response is strongly sensitive to harvest distance from the stream channel (Figure 3.8).

For our WS10 simulations, results suggest that streamflow increases linearly with harvest amount, irrespective of location, and is insignificant for a harvest area of less than 10% (Figure 3.14). *Stednick* [1996], who reviewed 95 paired-catchment studies across the United States, also found that annual streamflow increased linearly with increasing harvest area, and that changes in annual streamflow in the Pacific Northwest catchments were undetectable for harvest areas of less than 20% (Figure 3.16). *Bosh and Hewlett* [1982] reviewed 94 paired-catchment studies in Asia, Australia, Africa and North America, and found that annual water yield increased by ~ 40mm for every 10% reduction in coniferous forest cover. Likewise, *Sahin and Hall* [1996] analyzed the results of 145 experimental studies in Asia, Australia, Africa, Europe and North America, and found that annual streamflow increased linearly at a rate of 20 to 25mm/year for each 10% reduction in coniferous forest cover. *Grant et al.* [2008] analyzed the results of several experimental and modeling studies across the Pacific Northwest and found that the change in peak flow increased linearly with increasing harvest area and was

undetectable (i.e. relative change in peakflow is less than 10%) for harvested areas of less than 29% in rain dominated catchments and 15% for catchments in the transient snow zone.

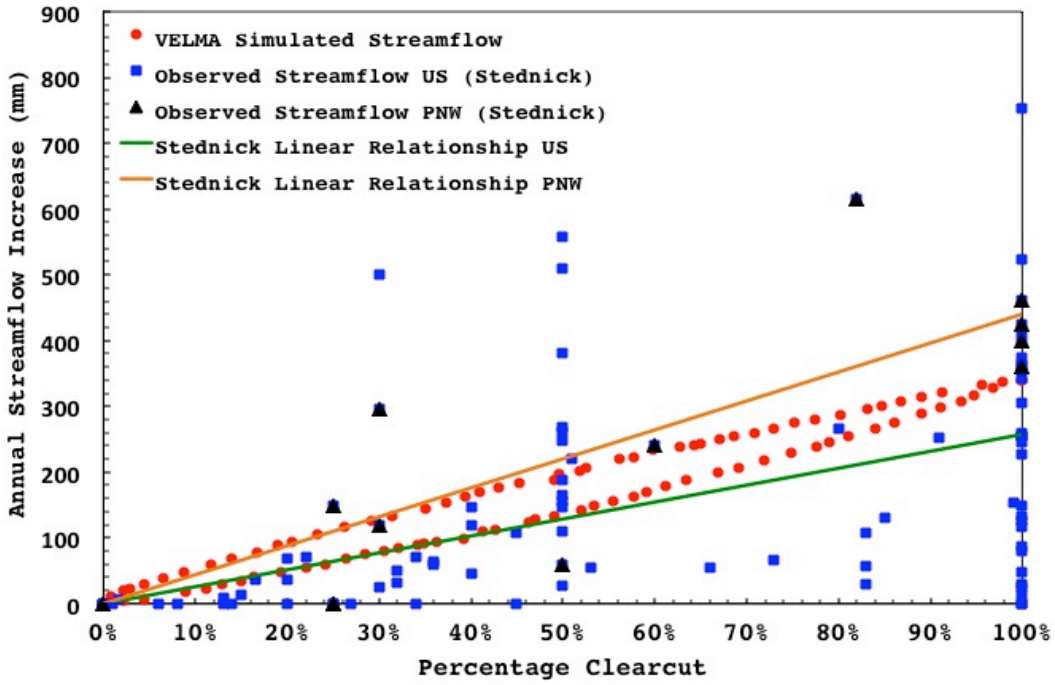

Figure 3.16*: Comparison of the simulated increase in annual streamflow in WS10 (red dots) with observed increase in annual streamflow for 95 catchments in the US [Stednick, 1996] (Green line), and for the Pacific Northwest (Stednick data) (Orange line) as a function of the percent of catchment harvested.*

For our WS10 simulations, the largest absolute increase in streamflow is in fall and winter, while the largest relative increase in streamflow is associated with summer months. Similar results have been found by *Harr et al.,* [1979], who examined the seasonal changes in streamflow following a 100% clearcut of two Coyote Creek experimental watersheds in Southwest Oregon. *Harr et al*., [1979] found that the largest absolute increase in streamflow (~ 120mm) was in winter, whereas the largest relative increase (~ 44%) was in the low flow summer months. Likewise, *Jones and Post* [2004] examined the seasonality of streamflow to forest clearcut in 14 experimental paired watersheds located in the northwest conifer and eastern deciduous forests. They found

that the absolute increase in streamflow was largest in moist seasons, whereas the relative increase in streamflow was highest in the warm seasons.

Our simulation results suggest that post-clearcut annual streamflow increases with decreasing harvest distance to the channel (Figure 3.8). This streamflow sensitivity to harvest location stems from the fact that subsurface flow generated from an upland clearcut area, as opposed to a lowland clearcut area, has a relatively longer flowpath. This longer flowpath subjects subsurface flow to downslope plant water uptake, which reduces the amount of water that reaches the stream channel. These results are consistent with previous findings on the importance of riparian forest buffers and lowland vegetation in reducing subsurface flow to streams [*Jordan et al.*, 1993; *Lowrance et al.*, 1997].

Forest harvest effects on streamflow in WS10 were simulated in a simplified way, with the ultimate goal of developing a framework that can be efficiently scaled up for larger watersheds of interest to land managers and policy makers. For example, one of our objectives is to provide a foundation for extrapolation to managed landscapes that are not as data rich as LTER sites (e.g., ungauged basins with little soil and vegetation data). However, our simplifying assumptions need to be examined. Below we discuss a number of harvest effects and watershed characteristics relevant to hydrological processes not explicitly addressed in this study.

(1) *Roads*: The impact of forest roads on hydrological processes have been well documented for the H.J. Andrews Experimental Forest [*Jones and Grant*, 1996; *Luce and Wemple*, 2001; *Swanson and Dyrness*, 1975; *Wemple and Jones*, 2003; *Wemple et al.*, 2001]. Roads have been shown to (1) intercept and route surface and shallow subsurface water to stream channels [*Luce and Wemple*, 2001], (2) increase the magnitude and frequency of peak flows [*Jones and Grant*, 1996], and (3) increase sediment transport to the stream [*Beschta*, 1978; *Swanston and Swanson*, 1976].

(2) *Harvest methods:* Forest harvest in many Pacific Northwest sites is conducted with skidders, tractors, or cable yarding [*Moore and Wondzell,* 2005]. WS10 was logged using a skyline cable system [*Hood et al.*, 2006], and trees were felled and dragged uphill to a single landing [*Sollins and McCorison*, 1981]. As a result, soils on about 50% of the

watershed were subjected to moderate or severe disturbance or compaction [*Harr and McCorison*, 1979]. Such soil compaction reduces soil infiltration capacity [*Startsev and McNabb*, 2000], saturated hydraulic conductivity [*Purser and Cundy*, 1992], pore size distribution, and pore space [*Huang et al.*, 1996], which in turn, impact watershed hydrological processes.

(3) *Forest succession*: Biomass recovery is complex, involving changes in species composition, growth rates and canopy structure. During post-clearcut succession, species composition often changes from colonizing shrubs to hardwood trees before returning to conifer dominance [*Yang et al.*, 2005]. To accurately model these successional dynamics would require the inclusion of multiple species, species interaction, overstory and understory dynamics, the seasonality of leaf area, and canopy interception, among others [*Bond-Lamberty et al.*, 2005]. However, including these dynamics would increase model complexity, decrease computational efficiency, and limit model application to sites rich in data. Instead our simulations use a Chapman-Richards growth function [*Hunt*, 1982; *Ratkowsky*, 1990; *Richards*, 1959] that relates canopy transpiration to forest age, as a simple proxy for plant/biomass recovery (Equation 3.21; Appendix B).

(4) *Soil spatial heterogeneity:* Soil texture and depth vary spatially within WS10 [*McGuire et al.*, 2007; *Ranken*, 1974; *Sayama and McDonnell*, 2009]. However, deriving high-resolution and catchment wide soil texture and depth maps from, typically, a small number of point measurements, is at best, uncertain. Instead, we assume uniform loam soil texture and uniform depth to bedrock of 2m to reflect, more or less, average conditions in the catchment [*Ranken*, 1974]. While a sensitivity analysis on the impact of the spatial distribution of soil texture and soil depth on streamflow dynamics would certainly provide insights into catchment dynamics, it is beyond the scope of this paper.

Finally, it is important to ask whether or not an explicit treatment of the preceding issues would improve model performance and the understanding of process-level controls on streamflow and other ecohydrological processes. However, an explicit treatment of these issues comes at the cost of computational efficiency, model complexity, and applicability to larger spatial and temporal scales. This is an important tradeoff to consider, given that data needed to apply complex models is not generally available at

scales relevant to formulating management decisions. The current version of VELMA is an initial attempt at a parsimonious solution to this dilemma.

3.8. Conclusion

Despite the limitations discussed above, the model presented here provides a relatively simple, spatially distributed framework for assessing the effects of changes in climate, land use and land cover on ecohydrological processes within watersheds. The WS10 simulations suggest that the model can predict, with reasonable accuracy, the effects of forest harvest on daily, seasonal, and annual changes in streamflow. The simulations describing the effects of harvest amount and spatial pattern provide process-level insights into important hydrological responses to harvest – details that would be difficult or impossible to capture through experimentation or observation alone. Moreover, the model provides an integrated ecohydrological framework for evaluating how alternative climate and forest management scenarios may interact to affect the functioning and health of forest and stream ecosystems. Finally, the simplicity of the model makes it potentially useful for applications across a range of spatial and temporal scales relevant to land managers and policy makers.

3.9. Appendix:

Appendix A describes the hydrology model, which includes the equations typically applied across watersheds and ecosystems. Appendix B describes the evapotranspiration recovery function used to mimic post-harvest transpiration dynamics.

3.9.1 Appendix A: Hydrological Model Description

VELMA is a spatially distributed ecohydrology model that accounts for hydrologic and biogeochemical processes within watersheds. The model simulates daily to century-scale changes in soil water storage, surface and subsurface runoff, vertical drainage, carbon (C) and nitrogen (N) cycling in plants and soils, as well as transport of nutrients from the terrestrial landscape to the streams. VELMA consists of multi-layered soil column models that communicate with each other through the downslope lateral transport of water (Figure 3.A.1). Each soil column model consists of three coupled sub-models: a

hydrological model, a soil temperature model, and a plant-soil model. What we describe below is the hydrology component of the model. First, we describe the soil column model and then place this soil column within a catchment framework.

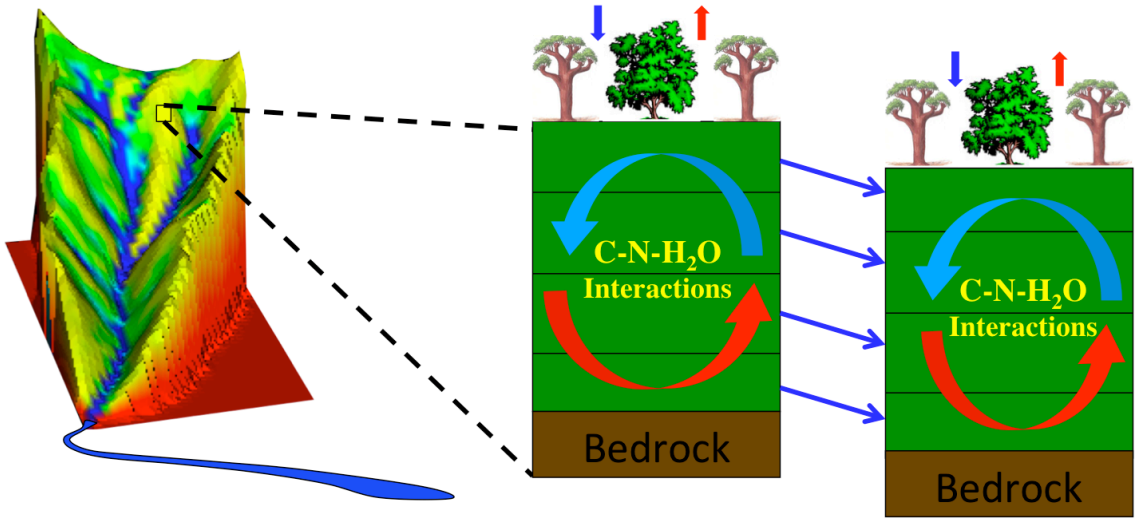

Figure 3.A.1: *Conceptual catchment modeling framework using multi-layered soil columns.*

3.9.1.1 Soil Column Framework

We employ a multi-layer soil column as the fundamental hydrologic unit. The soil column consists of n soil layers, a standing water layer, and a snow layer (Figure 3.A.2). Soil water balance is solved for each model layer (Equation 3.1-3.6). Soil water storage in layer i (s_i), surface standing water (s_{STW}), and snow water equivalent (s_{SWE}), are tracked and updated at each time step.

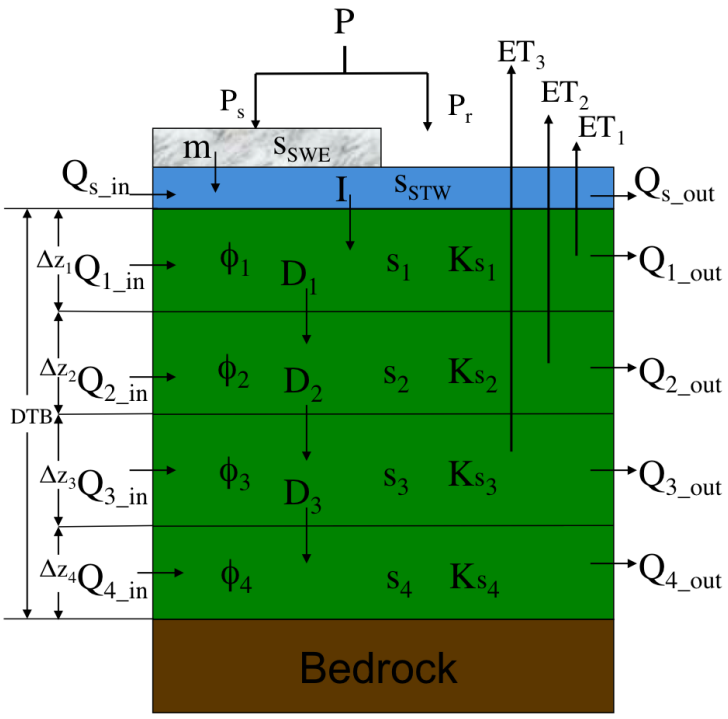

Figure 3.A.2: *The soil column framework consists of 4-layer soil column, a standing water layer, and a snow layer. DTB is the soil column depth to bedrock. z_i, Ks_i, ϕ_i, and s_i, are the thickness, the saturated hydraulic conductivity, the soil porosity, and the soil water storage of layer i, respectively.*

For a 4-layer soil model, such as the one used in this work:

$$\frac{ds_{SWE}}{dt} = P_s - m \tag{3.1}$$

$$\frac{ds_{STW}}{dt} = P_r - I + m - Q_{s\_out} + Q_{s\_in} \tag{3.2}$$

$$\frac{ds_1}{dt} = I - D_1 - ET_1 - Q_{1\_out} + Q_{1\_in} \tag{3.3}$$

$$\frac{ds_2}{dt} = D_1 - D_2 - ET_2 - Q_{2\_out} + Q_{2\_in} \tag{3.4}$$

$$\frac{ds_3}{dt} = D_2 - D_3 - ET_3 - Q_{3\_out} + Q_{3\_in} \tag{3.5}$$

$$\frac{ds_4}{dt} = D_3 - Q_{4\_out} + Q_{4\_in} \tag{3.6}$$

where P_r (*mm/day*) and P_s (*mm/day*) are rain and snow, respectively, ET_i (*mm/day*) is the water extracted from soil layer *i* due to evapotranspiration, s_i (*mm*) is the soil water storage in layer *i*; s_{SWE} (*mm*) is the snow water equivalent due to the accumulation of snow, s_{STW} (*mm*) is the standing water amount, *m* (*mm/day*) is the snowmelt that enters the standing water layer, *I* (*mm/day*) is the soil infiltration rate, D_i (*mm/day*) is the vertical drainage from layer *i* to layer *i+1* within a given soil column, Q_{i_in} (*mm/day*) and Q_{i_out} (*mm/day*) are the lateral subsurface flow into and out of layer *i*; Q_{s_in} (*mm/day*) is the surface water flow from the s_{STW} pool of an upslope soil column and Q_{s_out} (*mm/day*) is the surface water flow to the s_{STW} pool of a downslope soil column or into the stream.

3.9.1.1.1 *Vertical Water Drainage:*

The vertical water drainage (D_i) is modeled using a logistic function that is intended to capture the breakthrough characteristics of soil water movement. Specifically, we employ a logistic function $f\left(s_i / s_i^{\max}\right)$ that permits for fast "switching" from low to high flow as layer moisture approaches field capacity:

$$D_i = Ks_i^{vertical} \times f\left(s_i / s_i^{\max}\right) \qquad i = 1,2,\ldots n \tag{3.7}$$

where $Ks_i^{vertical}$ is the vertical saturated hydraulic conductivity in layer *i*, $\left(s_i / s_i^{\max}\right)$ is the soil degree of saturation in layer *i*, $s_i^{\max}$ (mm) is the maximum soil water storage in layer *i*, and $f\left(s_i / s_i^{\max}\right)$ is the logistic function for layer *i*. The vertical saturated hydraulic conductivity follows TOPMODEL formulations [*Beven and Kirkby*, 1979] and decreases exponentially with depth such that:

$$Ks_i^{vertical} = Ks \times e^{-f_v \times d_i} \qquad i = 1,2,\ldots n \tag{3.8}$$

where *Ks* is the soil surface saturated hydraulic conductivity [*Clapp and Hornberger*, 1978; *Dingman*, 1994], f_v is the vertical decay rate of *Ks* with depth, and d_i is the soil depth to the center of layer *i*.

The logistic function is modeled as:

$$f\left(s_i/s_i^{\max}\right)=\frac{1+\exp\left(-\left(s_i/s_i^{\max}\right)\right)}{1+a_{1,i}\exp\left(-a_{2,i}\left(s_i/s_i^{\max}\right)\right)}-\frac{2}{\left(1+a_{1,i}\right)} \qquad i=1,2,\ldots n$$

$$with\begin{cases}a_{1,i}=\exp\left(6+270.562\times\left(Ks_i^{vertical}\right)^{-0.574}\right)\\ a_{2,i}=6+144.749\times\left(Ks_i^{vertical}\right)^{-0.444}\end{cases} \tag{3.9}$$

3.9.1.1.2 *Precipitation, rain, snow and snowmelt:*

Below a threshold temperature (T_{th}), precipitation (P) falls as snow (P_s), otherwise as rain (P_r). Snow accumulates until air temperature (T_a) warms and reaches melting temperature (T_m). Snowmelt rate (m) follows a degree day approach [*Rango and Martinec*, 1995]), and includes for the heat provided by rain on snow [*Harr*, 1981]. Snowmelt (m) enters the s_{STW} pool and from there infiltrates into the top soil layer (or continues as lateral surface flow and enters a downslope s_{STW} pool, section 2.2).

$$P=\begin{cases}P_r & T_a>T_{th}\\ P_s & T_a\le T_{th}\end{cases}$$
$$m=\begin{cases}\alpha\left(T_a-T_m\right)+\sigma\times P_r\times T_a & T_a>T_m\\ 0 & T_a\le T_m\end{cases} \tag{3.10}$$

where α (mm °C^{-1} day^{-1}) is the degree-day factor for melt and σ is the rain on snow factor.

3.9.1.1.3 *Surface Soil Infiltration:*

Based on the large uncertainties associated in ascribing soil texture, soil structure, and soil properties, we simply assume that water stored in the s_{STW} pool is allowed to infiltrate (I) the top soil layer such that:

$$I=\left(P_r+m+Q_{s\_in}-Q_{s\_out}\right) \qquad for \quad \left(P_r+m+Q_{s\_in}-Q_{s\_out}\right)<Ks_{i=1}^{vertical}$$
$$I=Ks_{i=1}^{vertical} \qquad for \quad \left(P_r+m+Q_{s\_in}-Q_{s\_out}\right)\ge Ks_{i=1}^{vertical} \tag{3.11}$$

3.9.1.1.4 *Evapotranspiration:*

Evapotranspiration increases exponentially with increasing soil water storage and asymptotically approaches the potential evapotranspiration (*PET*) rate as water storage reaches saturation [*Davies and Allen*, 1973; *Federer*, 1979; 1982; *Spittlehouse and Black*, 1981].

$$ET_i = W_{E,i} \times PET \times \left(1 - \exp\left(-c_{ET} \times \left(s_i / s_i^{\max}\right)\right)\right) \qquad i = 1,2,...n \tag{3.12}$$

where $W_{E,i}$ is the soil water extraction fraction in layer *i*, and c_{ET} is an *ET* shape factor to ensure that *ET* approaches *PET* near field capacity.

PET is estimated using a simple temperature-based method [*Hamon*, 1963]:

$$PET = K_{PET} \times 0.0138 \times L \times \rho_{vsat}(T_a)$$
$$with \quad \begin{cases} \rho_{vsat}(T_a) = 0.622 \times \rho_a \times \left(\dfrac{e_{sat}(T_a)}{p_{SL}}\right) \\ e_{sat}(T_a) = 6.11 \times \exp\left(\dfrac{17.3 \times T_a}{T_a + 273.3}\right) \end{cases} \tag{3.13}$$

where $\rho_{vsat}(T_a)$ is the saturation absolute humidity (g/m^3) at the mean daily air temperature T_a (°C), ρ_a is the air density (1300 g/m^3), $e_{sat}(T_a)$ is the saturation vapor pressure (kPa) at T_a, p_{SL} is the mean pressure at sea level (101.3 kPa), K_{PET} is a calibration constant, and *L* is the local day length expressed in hours [*Dingman*, 1994].

The distribution of plant water extraction through the soil profile has a significant impact on the ability of vegetation to access water during the growing season [*Bond et al.*, 2008]. Roots, soil macropores and soil saturated hydraulic conductivity all tend to fall off exponentially with depth [*Beven and Kirkby*, 1979; *Gale and Grigal*, 1987; *Jackson et al.*, 1996; *Sidle et al.*, 2001; *Wigmosta and Perkins*, 2001], which suggests that the ability to extract water from the soil column decreases with soil depth. A number of studies have found that the majority of water uptake is in the shallow soils where water

and nutrients are abundant [*Jackson et al.*, 1996; *Warren et al.*, 2005]. However, these studies also suggest that water uptake shifts from shallow to deep layers as near surface soils dry out [*Brooks et al.*, 2006; *Hacke et al.*, 2000; *Warren et al.*, 2005]. To mimic these dynamics, soil water uptake is modeled as follows:

$$for\left(\frac{s_{i=(d_r-1)}}{s^{\max}_{i=(d_r-1)}}\right)\geq\left(\frac{\theta^{w}_{i=(d_r-1)}}{\phi_{i=(d_r-1)}}\right)\quad\begin{cases}W_{E,i}=\dfrac{s_i}{\sum_{j=1}^{d_r-1}s_j} & i=1,2,\ldots(d_r-1)\\ W_{E,i}=0 & i=d_r,\ldots..n\end{cases}\tag{3.14}$$

$$for\left(\frac{s_{i=(d_r-1)}}{s^{\max}_{i=(d_r-1)}}\right)<\left(\frac{\theta^{w}_{i=(d_r-1)}}{\phi_{i=(d_r-1)}}\right)\quad\begin{cases}W_{E,i}=\dfrac{\left(1-W_{E,deep}\right)\times s_i}{\sum_{j=1}^{d_r-1}s_j} & i=1,2,\ldots(d_r-1)\\ W_{E,i}=W_{E,deep} & i=d_r\\ W_{E,i}=0 & i=(d_r+1),\ldots..n\end{cases}\tag{3.15}$$

where θ^{w}_{i}, and ϕ_i are the soil wilting point and the soil porosity in layer *i*, respectively, Layer d_r is the deepest layer in which water extraction is possible, $\left(s_{i=(d_r-1)}/s^{\max}_{i=(d_r-1)}\right)$ is the degree of saturation of layer (d_r - 1), and $W_{E,deep}$ is the fraction of water uptake from layer d_r during droughts (a calibrated value). The depth of layer d_r is determined either experimentally (typically taken from rooting depth information) or through calibration. Based on Equation 14, water uptake is limited to shallow layers as long as water storage in these layers is above wilting point. When the water storage in the shallow layers is below wilting point, Equation 15 permits for deep soil water extraction.

3.9.1.2 Watershed Framework:

To place the above described soil column framework within a catchment framework, the catchment topography is gridded into a number of pixels (dependent upon the available DEM, e.g., 30 m), with each pixel consisting of one soil column model (Figure A.1). Soil columns communicate with each other through the downslope lateral

transport of water. For simplicity, lateral subsurface flow Q_i (Equation 16) from one soil column pixel to its downslope neighbor is from layer *i* of the upslope pixel to layer *i* of the downslope pixel. Lateral surface flow Q_s (Equation 18) is from the s_{STW} pool of an upslope pixel to the s_{STW} pool of a downslope pixel, where it can then either infiltrate into the top soil layer of the downslope pixel, or continue its downslope movement as lateral surface flow. A multiple flow direction method is used where flow from one pixel to its eight neighbors is fractionally allocated according to terrain slope [*Freeman*, 1991; *Quinn et al.*, 1991].

3.9.1.2.1 Lateral Subsurface Runoff:

Lateral downslope flow (Q_i) is triggered near field capacity using the logistic function presented in Equation 9 but (1) corrected for the local slope and (2) $Ks_i^{vertical}$ in $a_{1,i}$ and $a_{2,i}$ is replaced by $Ks_i^{lateral}$ such that:

$$Q_i = Ks_i^{lateral} \times SL \times f\left(s_i / s_i^{\max}\right) \qquad i = 1,2,...n \tag{3.16}$$

and

$$Ks_i^{lateral} = Ks \times e^{-f_l \times d_i} \qquad i = 1,2,...n \tag{3.17}$$

where $Ks_i^{lateral}$ is the lateral saturated hydraulic conductivity in layer *i*, *SL* is the local terrain slope, and f_l is the lateral decay rate of *Ks* with depth.

3.9.1.2.2 Surface Runoff:

Surface runoff (Q_s) from a pixel is calculated as a function of the standing water after infiltration (*I*) is accounted for, local terrain slope and a Chezy "like" coefficient (*Che*) (1/time) [*Dingman*, 1994]:

$$Q_s = Che \times SL \times S_{STW} \tag{3.18}$$

3.9.1.2.3 Total Runoff:

Total catchment discharge (Q_T) is computed as the sum of the lateral flows into the channel, the rain falling directly on the channel, and the snowmelt from channel pixels. The stream channel is defined as all pixels with a flow accumulation area above a pre-defined threshold. We assume that all flows entering the channel are directly routed to the outlet such that:

$$Q_T = \sum_{j=1}^{cn} \sum_{i=1}^{n} \left(Q_{s,j} + Q_{i,j} \right) + \sum_{k=1}^{cr} \left(P_r + m \right) \tag{3.19}$$

where *cn* is the number of pixels that are both adjacent to the channel and that have a flow direction into the channel, *n* is the number of layers in a soil column, and *cr* is the number of pixels within the channel.

3.9.2 Appendix B: Evapotranspiration Recovery Function Description

3.9.2.2 Background

Successional changes in forest transpiration are generally consistent with changes in forest Leaf Area Index (LAI), sapwood basal area, and net primary production (NPP) [*Watson et al.*, 1999; *Zimmermann et al.*, 2000]. *Ryan et al*., [1997] found that forest LAI increases initially after disturbance, reaches a maximum in young stands, and thereafter decreases. *Moore et al.,* [2004] found that young Douglas-fir forests in the Pacific Northwest have a higher sapwood basal area and use nearly three times as much water during the growing season as old-growth forests. *Acker et al.,* [2002] found that the NPP of young stands in the Pacific Northwest is larger than the NPP of mature and old stands (Figure 3.B.1). Furthermore, several experimental studies found that the streamflow in managed forest is reduced to below pre-harvest values due to rapidly transpiring young vegetation [*Bond et al.*, 2008; *Hicks et al.*, 1991]. Finally, *Yang et al.* [2005] examined conifer development in 153 stands in the Pacific Northwest using interpretation of historic aerial photographs from 1959 to 1997 and found that coniferous forests regenerate quickly and reach closed canopy (defined as >70% tree cover) approximately 50 years after disturbance.

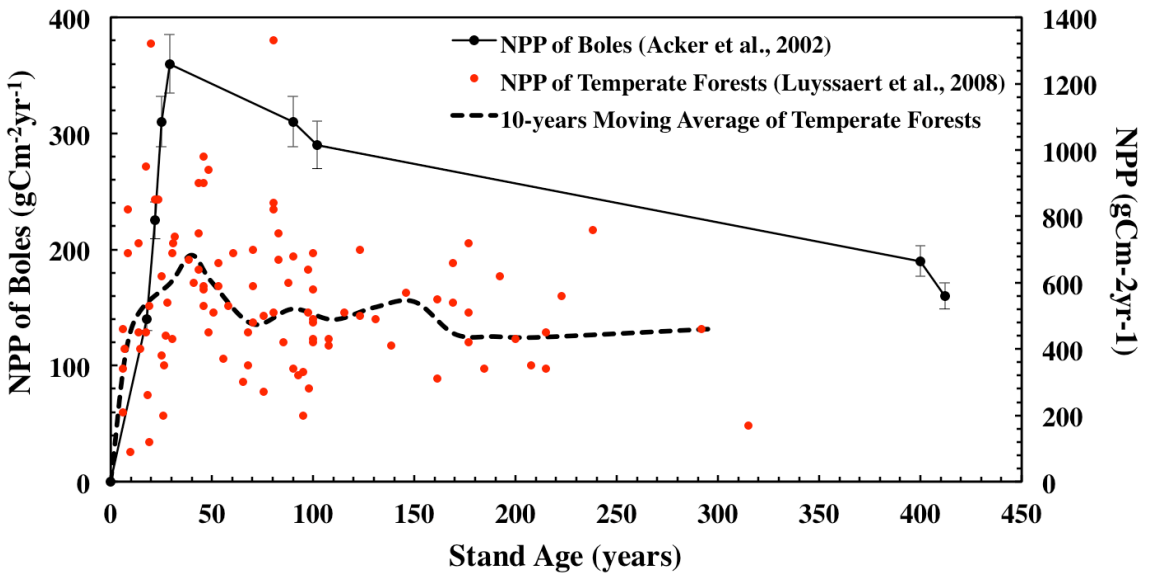

Figure 3.B.1: *Changes in net primary production (NPP) of temperate forests (red dots are individual forest stands sampled throughout the world; dashed black line is a 10-year moving average)* [*Luyssaert et al.,* 2008]*, and NPP of boles for Pacific Northwest coniferous forests (black circles and solid black line) as a function of stand age (i.e. time after stand-replacing disturbance)* [*Acker et al.,* 2002].

3.9.2.3 Evapotranspiration Recovery Function

Based on these findings, the ET function given in Equation 12 is modified to account for the 1) reduction in ET due to clearcut, 2) ET recovery during regrowth, 3) high transpiration demands of young forest, and 4) return to pre-clearcut ET values within 50 years. Thus

$$ET_i = f_{TP}(t_d) \times W_{E,i} \times PET \times \left(1 - \exp\left(-c_{ET} \times \left(s_i / s_i^{\max}\right)\right)\right) \qquad i = 1,2,\ldots n \tag{3.20}$$

where

$$f_{TP}(t_d) = f_{YF}(t_d) \times \left(\left(1 - r_{ET}\right) \times \left(1 - \exp\left(-t_d / r_T\right)\right) + r_{ET}\right) \tag{3.21}$$

and

$$for\ \left(25yrs \le t_d \le 45yrs\ \&\ t_d \in Jun - Sept\right) \quad f_{YF}(t_d) = \frac{\Omega}{\left(\left(1 - r_{ET}\right) \times \left(1 - \exp\left(-t_d / r_T\right)\right) + r_{ET}\right)} \tag{3.22}$$

$$else \quad f_{YF}(t_d) = 1$$

where $f_{TP}(t_d)$ is the ET recovery function, t_d is time in days after disturbance, r_{ET} is the residual ET immediately after clearcut, r_T is an ET recovery shape factor, and Ω is the percentage increase in transpiration of young stands over old-growth during the growing season (assumed here between June and September). The function $f_{YF}(t_d)$ accounts for the increase in ET of young stands over old-growth.

The ET recovery function, $f_{TP}(t_d)$, is a modified Chapman-Richards growth function [*Hunt*, 1982; *Ratkowsky*, 1990; *Richards*, 1959] that accounts for the higher transpiration rate of young vigorous stands over old-growth [*Bond et al.*, 2008; *Jones and Post*, 2004]. Specifically, $f_{TP}(t_d)$ increases exponentially (from a clearcut value of $f_{TP}(t_d = 0) = r_{ET}$) and asymptotes to pre-clearcut values within 50 years (i.e. $f_{TP}(t_d = 50yrs) = 1$). This ET recovery function Equation 3.21 is an initial attempt to capture the complex successional dynamics associated with canopy recovery. This function has been widely used in studies of trees and stand growth (e.g. at the H.J. Andrews, the Coweeta, and the Hubbard Brook Experimental Forests) [*Bosch and Von Gadow*, 1990; *Christina et al*., 2011; *Duan*, 1996; *Janisch and Harmon*, 2002; *Khamis et al*., 2005; *Waichler et al*., 2005; *Zeide*, 1993, amongst others]. *Waichler et al*., [2005] used the Chapman-Richards growth function to capture canopy recovery in 3 watersheds within H.J. Andrews. *Yang et al.*, [2005] used the Chapman-Richards growth function to simulate the recovery of shrubs, hardwood trees, conifer trees and mixed trees successional post-disturbance dynamics.

Calibration of the ET recovery function parameters is conducted as follows: Ω is calibrated to capture the observed 1975 – 2008 annual, seasonal and monthly streamflow. r_{ET} is calibrated based on the annual P and Q_T record at WS10 immediately after clearcut and yields a value of 30%, which is well within the range of observed values in forests across the United States and the Pacific Northwest [*Spittlehouse*, 2006; *Stednick*, 1996; *Stoy et al*., 2006; *Winkler et al*., 2010]. For example, a number of studies in the Pacific Northwest, including H.J. Andrews, have found that the initial ET after clearcut ranged from 280 mm to 550mm (30 to 55% of pre-clearcut ET) [*Bosch and Hewlett*, 1982; *Hibbert*, 1966; *Stednick*, 1996].

Table 3.B.1: Model parameters values used to simulate the hydrologic processes of WS10 in the H.J. Andrews Experimental Forest.

Parameters	Definition	Value	References
Soil Texture	Dominant Soil Texture	Loam*	*Ranken,* 1974
θ_i^{fc}	Field Capacity in layer *i*	0.27	Clapp and Hornberger, 1978
ϕ_i	Porosity in layer *i*	0.463	Clapp and Hornberger, 1978
θ_i^{w}	Wilting Point in layer *i*	0.117	Clapp and Hornberger, 1978
Pre-Harvest Calibrated Model Parameters			
Δz_1	Soil Surface Layer (Layer 1) Thickness (mm)	300	Calibrated
Δz_2	First Intermediate Soil Layer (layer 2) Thickness (mm)	750	Calibrated
Δz_3	Second Intermediate Soil Layer (layer 3) Thickness (mm)	750	Calibrated
Δz_4	Deep Soil Layer (Layer 4) Thickness (mm)	200	Calibrated
Ks	Surface Saturated Hydraulic Conductivity (mm/day)	950	Calibrated
f_v	Vertical Decay Rate of *Ks* (1/m)	1.3	Calibrated
f_l	Lateral Decay Rate of *Ks* (1/m)	1.55	Calibrated
d_r	Deepest layer in which water extraction is possible	3	*Santantonio et al.* 1977
$W_{E,deep}$	Fraction of water uptake from the deep layers during droughts	0.2	Calibrated
c_{ET}	*ET* Shape Factor	5	Calibrated
K_{PET}	Potential Evapotranspiration Calibration Parameter	2	Calibrated
α	Degree-day Factor for Melt (mm $°C^{-1}$ day^{-1})	5	Calibrated
T_{th}	Threshold Temperature (°C)	-1	Calibrated
T_m	Melting Temperature (°C)	2	Calibrated
σ	Rain on Snow Parameter	0.5	Calibrated
Che	Chezy "like" Coefficient (1/day)	540,000	Calibrated
Post-Harvest Calibrated Model Parameters			
r_{ET}	Residual Evapotranspiration fraction after Clearcut	0.3	Calibrated
r_T	Transpiration recovery shape factor	3000	Calibrated
Ω	Percentage Increase in daily transpiration due to young vigorous forest (%)	10	Calibrated

**Soil texture in WS10 range from gravelly, silty clay loam to very gravelly clay loam* [*Ranken, 1974*].

3.10. Acknowledgements

The information in this document has been funded in part by the US Environmental Protection Agency. It has been subjected to the Agency's peer and administrative review, and it has been approved for publication as an EPA document. Mention of trade names or commercial products does not constitute endorsement or recommendation for use. This research was additionally supported in part by the following NSF Grants 0439620, 0436118, and 0922100. We thank Sherri Johnson, Barbara Bond, Suzanne Remillard, Theresa Valentine and Don Henshaw for invaluable assistance in accessing and interpreting various H.J. Andrews LTER data sets used in this study. Data for streamflow, stream chemistry and climate were provided by the H.J. Andrews Experimental Forest research program, funded by the National Science Foundation's Long-Term Ecological Research Program (DEB 08-23380), US Forest Service Pacific Northwest Research Station, and Oregon State University.

3.11. References

Acker, S., C. Halpern, M. Harmon, and C. Dyrness (2002), Trends in bole biomass accumulation, net primary production and tree mortality in Pseudotsuga menziesii forests of contrasting age, *Tree Physiology*, *22*(2-3), 213.

Beckers, J., B. Smerdon, T. Redding, A. Anderson, R. Pike, and A. T. Werner (2009), Hydrologic Models for Forest Management Applications: Part 1: Model Selection, *Watershed Management Bulletin*, *13*(1), 35-44.

Beschta, R., M. Pyles, A. Skaugset, and C. Surfleet (2000), Peakflow responses to forest practices in the western Cascades of Oregon, USA, *Journal of Hydrology*, *233*(1-4), 102-120.

Beschta, R. L. (1978), Long-term patterns of sediment production following road construction and logging in the Oregon Coast Range, *Water Resources Research*, *14*(6), 1011-1016, doi:1010.1029/WR1014i1006p01011.

Beven, K., and M. Kirkby (1979), A physically based, variable contributing area model of basin hydrology, *Hydrological Sciences Bulletin*, *24*(1), 43-69.

Bond, B. J., F. C. Meinzer, and J. R. Brooks (2008), How trees influence the hydrological cycle in forest ecosystems, in *Hydroecology and Ecohydrology: Past, Present and Future (eds P. J. Wood, D. M. Hannah and J. P. Sadler), John Wiley & Sons, Ltd, Chichester, UK. doi: 10.1002/9780470010198.ch2*, edited, pp. 7-28.

Bond-Lamberty, B., S. T. Gower, D. E. Ahl, and P. E. Thornton (2005), Reimplementation of the Biome-BGC model to simulate successional change, *Tree Physiology*, *25*(4), 413.

Bosch, J., and J. Hewlett (1982), A review of catchment experiments to determine the effect of vegetation changes on water yield and evapotranspiration, *Journal of Hydrology*, *55*(1-4), 3-23.

Bosch, J., and K. Von Gadow (1990), Regulating afforestation for water conservation in South Africa, *South African Forestry Journal*, *153*(1), 41-54.

Bowling, L. C., P. Storck, and D. P. Lettenmaier (2000), Hydrologic effects of logging in western Washington, United States, *Water Resources Research*, *36*(11), 3223-3240.

Brooks, J. R., F. C. Meinzer, J. M. Warren, J. C. Domec, and R. Coulombe (2006), Hydraulic redistribution in a Douglas fir forest: lessons from system manipulations, *Plant, Cell & Environment*, *29*(1), 138-150.

Christina, M., J. P. Laclau, J. Goncalves, C. Jourdan, Y. Nouvellon, and J. P. Bouillet (2011), Almost symmetrical vertical growth rates above and below ground in one of the world's most productive forests, *Ecosphere 2(3):art27 doi:10.1890/ES10-00158.1*.

Clapp, R. B., and G. M. Hornberger (1978), Empirical equations for some soil hydraulic properties, *Water Resources Research*, *14*(4), 601-604, doi:610.1029/WR1014i1004p00601.

Daly, C., and W. McKee (2011), Meteorological data from benchmark stations at the Andrews Experimental Forest. Long-Term Ecological Research. Forest Science Data Bank, Corvallis, OR. [Database]. Available: http://andrewsforest.oregonstate.edu/data/abstract.cfm?dbcode=MS001 (16 July 2011).

Davies, J., and C. Allen (1973), Equilibrium, potential and actual evaporation from cropped surfaces in southern Ontario, *Journal of Applied Meteorology*, *12*(4), 649-657.

Dingman, S. (1994), *Physical hydrology*, Prentice Hall Upper Saddle River, NJ.

Duan, J. (1996), A coupled hydrologic-geomorphic model for evaluating effects of vegetation change on watersheds: Ph.D. Dissertation, Oregon State University, Corvallis, OR, 133p.

Dyrness, C. (1973), Early stages of plant succession following logging and burning in the western Cascades of Oregon, *Ecology*, *54*(1), 57-69.

Federer, C. A. (1979), A soil-plant-atmosphere model for transpiration and availability of soil water, *Water Resources Research*, *15*(3), 555-562, doi:510.1029/WR1015i1003p00555.

Federer, C. A. (1982), Transpirational supply and demand: plant, soil, and atmospheric effects evaluated by simulation, *Water Resources Research*, *18*(2), 355-362, doi:310.1029/WR1018i1002p00355.

Fredriksen, R. (1975), Nitrogen, phosphorus and particulate matter budgets of five coniferous forest ecosystems in the western Cascades Range, Oregon, Doctoral thesis, 71 pp, Oregon State University, Corvallis.

Freeman, T. (1991), Calculating catchment area with divergent flow based on a regular grid, *Computers & Geosciences*, *17*(3), 413-422.

Gale, M. R., and D. F. Grigal (1987), Vertical root distributions of northern tree species in relation to successional status, *Canadian Journal of Forest Research*, *17*(8), 829-834.

Garrick, M., C. Cunnane, and J. Nash (1978), A criterion of efficiency for rainfall-runoff models, *Journal of Hydrology*, *36*(3-4), 375-381.

Gholz, H. L., G. M. Hawk, A. Campbell, K. Cromack Jr, and A. T. Brown (1985), Early vegetation recovery and element cycles on a clear-cut watershed in western Oregon, *Canadian Journal of Forest Research*, *15*(2), 400-409.

Golding, D. L. (1987), Changes in streamflow peaks following timber harvest of a coastal British Columbia watershed, paper presented at Forest Hydrology and Watershed Management, IAHS, Vancouver.

Grant, G., S. Lewis, F. Swanson, J. Cissel, and J. McDonnell (2008), Effects of forest practices on peak flows and consequent channel response: a state-of-science report for western Oregon and Washington, *General Technical Report. PNW-GTR-760. Portland, OR: USDA Forest Service, Pacific Northwest Research Station*, *76*.

Grier, C., and R. Logan (1977), Old-growth Pseudotsuga menziesii communities of a western Oregon watershed: biomass distribution and production budgets, *Ecological Monographs*, *47*(4), 373-400.

Hacke, U., J. Sperry, B. Ewers, D. Ellsworth, K. Schäfer, and R. Oren (2000), Influence of soil porosity on water use in Pinus taeda, *Oecologia*, *124*(4), 495-505.

Hamon, W. (1963), Computation of Direct Runoff Amounts From Storm Rainfall *International Association of Scientific Hydrology, Symposium Surface Waters 3*, 52-62.

Harmon, M. E., W. K. Ferrell, and J. F. Franklin (1990), Effects on carbon storage of conversion of old-growth forests to young forests, *Science*, *247*(4943), 699-701.

Harr, R. (1981), Some characteristics and consequences of snowmelt during rainfall in western Oregon, *Journal of Hydrology*, *53*(3-4), 277-304.

Harr, R., and F. M. McCorison (1979), Initial effects of clearcut logging on size and timing of peak flows in a small watershed in western Oregon, *Water Resources Research*, *15*(1), 90-94, doi:10.1029/WR1015i1001p00090.

Harr, R., R. Fredriksen, and J. Rothacher (1979), Changes in streamflow following timber harvest in southwestern Oregon, *Research Paper PNW-RP-249. Portland, OR: U.S. Department of Agriculture, Forest Service, Pacific Northwest Research Station*, 22.

Harr, R., A. Levno, and R. Mersereau (1982), Streamflow changes after logging 130-year-old Douglas fir in two small watersheds, *Water Resources Research*, *18*(3), 637-644, doi:610.1029/WR1018i1003p00637.

Hibbert, A. (1966), Forest treatment effects on water yield, in *Proceedings of a National Science Foundation advanced science seminar, International symposium on forest hydrology. Pergamon Press, USA*, edited by W.E. Sopper and H.W. Lull, pp. 527-543, Pergamon Press, New York,.

Hicks, B., R. Beschta, and R. Harr (1991), Long-term changes in streamflow following logging in western Oregon and associated fisheries implications, *Water Resources Bulletin*, *27*(2), 217-226.

Hood, E., M. N. Gooseff, and S. L. Johnson (2006), Changes in the character of stream water dissolved organic carbon during flushing in three small watersheds, Oregon, *Journal of Geophysical Research*, *111*, G01007, doi:01010.01029/02005JG000082. .

Huang, J., S. Lacey, and P. Ryan (1996), Impact of forest harvesting on the hydraulic properties of surface soil, *Soil Science*, *161*(2), 79.

Hunt, R. (1982), *Plant Growth Curves: The Functional Approach to Plant Growth Analysis*, 248 pp., Edward Arnold, London.

Jackson, R., J. Canadell, J. Ehleringer, H. Mooney, O. Sala, and E. Schulze (1996), A global analysis of root distributions for terrestrial biomes, *Oecologia*, *108*(3), 389-411.

Janisch, J., and M. Harmon (2002), Successional changes in live and dead wood carbon stores: implications for net ecosystem productivity, *Tree Physiology*, *22*(2-3), 77.

Johnson, S., and J. Rothacher (2009), Stream discharge in gaged watersheds at the Andrews Experimental Forest. Long-Term Ecological Research. Forest Science Data Bank, Corvallis, OR. [Database]. Available: http://andrewsforest.oregonstate.edu/data/abstract.cfm?dbcode=HF004 (16 July 2011).

Jones, J. A. (2000), Hydrologic processes and peak discharge response to forest removal, regrowth, and roads in 10 small experimental basins, western Cascades, Oregon, *Water Resources Research*, *36*(9), 2621-2642, doi:2610.1029/2000WR900105.

Jones, J. A., and G. E. Grant (1996), Peak flow responses to clear-cutting and roads in small and large basins, western Cascades, Oregon, *Water Resources Research*, *32*(4), 959-974.

Jones, J. A., and D. A. Post (2004), Seasonal and successional streamflow response to forest cutting and regrowth in the northwest and eastern United States, *Water Resources Research*, *40*(5), W05203, doi:05210.01029/02003WR002952.

Jordan, T., D. Correll, and D. Weller (1993), Nutrient interception by a riparian forest receiving inputs from adjacent cropland, *Journal of Environmental Quality*, *22*(3), 467.

Keppeler, E. T., and R. R. Ziemer (1990), Logging effects on streamflow: water yield and summer low flows at Caspar Creek in northwestern California, *Water Resources Research*, *26*(7), 1669-1679.

Khamis, A., Z. Ismail, K. Haron, and A. T. Mohammed (2005), Nonlinear growth models for modeling oil palm yield growth, *Journal of Mathematics and Statistics*, *1*(3), 225-233.

Kirchner, J. (2003), A double paradox in catchment hydrology and geochemistry, *Hydrological Processes*, *17*(4), 871-874.

Legates, D. R., and G. J. McCabe Jr (1999), Evaluating the use of "goodness-of-fit" measures in hydrologic and hydroclimatic model validation, *Water Resources Research*, *35*(1), 233-241.

Lowrance, R., L. Altier, J. Newbold, R. Schnabel, P. Groffman, J. Denver, D. Correll, J. Gilliam, J. Robinson, and R. Brinsfield (1997), Water quality functions of riparian forest buffers in Chesapeake Bay watersheds, *Environmental Management*, *21*(5), 687-712.

Luce, C., and B. Wemple (2001), Introduction to special issue on hydrologic and geomorphic effects of forest roads, *Earth Surface Processes and Landforms*, *26*(2), 111-113.

Luyssaert, S., E. Schulze, A. Borner, A. Knohl, D. Hessenmoller, B. Law, P. Ciais, and J. Grace (2008), Old-growth forests as global carbon sinks, *Nature*, *455*(7210), 213-215.

McGuire, K., M. Weiler, and J. McDonnell (2007), Integrating tracer experiments with modeling to assess runoff processes and water transit times, *Advances in Water Resources*, *30*(4), 824-837.

McKane, R., E. Rastetter, G. Shaver, K. Nadelhoffer, A. Giblin, J. Laundre, and F. Chapin III (1997), Climatic effects on tundra carbon storage inferred from experimental data and a model, *Ecology*, *78*(4), 1170-1187.

Moore, G., B. Bond, J. Jones, N. Phillips, and F. Meinzer (2004), Structural and compositional controls on transpiration in 40-and 450-year-old riparian forests in western Oregon, USA, *Tree Physiology*, *24*(5), 481.

Moore, R., and S. Wondzell (2005), Physical Hydrology in the Pacific Northwest and the Effects of Forest HarvestingñA Review, *Journal of the American Water Resources Association*, *41*, 753-784.

Nash, J., and J. Sutcliffe (1970), River flow forecasting through conceptual models part I--A discussion of principles, *Journal of Hydrology*, *10*(3), 282-290.

Purser, M. D., and T. W. Cundy (1992), Changes in soil physical properties due to cable yarding and their hydrologic implications, *Western Journal of Applied Forestry*, *7*(2), 36-39.

Quinn, P., K. Beven, P. Chevallier, and O. Planchon (1991), Prediction of hillslope flow paths for distributed hydrological modelling using digital terrain models, *Hydrological Processes*, *5*(1), 59-79.

Rango, A., and J. Martinec (1995), Revisiting the degree-day method for snowmelt computations, *Water Resources Bulletin*, *31*(4), 657-669.

Ranken, D. W. (1974), Hydrologic properties of soil and subsoil on a steep, forested slope, Master's thesis, 117 pp, Oregon State University, Corvallis.

Ratkowsky, D. (1990), Handbook of Nonlinear Regression Models, volume 107 of Statistics: Textbooks and Monographs, edited, Marcel Dekker, Inc., New York, NY.

Richards, F. (1959), A flexible growth function for empirical use, *Journal of Experimental Botany*, *10*(29), 290-300.

Rothacher, J. (1965), Streamflow from small watersheds on the western slope of the Cascade Range of Oregon, *Water Resources Research*, *1*, 125-134, doi:110.1029/WR1001i1001p00125.

Rothacher, J. (1970), Increases in water yield following clear-cut logging in the Pacific Northwest, *Water Resources Research*, *6*(2), 653-658, doi:610.1029/WR1006i1002p00653.

Ryan, M., D. Binkley, and J. H. Fownes (1997), Age-related decline in forest productivity: pattern and process, *Advances in ecological research*, *27*, 213-262.

Sahin, V., and M. Hall (1996), The effects of afforestation and deforestation on water yields, *Journal of Hydrology*, *178*(1-4), 293-309.

Santantonio, D., R. Hermann, and W. Overton (1977), Root biomass studies in forest ecosystems. Pedobiologia, Bd. 17, S. 1-31. Paper 957, *Forest Research Laboratory, School of Forestry Oregon State University, Corvallis, Oregon*.

Sayama, T., and J. McDonnell (2009), A new time-space accounting scheme to predict stream water residence time and hydrograph source components at the watershed scale, *Water Resources Research*, *45*, W07401, doi:07410.01029/02008WR007549.

Sidle, R. C., S. Noguchi, Y. Tsuboyama, and K. Laursen (2001), A conceptual model of preferential flow systems in forested hillslopes: evidence of self organization, *Hydrological Processes*, *15*(10), 1675-1692.

Sollins, P., and F. M. McCorison (1981), Nitrogen and carbon solution chemistry of an old-growth coniferous forest watershed before and after cutting, *Water Resources Research*, *17*(5), 1409-1418, doi:1410.1029/WR1017i1005p01409.

Sollins, P., K. Cromack Jr, F. Mc Corison, R. Waring, and R. Harr (1981), Changes in nitrogen cycling at an old-growth Douglas-fir site after disturbance, *Journal of Environmental Quality*, *10*(1), 37.

Spittlehouse, D. (2006), Annual water balance of high elevation forests and clearcuts In: Proceedings of the 27th Conference on Agricultural and Forest Meteorology, San Diego, CA, American Meteorological Society, Boston, MA, 7 pp.

Spittlehouse, D. L., and T. A. Black (1981), Growing Season Water Balance Model Applied to Two Douglas Fir Stands, *Water Resources Research*, *17*(6), 1651-1656, doi:1610.1029/WR1017i1006p01651.

Startsev, A., and D. McNabb (2000), Effects of skidding on forest soil infiltration in west-central Alberta, *Canadian Journal of Soil Science*, *80*(4), 617-624.

Stednick, J. (1996), Monitoring the effects of timber harvest on annual water yield, *Journal of Hydrology*, *176*(1-4), 79-95.

Stoy, P. C., G. G. Katul, M. Siqueira, J. Y. Juang, K. A. Novick, H. R. Mccarthy, A. Christopher Oishi, J. M. Uebelherr, H. S. Kim, and R. Oren (2006), Separating the effects of climate and vegetation on evapotranspiration along a successional chronosequence in the southeastern US, *Global Change Biology*, *12*(11), 2115-2135.

Swanson, F., and C. Dyrness (1975), Impact of clear-cutting and road construction on soil erosion by landslides in the western Cascade Range, Oregon, *Geology*, *3*(7), 393.

Swanston, D., and F. Swanson (1976), Timber harvesting, mass erosion, and steepland forest geomorphology in the Pacific Northwest, *Geomorphology and Engineering, pp.199-221, Coates, ed. Dowden, Hutchinson, and Ross, Inc., Stroudsburg, Pa*.

Tachikawa, Y., G. Nagatani, and K. Takara (2004), Development of stage discharge relationship equation incorporating saturated-unsaturated flow mechanism, *Annual Journal of Hydraulic Engineering, Japan. Society of Civil Engineers*, *48*, 7-12.

Tague, C., and L. Band (2000), Simulating the impact of road construction and forest harvesting on hydrologic response, *Earth Surface Processes and Landforms*, *26*(2), 135-151.

Valentine, T., and G. Lienkaemper (2005), 30 meter digital elevation model (DEM) clipped to the Andrews Experimental Forest. Long-Term Ecological Research. Forest Science Data Bank, Corvallis, OR. [Database]. Available: http://andrewsforest.oregonstate.edu/data/abstract.cfm?dbcode=GI002 (16 July 2011).

Van Verseveld, W. J., J. J. McDonnell, and K. Lajtha (2008), A mechanistic assessment of nutrient flushing at the catchment scale, *Journal of Hydrology*, *358*(3-4), 268-287.

Vanderbilt, K., K. Lajtha, and F. Swanson (2003), Biogeochemistry of unpolluted forested watersheds in the Oregon Cascades: temporal patterns of precipitation and stream nitrogen fluxes, *Biogeochemistry*, *62*(1), 87-117.

Waichler, S. R., B. C. Wemple, and M. S. Wigmosta (2005), Simulation of water balance and forest treatment effects at the HJ Andrews Experimental Forest, *Hydrological Processes*, *19*(16), 3177-3199.

Warren, J., F. Meinzer, J. Brooks, and J. Domec (2005), Vertical stratification of soil water storage and release dynamics in Pacific Northwest coniferous forests, *Agricultural and Forest Meteorology*, *130*(1-2), 39-58.

Watson, F., R. Vertessy, and R. Grayson (1999), Large-scale modelling of forest hydrological processes and their long-term effect on water yield, *Hydrological Processes*, *13*(5), 689-700.

Wemple, B. C., and J. A. Jones (2003), Runoff production on forest roads in a steep, mountain catchment, *Water Resources Research*, *39*(8), 1220.

Wemple, B. C., F. J. Swanson, and J. A. Jones (2001), Forest roads and geomorphic process interactions, Cascade Range, Oregon, *Earth Surface Processes and Landforms*, *26*(2), 191-204.

Whitaker, A., Y. Alila, J. Beckers, and D. Toews (2002), Evaluating peak flow sensitivity to clear-cutting in different elevation bands of a snowmelt-dominated mountainous catchment, *Water Resources Research*, *38*(9), 1172, doi:1110.1029/2001WR000514.

Wigmosta, M. S., and W. A. Perkins (2001), Simulating the effects of forest roads on watershed hydrology, *Land use and watersheds: human influence on hydrology and geomorphology in urban and forest areas*, *2*, 127-143.

Wigmosta, M. S., L. W. Vail, and D. P. Lettenmaier (1994), A distributed hydrology-vegetation model for complex terrain, *Water Resources Research*, *30*(6), 1665-1680, doi:1610.1029/1694WR00436.

Willmott, C. J. (1981), On the validation of models, *Physical geography*, *2*(2), 184-194.

Winkler, R. D., R.D. Moore, T. Redding, D. Spittlehouse, B. Smerdon, and D. Carlyle-Moses. (2010), Chapter 7 - The effects of forest disturbance on hydrologic processes and watershed response In: R.G. Pike, T.E. Redding, R.D. Moore, R.D. Winkler and K.D. Bladon (editors) 2010. Compendium of forest hydrology and geomorphology in British Columbia. B.C. Min. For. Range, For. Sci. Prog., Victoria, B.C. and FORREX Forum for Research and Extension in Natural Resources, Kamloops, B.C. Land Manag. Handb. 66. pp. 179-212., B.C. Ministry of Forests and Range Research Branch, Victoria, B.C. and FORREX Forest Research Extension Partnership, Kamloops.

Yang, Z., W. Cohen, and M. Harmon (2005), Modeling early forest succession following clear-cutting in western Oregon, *Canadian Journal of Forest Research*, *35*(8), 1889-1900.

Zeide, B. (1993), Analysis of growth equations, *Forest science*, *39*(3), 594-616.

Zimmermann, R., E. D. Schulze, C. Wirth, E. E. Schulze, K. C. Mcdonald, N. N. Vygodskaya, and W. Ziegler (2000), Canopy transpiration in a chronosequence of Central Siberian pine forests, *Global Change Biology*, *6*(1), 25-37.

CHAPTER 4

EFFECTS OF FIRE AND HARVEST ON CARBON AND NITROGEN DYNAMICS IN A PACIFIC NORTHWEST FOREST CATCHMENT

Alex Abdelnour[1], Robert McKane[2], Marc Stieglitz[1,3], Feifei Pan[1,4], Yiwei Cheng[1]

[1] Department of Civil and Environmental Engineering, Georgia Institute of Technology, Atlanta, GA, USA.
[2]US Environmental Protection Agency, Corvallis, OR, USA
[3]School of Earth Atmospheric Sciences, Georgia Institute of Technology, Atlanta, GA, USA.
[4]Department of Geography, University of North Texas, Denton, TX, USA.

4.1. Abstract

Two significant disturbance events have shaped the life history of vegetation growth of a small intensively studied watershed in the Pacific Northwest. The first was a stand-replacing fire in *circa* 1525. The second was a clearcut harvest in 1975. To reconstruct and analyze the effects of these two historical disturbances events on vegetation and soil carbon and nitrogen dynamics, we use a new ecohydrological model, Visualizing Ecosystems for Land Management Assessments (VELMA). Observed ecological and hydro-biogeochemical data from this site in combination with published chronosequence data from Pacific Northwest forest ecosystems were used to calibrate and test the modeled response to fire and harvest. Model parameters were first calibrated to simulate the post-fire build-up trajectory of ecosystem carbon and nitrogen stocks for the period 1525 to 1968. Thereafter, model parameters are held fixed and the model is used to simulate the 1969 to 1974 biogeochemical dynamics of this old-growth forest. Finally, for the period 1975 to 2008, the model is used to simulate the impact of the 1975 100% clearcut. Results show that (1) losses of dissolved nutrients in an old-growth forest are generally low and consist primarily of DON and DOC, (2) following fire and harvest, C and N losses from the terrestrial system to the stream and atmosphere increase as a result of reduced N uptake from plants, high soil organic carbon decomposition, and high soil water content, and (3) plant biomass regrowth following clearcut was lower than the rate of regrowth after fire due to the greater amount of nitrogen released from decomposing detritus following fire than after clearcut.

4.2. Introduction:

Fire and harvest are two disturbances that have impacted the life history of the vegetation growth in forests of the Pacific Northwest [*Agee*, 1994; *Agee* 1990; *Franklin and Forman*, 1987; *Stednick*, 1996; *Wright and Agee*, 2004; *Wright and Heinselman*, 1973]. Forest fire and harvest in the Pacific Northwest have been found to increase water yield [*Bosch and Hewlett*, 1982; *Hibbert*, 1966; *Helvey*, 1980, *Amaranthus et al*., 1989], summer low flow [*Keppeler and Ziemer*, 1990; *Neary et al*., 2005], peak streamflow [*Beschta et al*., 2000; *Harr and McCorison*, 1979; *Ice et al*., 2004], stream nutrient concentrations [*Beschta*, 1990; *Sollins and McCorison*, 1981; *Sollins et al*., 1981; *Tiedemann et al.*, 1988; *Raison et al.*, 1990], greenhouse gas emissions [*Harmon et al*., 1990; *Turner et al.,* 2003], and soil microbial activity [*Bormann et al.*, 1968; *R Grant et al.*, 2007]. Forest fire and harvest have also been shown to reduce evapotranspiration [*Jones and Post*, 2004; *Jones*, 2000; *Ice et al*., 2004], plant N uptake, and forest productivity [*Sollins and McCorison*, 1981]. These changes to the ecosystem hydrological fluxes and biogeochemical dynamics affect key ecosystem services relevant to land managers and policy makers such as timber production, water quality and quantity, and wildlife habitat. For informed management decisions to be made, it is therefore important to understand how historical natural and man-made disturbances affected long-term watershed hydrology, carbon (C) and nitrogen (N) dynamics, and vegetation recovery, so as to draw insights into the impact of future managements on key ecosystem processes. Attempts at investigating the impact of forest disturbances have been addressed through paired-watershed experiments [*Harr and McCorison*, 1979; *Langford*, 1976; *Moore and Wondzell*, 2005; *Raison et al.*, 1990; *Weber and Flannigan*, 1997] and model simulations [*Janisch and Harmon*, 2002; *Storck et al.*, 1998; *C Tague and Band*, 2000; *Wright et al.*, 2002].

A number of experimental paired watershed studies have explored the impact of fire and harvest on ecosystem dynamics in the Pacific Northwest forests. These experimental studies have been conducted in places such as the H.J. Andrews Experimental forest in the western-central Cascade Mountains of Oregon, the Alsea watershed study in coastal Oregon, and the Yakima River basin in Washington State,

amongst others. For example, (1) *Giesen et al*., [2008] used field measurements (i.e. tree scars, dendrochronological records, soil C and N content measurements) at 24 forest stands in the western Cascade Range of Oregon to evaluate the long-term impacts of stand-replacing wildfire on carbon and nitrogen pools and dynamics, (2) *Stednick* [2008] used long-term measurement of nutrients losses to the stream to explore the impact of forest harvest on water quality in three watersheds in coastal Oregon, and (3) *Sollins and McCorison* [1981] measured nitrogen concentration in a small experimental watershed in western Oregon, to explore the impact of clearcut on nitrogen pool and losses. Nonetheless, the complexity of experimental ecosystem studies often prevents direct interpretation of relationships between responses and specific perturbations [*Grant et al*., 2008; *Thompson et al*., 2006]. Moreover, difficulties in separating the effects of plant biomass removal from the effects of roads have been identified and known to impact experimental results [*Yanai et al.*, 2003]. Furthermore, experimental studies are usually expensive, require a significant time commitment, and cannot be used alone to quantify the contribution of specific processes to specific observed biogeochemical responses [*Alila and Beckers*, 2001; *Giesen et al*., 2008; *Stednick*, 2008].

Process-based ecohydrological models can help address this need by providing a whole-system synthesis of disparate data sets (soils, vegetation, climate, etc.) and by exploring underlying process-level controls on catchment hydrological and biogeochemical responses to disturbance. Models can isolate the effect of a 'target' treatment factor from the effects of other factors that may be unavoidably altered within a single treatment [*McKane et al.*, 1997]. A number of models have been used to test forest management treatment scenarios, reproduce historical disturbances, and simulate post-disturbance successional changes in carbon and nitrogen, amongst others. For example: (1) *Harmon and Marks* [2002] developed a carbon model STANDCARB, to examine the effects of forest management treatments such as slash burning, partial harvest and clearcut, amongst others, on plant and soil carbon pools in Pacific Northwest forests, (2) *Wimberley* [2002] used a spatial simulation model of wildfire and forest succession to mimic pre-settlement landscape dynamics in the Oregon Coast Range, (3) *Keane et al*., [1997] used FIRE-BGC [*Keane et al.*, 1996], a mechanistic biogeochemical succession model, to simulate the effects of fire on carbon emissions to the atmosphere in

the coniferous forest landscapes of Glacier National Park, Montana, and (4) *Tague et al*., [2009] used the RHESSys model [*Tague and Band*, 2004] to simulate the ecohydrological response of a Mediterranean type ecosystem to the combined impacts of projected climate change and altered fire frequencies. These and other simulation models have provided an effective tool to complement field research and to examine the integrated responses of watershed hydrology, ecology, and biogeochemistry to interacting stressors.

However, existing process-based models have disadvantages. Many are too simple to capture the important process-level hydrological and biogeochemical controls on ecosystem responses to disturbance. At the other extreme, some models are so complex that they require forcing data that are often unavailable, or are too computationally expensive to simulate the local dynamics over large watershed areas, or require a high level of expertise to implement. There is therefore need for a balanced approach. Specifically an accessible, spatially-distributed, ecohydrological model that is both computationally efficient and relatively easy to implement for analyzing the effects of changes in climate, land-use and land cover on watershed processes at scales relevant to formulating management decisions.

Such an ecohydrological model, VELMA (Visualizing Ecosystems for Land Management Assessments, [*Abdelnour et al*., 2011]) was used to investigate the response of Pacific Northwest forests to natural and man-made disturbances. Specifically, the model was applied to a small intensively studied catchment (WS10), where a stand-replacing fire occurred in 1525 and a 100% clearcut in 1975. The temporal changes in measured and unmeasured biogeochemical fluxes such as nutrient losses, soil heterotrophic respiration, and N_2-N_2O emissions, amongst others, were explored for three periods of interest: (1) following the 1525 stand-replacing fire (1525 to 1968), (2) during old-growth condition when the ecosystem was relatively close to steady state (1969 to 1974), and (3) following the 1975 whole catchment clearcut (1975 to 2008). Section 4.3 of this paper describes the study site. Section 4.4 provides an overview of the VELMA modeling framework. Section 4.5 describes our simulation methods. Section 4.6 presents model results and discussion. Section 4.7 summarizes our major conclusions.

4.3. Site Description

Watershed 10 (WS10) of the H.J. Andrews Experimental Forest (HJA) is a small 10.2 hectares catchment located in the western-central Cascade Mountains of Oregon, at latitude 44°15′N, longitude 122°20′W (Figure 4.1).

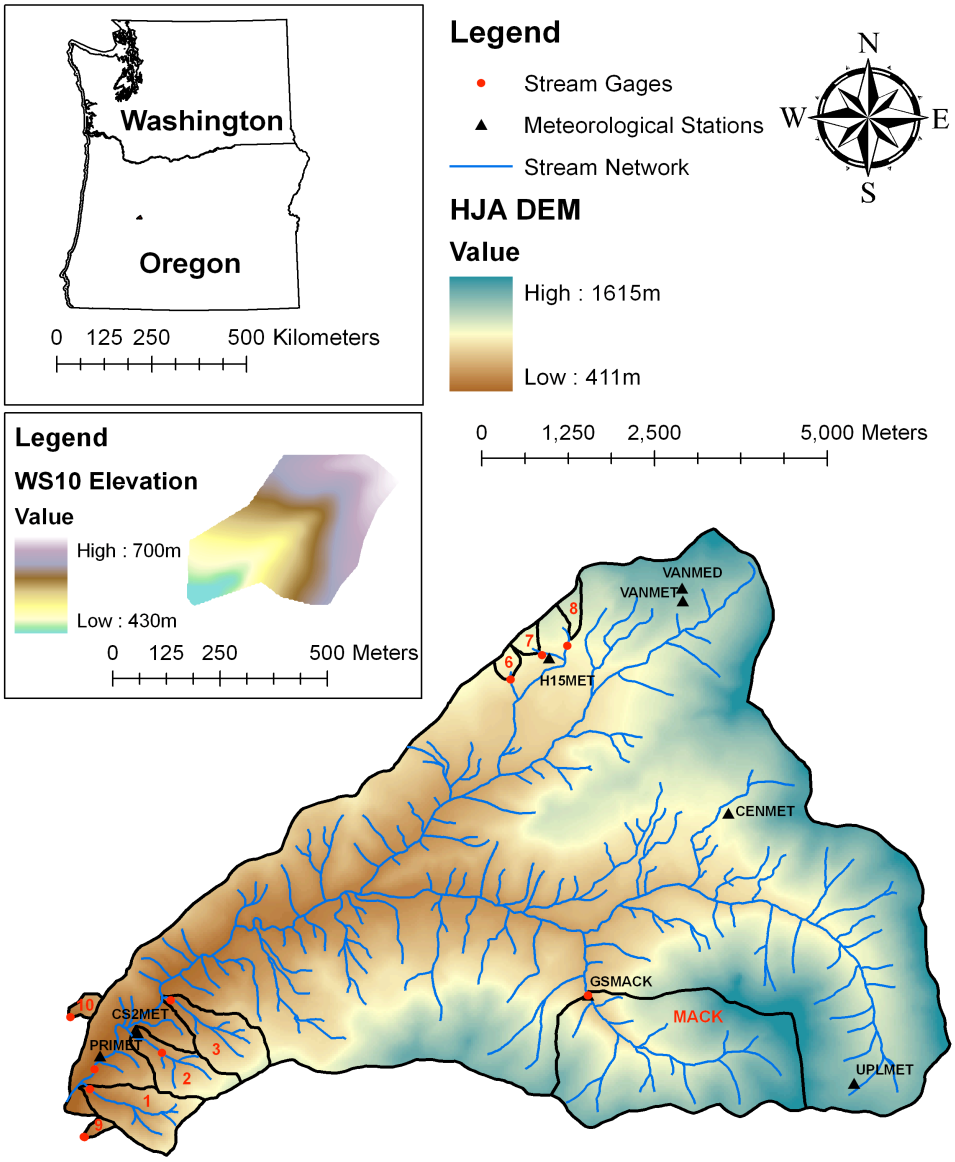

Figure 4.1: *The study site is the watershed 10 (WS10) of the H. J. Andrew Experimental Forest located in the western Cascade Range of Oregon. The red dots represent the locations of the stream gages. The black triangles represent the locations of the meteorological stations.*

WS10 has been the site of intensive research and manipulation by the U.S. forest Service since the 1960's, mainly to study the effects of forest harvest on hydrology, sediment transport, and nutrient loss [*Dyrness*, 1973; *Fredriksen*, 1975; *Harr and McCorison*, 1979; *Jones and Grant*, 1996; *Rothacher*, 1965; *Sollins and McCorison*, 1981; *Sollins et al.*, 1981]. Watershed 10 elevation ranges from 430 m at the stream gauging station to 700 m at the southeastern ridgeline. Near-stream and side-slope gradients are approximately 24° and 25° to 50°, respectively [*Grier and Logan*, 1977; *Sollins et al.*, 1981]. The climate is relatively mild with wet winters and dry summers [*Grier and Logan*, 1977]. Mean annual temperature is 8.5°C. Daily temperature extremes vary from 39°C in the summer to -20°C in the winter [*Sollins and McCorison*, 1981]. Mean annual precipitation is 2300 mm and falls primarily as rain between October and April [*Jones and Grant*, 1996]. Snow rarely persists longer than a couple of weeks and usually melts within 1 to 2 days [*Harr and McCorison*, 1979; *Harr et al.*, 1982; *Jones*, 2000]. Soils are of the Frissel series, which are classified as Typic Dystrochrepts with fine loamy to loamy-skeletal texture [*Sollins et al.*, 1981; *Vanderbilt et al.*, 2003] and are generally deep and well drained [*Grier and Logan*, 1977].

Two significant events determined the life history of the vegetation growth in WS10; a stand-replacing fire event in 1525 A.D. [*Wright et al*., 2002] and a man-made clearcut in 1975 A.D. [*Sollins and McCorison*, 1981]. Prior to the 100% clearcut in 1975, WS10 was a 450 year-old forest dominated by Douglas-fir (*Pseudotsuga menziessii*), western hemlock (*Tsuga heterophylla*), and western red cedar (*Thuja plicata*) [*C Grier and Logan*, 1977] reaching up to ~60m in height, with rooting depths rarely exceeding 100 cm [*Santantonio et al.*, 1977]. In the spring of 1975, WS10 was clearcut. All trees and woody materials larger than 20 cm in diameter or 2.4 m in length, including many logs on the ground, were removed from the site. Large woody slash was disposed of without burning [*Gholz et al.,* 1985]. Post-clearcut residual plants consisted of understory shade tolerant vegetation and shrubbery, undamaged by harvest [*Gholz et al.,* 1985]. Species such as the vine maple (*Acer circinatum*), Pacific rhododendron (*Rhododendron maximum*) and chinkapin (*Castanopsis chrysophylla*) regenerated during the spring after logging. In 1976, one year after clearcut, WS10 was planted with 2-year-

old seedlings of Douglas-fir [*Gholz et al.,* 1985]. The dominant vegetation of WS10 today is a ~35 year-old mixed Douglas-fir and western hemlock stand.

4.4. The Eco-Hydrological Model

A spatially distributed ecohydrological model, VELMA, was developed to simulate changes in soil water infiltration and redistribution, evapotranspiration, surface and subsurface runoff, carbon and nitrogen cycling in plants and soils, and the transport of dissolved forms of carbon and nitrogen from the terrestrial landscape to streams. VELMA was designed to simulate the integrated responses of ecohydrological processes to multiple forcing variables, e.g., changes in climate, land-use and land cover. It was intended to be broadly applicable to a variety of ecosystems (forest, grassland, agricultural, tundra, etc.) and to provide a computationally efficient means for scaling up ecohydrological responses across multiple spatial and temporal scales – hillslopes to basins, and days to centuries. A detailed description of VELMA is provided in Appendix A.

The model uses a distributed soil column framework to simulate the movement of water and nutrients (organically bound carbon (C) and nitrogen (N) in plants and soils; dissolved inorganic nitrogen (DIN), dissolved organic nitrogen (DON) and dissolved organic carbon (DOC); and gaseous forms of C and N including CO_2, N_2O and N_2) within the soil, between the soil and the vegetation, and from the soil surface and vegetation to the atmosphere. The soil column model consists of three coupled sub-models: (1) a *hydrological model* that simulates vertical and lateral movement of water within soil, losses of water from soil and vegetation to the atmosphere, and the growth and ablation of the seasonal snowpack – the hydrological model is described in Appendix A of *Abdelnour et al.,* [2011], (2) a *soil temperature model* [*Cheng et al.*, 2010] that simulates daily soil layer temperatures from surface air temperature and snow depth by propagating the air temperature first through the snowpack and then through the ground using the analytical solution of the one-dimensional thermal diffusion equation (Equations 4.1-4.6, Appendix A), and (3) a *plant-soil model* that simulates ecosystem carbon storage and the cycling of C and N between a plant biomass layer and the active soil pools. Specifically, the plant-soil model simulates the interaction between

aboveground plant biomass, soil organic carbon (SOC), soil nitrogen including dissolved nitrate (NO_3), ammonium (NH_4), and organic nitrogen, as well as dissolved organic carbon (Equation 4.7-4.12, Appendix A). Daily atmospheric inputs of wet and dry nitrogen deposition are accounted for in the ammonium pool of the shallow soil layer (Equation 4.13, Appendix A). Uptake of ammonium and nitrate by plants is modeled using a Type II Michaelis-Menton function (Equation 4.14, Appendix A). Loss of plant biomass is simulated through a density dependent mortality. The mortality rate and the nitrogen uptake rate mimic the exponential increase in biomass mortality and the accelerated growth rate, respectively, as plants go through succession and reach equilibrium (Equation 4.14-4.18, Appendix A). Vertical transport of nutrients from one layer to another in a soil column is function of water drainage (Equations 4.19-4.22, Appendix A). Decomposition of soil organic carbon follow first order kinetics controlled by soil temperature and moisture content as described in the TEM model (Terrestrial Ecosystem Model) of *Raich et al.,* [1991] (Equation 4.23-4.26, Appendix A). Nitrification (Equation 4.27-4.30, Appendix A) and denitrification (Equation 4.31-4.34, Appendix A) were simulated using the equations from the generalized model of N_2 and N_2O production of *Parton et al.,* [1996; 2001] and *Del Grosso et al.,* [2000].

The soil column model is placed within a catchment framework to create a spatially distributed model applicable to watersheds and landscapes. Adjacent soil columns interact with each other through the downslope lateral transport of water and nutrients. Surface and subsurface lateral flow are routed using a multiple flow direction method [*Freeman*, 1991; *Quinn et al.*, 1991]. As with vertical drainage of soil water, lateral subsurface downslope flow is modeled using a simple logistic function and corrected for the local topographic slope angle. Lateral transport of nutrients from one soil column to the subsequent soil column or towards the stream is simulated as a function of subsurface flow and nutrient-specific loss rates (Equations 4.35-4.38, Appendix A). Nutrients transported downslope from one soil column to another can be processed through the different C and N cycling sub-models in that downslope soil column, or continue to flow downslope, interacting with other soil columns, or ultimately discharging water and nutrients to the stream.

4.5. Simulations Methods

4.5.1. Data

The model is forced with observed data of daily temperature, precipitation, and atmospheric nitrogen deposition. Daily temperature and precipitation data for the period January 1, 1969 - December 31, 2008 were obtained from the H.J. Andrews LTER PRIMET, CS2MET, and H15MET meteorological stations located around WS10 [*Daly and McKee*, 2011] (Figure 4.1). At the H.J. Andrews Experimental forest, observed wet atmospheric nitrogen deposition is available approximately every 3 weeks, for the period 1968 to 2010, whereas observed dry atmospheric nitrogen deposition is available 2 to 4 times a year, for the period 1988 to 2010 [*Johnson and Fredriksen*, 2010]. However, for the purpose of our simulations, daily atmospheric inputs of wet and dry nitrogen deposition were calculated as a function of the average wet and dry annual nitrogen deposition found by *Sollins et al*., [1980] (Equation 4.13 in Appendix A). *Sollins et al*., [1980] measured the average wet and dry nitrogen deposition in WS10 for the period 1973 to 1975 and found that annual N input in precipitation and dust averaged 0.2$gNm^{-2}yr^{-1}$.

Observed data used for model calibration and validation include daily streamflow measured at the WS10 weir between 1969 to 2008 [*Johnson and Rothacher*, 2009], and NO_3, NH_4, DON and DOC losses to the stream measured for flow-weighted, composite samples collected approximately once every three weeks for the period 1978 to 2007, except DOC for which the period of record is 1992 to 2007 [*Johnson and Fredriksen*, 2011]. A 30-m resolution Digital Elevation Model of the H.J. Andrews's watershed 10 [*Valentine and Lienkaemper*, 2005] was used to compute flow direction, delineate watershed boundaries, and generate a channel network. Each 30x30-meter soil column was divided into 4 layers and was assumed to have an average soil column depth to bedrock of 2m [*Ranken*, 1974]. The dominant soil texture was specified as loam [*Ranken*, 1974]. Porosity, field capacity and wilting point values were obtained following *Dingman*, [1994].

4.5.2. Simulation Methods

Three WS10 simulations were conducted to simulate and analyze catchment biogeochemical responses to fire and harvest: First, a post-fire "build-up" simulation from 1525 to 1968, then an old-growth simulation from 1969 to 1974, and finally, a post-harvest simulation from 1975 to 2008 (Figure 4.2). For all simulations, model hydrological parameters have been previously calibrated to reproduce the observed daily streamflow for the period 1969 to 2008 [*Abdelnour et al.*, 2011]. Hydrological parameter names, values and references can be found in Table 3.A.1 and Table 3.A.2 of Chapter 3.

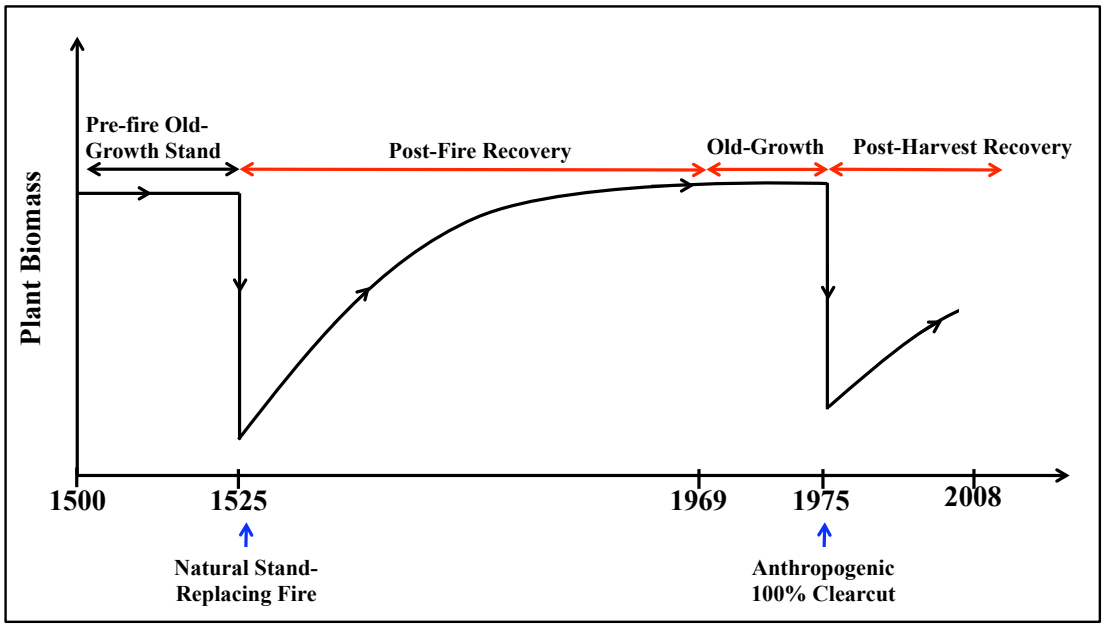

Figure 4.2: *Schematics of the historical events that shaped the landscape in WS10: a natural stand-replacing fire that occurred in 1525 A.D.* [*Wright et al.*, 2002] *and a 100% man-made clearcut in 1975. The three periods of interest are: a) the post-fire recovery period from 1525 to 1968, b) the old-growth period (1969-1974) chosen at the end of the post fire recovery period where temperature and precipitation data are available to drive the model, and c) the post-harvest period from 1975 to 2008*

1) *A post-fire "build-up" simulation* was conducted for the period 1525-1968 (Figure 4.2). This simulations was conducted in order to identify, through calibration, a single set of parameters that captures the accumulation of ecosystem C and N stocks following a stand-replacing fire in 1525 A.D. [*Grier and Logan*, 1977; *Wright et al.*, 2002] to 1968. Daily temperature and precipitation drivers were constructed from a

continuous loop of the available 1969 to 2008 observed climate station data. Typically following stand-replacing fires a large fraction of plant biomass is converted from live to dead matter [*Janisch and Harmon*, 2002], and a much smaller fraction is combusted as CO_2 [*Mitchell et al.*, 2009]. Consequently, there is a correspondingly large increase in coarse detrital matter that decomposes slowly during the decades following fire [*Janisch and Harmon*, 2002]. Therefore, the post-fire simulation was initialized by (1) reducing the initial live plant biomass value to 1% of its pre-fire old-growth value [*Wright et al*., 2002], (2) converting the dead plant biomass into detrital (soil) organic carbon [*Wright et al*., 2002], and (3) reducing the transpiration rate to zero initially, followed by an asymptotic increase to pre-disturbance values within 50 years [*Abdelnour et al*., 2011]. The 1525 initial conditions of plant biomass and soil organic carbon are $450gCm^{-2}$ and $70000gCm^{-2}$, respectively. Model parameters such as plant uptake rate, plant mortality rate, and soil organic carbon decomposition rate were calibrated to achieve a biomass buildup trajectory (1525-1968) that passed through observed chronosequence data taken at WS10 and other PNW forest ecosystems [*Grier and Logan*, 1977; *M Harmon et al.*, 2004; *Janisch and Harmon*, 2002; *Smithwick et al.*, 2002; *Sollins and McCorison*, 1981; *Sollins et al.*, 1980] (Table 4.1). Calibration parameters determined from this post-fire "build-up" simulation were then considered fixed for all subsequent WS10 simulations. A detailed description of the catchment biogeochemical dynamics associated with this calibration simulation is provided in section 4.6.1. Biogeochemical parameter names, values and references are provided in Tables 4.B.1.

2) *An old-growth simulation* was conducted for the period 1969-1974 (Figure 4.2) to explore daily, seasonal, and annual changes in C and N dynamics when the ecosystem was close to steady state conditions [*Sollins et al.*, 1980]. Initial values of plant biomass, SOC, NH_4, NO_3, DON and DOC pool were determined from the 1525-1968 post-fire simulation. A detailed description of the simulated nutrient flux dynamics for the old-growth period is provided in section 4.6.2.

3) *A post-harvest simulation* was conducted for the period 1975-2008 (Figure 4.2) in order to explore the impact of clearcut on measured and unmeasured nutrient losses, soil heterotrophic respiration, and N_2-N_2O land-atmosphere emissions, amongst others. WS10 was a 100% clearcut in the spring of 1975. All trees and woody material larger

than 20cm in diameter or 2.4m in length were removed from the site [*Sollins and McCorison*, 1981; *Halpern and Spies*, 1995]. The residual plants after the 1975 clearcut consisted of understory shade tolerant plants and shrubbery, undamaged by harvest [*Grier and Logan*, 1977; *Gholz et al.,* 1985]. To mimic the 1975 spring clearcut, the initial live plant biomass value was reduced to 10% (~ 4,500 gCm^{-2}) of its pre-harvest value [*Gholz et al.,* 1985; *Lee et al*., 2002] and the soil organic carbon pool was increased by 10% to account for new inputs of dead roots and stumps (all other plant biomass was assumed to have been removed from the site as logs) [*Grier and Logan*, 1977; *Gholz et al.,* 1985]. Plant transpiration rates were set to zero in 1975 and then increased asymptotically to pre-disturbance values within 50 years [*Abdelnour et al*., 2011]. A detailed description of the simulated nutrient fluxes dynamics for the post-harvest period is provided in section 4.6.3.

Table 4.1: Comparison of the post-fire simulation results, for the period 1960-1968, when the ecosystem is considered in steady state (i.e. old-growth condition) against observed old-growth values at other Pacific Northwest Forest.

Output Parameter	Simulated Mean Value	Simulated Range of Values	Observed Mean Value	Observed Range of Values	Reference
DIN Loss ($gNm^{-2}yr^{-1}$)	0.03	0.012-0.05	0.040	0.019-0.06	*Sollins et al.,* [1980]
DON Loss ($gNm^{-2}yr^{-1}$)	0.12	0.09-0.17	0.09	0.075-0.11	*Sollins and McCorison* [1981]
DOC Loss ($gCm^{-2}yr^{-1}$)	1.8	1.3-2.4	3.18	2.0-4.3	*Sollins and McCorison* [1981]
			3.000	1.0-10.0	*Grier and Logan* [1977]
Plant Biomass (gC/m^2)	42,500	42,300-42,600	39,807	34,800-44,800	*Harmon et al.,* [2004]
			45,500	14,700-60,600	*Smithwick et al.,*[2002]
			43,500	---	*Grier and Logan* [1977]
Soil Organic Carbon (gC/m^2)	25,600	25,500-25,800	22,092	20,600-23,600	*Harmon et al.,* [2004]
			19,000	---	*Grier and Logan* [1977]
			39,600	---	*Means et al.,* [1992]
			27,500	7,500-50,000	*Smithwick et al.,*[2002]
Total Carbon Storage (gC/m^2)	68,100	67,800-68,400	61,899	56,600-67,700	*Harmon et al.,* [2004]
			62,400	---	*Grier and Logan* [1977]
Heterotrophic Soil Respiration ($gCm^{-2}yr^{-1}$)	488	457-549	577	479 to 675	*Harmon et al.,* [2004]
Denitrification Rate ($gNm^{-2}yr^{-1}$)	0.05	0.04-0.06	0.04	0.03-0.09	*Schmidt et al.,* [1988]
			0.013	0.008-0.021	*Binkley et al.,* [1992]
NPP ($gCm^{-2}yr^{-1}$)	498	463-563	597	453 to 741	*Harmon et al.,* [2004]
			544	---	*Grier and Logan* [1977]
NEP ($gCm^{-2}yr^{-1}$)	9	5-10	20	(-116) to (+156)	*Harmon et al.,* [2004]
			44	---	*Grier and Logan* [1977]

4.6. Simulation Results and Discussion

Results and discussion are generally presented in the following sequence: (1) changes in plant biomass and SOC, (2) changes in dissolved organic and inorganic C and N losses to the stream, (3) changes in gaseous losses of C and N to the atmosphere, and (4) changes in net primary production (NPP) and net ecosystem production (NEP).

4.6.1. Post-fire "build-up" of Ecosystem C and N Stocks (1525-1968)

4.6.1.1. Post-Fire Plant Biomass and SOC (1525-1968)

Post-fire simulated plant biomass increased from the 1525 value of 450gCm^{-2} at an average rate of 580gCm^{-2}yr^{-1} for the first 30 years and at a rate of 300 gCm^{-2}yr^{-1} for the next 70 years (Figure 4.3). Thereafter, simulated plant biomass gradually leveled off, reaching an old-growth value of ~ 42,500gCm^{-2} after approximately 400 years. Post-fire SOC decreased exponentially from the 1525 value of 70,000 gCm^{-2} as a result of high decomposition and low detritus input to the soil, and reached its lowest level after about 100 years (Figure 4.3). At that point, re-growing plant biomass provided increasing amounts of detritus input to the soil, thereby replenishing the soil carbon pool. Soil carbon subsequently rose and stabilized at ~25,600gCm^{-2}, 300 years into the simulation (Figure 4.3). Simulated post-fire recovery of plant biomass and SOC were generally consistent with observed successional changes in live and dead wood carbon stores in other forests of the PNW [*Janisch and Harmon*, 2002; *Spies et al.*, 1988; *Turner et al.*, 2004]. However, early (less than 100 years old) simulated successional rates of increase in plant biomass exceeded the reported observed values by *Janisch and Harmon*, [2002] (see Figure 4.3). In figure 4.3, observed data for all stands less than 100 years old were after clearcut, whereas all stands older than 100 years were after a stand replacing fire. As a result, the difference between observed and simulated early successional plant biomass may owe in part to the greater amount of nitrogen released from decomposing detritus following fire than after clearcut.

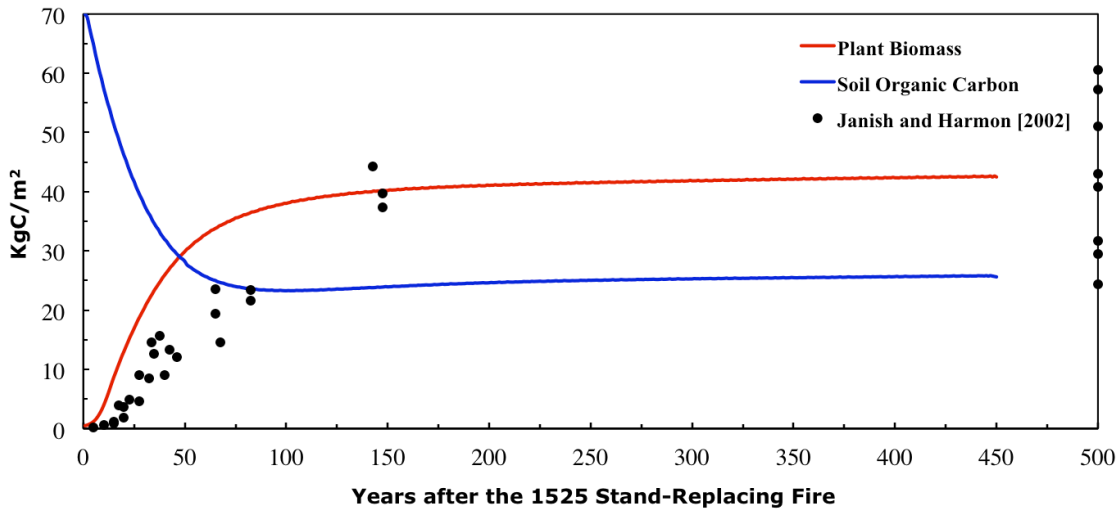

Figure 4.3: *Simulated biomass (red-line) and soil organic carbon (blue-line) recovery after the 1525 A.D. stand-replacing fire. The black-dots are the observed [Janisch and Harmon, 2002] accumulation of bole biomass (multiplied by 1.3 to get total plant biomass) for a 500-year chronosequence of 36 Pseudotsuga-Tsuga dominated forest stands in southwestern Washington State. The x-axis is years since disturbance or age of the stand.*

4.6.1.2. Post-Fire Dissolved C and N losses (1525-1968)

Post-fire losses of dissolved C and N to the stream increased as a result of high SOC decomposition, low levels of plant N uptake prior to significant re-establishment of plant biomass, and high subsurface flow. Specifically, simulated DIN losses peaked (~ 15$gNm^{-2}yr^{-1}$) three years after the fire and averaged 10$gNm^{-2}yr^{-1}$ (~300-fold increase) over the first five years after disturbance. Thereafter, DIN losses decreased exponentially and were within 20% of the equilibrium value (~ 0.036$gNm^{-2}yr^{-1}$) after 250 years. DON losses increased slightly immediately after fire and then approached equilibrium (~ 0.13$gNm^{-2}yr^{-1}$) within 100 years. DOC losses peaked (~ 10$gCm^{-2}yr^{-1}$) immediately after fire and then decreased exponentially and approached equilibrium within 100 years. Post-fire changes in dissolved C and N losses to the stream are generally consistent with measured impacts of fire on nutrient losses [*Carignan et al.*, 2000; *Chanasyk et al.*, 2003; *Williams and Melack*, 1997]. However, our simulated DIN losses were generally higher than the observed post–fire DIN losses to the stream [*Carignan and al.,* 2000; *Williams*

and Melack, 1997]. This may be due to our simplifying assumption that the stand-replacing fire does not impact and reduce soil nitrogen pool as a result of combustion and convection losses. However, *Grier* [1975] found that N losses from the forest soils due to convection and combustion reached 907kgN/ha or 39% of total N during a stand-replacing fire in a mixed-conifer forest in north central Washington.

4.6.1.3. Post-Fire Gaseous C and N losses (1525-1968)

Post-fire simulated gaseous losses of C and N increased as a result of high SOC decomposition, high soil water content, and low levels of plant N uptake. Specifically, simulated soil heterotrophic respiration (R_h) followed a similar trajectory as SOC, peaking ($1500gCm^{-2}yr^{-1}$) in the year 1525, and then falling exponentially until reaching its lowest value 120 years after disturbance (Figure 4.4). Thereafter, R_h increased with increasing SOC and reached an equilibrium value of ~ $488gCm^{-2}yr^{-1}$. Post-fire simulated soil denitrification rates (N_2 and N_2O emissions to the atmosphere) increased rapidly and peaked 8 years after disturbance. Thereafter, soil denitrification decreased exponentially due to a reduction in soil nitrate availability and reached a steady state value of ~ $0.06gNm^{-2}yr^{-1}$ approximately 300 years into the simulation. Similar results were found by *Turner et al.,* [2003] who used the carbon cycle model, Biome-BGC, to explore the temporal dynamics of carbon fluxes in two western Oregon watersheds. *Turner et al.,* [2003] found that R_h peaked (~ $1300gCm^{-2}yr^{-1}$) at the onset of the disturbance, then decreased exponentially and reached equilibrium value (~ $600gCm^{-2}yr^{-1}$) within 200 years.

4.6.1.4. Post-Fire NPP and NEP (1525-1968)

As a result of vegetation removal and the large soil decomposition-driven losses of C as CO_2 to the atmosphere and as DOC to the stream, the initial 1525 post-fire simulated value of NPP and NEP was $90gCm^{-2}yr^{-1}$ and $-1500gCm^{-2}yr^{-1}$, respectively (Figure 4.4). Thereafter, simulated NPP increased with increasing N availability in the soil, reached a peak value of ~ $1300gCm^{-2}yr^{-1}$ 14 years after fire, then decreased exponentially due to the decrease in N availability, and finally reached a stable value of ~ $500gCm^{-2}yr^{-1}$ within 200 years. Similarly, post-fire simulated NEP increased with the rapid regrowth of plant

biomass and became positive, peaking at ~150gCm^{-2}yr^{-1} after only 15 years. Thereafter, NEP decreased exponentially, reaching a steady state average equilibrium value of ~9gCm^{-2} after 200 years. Post-fire changes in NPP and NEP are generally consistent with a variety of chronosequence observations and modeling studies (Figure 4.5) [e.g. *Luyssaert et al.,* 2008*; Turner et al.,* 2003; *Hicke et al.,*2003*; Law et al.,* 2001, and *Janisch and Harmon*, 2002, amongst others]. For example, *Turner et al.,* [2003] used the Biome-BGC model to analyze forest carbon dynamics in the H.J. Andrews forest and found that 1) NPP was near zero early in succession, increased and reached 1200gCm^{-2}yr^{-1}, 15 years after disturbance, then decreased exponentially and reached an equilibrium value of ~ 620gCm^{-2}yr^{-1} within 200 years, and 2) NEP was strongly negative (~ -1300gCm^{-2}yr^{-1}) at the onset of the disturbance, peaked at ~ 700gCm^{-2}yr^{-1} 15 years after disturbance, then decreased exponentially and reached an equilibrium value of ~ 20gCm^{-2}yr^{-1} within 200 years.

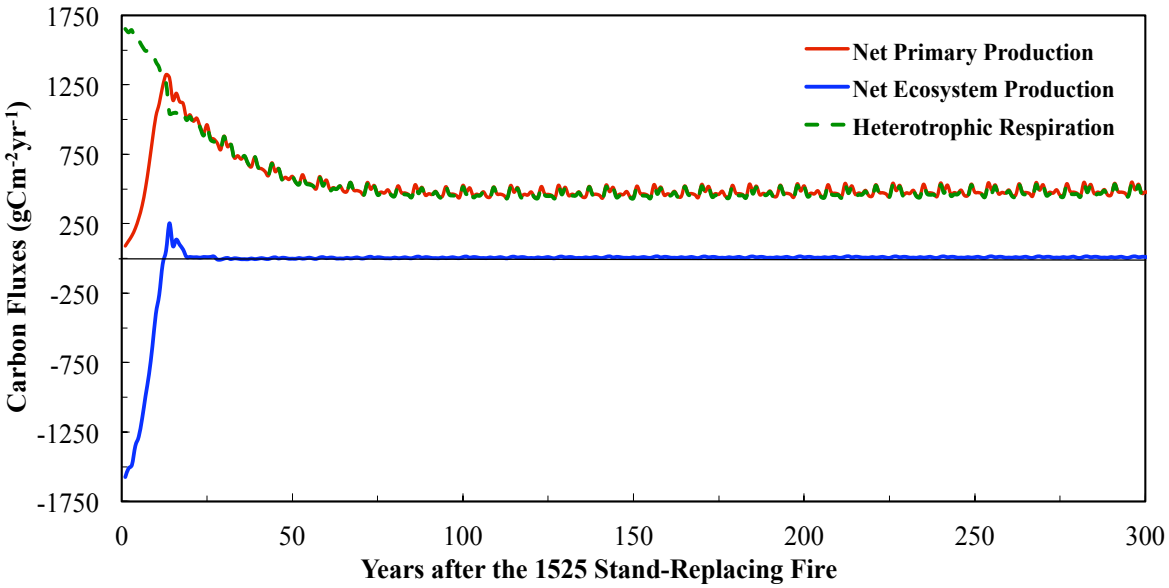

Figure 4.4: *Simulated net primary production (red-line), net ecosystem production (blue-line) and soil heterotrophic respiration (green dashed line) recovery after the 1525 A.D. stand-replacing fire. The x-axis is years since disturbance or age of the stand.*

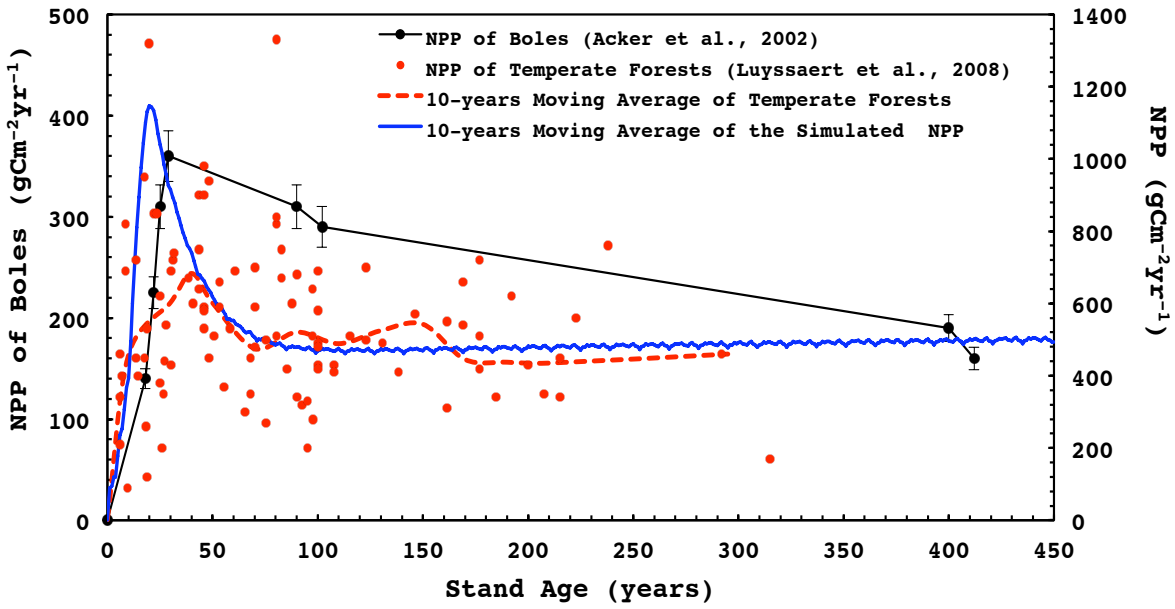

Figure 4.5: *Comparison between the simulated post-fire 10-year moving average of ecosystem net primary production NPP (blue-line) and the observed (1) NPP of temperate forests (red dots are individual forest stands sampled throughout the world; dashed red line is a 10-year moving average)* [*Luyssaert et al.*, 2008], *and (2) NPP of boles for Pacific Northwest coniferous forests (black dots and solid black line) as a function of stand age (i.e. time after stand-replacing disturbance)* [*Acker et al.*, 2002].

4.6.2. Old-Growth Biogeochemical Dynamics (1969-1974)

At daily time scales, simulated nutrient losses were generally high in the wet season and low in the summer dry season. Specifically, simulated daily NH_4 losses averaged 0.06mgNm^{-2}day^{-1} and were strongly correlated to precipitation (R^2=0.8) and stream discharge (R^2=0.6). NH_4 losses peaked in fall and winter with the peaks in streamflow and reached 1.2mgNm^{-2}day^{-1}. Summer NH_4 losses were low, averaging 0.03mgNm^{-2}day^{-1}. Simulated daily NO_3 losses averaged 0.02mgNm^{-2}day^{-1} and were strongly correlated to streamflow (R^2=0.7), but weakly correlated to precipitation (R^2=0.4). Simulated NO_3 losses were largest (1) in the summer as a result of high nitrification rates, and (2) in the fall, at the onset of the rainy season when hydrological connectivity within hillslopes is re-established and nutrients accumulated in soils during drier summer months are more readily flushed downslope [*Creed et al.*, 1996; *Stieglitz et*

al., 2003]. Simulated daily DOC and DON losses averaged 7.6mgCm^{-2}day^{-1}, and 0.5mgNm^{-2}day^{-1}, respectively, and were strongly correlated to stream discharge (R^2=0.8 and 0.9, respectively). DOC and DON losses peaked with peakflow, reaching 115.5mgCm^{-2}day^{-1} and 6.7mgNm^{-2}day^{-1}, respectively, and were largest in fall and winter. In the summer season, DOC and DON losses were minimal and averaged 0.8mgCm^{-2}day^{-1} and 0.05mgNm^{-2}day^{-1}, respectively. Similar results have been found by *Vanderbilt et al.,* [2003], who analyzed long-term organic and inorganic nitrogen outputs in stream water in six watersheds at the H.J. Andrews Experimental Forest in Oregon. They found that NH_4, NO_3 and DON losses to the stream were correlated to stream discharge with a R^2 of 0.5, 0.5, and 0.8, respectively. Note: observed daily nutrient losses data for the period 1969 to 1975 were unavailable at WS10 for a comparison with our simulated daily values.

On an annual basis, simulated losses of dissolved inorganic nitrogen (NH_4 and NO_3) averaged 0.03gNm^{-2}yr^{-1} with NH_4 losses being three times NO_3 losses to the stream (NO_3/NH_4 ~33%). Specifically, simulated annual NO_3 and NH_4 losses averaged 0.008gNm^{-2}yr^{-1} and 0.023gNm^{-2}yr^{-1}, respectively. Simulated annual DON losses averaged 0.14gNm^{-2}yr^{-1} and accounted for 81% of the nitrogen that reached the stream (DON/DIN = 4.4). Simulated annual DOC losses averaged 2.9gCm^{-2}yr^{-1} and ranged between 1.7 and 4.5 gCm^{-2}yr^{-1}. These simulated old-growth nutrient fluxes were consistent with other studies of the biogeochemical dynamics of old-growth forests in the PNW (Table 4.2). For example, *Sollins and McCorison* [1981] measured nitrogen and carbon solution chemistry in WS10 before the 1975 clearcut, and found that, in an undisturbed watershed, NH_4 accounted for 18 to 33% of total dissolved nitrogen, DON accounted for the rest, and NO_3 concentration was very low. Similarly, *Fredriksen* [1975] found that nitrogen losses in undisturbed forests are small and occur primarily as DON.

Table 4.2: Comparison of simulation results from the old-growth simulation against observed values at WS10 and other old-growth Pacific Northwest Forests.

Output Parameter	Simulated Mean Value	Observed Mean Value	Reference
NH_4 Loss ($gNm^{-2}yr^{-1}$)	0.023 (0.018-0.03)	0.01	*Vanderbilt et al.,* [2003]
NO_3 Loss (gN/m^2yr)	0.008 (0.003-0.01)	0.01 (0.009-0.011)	*Martin and Harr* [1989]
		0.003	*Vanderbilt et al.,* [2003]
DIN Loss (gN/m^2yr)	0.032 (0.02-0.04)	0.04 (0.01937-0.06)	*Sollins et al.,* [1980]
DON Loss (gN/m^2yr)	0.14 (0.12-0.18)	0.089 (0.0745-0.1043)	*Sollins and McCorison* [1981]
DOC Loss (gC/m^2yr)	2.94 (1.7-4.54)	3.178 (2.015-4.34)	*Sollins and McCorison* [1981]
		3 (1-10)	*Grier and Logan* [1977]
$\frac{NH_4\ Loss}{NO_3\ Loss}$	3	2	*Vanderbilt et al.,* [2003]
$\frac{NH_4\ Loss}{Total\ N\ Loss}$	14%	18-33%	*Sollins and McCorison* [1981]
$\frac{DON\ Loss}{Total\ N\ Loss}$	81%	80%	*Vanderbilt et al.,* [2003]
$\frac{DOC\ Loss}{DON\ Loss}$	21 (14-36)	21-52	*Cairns and Lajtha* [2005]
Q vs DON	R^2=0.8	R^2= (0.4-0.79)	*Vanderbilt et al.,* [2003]
Q vs NH_4	R^2=0.6	R^2= 0.51	*Vanderbilt et al.,* [2003]

4.6.3. Post-Harvest Biogeochemical Dynamics (1975-2008)

To explore the impact of the 1975 WS10 clearcut on C and N dynamics, we conducted two simulations: a post-harvest simulation for the period 1975 to 2008 (described in section 4.6.2), and a control simulation, over the same period, in which no vegetation is removed (i.e. soil and plant C and N dynamics are at steady state and similar to old-growth dynamics, Table 4.1 and 4.2). Post-clearcut simulated relative changes in C and N fluxes are presented in terms of the difference between the post-harvest simulation values and the control simulation values.

4.6.3.1. Post-Clearcut Plant biomass and SOC (1975-2008)

Simulated post-clearcut plant biomass increased rapidly at a rate of ~ $400gCm^{-2}yr^{-1}$ as a result of large early successional N uptake rates and N availability, and reached a value of ~ $16000gCm^{-2}$, thirty years after disturbance (Figure 4.6). Simulated post-clearcut SOC decreased as a result of high SOC decomposition and low detritus input

into the soil. Simulated SOC reached 55% of its initial value (~ 15000gCm^{-2}) thirty years after clearcut (Figure 4.6). Simulated recoveries of plant biomass and SOC were consistent with observed early successional changes in live and dead wood carbon stores in PNW forests [*Janisch and Harmon*, 2002; *Spies et al.*, 1988]. However, post-clearcut simulated successional rates of change in plant biomass and SOC exceeded the reported observed values by *Janisch and Harmon*, [2002]. *Janisch and Harmon*, [2002] found that live tree bole carbon stores increased after disturbance and reached ~ 7500gCm^{-2} (i.e. ~ 9500gCm^{-2} for total plant biomass), thirty years after disturbance. Moreover, *Janisch and Harmon*, [2002] found that coarse woody detritus carbon stores decreased after clearcut and reached 50% of its initial mass (~ 2800gCm^{-2}), thirty years after disturbance. Nevertheless, *Janisch and Harmon*, [2002] simulated old-growth values of live and dead carbon stores (31900gCm^{-2} and 7200gCm^{-2}, respectively) were generally at the lower end of the range reported for Oregon forests (29500-58500gCm^{-2} [*Grier and Logan*, 1977; *Harmon et al.,* 2004] and 12700-32600gCm^{-2} [*Grier and Logan*, 1977; *Harmon et al.,* 2004; *Means et al.,* 1992]).

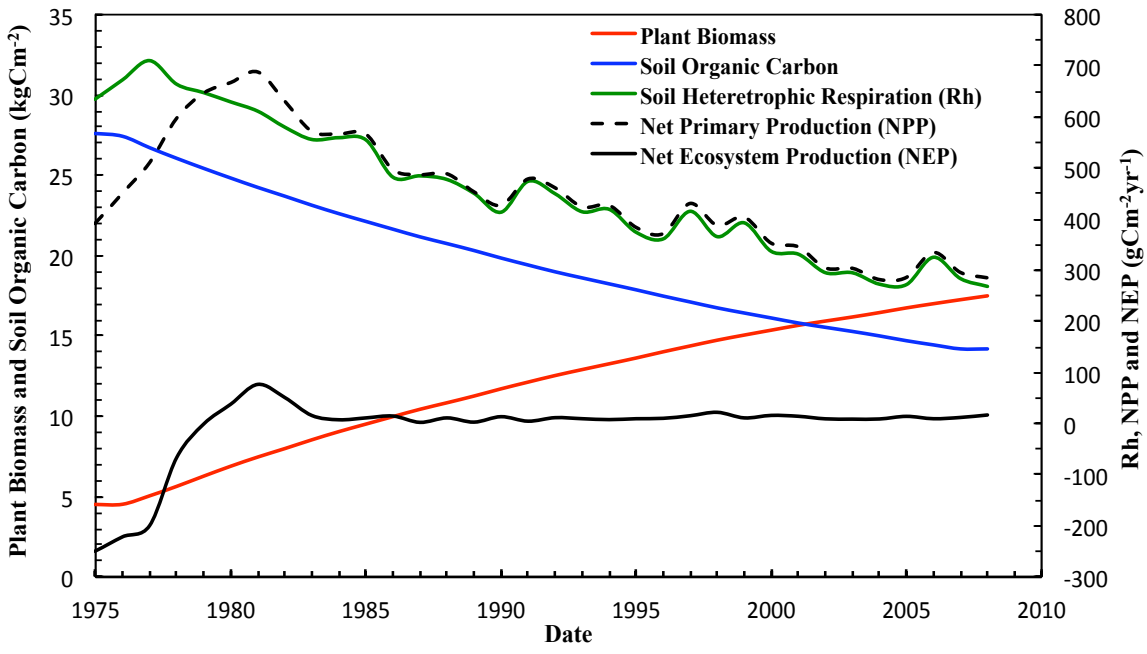

Figure 4.6: *Simulated recovery of plant biomass (kgCm^{-2}; red-line), soil organic carbon (kgCm^{-2}; blue-line), net primary production (gCm^{-2}yr^{-1}; black-dashed line), net ecosystem production (gCm^{-2}yr^{-1}; black-line), and soil heterotrophic respiration (gCm^{-2}yr^{-1}; green-line) after a 100% clearcut in 1975. The x-axis represents the 1975-2008 period of available precipitation and temperature data.*

4.6.3.2. Post-Clearcut Dissolved C and N losses (1975-2008)

Post-clearcut losses of dissolved inorganic N to the stream peaked a few years after disturbance as a result of high SOC decomposition, low levels of plant N uptake prior to significant re-establishment of plant biomass, and the increase in streamflow. Specifically, simulated annual NH_4 and NO_3 losses peaked 2 years after clearcut, and averaged $0.08 gNm^{-2}yr^{-1}$ (4-fold higher than control values) and $0.9 gNm^{-2}yr^{-1}$ (150-fold higher than control values), respectively, over the first five years. Thereafter, simulated annual NH_4 and NO_3 losses decreased as a result of a decreasing SOC pool and an increase in N uptake by plants, and reached $0.015 gNm^{-2}yr^{-1}$ (25% lower than control values) and $0.008 gNm^{-2}yr^{-1}$ (10% lower than control values), respectively, thirty years after clearcut. The simulated changes in NH_4 and NO_3 losses to the stream were consistent with observed data at WS10 (see Figure 4.7 and Table 4.3) as well as previously published studies of biogeochemical dynamics in recently clearcut old-growth forests [e.g. *Cairns and Latjtha* 2005; *Sollins and McCorison*, 1981; *Fredriksen* 1975]. For example, *Sollins and McCorison* [1981] found that NO_3 concentration increased as much as 100-fold, 7 to 18 months after the 1975 clearcut of WS10. *Fredriksen* [1975] found that following forest clearcut at two experimental watersheds in western Oregon, sharp increases in stream N concentrations were attributed to decreased plant N uptake and increased detritus N subject to mineralization into ammonium. *Vitousek and Reiners* [1975] found that vegetation removal by fire or forest harvest results in an immediate but transient flush of N to streams, which is quickly followed by tight retention of N in young vigorously growing stands.

Post-clearcut simulated dissolved organic C and N losses to the stream were driven by high SOC decomposition and high subsurface flow. Specifically, simulated annual DON and DOC losses peaked two years after clearcut, and averaged $0.15 gNm^{-2}yr^{-1}$ (~20% higher than control values) and $3.2 gCm^{-2}yr^{-1}$ (~18% higher than control values) over the first five years, respectively. Thereafter, simulated annual DON and DOC losses decreased with decreasing SOC and averaged $0.07 gNm^{-2}yr^{-1}$ (~30% lower than control values) and $1.1 gCm^{-2}yr^{-1}$ (~35% lower than control values) thirty years after clearcut, respectively. Changes in DON and DOC losses to the stream were consistent with

observed post-clearcut nutrients dynamics in WS10 (see Figure 4.7 and Table 4.3) and other PNW forests. *Cairns and Latjtha* [2005] found that DON and DOC losses in young watersheds were approximately 30% and 25% higher than in old watersheds. *Sollins and McCorison* [1981] found that DOC concentrations were higher in the clearcut watershed compared to the control watershed.

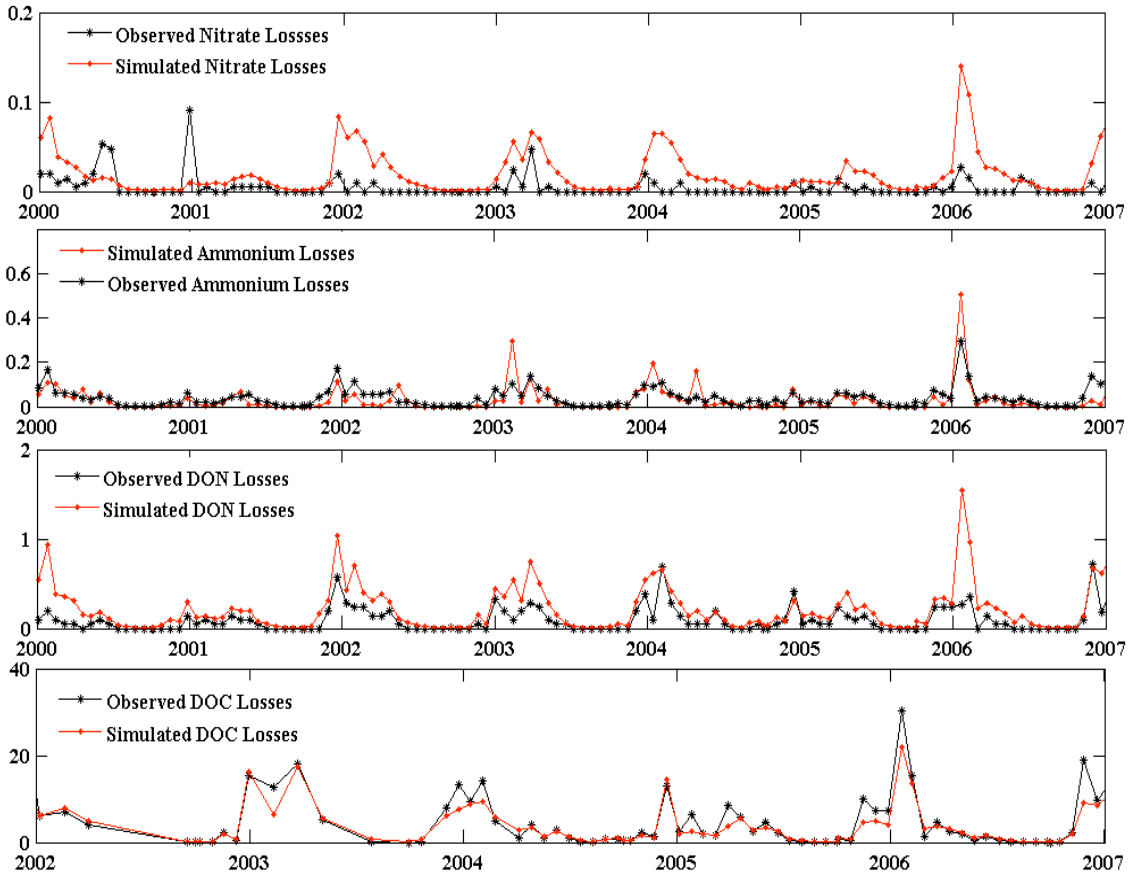

Figure 4.7: *Simulated (red-dots) versus observed (black-dots) nitrate NO_3 ($mgNm^{-2}$), ammonium NH_4 ($mgNm^{-2}$), DON ($mgNm^{-2}$), and DOC losses ($mgCm^{-2}$) to the stream after the 1975 clearcut of watershed 10 in the H.J. Andrews. The simulated values are averages over the same time interval as the observed values. The x-axis represents the selected set of data between 2000 and 2007 for nitrate, ammonium and DON losses and between 2002 and 2007.*

Table 4.3: Streamflow and nutrient losses modeling skills for the post-harvest period (1975-2008) (Observed daily streamflow from 1975 to 2008; Observed tri-weekly NH_4 ($mgNm^{-2}yr^{-1}$), NO_3 ($mgNm^{-2}yr^{-1}$), and DON ($mgNm^{-2}yr^{-1}$) losses from 1979 to 2007; Observed tri-weekly DOC ($mgCm^{-2}yr^{-1}$) losses from 2001 to 2007).

Parameter	Streamflow and Nutrient Losses Modeling Skills		
	Correlation Coefficient R^2	Baseline adjusted modified index of agreement d'_1	Root Mean Square Error RMSE
Streamflow	0.913	0.821	3.341
NH_4 Loss	0.7	0.52	0.02
NO_3 Loss	0.47	0.176	0.64
DON Loss	0.82	0.5	0.06
DOC Loss	0.94	0.84	0.19

4.6.3.3. Post-Clearcut Gaseous C and N losses (1975-2008)

Post-clearcut simulated gaseous losses of C and N increased as a result of high SOC decomposition, high soil water content, and low levels of plant N uptake prior to significant plant regrowth. Specifically, simulated annual denitrification rates and soil heterotrophic respiration (R_h) peaked two years after clearcut, and averaged $0.9gNm^{-2}yr^{-1}$ (~ 13-fold higher than control values) and ~ $710gCm^{-2}yr^{-1}$ (30% higher than control values) from 1975 to 1980, respectively (Figure 4.6). Thereafter, simulated annual denitrification rates and R_h decreased with increasing plant biomass, increasing N uptake, and decreasing SOC and soil water content. By 2005, thirty years after clearcut simulated annual denitrification rates and R_h averaged $0.07gNm^{-2}yr^{-1}$ (30% lower than control values) and $280gCm^{-2}yr^{-1}$ (40% lower than control values), respectively. The simulated changes in gaseous losses of C and N were consistent with previously published studies of biogeochemical dynamics in recently clearcut old-growth forests. For example, *Grant et al.,* [2007] used an ecosystem model *ecosys* [*Grant et al.,* 2001] to simulate the impact of clearcutting on R_h in an old-growth forest of the PNW, and found that R_h peaked (~ $1200gCm^{-2}yr^{-1}$) two years after clearcut and then decreased and reached ~ $350gCm^{-2}yr^{-1}$, 50 years after clearcut. *Griffiths and Swanson* [2001] measured the microbiological characteristics of forest soils in recently harvested and old-growth Douglas-fir in the HJA Forest, and found that the denitrification rate increased six-fold

five years after clearcut, then decreased and was 20% lower than old-growth values, for a 40-year-old stand.

4.6.3.4. Post-Clearcut NPP and NEP (1975-2008)

Post-clearcut simulated NPP and NEP decreased from an old-growth value of 498 $gCm^{-2}yr^{-1}$ and 9 $gCm^{-2}yr^{-1}$ respectively, as a result of vegetation removal, and large decomposition-driven losses of C as CO_2 to the atmosphere and as DOC to the stream (Figure 4.6). Specifically, simulated annual NPP decreased by 45%, to ~ $390gCm^{-2}yr^{-1}$ at the onset of clearcut, then increased with the rapid re-growth of plant biomass, and peaked (~ $700gCm^{-2}yr^{-1}$) seven years after clearcut. Thereafter, annual NPP decreased and reached an average value of ~ $300gCm^{-2}yr^{-1}$ (~ 45% lower than control values), thirty years after clearcut. Similarly, simulated annual NEP dropped to -$250gCm^{-2}yr^{-1}$ at the onset of the clearcut, peaked at $75gCm^{-2}yr^{-1}$ seven years after disturbance as a result of rapid regrowth of plant biomass, high N uptakes, and a decrease in soil C losses, and then decreased and reached $12gCm^{-2}yr^{-1}$, thirty years after clearcut. The simulated early successional trends in NPP and NEP are generally consistent with a variety of chronosequence simulations of recently clearcut forests of the PNW [e.g. *Grant et al.,* 2007; *Turner et al.,* 2004; *Janisch and Harmon*, 2002]. *Grant et al.,* [2007] simulated the change in NEP with forest age in a coastal Douglas–fir forest of the PNW, and found that NEP decreased (-$620gCm^{-2}yr^{-1}$) at the onset of the disturbance, then became positive, and peaked (~$450gCm^{-2}yr^{-1}$) ~ 18 years after clearcut. *Janisch and Harmon*, [2002] found that post-clearcut NEP was negative (-$250gCm^{-2}yr^{-1}$) at the onset of clearcut, increased and became positive 12 to 14 years after disturbance, then peaked at ~ $200gCm^{-2}yr^{-1}$, 50 to 70 years after disturbance. However, post-clearcut NEP values simulated by VELMA for WS10 were less than simulated NEP values of other PNW forest, and were negative for a shorter period of time. This difference might be due in part to 1) the simulated removal of slash and woody debris from the clearcut watershed, which has been found to hastened the recovery of simulated NEP [*Grant et al.,* 2007] and 2) VELMA's simplified assumption of a single stand instead of complex regenerating stands, which has been found to introduce a bias towards lower NEP [*Grant et al.,* 2007].

4.7. Conclusion

The ecohydrological model presented here, VELMA, provides a relatively simple, spatially distributed framework for assessing the effects of changes in climate, land-use (harvest, fire, etc.) and land cover on hydrological, ecological, and biogeochemical processes within watersheds. VELMA was used to provide process-level insights into the impact of forest fire and harvest on catchment biogeochemical fluxes at a small intensively studied catchment in the Pacific Northwest (WS10) – details that would be difficult or impossible to capture through experimentation or observation alone. Moreover, VELMA provides a framework for understanding how limited supplies of available N tightly constrains ecosystem responses (production and accumulation of biomass, net ecosystem production, etc.) to major disturbances in WS10, and perhaps, more generally for Douglas-fir dominated forests in the western Oregon Cascades of the Pacific Northwest. Although the impact of disturbances on catchment biogeochemical fluxes have already been investigated in earlier experimental studies [e.g., *Sollins and McCorison*, 1981; *Sollins et al*., 1980, *Vitousek and Reiners,* 1975; *Vitousek et al*., 1979; amongst others), the interaction of hydrological and biogeochemical processes represented in VELMA provide additional insight into how feedbacks among the cycles of C, N and water regulate N supplies. The main insights from this exercise included the following:

1) Following fire and harvest, nutrient losses from the terrestrial system to the stream were tightly constrained by the hydrological cycle, particularly at the hillslope scale. Losses of NH_4, DON, and DOC to the stream were primarily driven by wet-season rain events that were large enough to generate hydrologic connectivity and flushing of nutrients down hillslopes. By contrast, losses of nitrate to the stream were less predictable, owing to complex spatial and temporal patterns of nitrification and denitrification (e.g., hillslope vs. riparian zone).

2) Gaseous losses of C and N to the atmosphere, following disturbance, were primarily driven by high soil water content, high soil organic carbon decomposition, and low N uptake. Specifically, post-disturbance increase in soil moisture and nitrate availability enhanced the anaerobic process of soil denitrification and substantially

increased N_2-N_2O emissions to the atmosphere, whereas post-disturbance increase in soil organic carbon decomposition enhanced soil heterotrophic respiration and increased CO_2 emission to the atmosphere.

3) Beyond the short-term loss of N after fire, the supply of available N for vegetation regrowth was enhanced by the decades-long release of N from the large pulse of decomposing bole wood killed by the fire. In contrast, the regrowth of plant biomass following the 1975 A.D. clearcut was about 30% lower than the rate of regrowth after fire, owing to the large loss of N in harvested bolewood, into the stream and to the atmosphere, as well as a rather small increase in detritus N from decomposing roots.

Although this exercise is intended to illustrate how a process-based ecohydrological modeling framework can provide useful insights into ecosystem responses to disturbance, we emphasize that VELMA uses a simplified modeling approach with comparatively few parameters and data input requirements. While one of our objectives is to provide a framework that can be efficiently scaled up to much larger watersheds and times scales of interest to land managers and policymakers, it is important to examine a few of the simplifying assumptions we made to conduct this study. The following three points are a brief summary of watershed characteristics relevant to biogeochemical processes and nutrient export that are not addressed in this study.

1) *Multiple species*: Aboveground and belowground biomass as well as the different species that usually populate a forested watershed is simplified by using an aggregated biomass pool. However, co-existing grass, shrubs and trees compete for nutrients, moisture and energy (i.e. interspecific competition) [*Rozzell*, 2003; *West and Chilcote*, 1968]. As a result, species tend to be spatially distributed based on their tolerance to local conditions (soil water content, nutrient availability, energy, amongst others) [*Van Breemen et al.*, 1997]. *Gholz et al.,* [1985] found that, a few years after clearcut, the riparian zone in WS10 had the greatest annual increase in biomass and was dominated by *Aralia californica*, whereas *Senecio sylvaticus* dominated the midlands. This spatial variability in biomass accumulation and species affects biogeochemical process such as nutrient uptakes and nutrient fixation, leads to higher nutrient uptakes in the lowlands, which in turn reduces nutrient losses to the stream. Incorporating multiple

species and their interactions in VELMA would reduce the amount of simulated nitrogen that reaches the stream and would allow exploration of post-harvest successional changes in the spatial and temporal distribution of species within watersheds.

2) *In stream processes*: Our simulations assume that the stream nutrient concentration reflects forest processes and do not include in-stream processes. In-stream processes are responsible for temporary retention and recycling of nutrients by a wide variety of physical, chemical and biological mechanisms [*Bilby and Likens*, 1980; *Triska et al.*, 1984; *Wallace and Benke*, 1984] such as adsorption mechanisms, algae uptake, benthic release, denitrification, and decomposition, among others [*Bernot and Dodds*, 2005], and are usually important for large watersheds and short time scales [*Tague and Band*, 2004]. *Peterson et al.,* [2001] found that in-stream processes such as nitrification rates in a third–order stream in the H.J. Andrews Experimental forest is responsible for the removal of 40% of the ammonium losses that reach the stream. Although the incorporation of in-stream processes in VELMA is beyond the scope of this paper, doing so would provide a more accurate representation of mechanisms controlling catchment-scale N export. In its present configuration, VELMA is calibrated to provide a best fit for observed N export at a particular stream sampling point, typically a stream gauging station. Thus, in-stream processes affecting measured concentrations of dissolved N are implicitly included in this model calibration. Consequently, an explicit treatment of in-stream processes would require recalibration of the terrestrial processes controlling N transport to the stream.

3) *N fixation*: VELMA does not include the effect of N fixation on plant biomass dynamics and N cycling. N fixation can be an important source of N input into Pacific Northwest coniferous forests [*Sollins et al.*, 1980], and usually occurs during early successional stages following disturbance, when N fixing plants and microorganisms tend to be more abundant [*Rastetter et al.*, 2001]. However, this simplification is acceptable for WS10 given the low abundance of N fixers in the young, post-harvest forest. *Gholz et al.,* [1985] found that post clearcut N fixers such as red alder (*Alnus rubra*) and snowbush (*Ceanothus veluntinus*) were sparse and limited to the riparian zone of WS10.

For some applications, the explicit treatment of these processes may be needed. However, it must be recognized that such added processes come at the cost of increased model complexity, computational efficiency, and applicability to larger spatial and temporal scales. These are important tradeoffs to consider, given that data needed to implement complex models are not generally available.

4.8. Appendix A: Model Description

VELMA is a spatially distributed ecohydrology model that accounts for hydrologic and biogeochemical processes within watersheds. The model simulates daily to century-scale changes in soil water storage, surface and subsurface runoff, vertical drainage, carbon and nitrogen cycling in plants and soils, as well as transport of nutrients from the terrestrial landscape to the streams. VELMA consists of multi-layered soil column models that communicate with each other through the downslope lateral transport of water and nutrients (Figure 4.A.1). Each soil column model consists of three coupled sub-models: a hydrological model, a soil temperature model, and a plant-soil model. Described below are the soil temperature and plant-soil component of the model. The hydrological component was described in a previous manuscript [*Abdelnour et al.,* 2011]. First, we describe the soil column model and then place this soil column within a catchment framework.

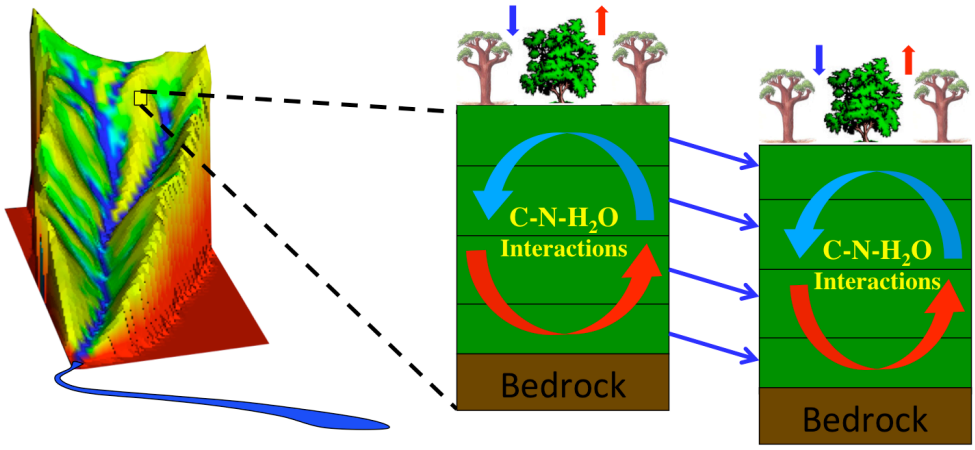

Figure 4.A.1*: Conceptual catchment modeling framework using multi-layered soil columns.*

4.8.1. Soil Column Framework

We employ a multi-layer soil column as a fundamental hydrologic and ecological unit. The soil column consists of *n* soil layers (Figure 4.A.2 and 4.A.3). Soil water balance, soil subsurface temperature and soil C and N pools are computed for each layer.

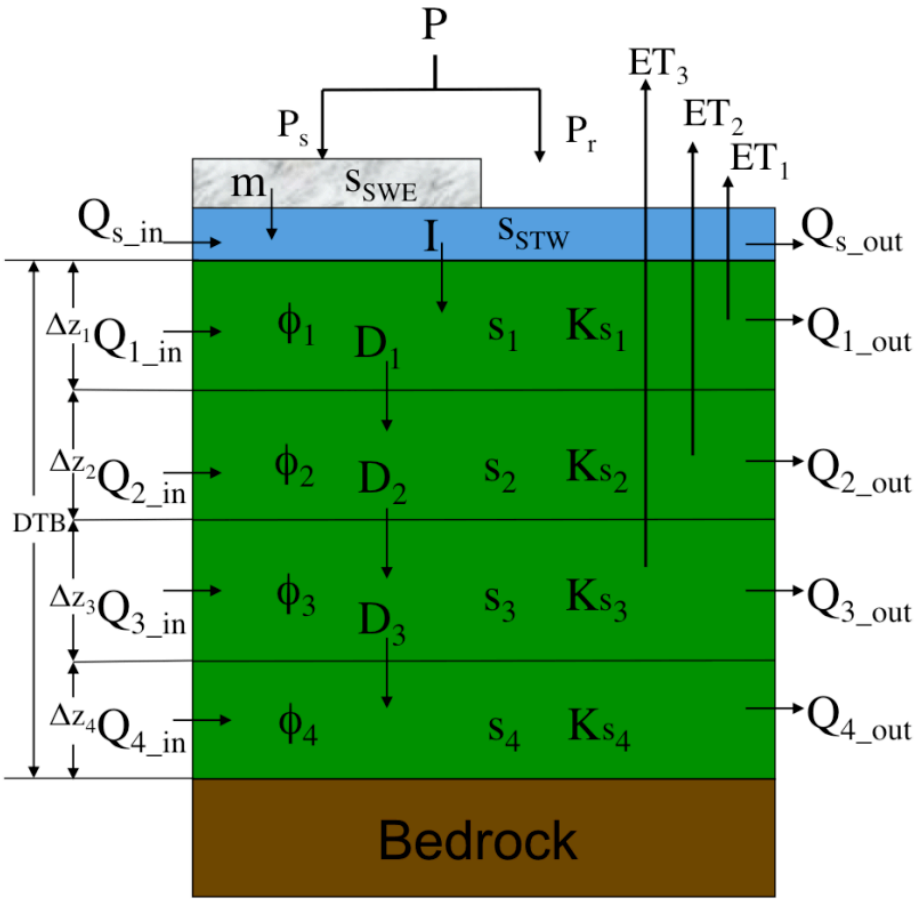

Figure 4.A.2*: The soil column hydrological framework consists of 4-layer soil column, a standing water layer, and a snow layer. DTB is the soil column depth to bedrock.* Δz_i, Ks_i, ϕ_i, *and* s_i, *are the thickness, the saturated hydraulic conductivity, the soil porosity, and the soil water storage of layer i, respectively;* P, P_s *and* P_r, *are the precipitation, snow, and rain, respectively;* m *is the snowmelt and* s_{SWE} *is the snow water equivalent depth;* I *is the infiltration and* s_{STW} *is the standing water amount;* Q_s *is the surface runoff;* Q_i, D_i *and* ET_i, *are the subsurface runoff, the drainage and the evapotranspiration of layer i, respectively.*

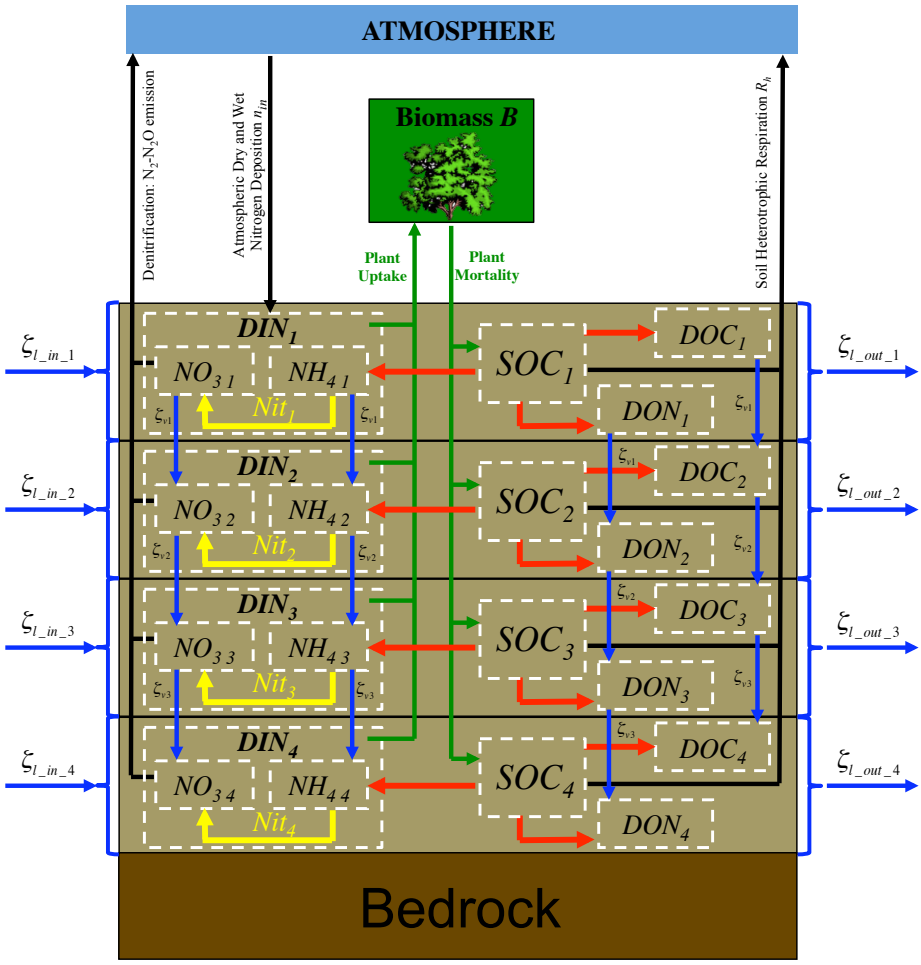

Figure 4.A.3: *The soil column biogeochemical framework simulates ecosystem carbon storage and the cycling of carbon and nitrogen between a plant biomass layer and a 4-layer soil column. B is the aboveground and belowground plant biomass. DIN_i is the dissolved inorganic nitrogen pool in layer i. The DIN pool consists of a nitrate pool and an ammonium pool, and constitutes the available soil nitrogen for plant uptake. Nit_i is the ammonium nitrification into nitrate in layer i (Yellow Arrow). The NO_3 pool decomposes through denitrification, which releases N_2-N_2O gases into the atmosphere. n_{in} is the atmospheric wet and dry nitrogen deposition and is accounted for in the first layer nitrogen pool. DON_i and DOC_i are the dissolved organic nitrogen and carbon pool in layer i, respectively. SOC_i is the soil organic carbon pool in layer i. Plant mortality is a source of carbon into the SOC pool. The SOC pool decomposes through soil microbial activity into DON, DOC, and NH_4 (Red Arrows). Soil heterotrophic respiration R_h from SOC decomposition in each layer i is released into the atmosphere. NO_3, NH_4, DON and DOC are soluble and transported through water drainage from layer i to layer i+1, and through subsurface runoff from layer i of the soil column to layer i of a downslope soil column (Blue Arrows). $\xi_{v,i}$ is the vertical losses of nutrients from layer i to layer i+1. $\xi_{l\_in\_i}$ and $\xi_{l\_out\_i}$ are the lateral soluble nutrients in and out of layer i.*

4.8.1.1. The Soil Temperature Model:

The soil temperature model first simulates the ground surface temperature (*GST*) from the available mean surface air temperature (T_a) in the presence of snow cover.

The ground surface temperature is calculated as follows:

$$GST(t) = T_a \times e^{\left(\frac{SD(t)}{\lambda_{snow}}\right)} \tag{4.1}$$

where *SD(t)* is the snow depth (*mm*) at time *t* and λ_{snow} is the seasonal damping depth for snow which is approximately equal to 670 mm [*Hillel*, 1998] for a snowpack of density 300kgm^{-3}. In this model, snow is an insulative material that only attenuates the mean surface air temperature signal [*Cheng et al.*, 2010]. The attenuation of the T_a signal is assumed proportional to the depth of the snowpack [*Cheng et al*., 2010]. As a result, during snow free periods, the ground surface temperature is assumed equal to the mean surface air temperature: *SD* = 0, *GST* = T_a.

Subsurface heat transfer is then simulated using the analytical solution of the one-dimensional heat conduction equation [*Carslaw and Jaeger*, 1959; *Hillel*, 1998].

The subsurface soil temperature in layer *i* is calculated as follows:

$$T_{s,i}(d_i, t) = \overline{GST} + \left(GST\left(t - \phi(d_i, t)\right) - \overline{GST}\right) \times e^{\left(-\frac{d_i}{\lambda(t)}\right)} \quad i = 1,2 \ldots n \tag{4.2}$$

where $\overline{GST}$ is the annual mean soil temperature (°C), d_i is the soil depth to the middle of layer *i* (mm), $\phi(d_i, t)$ is the phase lag of $T_{s,i}$ relative to *GST* at depth d_i:

$$\phi(d_i, t) = \left(\frac{d_i}{\lambda(t)} \times \frac{360}{(2 \times \pi)}\right) \quad i = 1,2, \ldots n \tag{4.3}$$

and $\lambda(t)$ is the damping depth of the soil (mm), defined as the characteristic depth at which the temperature signal is attenuated to *1/e* of the *GST*. $\lambda(t)$ is function of the thermal properties of the soil and the frequency of the temperature fluctuation:

$$\lambda(t) = \left(\frac{2D_h(t)}{w}\right)^{\frac{1}{2}} \tag{4.4}$$

where $D_h(t)$ is the time dependent thermal diffusivity of the soil (mm^2/day) and is function of the simulated soil moisture $\left(\frac{s_i}{s_i^{max}}\right)$ [*De Vries*, 1975]. For each layer *i* of the soil column:

$$D_h(t) = \left(19.45\times10^{-3}\right)\times\left(\frac{s_i}{s_i^{\max}}\right)+2\times10^{-3} \qquad for\left(\frac{s_i}{s_i^{\max}}\right)<0.18$$
$$D_h(t) = \left(-4.055\times10^{-3}\right)\times\left(\frac{s_i}{s_i^{\max}}\right)+6.23\times10^{-3} \qquad for\left(\frac{s_i}{s_i^{\max}}\right)\geq 0.18 \qquad i=1,2,\ldots n \qquad (4.5)$$

and w is the frequency of annual temperature fluctuation (day^{-1}):

$$w=\frac{2\pi}{365} \qquad (4.6)$$

4.8.1.2. The Plant-Soil Model:

The plant-soil model simulates ecosystem carbon storage and the cycling of carbon and nitrogen between a plant biomass layer and the active soil pools (Figure 4.A.3). Specifically, the model simulates the interaction between plant biomass (*B*), soil organic carbon including humus and detritus (*SOC*), plant available soil nitrogen (*N*) including dissolved organic and inorganic nitrogen (*DON* & *DIN*) as well as dissolved organic carbon (*DOC*). The dissolved organic nitrogen (*DIN*) pool is divided into an ammonium (NH_4) and nitrate (NO_3) pool. *B*, *SOC*, NH_4, NO_3, *DON* and *DOC* pools are updated at each time step. For an *n*-layer soil model (*i=1,2…n*):

$$\frac{dB}{dt}=\left[\left(\sum_{i=1}^{n}\frac{r_i\times\mu_i\times\delta_{NH_4}\times NH_{4,i}}{NH_{4,i}\times kn}\right)\left(\sum_{i=1}^{n}\frac{r_i\times\mu_i\times\delta_{NO_3}\times NO_{3,i}}{NH_{3,i}\times kn}\right)\right]\times WS\left(\frac{s_i}{s_i^{max}}\right)\times B-m(B)\times B \qquad (4.7)$$

$$\frac{dSOC_i}{dt}=r_i\times m(B)\times B-\nu_i\left(T_{s,i},s_i\right)\times SOC_i \qquad (4.8)$$

$$\frac{dNH_{4,i}}{dt}=n_{in}-r_i\times\mu_i\times\delta_{NH_4}\times f_M\left(NH_{4,i}\right)\times WS\left(\frac{s_i}{s_i^{max}}\right)\times B+(1-q)\times SOC_i\times\nu_i\left(T_{s,i},s_i\right)-$$
$$Nit_i-\zeta_v\left(NH_{4,i}\right)+\zeta_v\left(NH_{4,i-1}\right)+\zeta_{l_{in}}\left(NH_{4,i}\right)-\zeta_{l_{out}}\left(NH_{4,i}\right) \qquad (4.9)$$

$$\frac{dNO_{3,i}}{dt} = Nit_i - r_i \times \mu_i \times \delta_{NO_3} \times f_M(NO_{3,i}) \times WS\left(\frac{s_i}{s_i^{max}}\right) \times B - Den_i - \zeta_v(NO_{3,i}) +$$

$$\zeta_v(NO_{3,i-1}) + \zeta_{l\_in}(NO_{3,i}) - \zeta_{l\_out}(NO_{3,i}) \quad (4.10)$$

$$\frac{dDOC_i}{dt} = \alpha_{CN} \times c_d \times SOC_i \times \nu_i(T_{s,i}, s_i) - \zeta_v(DOC_i) + \zeta_v(DOC_{i-1}) + \zeta_{l\_in}(DOC_i) -$$

$$\zeta_{l\_out}(DOC_i) \quad (4.11)$$

$$\frac{dDON_i}{dt} =$$

$$q \times SOC_i \times \nu_i(T_{s,i}, s_i) - \zeta_v(DON_i) + \zeta_v(DON_{i-1}) + \zeta_{l_{in}}(DON_i) - \zeta_{l_{out}}(DON_i) \quad (4.12)$$

where *m(B)* is the plant mortality rate (day^{-1}); r_i and μ_i are the biomass root fraction and the uptake rate function (day^{-1}) in layer *i*, respectively; δ_{NH_4} and δ_{NO_3} are the fraction of nitrogen uptake from the ammonium and nitrate pool, respectively; SOC_i, $NH_{4,i}$, $NO_{3,i}$, DOC_i and DON_i are the soil organic carbon, ammonium, nitrate, dissolved organic carbon and dissolved organic nitrogen pools in layer *i*, respectively (gNm^{-2}); *kn* (gNm^{-2}) is the Michealis Menton calibration parameter; $WS(s_i/s_i^{max})$ is the water stress function; $\nu_i(T_{s,i}, s_i)$ is a first order soil organic carbon decomposition rate (day^{-1}); n_{in} is the atmospheric input of wet and dry nitrogen deposition (gNm^{-2}day^{-1}); $(1-q)\times SOC_i \times \nu_i(T_{s,i}, s_i)$ is the flux of carbon into the ammonium pool due to soil organic carbon decomposition in layer *i* ($gNm^{-2}day^{-1}$); $q \times SOC_i \times \nu_i(T_{s,i}, s_i)$ is the flux of carbon into the DON pool due to soil organic carbon decomposition in layer *i* (gNm^{-2}day^{-1}); $\alpha \times c_d \times SOC_i \times \nu_i(T_{s,i}, s_i)$ is the flux of carbon from the SOC pool into the DOC pool within layer *i* (gCm^{-2}day^{-1}); $f_M(NH_{4,i})$ *and* $f_M(NO_{3,i})$ are the Type II Michealis Menton functions for ammonium and nitrate uptake in layer *i*, respectively; Nit_i and Den_i are the ammonium nitrification (gNm^{-2}day^{-1}) and nitrate denitrification (gNm^{-2}day^{-1}) amounts in layer *i*, respectively; $\zeta_v(NH_{4i})$, $\zeta_v(NO_{3i})$, $\zeta_v(DOC_i)$, and $\zeta_v(DON_i)$ are the NH_4 (gNm^{-2}day^{-1}), NO_3 (gNm^{-2}day^{-1}), DOC (gCm^{-2}day^{-1}), and DON (gNm^{-2}day^{-1}) losses through vertical transport of water (i.e. Drainage) from layer *i* to layer *i+1*; $\zeta_{l\_out}(NH_{4i})$, $\zeta_{l\_out}(NO_{3i})$, $\zeta_{l\_out}(DOC_i)$, and $\zeta_{l\_out}(DON_i)$ are the NH_4 (gNm^{-2}day^{-1}), NO_3 (gNm^{-2}day^{-1}), DOC (gCm^{-2}day^{-1}), and DON (gNm^{-2}day^{-1}) losses out of layer *i*, through lateral transport of water

(i.e. subsurface runoff) from layer *i* of the soil column to layer *i* of a downslope soil column or towards the stream; $\zeta_{l\_in}(NH_{4i})$, $\zeta_{l\_in}(NO_{3i})$, $\zeta_{l\_in}(DOC_i)$, and $\zeta_{l\_in}(DON_i)$ are the NH_4, NO_3, DOC and DON fluxes into layer *i*, through lateral transport of water (i.e. subsurface runoff) from layer *i* of an upslope soil column; α is the C:N ratio for plants and soils and is currently assumed constant for the entire simulations; c_d is the fraction of carbon that is not lost to the atmosphere due to the soil heterotrophic respiration.

4.8.1.2.1. Atmospheric Nitrogen Deposition:

Atmospheric inputs of wet and dry nitrogen deposition are assumed to affect only the first soil layer and to be temporally distributed throughout the year as a function of precipitation.

$$n_{in} = \overline{n_{in}} \times \frac{\left(P_r + m\right)}{P_{ann}} \tag{4.13}$$

where $\overline{n_{in}}$ is the long-term average annual wet and dry nitrogen deposition ($gNm^{-2}yr^{-1}$), P_r is rain (mm/day), m is snowmelt (mm/day), and P_{ann} is the long-term average annual precipitation (mm/yr).

4.8.1.2.2. Michealis Menton functions:

The Type II Michealis Menton functions are used to limit NH_4 and NO_3 uptake.

$$f_M\left(NH_{4i}\right) = \frac{NH_{4i}}{NH_{4i} + kn}$$
$$f_M\left(NO_{3i}\right) = \frac{NO_{3i}}{NO_{3i} + kn} \qquad i = 1,2...n \tag{4.14}$$

4.8.1.2.3. Plant Mortality:

Plant mortality rate is simulated as a function of plant biomass. *Acker et al.,* [2002] found that biomass mortality increases slowly with age for young stand until it reaches the mortality of mature and old-growth stands. In VELMA, plant mortality is assumed to increase exponentially with biomass value and to reach a steady state value for

mature/old-growth stands.

$$m(B) = \begin{cases} \left(\dfrac{\left(m_a \times B\right)^{m_b} \times m_c}{B} \right) & for\ B < B_{st} \\ m_{st} & for\ B \geq B_{st} \end{cases} \tag{4.15}$$

where m_a, m_b, and m_c are the mortality rate parameters, m_{st} is the equilibrium mortality rate of old-growth stands (day^{-1}), and B_{st} is the biomass value at equilibrium for an old-growth stand (gNm^{-2} or gCm^{-2} /α).

4.8.1.2.4. Plant Uptake:

Plant uptake rate is assumed to increase with increasing stand age (S_{age}), reach a maximum value for young stand and then decrease and reach equilibrium value for mature/old-growth stand [*Acker et al.*, 2002; *Waring and Franklin*, 1979].

$$\mu_i = \begin{cases} \mu_{\min} + 1.44 \times \left(\dfrac{W_{k1}}{W_{\lambda 1}}\right) \times \left(\dfrac{S_{age}}{W_{\lambda 1} \times S_{age}^{\max}}\right)^{W_{k1}-1} \times e^{\left(\frac{S_{age}}{W_{\lambda 1} \times S_{age}^{\max}}\right)^{W_{k1}}} & for\ S_{age} \leq S_{age}^{\max} \\ \mu_{st} + \left(\dfrac{W_{k2}}{W_{\lambda 2}}\right) \times \left(\dfrac{S_{age}}{W_{\lambda 2} \times S_{age}^{\max}}\right)^{W_{k2}-1} \times e^{\left(\frac{S_{age}}{W_{\lambda 2} \times S_{age}^{\max}}\right)^{W_{k2}}} & for\ S_{age} > S_{age}^{\max} \end{cases} \quad i = 1,2,\ldots n \tag{4.16}$$

where μ_{min} is the minimum uptake rate of plant (day^{-1}), μ_{st} is the steady state/equilibrium value of plant uptake (day^{-1}), S_{age}^{max} is the stand age for which plant uptake is the highest (days), W_{k1}, $W_{\lambda 1}$, W_{k2}, and $W_{\lambda 2}$ are the Weibull distribution parameters to calibrate.

4.8.1.2.5. Water Stress Function:

The water stress function varies between 0 and 1, and is proportional to the soil layer water saturation. The water stress function limits plant growth (i.e. plant nutrient uptake capacity) [*Pugnaire et al.*, 1993] as soil layer wetness approaches zero or saturation.

$$WS\left(\frac{s_i}{s_i^{\max}}\right)=\begin{cases}0.002154\times e^{\left(15.3511\times\left(\frac{s_i}{s_i^{\max}}\right)\right)} & for\left(\frac{s_i}{s_i^{\max}}\right)<WS^{\min}\\ 1 & for\ WS^{\min}\le\left(\frac{s_i}{s_i^{\max}}\right)\le WS^{\max}\\ 2.44141\times e^{\left(-1.116\times\left(\frac{s_i}{s_i^{\max}}\right)\right)} & for\left(\frac{s_i}{s_i^{\max}}\right)>WS^{\max}\end{cases}\qquad i=1,2,...n \tag{4.17}$$

where $WS^{\min}$ and $WS^{\max}$ are the minimum and maximum soil layer water saturation values between which water stress function has no effect on plant nutrient uptake.

4.8.1.2.6. *Biomass Root Fraction:*

Biomass root fraction distribution with depth follows *Gale and Grigal* [1987] model of vertical root distribution:

$$r_i = 1-\beta^{d_i}-\sum_{j=1}^{i} r_j \qquad i=1,2,...n \tag{4.18}$$

where β is a fitted "extinction coefficient" that depends on the vegetation type.

4.8.1.2.7. *Vertical Transport of Nutrients:*

Vertical transport of nutrients within the soil column is a function of the vertical water drainage and the size of the nutrient pool in layer *i*:

$$\xi_v\left(NH_{4i}\right)=qf_{NH_4}\times\frac{D_i}{s_i}\times NH_{4i} \qquad i=1,2...n \tag{4.19}$$

$$\xi_v\left(NO_{3i}\right)=qf_{NO_3}\times\frac{D_i}{s_i}\times NO_{3i} \qquad i=1,2...n \tag{4.20}$$

$$\xi_v\left(DON_i\right)=qf_{DON}\times\frac{D_i}{s_i}\times DON_i \qquad i=1,2...n \tag{4.21}$$

$$\xi_v\left(DOC_i\right)=qf_{DOC}\times\frac{D_i}{s_i}\times DOC_i \qquad i=1,2...n \tag{4.22}$$

where D_i (*mm/day*) is the vertical water drainage from layer *i* to layer *i*+1 (Equation 3.14 in Chapter 3); s_i (*mm*) is the amount of water in layer *i*; qf_{NH_4}, qf_{NO_3}, qf_{DON}, and qf_{DOC} are the maximum fractions of NH_4, NO_3, DON and DOC pool that can be lost through transport of water.

4.8.1.2.8. *Soil Organic Carbon Decomposition*

Soil organic carbon decomposition rate varies with environmental factors such as soil temperature [*Katterer et al.*, 1998; *Lloyd and Taylor*, 1994; *Rustad and Fernandez*, 1998] and soil moisture [*Davidson et al.*, 2000] and is based on the process-based Terrestrial Ecosystem Model (TEM) presented by *Raich et al.,* [1991]. Soil moisture impacts SOC decomposition rate via moisture availability in dry soil and via oxygen availability in wet soil, such as:

$$\nu_i\left(T_{s,i}, s_i\right) = k_c \times F_c^{temp}\left(T_{s,i}\right) \times F_c^{moisture}\left(\frac{s_i}{s_i^{\max}}\right) \qquad i = 1,2,\ldots n \tag{4.23}$$

$$F_c^{temp}\left(T_{s,i}\right) = 0.00442 \times e^{\left(0.0693 \times T_{s,i}\right)} \qquad i = 1,2,\ldots n \tag{4.24}$$

$$F_c^{moisture}\left(\frac{s_i}{s_i^{\max}}\right) = 0.8 \times M_{sat}^{A} + 0.2 \qquad i = 1,2,\ldots n \tag{4.25}$$

$$A = \left(\frac{\left(100 \times \left(\frac{s_i}{s_i^{\max}}\right)\right)^{ma_1} - \left(\frac{s_i}{s_i^{\max}}\right)_{opt}^{ma_1}}{\left(\frac{s_i}{s_i^{\max}}\right)_{opt}^{ma_1} - 100^{ma_1}} \right)^2 \qquad i = 1,2,\ldots n \tag{4.26}$$

where k_c (day^{-1}) is the potential decomposition rate determined by model calibration; $F_c^{temp}\left(T_{s,i}\right)$ relates the microbial activity rate to changes in soil temperature (Equation 1.13; [*Raich et al.,* 1991]); $F_c^{moisture}\left(s_i / s_i^{\max}\right)$ defines the impact of soil moisture on decomposition (Equation 1.14b; [*Raich et al.,* 1991]); M_{sat} is a parameter that determines the value of $F_c^{moisture}\left(s_i / s_i^{\max}\right)$ when the soil is saturated (Table A5; [*Raich et al.,* 1991]);

ma_1 is a shape parameter defining the skewness of the curve (Table A5; [*Raich et al.,* 1991]); $\left(s_i/s_i^{\max}\right)_{opt}$ is the optimal soil wetness value for which carbon decomposition is maximal; $F_c^{temp}\left(T_{s,i}\right)$ and $F_c^{moisture}\left(s_i/s_i^{\max}\right)$ vary between the values of 0 and 1.

4.8.1.2.9. *Nitrification Rate:*

Nitrification is the biological oxidation of ammonium into nitrite and subsequently nitrate under aerobic conditions. Nitrification occurs naturally in the environment and is carried out by autotrophic bacteria. Soil nitrification rates depend on a number of environmental factors such as soil ammonium level [*Smart et al.*, 1999], soil moisture [*Davidson et al.*, 1993], soil temperature [*Malhi and McGill*, 1982] and soil pH [*DeGroot et al.*, 1994]. In VELMA, nitrification is simulated using similar equations to the generalized model of N_2 and N_2O production of *Parton et al.,* [1996; 2001]. Soil nitrification rate is assumed to (1) increase exponentially with soil temperature ($F_N^{temp}\left(T_{s,i}\right)$; Figure 2b; [*Parton et al.,* 1996]), (2) increase as soil layer water saturation reaches optimal value for bacterial decomposition and then decrease rapidly as soil layer reaches saturation ($F_N^{moisture}\left(s_i/s_i^{\max}\right)$; Figure 2a; [*Parton et al.,* 1996]), (3) decrease exponentially as soil layer acidity (pH_i) increases ($F_N^{moisture}\left(s_i/s_i^{\max}\right)$; Figure 2c, [*Parton et al.,* 1996]), and (4) be limited by the amounted of ammonium available for nitrification.

The nitrification rate in layer *i* is calculated as follows:

$$Nit_i = K_N^{\max} \times F_N^{temp}\left(T_{s,i}\right) \times F_N^{acidity}\left(pH_i\right) \times F_N^{moisture}\left(\frac{s_i}{s_i^{\max}}\right) \times f_M\left(NH_{4i}\right) \times NH_{4i} \quad i = 1,2...n \tag{4.27}$$

$$F_N^{temp}\left(T_{s,i}\right) = -0.06 + 0.13 \times e^{\left(0.07 \times T_{s,i}\right)} \quad i = 1,2...n \tag{4.28}$$

$$F_N^{acidity}\left(pH_i\right) = 0.56 + \frac{\arctan\left(\pi \times 0.45 \times \left(-5 \times pH_i\right)\right)}{\pi} \quad i = 1,2...n \tag{4.29}$$

$$F_N^{moisture}\left(\frac{s_i}{s_i^{\max}}\right)=\left(\frac{\left(\frac{s_i}{s_i^{\max}}\right)-N_b}{N_a-N_b}\right)^{\left(N_d\times\frac{N_b-N_a}{N_a+N_c}\right)}\times\left(\frac{\left(\frac{s_i}{s_i^{\max}}\right)-N_c}{N_a-N_c}\right)^{N_d} \qquad i=1,2...n \qquad (4.30)$$

where $K_N^{\max}$ (day^{-1}) is the maximum nitrification rate determined by model calibration; N_a, N_b, N_c and N_d are soil parameters set according to soil texture and described in *Parton et al.,* [1996].

4.8.1.2.10. <u>*Denitrification Rate:*</u>

Denitrification is the biological reduction of nitrate under anaerobic conditions. During denitrification, heterotrophic microbes contribute to the NO_3 reduction into NO_2, NO and N_2O intermediates and ultimately into molecular nitrogen N_2 lost to the atmosphere. The denitrification process is controlled by environmental factors such as soil nitrate level, soil oxygen availability and soil labile carbon availability (e^- donor) [*Weier et al.*, 1993]. In VELMA, denitrification is simulated using the denitrification sub-model of N_2 and N_2O production presented by *Parton et al.,* [1996; 2001] and *Del Grosso et al.,* [2000]. The rate of denitrification is proportional to the amount of bio-available soil organic carbon level. However, VELMA does not differentiate between labile and non-labile soil organic matter. Therefore simulated ecosystem CO_2 loss (soil heterotrophic respiration) is used as a proxy for the amount of bio-available soil organic carbon [*Del Grosso et al.*, 2000; *Parton et al.*, 1996]. The rate of denitrification increases with decreasing oxygen availability. Oxygen availability is another critical factor not simulated by VELMA but assumed as a function of soil moisture, soil gaz diffusivity and oxygen demand. Gas diffusivity is simulated as a function of soil moisture and soil properties, whereas oxygen demand is a function of the simulated soil heterotrophic respiration [*Del Grosso et al.*, 2000; *Parton et al.*, 1996]. As a result, soil denitrification rate is simulated as a function of soil saturation $F_D^{moisture}\left(s_i/s_i^{\max}\right)$ (Equation 1, [*Parton et al.,* 2001]), soil heterotrophic respiration $F_D^{carbon}\left(CO_{2,i}\right)$ (Figure 1d, [*del Grosso et al.,* 2000]), and soil available nitrate $F_D^{nitrate}\left(NO_{3i}\right)$ (Figure 1c, [*del Grosso et al.,* 2000]).

Currently VELMA simulates the total denitrification or N_2+N_2O emission without the partition between N_2 and N_2O, such that:

$$Den_i = \min\left[F_D^{carbon}\left(CO_{2i}\right), F_D^{nitrate}\left(NO_{3i}\right)\right] \times F_D^{moisture}\left(\frac{s_i}{s_i^{\max}}\right) \qquad i = 1,2...n \tag{4.31}$$

$$F_D^{moisture}\left(\frac{s_i}{s_i^{\max}}\right) = 0.5 + \frac{\arctan\left(\pi \times 0.6 \times \left(0.1 \times \left(\frac{s_i}{s_i^{\max}}\right)\right) - \vartheta_a\right)}{\pi} \qquad i = 1,2...n \tag{4.32}$$

$$F_D^{carbon}\left(CO_{2,i}\right) = 0.1 \times \left(\alpha \times c_d \times SOC_i \times \nu_i\left(T_{s,i}, s_i\right)\right)^{1.3} \qquad i = 1,2...n \tag{4.33}$$

$$F_D^{nitrate}\left(NO_{3i}\right) = 0.005 \times \left(NO_{3i}\right)^{0.57} \qquad i = 1,2...n \tag{4.34}$$

where $F_D^{carbon}\left(CO_{2,i}\right)$ and $F_D^{nitrate}\left(NO_{3i}\right)$ represent the maximum possible N gas flux from layer *i* for a given soil heterotrophic respiration rate and nitrate level, respectively ($gNm^{-2}day^{-1}$); ϑ_a is a shape parameter that depends on soil texture; $F_D^{moisture}\left(s_i/s_i^{\max}\right)$ varies between zero and 1.

4.8.2. Watershed Framework

To place the above described soil column framework within a catchment framework, the catchment topography is gridded into a number of pixels, with each pixel consisting of one coupled soil column. Soil columns communicate with each other through the downslope lateral transport of water and nutrients. Surface and subsurface runoff are responsible for this lateral transport and link each soil column to the surrounding downslope soil columns. A multiple flow direction method is used where flow and nutrients from one pixel to its eight neighbors is fractionally allocated according to terrain slope [*Freeman*, 1991; *Quinn et al.*, 1991]. Moreover, nutrients transported downslope from one soil column to another can be processed through the different sub-models in that downslope soil column, or continue to flow downslope, interacting with other soil columns, or ultimately discharging water and nutrients to the stream.

4.8.2.1. Lateral Transport of Nutrients

Lateral transport of nutrients from layer *i* of an upslope soil column to layer *i* of a downslope soil column or towards the stream is based on the flow routing information and on terrain slope. As with the vertical transport of nutrients, the lateral transport of nutrient is a function of the lateral runoff and the size of the nutrient pool in layer *i*. For simplicity, we assume that both surface runoff and layer 1 subsurface runoff impact the nutrient pool in layer 1 of the soil column.

$$\zeta_l\left(NH_{4i}\right) = qf_{NH_4} \times \frac{\left(Q_i + q_{surf} \times Q_s\right)}{s_i} \times NH_{4i} \qquad i = 1,2 \ldots n \tag{4.35}$$

$$\zeta_l\left(NO_{3i}\right) = qf_{NO_3} \times \frac{\left(Q_i + q_{surf} \times Q_s\right)}{s_i} \times NO_{3i} \qquad i = 1,2 \ldots n \tag{4.36}$$

$$\zeta_l\left(DON_i\right) = qf_{DON_i} \times \frac{\left(Q_i + q_{surf} \times Q_s\right)}{s_i} \times DON_i \qquad i = 1,2 \ldots n \tag{4.37}$$

$$\zeta_l\left(DOC_i\right) = qf_{DOC_i} \times \frac{\left(Q_i + q_{surf} \times Q_s\right)}{s_i} \times DOC_i \qquad i = 1,2 \ldots n \tag{4.38}$$

with $q_{surf} = \begin{cases} 1 & for\ i = 1 \\ 0 & for\ i = 2,3 \ldots n \end{cases}$

where Q_i (mm/day) is the lateral subsurface runoff from layer *i* (Equation 3.16 in Chapter 3); Q_s (mm/day) is the surface runoff that impact the nutrients pools in layer 1 (Equation 3.18 in Chapter 3).

Table 4.B.1: Model parameter values used to simulate the biogeochemical processes of watershed 10 in the H.J. Andrews Experimental Forest.

Parameters	Definition	Value	References
λ_{snow}	Seasonal damping depth for snow (mm)	670	*Hillel*, [1998]
$\overline{GST}$	Annual mean soil temperature (°*C*)	8.5	*Sollins and McCorison,* [1981]
kn	Michealis Menton calibration parameter (gN/m^2)	0.1	Calibrated
δ_{NO3}	Fraction of nitrogen uptake from the nitrate pool	0.3	*Rygiewicz and Bledsoe,* [1986]; *Kamminga-Van Wijk and Prins.,* [1993]
δ_{NH4}	Fraction of nitrogen uptake from the ammonium pool	0.7	*Rygiewicz and Bledsoe,* [1986]; *Kamminga-Van Wijk and Prins.,* [1993]
α_{CN}	C:N ratio for plants and soils	50	*Sollins and McCorison,* [1981]
c_d	Fraction of carbon that is not lost to the atmosphere due to the soil heterotrophic respiration	0.004	Calibrated
$\overline{n_{in}}$	Annual wet and dry deposition of atmospheric N ($gNm^{-2}yr^{-1}$)	0.2	*Sollins et al*., [1980]
β	Fitted extinction coefficient	0.976	*Jackson et al*., [1996]
q	Fraction of carbon decomposition that feeds into the DON pool	0.015	Calibrated
m_{st}	Steady state average mortality rate of old-growth forest (yr^{-1})	0.0125	*Lutz and Halpern*., [2006]
B_{st}	Average biomass value for an old-growth forest (gN/m^2)	42350	*Harmon et al*., [2004]; *Sollins et al.*, [1980]
m_a	Mortality rate parameter	1.55	Fixed a priori
m_b	Mortality rate parameter	4	Fixed a priori
m_c	Mortality rate parameter	1.E-14	Fixed a priori
μ_{min}	Minimum uptake rate of vegetation after disturbance (yr^{-1})	0.20	Fixed a priori
μ_{st}	Steady state value of plant uptake (yr^{-1})	0.25	Calibrated
S_{age}^{max}	Stand age for which plant uptake is the highest (years)	35	*Luyssaert et al*., [2008]
W_{k1}	Weibull distribution parameter for plant uptake	1.60	Fixed a priori
$W_{\lambda 1}$	Weibull distribution parameter for plant uptake	1.70	Fixed a priori
W_{k2}	Weibull distribution parameter for plant uptake	0.95	Fixed a priori
$W_{\lambda 2}$	Weibull distribution parameter for plant uptake	0.85	Fixed a priori
WS^{min}	Lower limit of soil water saturation, below which plant uptake is reduced (%).	40	Fixed a priori
WS^{max}	Upper limit of soil water saturation, above which plant uptake is reduced (%).	80	Fixed a priori
k_c	Potential carbon decomposition rate (vegetation dependent) (yr^{-1})	0.45	Calibrated
M_{sat}	Parameter that determines the value $F_N^{moisture}(s_i/s_i^{max})$	0.25	*Raich et al*., [1991]
ma_1	Shape parameter defining the skewness of the $F_N^{moisture}(s_i/s_i^{max})$ curve	0.14	*Raich et al*., [1991]
	Optimal soil wetness for which decomposition is maximal	40%	*Alexander*, [1977]
pH	Average pH value for the soils in WS10	4.5	*Chaer et al*., [2009]
$K_N^{\max}$	Maximum nitrification rate (day^{-1})	0.15	*Parton et al.,* [2001]
N_a	Soil moisture function parameter for ammonium nitrification	0.4	*Parton et al*., [1996]
N_b	Soil moisture function parameter for ammonium nitrification	1.7	*Parton et al*., [1996]
N_c	Soil moisture function parameter for ammonium nitrification	3.22	*Parton et al*., [1996]
N_d	Soil moisture function parameter for ammonium nitrification	0.007	*Parton et al*., [1996]
ϑ_a	Soil moisture function shape parameter	5.0	*Del Grosso et al*., [2000]
qf_{NH_4}	Maximum fraction of NH_4 pool that can be lost through transport of water	0.12	Calibrated
qf_{NO_3}	Maximum fraction of NH_4 pool that can be lost through transport of water	0.04	Calibrated
qf_{DON}	Maximum fraction of NH_4 pool that can be lost through transport of water	0.02	Calibrated
qf_{DOC}	Maximum fraction of NH_4 pool that can be lost through transport of water	0.06	Calibrated

4.9. Acknowledgements

The information in this document has been funded in part by the US Environmental Protection Agency. It has been subjected to the Agency's peer and administrative review, and it has been approved for publication as an EPA document. Mention of trade names or commercial products does not constitute endorsement or recommendation for use. This research was additionally supported in part by the following NSF Grants 0439620, 0436118, and 0922100. We thank Sherri Johnson, Barbara Bond, Suzanne Remillard, Theresa Valentine and Don Henshaw for invaluable assistance in accessing and interpreting various H.J. Andrews LTER data sets used in this study. Sherri Johnson also provided helpful comments on an earlier draft. Data for streamflow, stream chemistry and climate were provided by the H.J. Andrews Experimental Forest research program, funded by the National Science Foundation's Long-Term Ecological Research Program (DEB 08-23380), US Forest Service Pacific Northwest Research Station, and Oregon State University.

4.10. References:

Abdelnour, A., M. Stieglitz, F. Pan, and R. McKane (2011), Catchment Hydrological Responses to Forest Harvest Amount and Spatial Pattern, *Water Resour. Res., doi:10.1029/2010WR010165, in press.*

Acker, S., C. Halpern, M. Harmon, and C. Dyrness (2002), Trends in bole biomass accumulation, net primary production and tree mortality in Pseudotsuga menziesii forests of contrasting age, *Tree Physiology*, *22*(2-3), 213.

Agee, J. (1994), Fire and weather disturbances in terrestrial ecosystems of the eastern Cascades. US Forest Service, *Pacific Northwest Research Station. General Technical Report PNW-GTR-320*.

Agee, J. K. (1990), The historical role of fire in Pacific Northwest forests, *Walstad, JD, and SR Radosevich, DV Sandberg, editors*.

Alila, Y., and J. Beckers (2001), Using numerical modelling to address hydrologic forest management issues in British Columbia, *Hydrological Processes*, *15*(18), 3371-3387.

Amaranthus, M., H. Jubas, and D. Arthur (1989), Stream Shading, Summer Streamflow and Maximum Water Temperature Following Intense Wildfire In Headwater Streams1, *on Fire and Watershed Management*, 75.

Bernot, M., and W. Dodds (2005), Nitrogen retention, removal, and saturation in lotic ecosystems, *Ecosystems*, *8*(4), 442-453.

Beschta, R., M. Pyles, A. Skaugset, and C. Surfleet (2000), Peakflow responses to forest practices in the western Cascades of Oregon, USA, *Journal of Hydrology*, *233*(1-4), 102-120.

Beschta, R. L. (1990), Effects of fire on water quantity and quality, *Natural and prescribed fire in Pacific Northwest forests, Walstad, J.D., S.R. Radosevich, and D.V. Sandberg (eds.). Corvallis, OR: Oregon State University Press*, 219-232.

Bilby, R., and G. Likens (1980), Importance of organic debris dams in the structure and function of stream ecosystems, *Ecology*, *61*(5), 1107-1113.

Binkley, D., P. Sollins, R. Bell, D. Sachs, and D. Myrold (1992), Biogeochemistry of adjacent conifer and alder-conifer stands, *Ecology*, 2022-2033.

Bormann, F., G. Likens, D. Fisher, and R. Pierce (1968), Nutrient loss accelerated by clear-cutting of a forest ecosystem, *Science*, *159*(3817), 882.

Bosch, J., and J. Hewlett (1982), A review of catchment experiments to determine the effect of vegetation changes on water yield and evapotranspiration, *Journal of Hydrology*, *55*(1-4), 3-23.

Cairns, M., and K. Lajtha (2005), Effects of succession on nitrogen export in the west-central Cascades, Oregon, *Ecosystems*, *8*(5), 583-601.

Carignan, R., P. D'Arcy, and S. Lamontagne (2000), Comparative impacts of fire and forest harvesting on water quality in Boreal Shield lakes, *Canadian Journal of Fisheries and Aquatic Sciences*, *57*(S2), 105-117.

Carslaw, H., and J. Jaeger (1959), Conduction of heat in solids, 2nd Edition, Oxford University Press, New York.

Chanasyk, D., I. Whitson, E. Mapfumo, J. Burke, and E. Prepas (2003), The impacts of forest harvest and wildfire on soils and hydrology in temperate forests: A baseline to develop hypotheses for the Boreal Plain, *Journal of Environmental Engineering and Science*, *2*(S1), 51-62.

Cheng, Y., M. Stieglitz, and F. Pan (2010), A Simple Method to Evolve Daily Ground Temperatures From Surface Air Temperatures in Snow Dominated Regions, *Journal of Hydrometeorology*.

Creed, I., L. Band, N. Foster, I. Morrison, J. Nicolson, R. Semkin, and D. Jeffries (1996), Regulation of nitrate-N release from temperate forests: a test of the N flushing hypothesis, *Water Resources Research*, *32*(11), 3337-3354.

Daly, C., and W. McKee (2011), Meteorological data from benchmark stations at the Andrews Experimental Forest. Long-Term Ecological Research. Forest Science Data Bank, Corvallis, OR. [Database]. Available: http://andrewsforest.oregonstate.edu/data/abstract.cfm?dbcode=MS001 (16 July 2011).

Davidson, E., L. Verchot, J. Catt,nio, I. Ackerman, and J. Carvalho (2000), Effects of soil water content on soil respiration in forests and cattle pastures of eastern Amazonia, *Biogeochemistry*, *48*(1), 53-69.

Davidson, E., P. Matson, P. Vitousek, R. Riley, K. Dunkin, G. Garcia-Mendez, and J. Maass (1993), Processes regulating soil emissions of NO and N20 in a seasonally dry tropical forest, *Ecology*, *74*(1), 130-139.

De Vries, D. (1975), Heat transfer in soils, *Heat and mass transfer in the biosphere*, *1*, 594.

DeGroot, C., A. Vermoesen, and O. Cleemput (1994), Laboratory study of the emission of NO and N 2 O from some Belgian soils, *Environmental Monitoring and Assessment*, *31*(1), 183-189.

Del Grosso, S., W. Parton, A. Mosier, D. Ojima, A. Kulmala, and S. Phongpan (2000), General model for N2O and N2 gas emissions from soils due to dentrification, *Global Biogeochemical Cycles*, *14*(4).

Dingman, S. (1994), *Physical hydrology*, Prentice Hall Upper Saddle River, NJ.

Dyrness, C. (1973), Early stages of plant succession following logging and burning in the western Cascades of Oregon, *Ecology*, *54*(1), 57-69.

Franklin, J. F., and R. T. T. Forman (1987), Creating landscape patterns by forest cutting: ecological consequences and principles, *Landscape Ecology*, *1*(1), 5-18.

Fredriksen, R. (1975), Nitrogen, phosphorus and particulate matter budgets of five coniferous forest ecosystems in the western Cascades Range, Oregon, Doctoral thesis, 71 pp, Oregon State University, Corvallis.

Freeman, T. (1991), Calculating catchment area with divergent flow based on a regular grid, *Computers & Geosciences*, *17*(3), 413-422.

Gale, M. R., and D. F. Grigal (1987), Vertical root distributions of northern tree species in relation to successional status, *Canadian Journal of Forest Research*, *17*(8), 829-834.

Gholz, H., G. Hawk, A. Campbell, K. Cromack Jr, and A. Brown (1985), Early vegetation recovery and element cycles on a clear-cut watershed in western Oregon, *CAN. J. FOR. RES.*, *15*(2), 400-409.

Gholz, H. L., G. M. Hawk, A. Campbell, K. Cromack Jr, and A. T. Brown (1985), Early vegetation recovery and element cycles on a clear-cut watershed in western Oregon, *Canadian Journal of Forest Research*, *15*(2), 400-409.

Giesen, T. W. G. T., S. S. P. S. S. Perakis, and K. C. K. Cromack Jr (2008), Four centuries of soil carbon and nitrogen change after stand-replacing fire in a forest landscape in the western Cascade Range of Oregon, *Canadian Journal of Forest Research*, *38*(9), 2455-2464.

Grant, G., S. Lewis, F. Swanson, J. Cissel, and J. McDonnell (2008), Effects of forest practices on peak flows and consequent channel response: a state-of-science report for western Oregon and Washington, *General Technical Report. PNW-*

GTR-760. Portland, OR: USDA Forest Service, Pacific Northwest Research Station, *76*.

Grant, R., T. Black, E. Humphreys, and K. Morgenstern (2007), Changes in net ecosystem productivity with forest age following clearcutting of a coastal Douglas-fir forest: testing a mathematical model with eddy covariance measurements along a forest chronosequence, *Tree Physiology*, *27*(1), 115.

Grant, R., N. Juma, J. Robertson, R. Izaurralde, and W. B. Mcgill (2001), Long-Term Changes in Soil Carbon under Different Fertilizer, Manure, and Rotation--Testing the Mathematical Model ecosys with Data from the Breton Plots, *Soil Science Society of America Journal*, *65*(1), 205-214.

Grier, C., and R. Logan (1977), Old-growth Pseudotsuga menziesii communities of a western Oregon watershed: biomass distribution and production budgets, *Ecological Monographs*, *47*(4), 373-400.

Grier, C. C. (1975), Wildfire effects on nutrient distribution and leaching in a coniferous ecosystem, *Canadian Journal of Forest Research*, *5*(4), 599-607.

Griffiths, R., and A. Swanson (2001), Forest soil characteristics in a chronosequence of harvested Douglas-fir forests, *Canadian Journal of Forest Research*, *31*(11), 1871-1879.

Harmon, M., K. Bible, M. Ryan, D. Shaw, H. Chen, J. Klopatek, and X. Li (2004), Production, respiration, and overall carbon balance in an old-growth Pseudotsuga-Tsuga forest ecosystem, *Ecosystems*, *7*(5), 498-512.

Harmon, M. E., and B. Marks (2002), Effects of silvicultural practices on carbon stores in Douglas-fir western hemlock forests in the Pacific Northwest, USA: results from a simulation model, *Canadian Journal of Forest Research*, *32*(5), 863-877.

Harmon, M. E., W. K. Ferrell, and J. F. Franklin (1990), Effects on carbon storage of conversion of old-growth forests to young forests, *Science*, *247*(4943), 699-701.

Harr, R., and F. M. McCorison (1979), Initial effects of clearcut logging on size and timing of peak flows in a small watershed in western Oregon, *Water Resources Research*, *15*(1), 90-94, doi:10.1029/WR1015i1001p00090.

Harr, R., A. Levno, and R. Mersereau (1982), Streamflow changes after logging 130-year-old Douglas fir in two small watersheds, *Water Resources Research*, *18*(3), 637-644, doi:610.1029/WR1018i1003p00637.

Helvey, J. (1980), Effects of a North Central Washington wildfire on Runoff and Sediment Production, *JAWRA Journal of the American Water Resources Association*, *16*(4), 627-634.

Hibbert, A. (1966), Forest treatment effects on water yield, in *Proceedings of a National Science Foundation advanced science seminar, International symposium on forest hydrology. Pergamon Press, USA*, edited by W.E. Sopper and H.W. Lull, pp. 527-543, Pergamon Press, New York,.

Hicke, J. A., G. P. Asner, E. S. Kasischke, N. H. F. French, J. T. Randerson, G. James Collatz, B. J. Stocks, C. J. Tucker, S. O. Los, and C. B. Field (2003), Postfire

response of North American boreal forest net primary productivity analyzed with satellite observations, *Global Change Biology*, *9*(8), 1145-1157.

Hillel, D. (1998), *Environmental soil physics*, Academic Pr.

Ice, G. G., D. G. Neary, and P. W. Adams (2004), Effects of wildfire on soils and watershed processes, *Journal of Forestry*, *102*(6), 16-20.

Janisch, J., and M. Harmon (2002), Successional changes in live and dead wood carbon stores: implications for net ecosystem productivity, *Tree Physiology*, *22*(2-3), 77.

Johnson, S., and J. Rothacher (2009), Stream discharge in gaged watersheds at the Andrews Experimental Forest. Long-Term Ecological Research. Forest Science Data Bank, Corvallis, OR. [Database]. Available: http://andrewsforest.oregonstate.edu/data/abstract.cfm?dbcode=HF004 (16 July 2011).

Johnson, S., and R. Fredriksen (2010), Long-term precipitation and dry deposition chemistry concentrations and fluxes: Andrews Experimental Forest rain collector samples. Long-Term Ecological Research. Forest Science Data Bank, Corvallis, OR. [Database]. Available: http://andrewsforest.oregonstate.edu/data/abstract.cfm?dbcode=CP002 (31 August 2011). .

Johnson, S., and R. Fredriksen (2011), Long-term stream chemistry concentrations and fluxes: Small watershed proportional samples in the Andrews Experimental Forest. Long-Term Ecological Research. Forest Science Data Bank, Corvallis, OR. [Database]. Available: http://andrewsforest.oregonstate.edu/data/abstract.cfm?dbcode=CF002 (18 July 2011).

Jones, J. A. (2000), Hydrologic processes and peak discharge response to forest removal, regrowth, and roads in 10 small experimental basins, western Cascades, Oregon, *Water Resources Research*, *36*(9), 2621-2642, doi:2610.1029/2000WR900105.

Jones, J. A., and G. E. Grant (1996), Peak flow responses to clear-cutting and roads in small and large basins, western Cascades, Oregon, *Water Resources Research*, *32*(4), 959-974.

Jones, J. A., and D. A. Post (2004), Seasonal and successional streamflow response to forest cutting and regrowth in the northwest and eastern United States, *Water Resources Research*, *40*(5), W05203, doi:05210.01029/02003WR002952.

Katterer, T., M. Reichstein, O. Andren, and A. Lomander (1998), Temperature dependence of organic matter decomposition: a critical review using literature data analyzed with different models, *Biology and Fertility of Soils*, *27*(3), 258-262.

Keane, R. E., P. Morgan, and S. W. Running (1996), Fire-BGC: A mechanistic ecological process model for simulating fire succession on coniferous forest landscapes of the northern Rocky Mountains. Forest Service research paper*Rep.*, Forest Service, Ogden, UT (United States). Intermountain Research Station.

Keane, R. E., C. C. Hardy, K. C. Ryan, and M. A. Finney (1997), Simulating effects of fire on gaseous emissions and atmospheric carbon fluxes from coniferous forest landscapes, *World Resource Review*, *9*(2), 177-205.

Keppeler, E. T., and R. R. Ziemer (1990), Logging effects on streamflow: water yield and summer low flows at Caspar Creek in northwestern California, *Water Resources Research*, *26*(7), 1669-1679.

Langford, K. (1976), Change in yield of water following a bushfire in a forest of Eucalyptus regnans, *Journal of Hydrology*, *29*(1-2), 87-114.

Law, B., P. Thornton, J. Irvine, P. Anthoni, and S. Van Tuyl (2001), Carbon storage and fluxes in ponderosa pine forests at different developmental stages, *Global Change Biology*, *7*(7), 755-777.

Lee, J., I. K. Morrison, J. D. Leblanc, M. T. Dumas, and D. A. Cameron (2002), Carbon sequestration in trees and regrowth vegetation as affected by clearcut and partial cut harvesting in a second-growth boreal mixedwood, *Forest Ecology and Management*, *169*(1-2), 83-101.

Lloyd, J., and J. Taylor (1994), On the temperature dependence of soil respiration, *Functional ecology*, *8*(3), 315-323.

Lutz, J. A., and C. B. Halpern (2006), Tree mortality during early forest development: a long-term study of rates, causes, and consequences, *Ecological Monographs*, *76*(2), 257-275.

Luyssaert, S., E. Schulze, A. Borner, A. Knohl, D. Hessenmoller, B. Law, P. Ciais, and J. Grace (2008), Old-growth forests as global carbon sinks, *Nature*, *455*(7210), 213-215.

Malhi, S., and W. McGill (1982), Nitrification in three Alberta soils: effect of temperature, moisture and substrate concentration, *Soil Biology and Biochemistry*, *14*(4), 393-399.

Martin, W. C., and H. Dennis (1989), Logging of mature Douglas-fir in western Oregon has little effect on nutrient output budgets, *Canadian Journal of Forest Research*, *19*(1), 35-43.

McKane, R., E. Rastetter, G. Shaver, K. Nadelhoffer, A. Giblin, J. Laundre, and F. Chapin III (1997), Climatic effects on tundra carbon storage inferred from experimental data and a model, *Ecology*, *78*(4), 1170-1187.

Means, J., P. MacMillan, and K. CROMACK (1992), Biomass and nutrient content of Douglas-fir logs and other detrital pools in an old-growth forest, Oregon, U. S. A, *Canadian journal of forest research(Print)*, *22*(10), 1536-1546.

Mitchell, S. R., M. E. Harmon, and K. E. B. O'Connell (2009), Forest fuel reduction alters fire severity and long-term carbon storage in three Pacific Northwest ecosystems, *Ecological Applications*, *19*(3), 643-655.

Moore, R., and S. Wondzell (2005), Physical Hydrology in the Pacific Northwest and the Effects of Forest HarvestingñA Review, *Journal of the American Water Resources Association*, *41*, 753-784.

Neary, D., K. Ryan, and L. DeBano (2005), Fire effects on soil and water. USDA Forest Service, Rocky Mountain Research Station, General Technical Report RMRS-GTR-42.

Parton, W., A. Mosier, D. Ojima, D. Valentine, D. Schimel, K. Weier, and A. Kulmala (1996), Generalized model for N2 and N2O production from nitrification and denitrification, *Global Biogeochemical Cycles*, *10*(3).

Parton, W., E. Holland, S. Del Grosso, M. Hartman, R. Martin, A. Mosier, D. Ojima, and D. Schimel (2001), Generalized model for NO x and N2O emissions from soils, *Journal of Geophysical Research-Atmospheres*, *106*(D15).

Peterson, B., W. Wollheim, P. Mulholland, J. Webster, J. Meyer, J. Tank, E. Marti, W. Bowden, H. Valett, and A. Hershey (2001), Control of nitrogen export from watersheds by headwater streams, *Science*, *292*(5514), 86.

Pugnaire, F., L. Serrano, and J. Pardos (1993), Constraints by water stress on plant growth, *Handbook of plant and crop stress*, 271ñ283.

Quinn, P., K. Beven, P. Chevallier, and O. Planchon (1991), Prediction of hillslope flow paths for distributed hydrological modelling using digital terrain models, *Hydrological Processes*, *5*(1), 59-79.

Raich, J., E. Rastetter, J. Melillo, D. Kicklighter, P. Steudler, B. Peterson, A. Grace, B. Moore Iii, and C. Vorosmarty (1991), Potential net primary productivity in South America: application of a global model, *Ecological Applications*, *1*(4), 399-429.

Raison, R., H. Keith, and P. Khanna (1990), Effects of fire on the nutrient-supplying capacity of forest soils, *Impact of Intensive Harvesting on Forest Site Productivity. Forest Research Institute Bulletin*, *159*, 39-54.

Ranken, D. W. (1974), Hydrologic properties of soil and subsoil on a steep, forested slope, Master's thesis, 117 pp, Oregon State University, Corvallis.

Rastetter, E., P. Vitousek, C. Field, G. Shaver, D. Herbert, and G. Gren (2001), Resource optimization and symbiotic nitrogen fixation, *Ecosystems*, *4*(4), 369-388.

Rothacher, J. (1965), Streamflow from small watersheds on the western slope of the Cascade Range of Oregon, *Water Resources Research*, *1*, 125-134, doi:110.1029/WR1001i1001p00125.

Rozzell, L. R. (2003), Species pairwise associations over nine years of secondary succession: assessing alternative explanations and successional mechanisms, Master's thesis. Utah State University, Logan, Utah.

Rustad, L., and I. Fernandez (1998), Soil warming: Consequences for foliar litter decay in a spruce-fir forest in Maine, USA, *Soil Science Society of America Journal*, *62*(4), 1072.

Santantonio, D., R. Hermann, and W. Overton (1977), Root biomass studies in forest ecosystems. Pedobiologia, Bd. 17, S. 1-31. Paper 957, *Forest Research Laboratory, School of Forestry Oregon State University, Corvallis, Oregon*.

Schmidt, J., W. Seiler, and R. Conrad (1988), Emission of nitrous oxide from temperate forest soils into the atmosphere, *Journal of atmospheric chemistry*, *6*(1), 95-115.

Smart, D., J. Stark, and V. Diego (1999), Resource limitations to nitric oxide emissions from a sagebrush-steppe ecosystem, *Biogeochemistry*, *47*(1), 63-86.

Smithwick, E., M. Harmon, S. Remillard, S. Acker, and J. Franklin (2002), Potential upper bounds of carbon stores in forests of the Pacific Northwest, *Ecological Applications*, *12*(5), 1303-1317.

Sollins, P., and F. M. McCorison (1981), Nitrogen and carbon solution chemistry of an old growth coniferous forest watershed before and after cutting, *Water Resources Research*, *17*(5), 1409–1418, doi:1410.1029/WR1017i1005p01409. .

Sollins, P., K. Cromack Jr, F. Mc Corison, R. Waring, and R. Harr (1981), Changes in nitrogen cycling at an old-growth Douglas-fir site after disturbance, *Journal of Environmental Quality*, *10*(1), 37.

Sollins, P., C. Grier, F. McCorison, K. Cromack Jr, R. Fogel, and R. Fredriksen (1980), The internal element cycles of an old-growth Douglas-fir ecosystem in western Oregon, *Ecological Monographs*, *50*(3), 261-285.

Spies, T. A., J. F. Franklin, and T. B. Thomas (1988), Coarse woody debris in Douglas-fir forests of western Oregon and Washington, *Ecology*, *69*(6), 1689-1702.

Stednick, J. (1996), Monitoring the effects of timber harvest on annual water yield, *Journal of Hydrology*, *176*(1-4), 79-95.

Stednick, J. (2008), Long-term Water Quality Changes Following Timber Harvesting, *ECOLOGICAL STUDIES*, *199*, 157.

Stednick, J. D. (2008), *Hydrological and biological responses to forest practices: the Alsea watershed study*, Springer Verlag.

Stieglitz, M., J. Shaman, J. McNamara, V. Engel, J. Shanley, and G. Kling (2003), An approach to understanding hydrologic connectivity on the hillslope and the implications for nutrient transport, *Global Biogeochemical Cycles*, *17*(4), 1105.

Storck, P., L. Bowling, P. Wetherbee, and D. Lettenmaier (1998), Application of a GIS-based distributed hydrology model for prediction of forest harvest effects on peak stream flow in the Pacific Northwest, *Hydrological Processes*, *12*(6), 889-904.

Tague, C., and L. Band (2000), Simulating the impact of road construction and forest harvesting on hydrologic response, *Earth Surface Processes and Landforms*, *26*(2), 135-151.

Tague, C., and L. Band (2004), RHESSys: Regional Hydro-Ecologic Simulation System-An object-oriented approach to spatially distributed modeling of carbon, water, and nutrient cycling, *Earth Interactions*, *8*, 1-42.

Tague, C., L. Seaby, and A. Hope (2009), Modeling the eco-hydrologic response of a Mediterranean type ecosystem to the combined impacts of projected climate change and altered fire frequencies, *Climatic Change*, *93*(1), 137-155.

Thompson, J. (2006), Society's choices: land use changes, forest fragmentation, and conservation, *Notes*.

Tiedemann, A., T. Quigley, and T. Anderson (1988), Effects of timber harvest on stream chemistry and dissolved nutrient losses in northeast Oregon, *Forest Science*, *34*(2), 344-358.

Triska, F. J., J. R. Sedell, K. Cromack, S. V. Gregory, and F. M. McCorison (1984), Nitrogen budget for a small coniferous forest stream, *Ecological Monographs*, *54*(1), 119-140.

Turner, D. P., M. Guzy, M. A. Lefsky, and T. Van (2003a), Effects of land use and fine scale environmental heterogeneity on net ecosystem production over a temperate coniferous forest landscape, *Tellus B*, *55*(2), 657-668.

Turner, D. P., M. Guzy, M. A. Lefsky, W. D. Ritts, S. Van Tuyl, and B. E. Law (2004), Monitoring forest carbon sequestration with remote sensing and carbon cycle modeling, *Environmental Management*, *33*(4), 457-466.

Turner, D. P., M. Guzy, M. A. Lefsky, S. Van Tuyl, O. Sun, C. Daly, and B. E. Law (2003b), Effects of land use and fine scale environmental heterogeneity on net ecosystem production over a temperate coniferous forest landscape, *Tellus B*, *55*(2), 657-668.

Valentine, T., and G. Lienkaemper (2005), 30 meter digital elevation model (DEM) clipped to the Andrews Experimental Forest. Long-Term Ecological Research. Forest Science Data Bank, Corvallis, OR. [Database]. Available: http://andrewsforest.oregonstate.edu/data/abstract.cfm?dbcode=GI002 (16 July 2011).

Van Breemen, N., A. C. Finzi, and C. D. Canham (1997), Canopy tree–soil interactions within temperate forests: effects of soil elemental composition and texture on species distributions, *Can. J. For. Res*, *27*(7), 1110-1116.

Vanderbilt, K., K. Lajtha, and F. Swanson (2003), Biogeochemistry of unpolluted forested watersheds in the Oregon Cascades: temporal patterns of precipitation and stream nitrogen fluxes, *Biogeochemistry*, *62*(1), 87-117.

Vitousek, P., and W. Reiners (1975), Ecosystem succession and nutrient retention: a hypothesis, *BioScience*, *25*(6), 376-381.

Wallace, J., and A. Benke (1984), Quantification of wood habitat in subtropical coastal plain streams, *Canadian Journal of Fisheries and Aquatic Sciences*, *41*(11), 1643-1652.

Waring, R., and J. Franklin (1979), Evergreen coniferous forests of the Pacific Northwest, *Science*, *204*(4400), 1380-1386.

Weber, M., and M. Flannigan (1997), Canadian boreal forest ecosystem structure and function in a changing climate: impact on fire regimes, *Environmental Reviews*, *5*(3-4), 145-166.

Weier, K., J. Doran, J. Power, D. Walters, and A. USDA (1993), Denitrification and the dinitrogen/nitrous oxide ratio as affected by soil water, available carbon, and nitrate.

West, N. E., and W. W. Chilcote (1968), Senecio sylvaticus in relation to Douglas-fir clear-cut succession in the Oregon Coast Range, *Ecology*, *49*(6), 1101-1107.

Williams, M. R., and J. M. Melack (1997), Effects of prescribed burning and drought on the solute chemistry of mixed-conifer forest streams of the Sierra Nevada, California, *Biogeochemistry*, *39*(3), 225-253.

Wimberly, M. C. (2002), Spatial simulation of historical landscape patterns in coastal forests of the Pacific Northwest, *Canadian Journal of Forest Research*, *32*(8), 1316-1328.

Wright, C. S., and J. K. Agee (2004), Fire and vegetation history in the eastern Cascade Mountains, Washington, *Ecological Applications*, *14*(2), 443-459.

Wright, H. E., and M. L. Heinselman (1973), The ecological role of fire in natural conifer forests of western and northern North America: introduction. Quaternary Research 3:319 –328.

Wright, P., M. Harmon, and F. Swanson (2002), Assessing the effect of fire regime on coarse woody debris, *USDA Forest Service General Technical Report PSW-GTR*, *181*, 621-634.

Yanai, R. D., W. S. Currie, and C. L. Goodale (2003), Soil carbon dynamics after forest harvest: an ecosystem paradigm reconsidered, *Ecosystems*, *6*(3), 197-212.

CHAPTER 5

CATCHMENT BIOGEOCHEMICAL RESPONSES TO FOREST HARVEST AMOUNT AND SPATIAL PATTERN

Alex Abdelnour[1], Robert McKane[2], Marc Stieglitz[1,3], Feifei Pan[1,4]

[1] Department of Civil and Environmental Engineering, Georgia Institute of Technology, Atlanta, GA, USA.
[2]US Environmental Protection Agency, Corvallis, OR, USA
[3]School of Earth Atmospheric Sciences, Georgia Institute of Technology, Atlanta, GA, USA.
[4]Department of Geography, University of North Texas, Denton, TX, USA.

5.1. Abstract

A new ecohydrological model, Visualizing Ecosystems for Land Management Assessments (VELMA), was used to analyze effects of forest harvest location and amount on ecosystem carbon (C) and nitrogen (N) dynamics in an intensively studied headwater catchment (WS10) in western Oregon, USA. The goal is to elucidate how the interaction of hydrological and biogeochemical processes within harvested and unharvested areas regulates losses of dissolved C and N from the terrestrial system to the stream and atmosphere. The model was previously calibrated to simulate observed ecohydrological responses of WS10 to a whole-catchment clearcut in 1975. Here we apply 100 scenarios for which harvest amount ranged from 2% to 100% of catchment area. Model results show that (1) NH_4 and NO_3 losses increased exponentially when unharvested riparian buffer zones fell below 60% of total catchment area, and (2) for each 1% increase in harvest area DON and DOC losses increased linearly. We then apply 20 scenarios for which harvest amount was fixed at 20% but harvest location varied with respect to hillslope position. As harvest distance to the stream decreased, simulated NH_4 and NO_3 losses increased exponentially, and DON and DOC losses increased linearly. Our analysis examines how specific biogeochemical processes (decomposition, nitrification, denitrification and plant N uptake) and hydrological processes (evapotranspiration, soil moisture, and vertical and lateral flow) interact within soil profiles and hillslopes to regulate short and long-term losses of nutrients following harvest. This exercise demonstrates VELMA's potential for informing riparian forest management practices aimed at protecting stream water quality.

5.2. Introduction:

Forest harvest effects on watershed hydrological and biogeochemical processes have been well described experimentally [*Bormann et al.*, 1968; *Harr*, 1976; *Hicks et al.*, 1991; *Jones*, 2000; *Jones and Post*, 2004; *Likens and Bormann*, 1995; *Rothacher*, 1970; *Sollins et al.*, 1981; *Swank et al.*, 2001; *Waichler et al.*, 2005], but a clear understanding of process-level hydro-biogeochemical controls can be difficult to ascertain from data alone. Forest removal experiments have been widely used across the United States in places such as the H.J. Andrews, Hubbard Brook, and Coweeta Experimental Forests. Multiple paired-basin experiments have been conducted at each of these sites to identify vegetation removal effects on streamflow [*Hibbert*, 1966; *Stednick*, 1996], peakflow [*Golding*, 1987; *Jones and Grant*, 1996], summer lowflow [*Keppeler and Ziemer*, 1990; *Rothacher*, 1965], carbon (C) and nitrogen (N) dynamics [*Sollins and McCorison*, 1981; *Sollins et al.*, 1981], and nutrient export to the stream [*Aust and Blinn*, 2004; *Sollins and McCorison*, 1981; *Stednick*, 2008; *Vitousek et al.*, 1979]. A number of generalizations concerning the effects of harvest on C and N dynamics have emerged from these analyses: (1) removal of forest cover increases nutrient concentration in streams [*Bormann et al.*, 1968; *Bormann et al.*, 1974; *Sollins and McCorison*, 1981], greenhouse gas emissions [*Harmon et al.*, 1990], and soil microbial activity (i.e. nitrification [*Bormann et al.,* 1968], denitrification [*Likens et al.*, 1978], soil heterotrophic respiration [*Grant et al.*, 2007], among others), and reduces plant N uptake and forest productivity [*Sollins et al.,* 1981]; (2) forest regrowth decreases nitrogen export to streams [*Likens et al.*, 1978; *Marks and Bormann*, 1972; *Vitousek and Reiners*, 1975]; and (3) the initial response to harvest and the subsequent recovery of forest productivity, nutrient pools, and nutrient losses are highly variable and difficult to predict [*Vitousek et al.*, 1979].

The factors that control the variability in biogeochemical response to harvest include harvest amount, harvest location, vegetation type, and climatic/hydrologic regimes, amongst others. For example, *Vitousek et al.,* [1979] analyzed 19 experimental studies to explore the quantitative and temporal dynamics of nutrient losses after forest harvest, and found that the extent of nitrogen losses following forest harvest varies tremendously from site to site and can be in part attributed to site characteristics. *Binkley*

and Brown [1993] analyzed the effects of harvesting on streamwater concentrations of nitrate from 31 experimental studies in the US and Canada, and found that post-harvest streamwater nitrate concentrations were usually higher in the eastern US compared to central and western regions. Variability in biogeochemical responses to harvest was also apparent within a region. For example, following whole-catchment clearcutting in western US locations, stream nitrate concentrations increased by 3-fold (0.08 $mgL^{-1}yr^{-1}$), 53-fold (0.16 $mgL^{-1}yr^{-1}$), and 11-fold (0.46 $mgL^{-1}yr^{-1}$) in Coyote Creek Oregon, High Ridge Oregon, and UBC Research Forest British Columbia, respectively, but decreased by 29% (0.05 $mgL^{-1}yr^{-1}$) in Bitterroot Montana. Moreover, *Binkley and Brown* [1993] reported that clearcutting 33% of a catchment in Fraser Colorado resulted in a 9-fold (0.054 $mgL^{-1}yr^{-1}$) increase in stream nitrate, whereas an 88% clearcut in Alsea Oregon resulted in no annual increase in stream nitrate concentration. It was also unclear how harvest location within these watersheds, as opposed to site characteristics, might have influenced nutrient fluxes. Thus, although carefully designed paired-catchment experiments and statistical analyses can provide strong circumstantial evidence for process-level controls, they generally cannot be used alone to quantify the contribution of specific processes to observed stream chemistry responses.

Process-based ecohydrological models can help address this need by (1) providing a whole-system synthesis of disparate data sets (soils, vegetation, climate, etc.) and (2) analyzing underlying process-level controls on catchment hydrological and biogeochemical responses to disturbance. In so doing, well-constrained models can extend a data set by providing a framework for exploring conditions that would be too difficult or costly to implement in practice. Moreover, models can isolate the effect of a 'target' treatment factor from the effects of other factors that may be unavoidably altered within a single treatment [*McKane et al.*, 1997]. For example: (1) *Aber et al.* [2002] applied the PnET-CN model [*Aber et al.,* 1997] on Watershed 6 of the Hubbard Brook Experimental Forest, to test the individual and combined effects of climate variability, changes in atmospheric chemistry, and physical and biotic disturbances on DIN loss rate; (2) *Arheimer et al.* [2005] used the HBV-N model [*Arheimer and Brandt*, 1998] to explore the impact of climate change on nitrogen leaching, water discharge, and nitrogen retention in a catchment in southern Sweden; (3) *Lam et al.* [2009] used the SWAT

model (Soil and Water Assessment Tool [*Arnold et al.*, 1998]) to assess the impact of point and non-point source pollution on nitrate loads in a complex lowland catchment in Germany; (4) *Krysanova and Haberlandt* [2002] used the SWIM ecohydrological model (Soil and Water Integrated Model [*Krysanova et al.*, 1998]) to study the impact of various fertilization schemes on nitrogen leaching from arable land in large river basins; and (5) *Band et al.* [2001] applied the RHESSys ecohydrological model [*Band et al.,* 1993] to the Baltimore Long Term Ecological Research site to simulate water spatial distribution, C and N cycling, and nitrate losses to streams. Thus, simulation models provide an effective tool to complement field research and to examine the integrated responses of watershed hydrology, ecology, and biogeochemistry to interacting stressors.

However, existing process-based models have some disadvantages. Many models are too simple to capture important process-level hydrological and biogeochemical controls on ecosystem responses to disturbance. At the other extreme, some models are so complex that they require calibration and forcing data that are often unavailable, or are too computationally expensive to simulate large watersheds and landscapes, or require a high level of expertise to implement. Therefore, there is a need for a balanced approach; specifically an accessible, spatially-distributed, ecohydrological model that is both computationally efficient and relatively easy to implement for analyzing the effects of changes in climate, land use and land cover on watershed processes at scales relevant to formulating management decisions.

We present a relatively simple spatially-distributed ecohydrological model – VELMA (Visualizing Ecosystems for Land Management Assessments; [*Abdelnour et al.*, 2011]) – that simulates changes in soil water infiltration and redistribution, evapotranspiration, surface and subsurface runoff, C and N cycling in plants and soils, and the transport of dissolved forms of C and N from the terrestrial landscape to streams. We apply this model to a small, intensively studied catchment in the Cascade Range in western Oregon, USA, to address three main questions: (1) how do losses of NH_4 and NO_3 to the stream vary with harvest amount (percentage of total catchment area cut); (2) to what extent do unharvested riparian buffers reduce NH_4 and NO_3 losses to the stream; (3) for a given level of harvest, how does harvest location within the catchment affect important biogeochemical fluxes, including losses of NH_4, NO_3, DON and DOC, N_2 and

N_2O emissions, and soil heterotrophic respiration; and (4) how does the interaction of hydrological and biogeochemical processes within the terrestrial ecosystem mediate post-harvest nutrient losses to the stream?

Section 5.3 of this paper describes the study site. Section 5.4 provides an overview of the VELMA modeling framework. Section 5.5 describes our model calibration and simulation methods. Section 5.6 presents model results and discussion for the harvest amount and location scenarios. Section 5.7 summarizes our major conclusions.

5.3. Site Description

Watershed 10 (WS10) of the H.J. Andrews Experimental Forest (HJA) is a 10.2 hectare headwater catchment located in the Cascade Range of western Oregon, at latitude 44°15′N, longitude 122°20′W (Figure 5.1). WS10 has been the site of intensive research and manipulation by the U.S. forest Service since the 1960's, mainly to study the effects of forest harvest on hydrology, sediment transport, and nutrient loss [*Dyrness*, 1973; *Fredriksen*, 1975; *Harr and McCorison*, 1979; *Jones and Grant*, 1996; *Rothacher*, 1965; *Sollins and McCorison*, 1981; *Sollins et al.*, 1981].

Basin elevation ranges from 430 m at the stream gauging station to 700 m at the southeastern ridgeline. Near-stream and side-slope gradients are approximately 24° and 25° to 50°, respectively [*Grier and Logan*, 1977; *Sollins et al.*, 1981]. The climate is relatively mild with wet winters and dry summers [*Grier and Logan*, 1977]. Mean annual temperature is 8.5°C. Daily temperature extremes vary from 39°C in the summer to -20°C in the winter [*Sollins and McCorison*, 1981]. Mean annual precipitation is 2300 mm and falls primarily as rain between October and April [*Jones and Grant*, 1996]. Snow rarely persists longer than a couple of weeks and usually melts within 1 to 2 days after snowfall [*Harr and McCorison*, 1979; *Harr et al.*, 1982; *Jones*, 2000].

Soils are of the Frissel series, which are classified as Typic Dystrochrepts with fine loamy to loamy-skeletal texture [*Sollins et al.*, 1981; *Vanderbilt et al.*, 2003] and are generally deep and well drained [*Grier and Logan*, 1977]. Prior to the 100% clearcut in 1975, WS10 was a 400 to 500 year-old forest dominated by Douglas-fir (*Pseudotsuga menziessii*), western hemlock (*Tsuga heterophylla*), and western red cedar (*Thuja plicata*)

[*Grier and Logan*, 1977] reaching up to ~60 m in height. Rooting depths rarely exceed 100 cm [*Santantonio et al.*, 1977]. Species such as the vine maple (*Acer circinatum*), Pacific rhododendron (*Rhododendron maximum*) and chinkapin (*Castanopsis chrysophylla*) regenerated during the spring after logging. Forest regrowth was rapid after the 1975 clearcut, initially by small trees and shrubs that survived logging, and soon after by planted seedlings of Douglas-fir [*Gholz et al.,* 1985]. The dominant vegetation of WS10 today is a ~35 year-old mixed Douglas-fir and western hemlock stand.

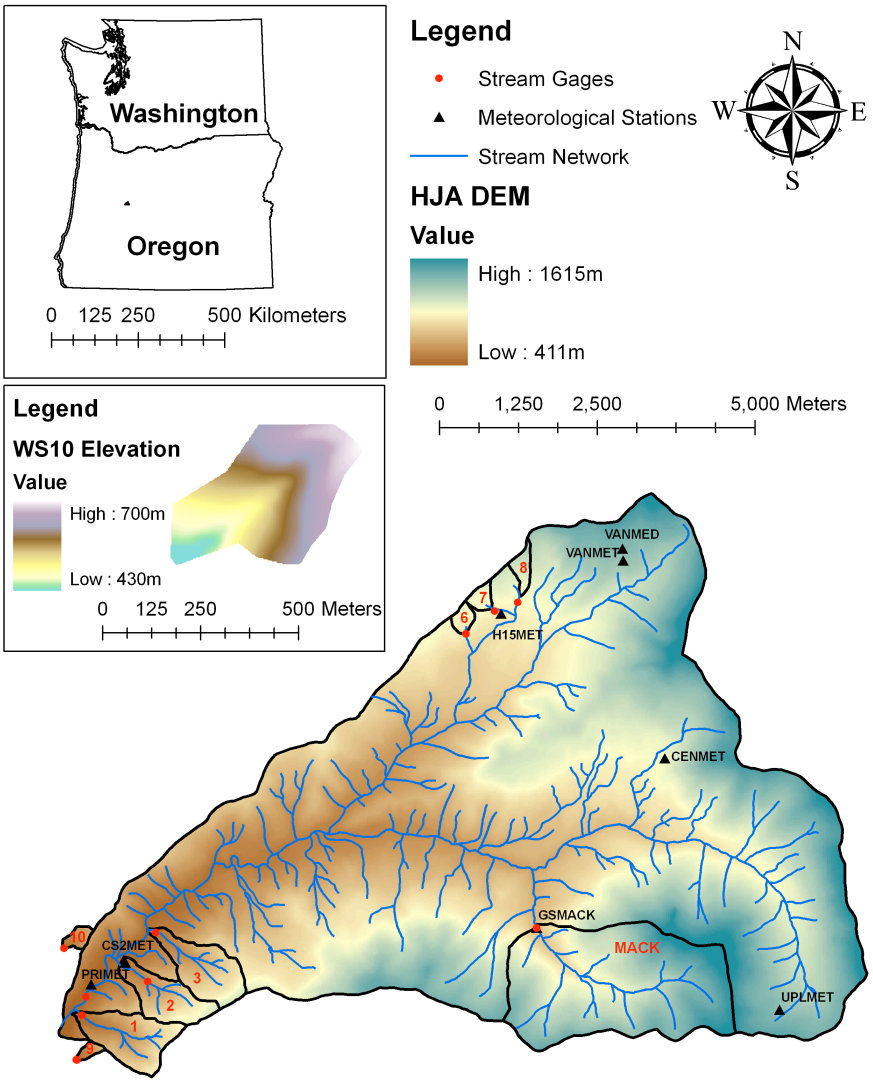

Figure 5.1: *The study site is the watershed 10 (WS10) of the H. J. Andrew Experimental Forest located in the western Cascade Range of Oregon. The red dots represent the locations of the stream gages. The black triangles represent the locations of the meteorological stations.*

5.4. The Eco-Hydrological Model

VELMA (Visualizing Ecosystems for Land Management Assessment) is a spatially distributed ecohydrological model designed to simulate the integrated responses of vegetation, soil, and water resources to multiple forcing variables, e.g., changes in climate, land use and land cover. It is intended to be broadly applicable to a variety of ecosystems (forest, grassland, agricultural, tundra, etc.) and to provide a computationally efficient means for scaling up ecohydrological responses across multiple spatial and temporal scales – hillslopes to basins, and days to centuries (Figure 5.2).

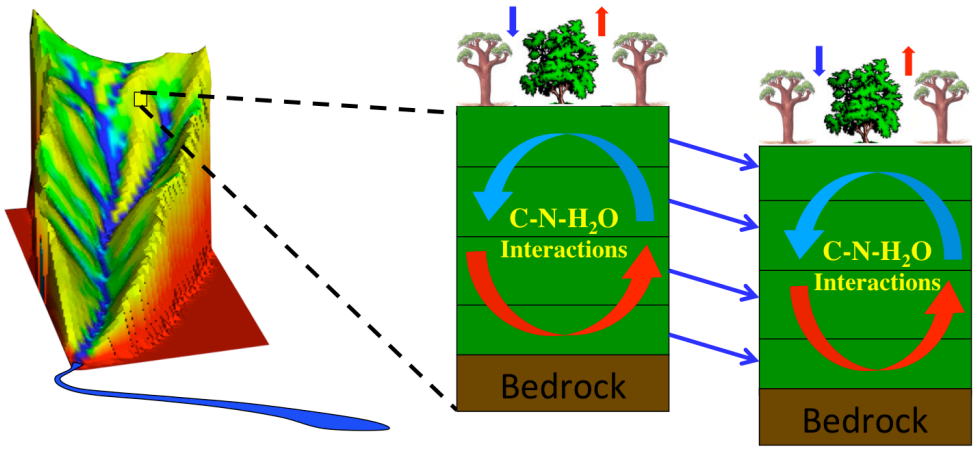

Figure 5.2: *Conceptual catchment modeling framework using multi-layered soil columns.*

The model uses a distributed soil column framework to simulate the movement of water and nutrients (organically bound C and N in plants and soils; dissolved NH_4, NO_3, DON and DOC; and gaseous forms of C and N including CO_2, N_2O and N_2) within the soil, between the soil and the vegetation, and from the soil surface and vegetation to the atmosphere. The soil column model consists of three coupled sub-models:

(1) A *hydrological model* (Figure 5.3) that simulates vertical and lateral movement of water within soil, losses of water from soil and vegetation to the atmosphere, and the growth and ablation of the seasonal snowpack – a detailed description of the hydrological model is provided in Appendix A of Chapter 3 [*Abdelnour et al.*, 2011];

(2) A *soil temperature model* [*Cheng et al.*, 2010] that simulates daily soil layer temperatures from surface air temperature and snow depth by propagating the air

temperature first through the snowpack and then through the ground using the analytical solution of the one-dimensional thermal diffusion equation;

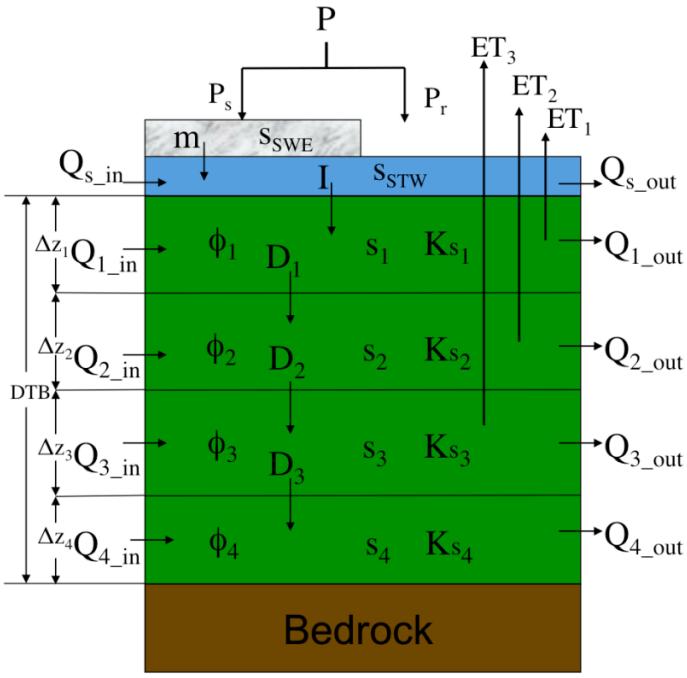

Figure 5.3: *The soil column hydrological framework consists of 4-layer soil column, a standing water layer, and a snow layer. DTB is the soil column depth to bedrock. Δz_i, Ks_i, $\phi_{i,}$, and s_i, are the thickness, the saturated hydraulic conductivity, the soil porosity, and the soil water storage of layer i, respectively; P, P_s and P_r, are the precipitation, snow, and rain, respectively; m is the snowmelt and s_{SWE} is the snow water equivalent depth; I is the infiltration and s_{STW} is the standing water amount; Q_s is the surface runoff; Q_i, D_i and ET_i, are the subsurface runoff, the drainage and the evapotranspiration of layer i, respectively.*

(3) A *plant-soil model* (Figure 4.4) that simulates ecosystem carbon storage and the cycling of C and N between a plant biomass layer and the active soil pools [*Abdelnour et al.*, In review]. Specifically, the plant-soil model simulates the interaction between aboveground plant biomass, soil organic carbon (SOC), soil nitrogen including dissolved nitrate (NO_3), ammonium (NH_4), and organic nitrogen (DON), as well as dissolved organic carbon (DOC). Daily atmospheric inputs of wet and dry nitrogen deposition are accounted for in the ammonium pool of the shallow soil layer. Uptake of ammonium and nitrate by plants is modeled using a Type II Michaelis-Menton function. Loss of plant biomass is simulated through density dependent mortality. The mortality rate and the

nitrogen uptake rate mimic the exponential increase in biomass mortality and the accelerated growth rate, respectively, as plants go through succession and reach equilibrium. Nitrification and denitrification are simulated using the equations from the generalized model of N_2 and N_2O production of *Parton et al.,* [1996; 2001] and *Del Grosso et al.,* [2000]. Decomposition of SOC follows first order kinetics controlled by soil temperature and moisture content as described in the TEM model (Terrestrial Ecosystem Model) of *Raich et al.,* [1991]. Vertical transport of nutrients from one layer to another in a soil column is function of water drainage.

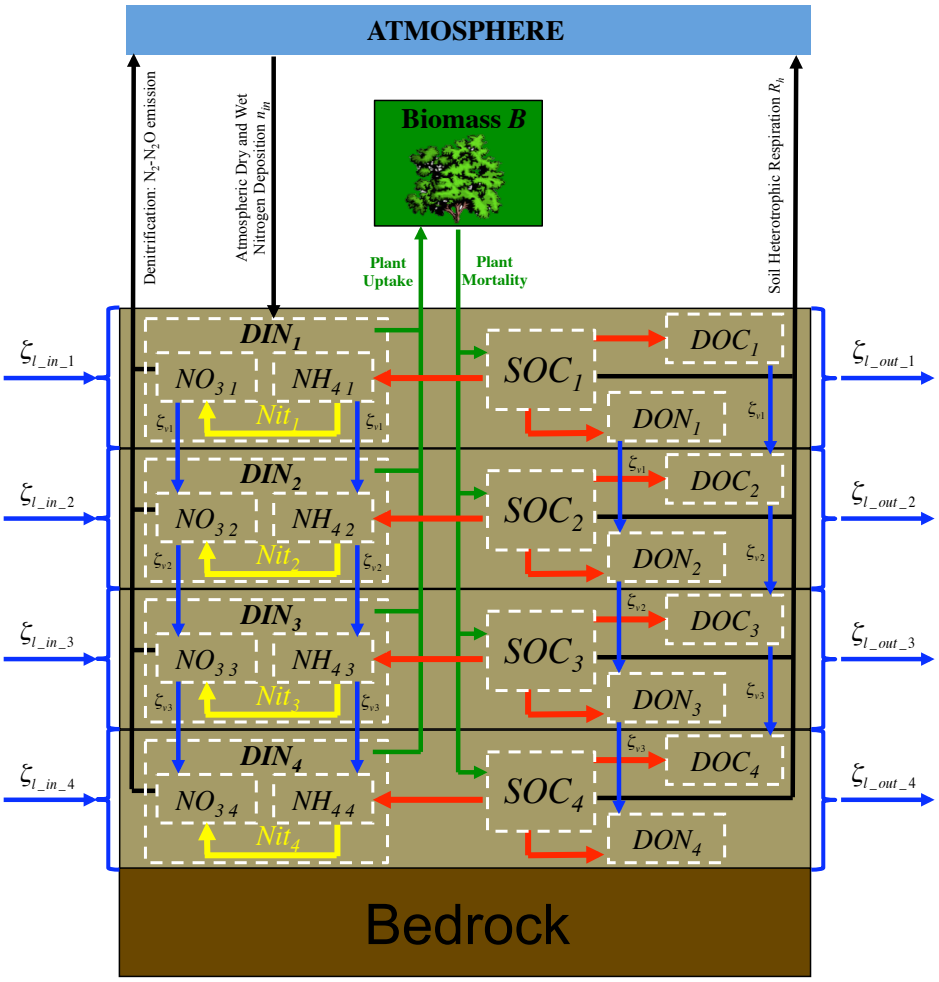

Figure 5.4: *The soil column biogeochemical framework simulates ecosystem carbon storage and the cycling of carbon and nitrogen between a plant biomass layer and a 4-layer soil column.*

The soil column model is placed within a catchment framework to create a spatially distributed model applicable to watersheds and landscapes. Adjacent soil columns interact with each other through the downslope lateral transport of water and nutrients. Surface and subsurface lateral flow are routed using a multiple flow direction method [*Freeman*, 1991; *Quinn et al.*, 1991]. As with vertical drainage of soil water, lateral subsurface downslope flow is modeled using a simple logistic function and corrected for the local slope angle. Lateral transport of nutrients from one soil column to the subsequent soil column or towards the stream is simulated as a function of subsurface flow and nutrient-specific loss rates. Nutrients transported downslope from one soil column to another can be processed through the different C and N cycling sub-models in that downslope soil column, or continue to flow downslope, interacting with other soil columns, or ultimately discharging water and nutrients to the stream.

5.5. Simulation Methods

5.5.1. *Data*

The model is forced with observed data of daily temperature, precipitation, and atmospheric nitrogen deposition. For simulations presented here, daily temperature and precipitation data for the period January 1, 1969 - December 31, 2008 were obtained from the H.J. Andrews LTER PRIMET, CS2MET, and H15MET meteorological stations located in the vicinity of WS10 [*Daly and McKee*, 2011] (see Figure 5.1). Daily atmospheric inputs of wet and dry nitrogen deposition were simulated as a function of the long-term average annual atmospheric nitrogen deposition, daily precipitation, and the long-term average annual precipitation. Specifically, we partitioned the historical mean wet and dry annual atmospheric nitrogen deposition of $0.2 gNm^{-2}yr^{-1}$ [*Sollins et al*., 1980] based on the ratio of daily precipitation to the long-term average annual precipitation. Thus, in any given year, the annual amount of dry and wet nitrogen deposition can either be higher or lower than the long-term average nitrogen deposition based on the amount of precipitation that falls during that year.

Observed data used for model calibration and validation included (1) daily streamflow measured at the WS10 weir between 1969 to 2008 [*Johnson and Rothacher*,

2009]; and (2) NO_3, NH_4, and DON and DOC losses to the stream measured for flow-weighted, composite samples collected approximately once every three weeks for the period 1978 to 2007, except DOC for which the period of record is 1992 to 2007 [*Johnson and Fredriksen*, 2011]; and (3) soil data describing texture, depth to bedrock, and total carbon and nitrogen content [*Abdelnour et al.*, 2011; *Dingman*, 1994]. Model calibration and validation methods are presented in section 5.5.3.

5.5.2. *Model Spatial Structure*

A 30-m resolution Digital Elevation Model (DEM) of the H.J. Andrews's watershed 10 [*Valentine and Lienkaemper*, 2005] was used to compute flow direction, delineate watershed boundaries, and generate a channel network. Each 30x30 m soil column was divided into 4 layers: a surface layer, intermediate layers, and a deep layer. The average soil column depth to bedrock is taken to be 2m [*Ranken*, 1974]. The dominant soil texture is specified as loam [*Ranken*, 1974]. Porosity, field capacity and wilting point values are obtained accordingly [*Dingman*, 1994].

5.5.3. *Model Simulations*

Abdelnour et al., [2011] and *Abdelnour et al.,* [in review] previously calibrated and validated VELMA's hydrological and biogeochemical parameters to simulate long-term (1525–2008 A.D.) changes in WS10 stream hydrology and chemistry and ecosystem C and N dynamics following a stand-replacing fire *circa* 1525, and a 100% clearcut in 1975 of the then 450-year-old forest (Chapter 3 and 4). *Abdelnour et al.,* [in review] used the calibrated set of parameters to simulate and analyze biogeochemical effects of those historical fire and harvest events that occurred over the entire catchment (Chapter 4). A comparison of post-harvest (1975–2008) simulated and observed streamflow and nutrient losses to the stream shows that the calibrated model was able to capture the temporal dynamics of streamflow, NH_4, NO_3, DON and DOC losses with a correlation coefficient of 0.91, 0.7, 0.47, 0.82, and 0.94, respectively. A short description of post-harvest C and N temporal dynamics relevant to this study is presented in section 5.1. All hydrological and biogeochemical parameter names, values and references can be found in *Abdelnour et al.,* [2011] and *Abdelnour et al.,* [in review] (Chapter 3 and 4).

Here we apply these same VELMA parameter values to simulate a series of virtual harvest scenarios to investigate biogeochemical responses to harvest amount (percentage of total catchment area clearcut) and harvest location (clearcut area average distance to stream). These simulations were designed to explore how ecosystem dissolved and gaseous C and N losses (i.e. NH_4, NO_3, DON, DOC losses, N_2-N_2O emissions and soil heterotrophic respiration) respond to harvest amounts ranging from 2% to 100% of total catchment area, as well as variations in the spatial pattern of where these harvests occur. Scenarios for the simulations examining the effects of harvest amount and harvest location are described in sections 5.5.3.1 and 5.5.3.2.

5.5.3.1. ***Harvest Location Scenarios (1975-2008)***

Harvest location simulations were designed to assess the importance of harvest spatial pattern on catchment biogeochemical fluxes, specifically, dissolved C and N losses from the terrestrial system to the stream and atmosphere as well as the terrestrial processes controlling those losses. Twenty harvest location scenarios were simulated from 1975 to 2008 to explore harvest location effects. Each scenario had the harvest amount fixed at 20% of the total catchment area. However, harvest location within the watershed varied. The location of each 20% clearcut varied from an all-ridge location (Figure 5.5; scenario A) to an all-valley location (Figure 5.5; scenario T). Catchment pixels within each 20% clearcut were selected based on flow accumulation (upslope contributing area). Forest removal was simulated by decreasing the initial plant biomass to 10% of its old-growth value, increasing the SOC pool by 10%, and reducing plant transpiration rates to zero at the onset of the disturbance [*Abdelnour et al*., 2011; in review]. A detailed description of the simulated nutrient flux dynamics for the harvest location scenarios is provided in section 5.6.2.

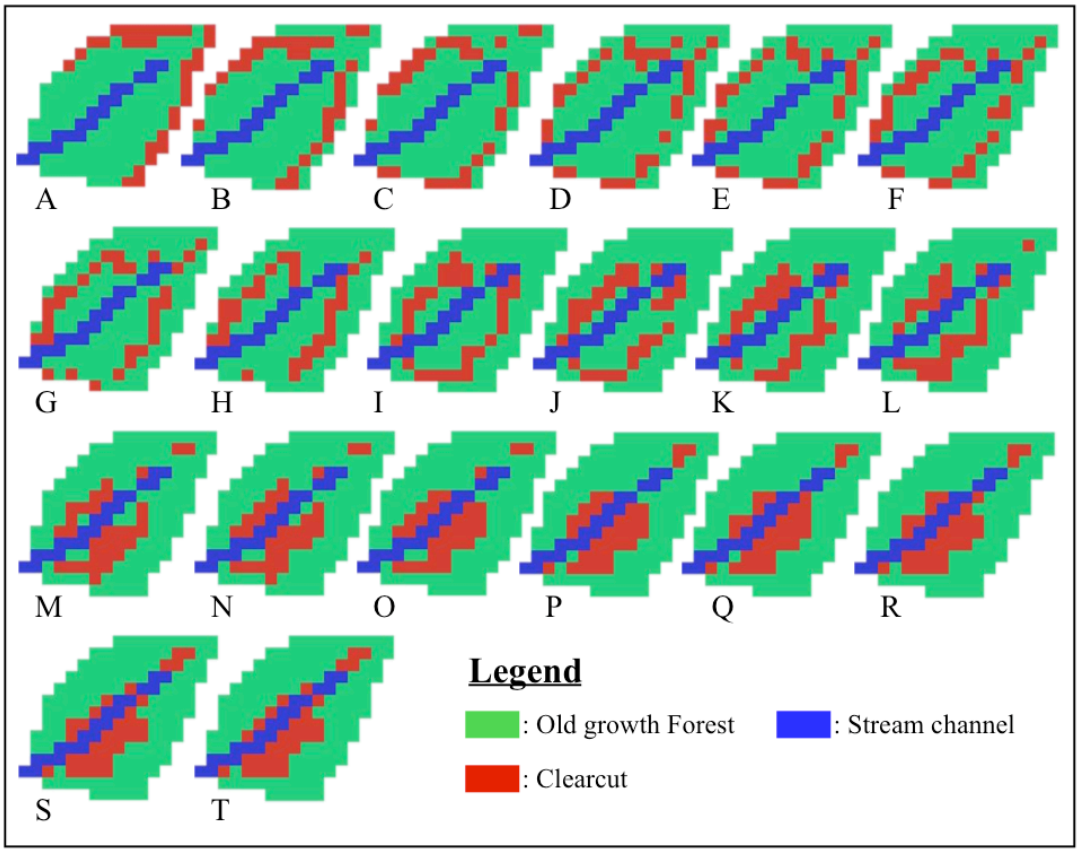

Figure 5.5: *Spatial pattern of forest harvest. Twenty scenarios of 20% clearcut area each were simulated. The location of the 20% clearcut area varied from an all-ridge location (scenario A) to an all-valley location (Scenario T).*

5.5.3.2. ***Harvest Amount Scenarios (1975-2008)***

Harvest amount simulations were designed to (1) explore whether biogeochemical responses to harvest amount exhibit threshold (non-linear) behavior, and (2) assess the effectiveness of riparian buffers in reducing stream nutrients loads. One-hundred harvest amount simulations were conducted from 1975 to 2008 to explore the impact of harvest amount, irrespective of location, on nutrient fluxes. Specifically, fifty harvest amount scenarios ranging from 2% to 100% of total catchment area, with an approximate increment of 2% in harvest area, were simulated from ridge to valley (Figure 5.6). Thereafter, fifty harvest amount scenarios ranging from 2% to 100% of total catchment area, with an approximate increment of 2% in harvest area, were simulated from valley to

ridge (Figure 5.6). As in the harvest location simulations, catchment pixels for a given clearcut amount were based on flow accumulation. Forest harvest was simulated by decreasing the initial plant biomass to 10% of its old-growth value, increasing the SOC pool by 10%, and reducing plant transpiration rates to zero at the onset of the disturbance [*Abdelnour et al*., 2011; in review]. A detailed description of the simulated nutrient flux dynamics for the ridge-to-valley and valley-to-ridge set of scenarios is provided in section 5.6.3.

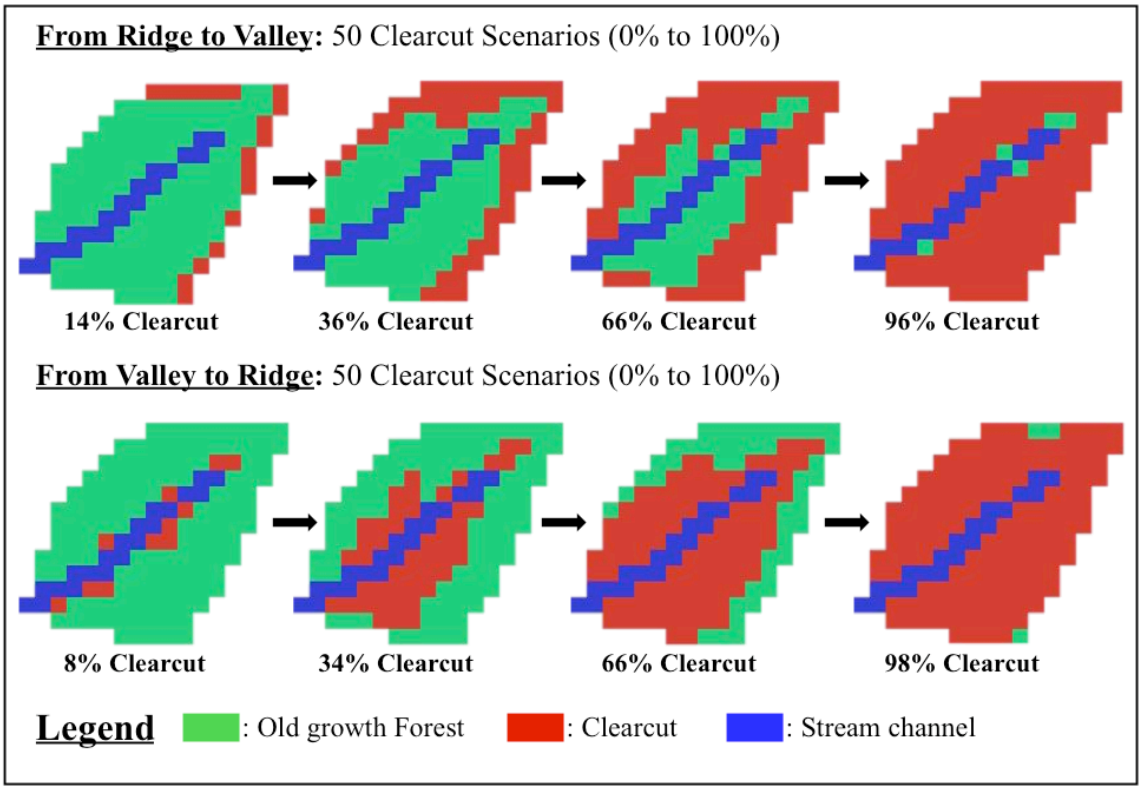

Figure 5.6: *Harvest amount scenarios. Selected examples of fifty clearcut scenarios ranging from 0% to 100% with a ~2% increment in harvest area were simulated (1) from ridge to valley, and (2) from valley to ridge, to assess the impact of increasing harvest area, irrespective of location, on catchment hydrological response.*

5.5.3.3. *Old-growth Control Scenario (1975-2008)*

To establish a baseline reference against which the simulations of harvest amount and location can be compared, we simulated an old-growth forest scenario for which no harvest occurred in 1975. That is, all drivers, parameters and simulation years (1975-2008) for the old-growth simulation were identical to the harvest amount and location

scenario simulations, except that initial (1975) state variables for plant biomass and SOC were set to the old-growth values for 1974, i.e., when the intact WS10 forest was ~450 years-old. A detailed description of the hydrological and biogeochemical dynamics associated with an old-growth simulation can be found in Chapter 3 and 4.

5.6. Results and Discussion

Our discussion of the simulation results will focus on losses of dissolved C and N from the terrestrial system to the stream and to the atmosphere, as well as how the interaction of hydrological and biogeochemical processes within the terrestrial ecosystem regulates these losses. We are particularly interested in examining how harvest amount and spatial pattern alters hydro-biogeochemical interactions within soil profiles and hillslopes. We specifically examine the hypothesis that forest harvest produces three immediate effects – reduced evapotranspiration, reduced plant uptake of nutrients, and a pulse of new detritus (SOC) – that in turn lead to an interacting series of changes in additional processes, such that effects on one process lead to effects on others. Specifically, to what extent do observed increases in the post-harvest mobilization and transport of N to streams depend on an interacting series of biogeochemical transformations (mineralization of organic N contained in decomposing SOC, diminished plant uptake of inorganic N, nitrification of NH_4 to NO_3, and denitrification of NO_3 to gaseous N products (N_2, NO_x, N_2O)) that are in turn mediated by hydrological processes affecting the availability and transport of water within soil profiles and hillslopes (decreased transpiration, increased soil water storage, and increased vertical and lateral flow)? We are also interested in examining how these processes change through time as forest vegetation regrows following harvest.

The model results and discussion are presented in the following sequence. In section 5.6.1, to provide context for the harvest amount and location simulation results conducted in the present study, we briefly review the results of *Abdelnour et al*., [in review] describing the effects of the WS10 whole-catchment clearcut on simulated and observed temporal changes (1975 – 2008) in dissolved and gaseous losses of C and N. In section 5.6.2, we present the simulated effects of harvest location on nutrient losses. Finally, in section 5.6.3, we present the simulated effects of harvest amount on nutrient losses.

5.6.1. Whole-Catchment Clearcut Simulation

For the simulation of the actual whole-catchment clearcut of the WS10 old-growth forest in 1975, streamflow increased by an average of 29% (345 mm) during the first five years after harvest, compared to values for the old-growth simulation described in Section 5.5.3.3, henceforth referred to as "old-growth values". The increase in streamflow reflected the sudden, sharp decrease in transpiration following the complete removal of the canopy. Losses of dissolved C and N to the stream consequently peaked a few years after disturbance, as a result of the combined effects of increases in soil water content, vertical drainage and lateral flow, SOC decomposition, and nitrification, and a decrease in plant N uptake prior to significant re-establishment of plant biomass [*Abdelnour et al.*, in review]. Specifically, simulated annual NH_4 and NO_3 losses peaked 2 years after clearcut, and over the first 5 years averaged 0.08 and 0.9 $gNm^{-2}yr^{-1}$ (4-fold and 150-fold higher than old-growth values). Thereafter, losses of NH_4 and NO_3 to the stream declined exponentially as a result of decreases in SOC decomposition and increases in N uptake by regrowing vegetation. By 2005, thirty years after clearcut, simulated annual NH_4 and NO_3 losses had declined to 0.015 and 0.008 $gNm^{-2}yr^{-1}$ (25% and 10% lower than old-growth values). Similarly, simulated annual DON and DOC losses peaked 2 years after clearcut, as a result of increases in subsurface flow and SOC decomposition. Over the first 5 years, DON and DOC losses averaged 0.15$gNm^{-2}yr^{-1}$ and 3.2 $gCm^{-2}yr^{-1}$ (~20% and 18% higher than old-growth values). Thereafter, annual DON and DOC losses to the stream decreased with decreases in SOC and subsurface flow associated with increases in plant transpiration. By 2005, thirty years after clearcut, simulated annual DON and DOC losses declined to ~0.07$gNm^{-2}yr^{-1}$ and 1.1 $gCm^{-2}yr^{-1}$ (~30% and 35% lower than old-growth values).

Simulated gaseous losses of dissolved C and N to the atmosphere peaked a few years after clearcut due to high SOC decomposition, high soil water content, and low N uptake prior to significant re-establishment of plant biomass. Specifically, simulated annual denitrification rates peaked two years after clearcut as a result of high soil nitrate availability and high soil water content, which enhanced the anaerobic process of denitrification. Simulated annual denitrification rates (i.e. N_2-N_2O emissions to the

atmosphere) averaged 0.9 $gNm^{-2}yr^{-1}$ (~13-fold higher than old-growth values) from 1975 to 1979, then decreased with increases in plant biomass and N uptake, and decreases in SOC and soil water content. By 2005, thirty years after clearcut, simulated denitrification rate had declined to 0.07 $gNm^{-2}yr^{-1}$ (30% lower than old-growth values). Similarly, simulated annual soil heterotrophic respiration peaked 2 years after clearcut as a result of increased SOC decomposition and lower water stress conditions. Simulated annual soil heterotrophic respiration averaged 710 $gCm^{-2}yr^{-1}$ (~30% higher than old-growth values) from 1975 to 1979, and then decreased with decreases in SOC. By 2005, thirty years after clearcut simulated annual soil heterotrophic respiration averaged 280$gCm^{-2}yr^{-1}$ (40% lower than old-growth values).

Thus, processes that favored nutrient losses to the stream dominated ecohydrological responses during the first 5 years after the whole-catchment clearcut in 1975, i.e., before significant re-establishment of vegetation had occurred. These mobilizing processes mainly included decreased plant uptake of NH_4 and NO_3, increased production of NH_4, NO_3, DON and DOC, and increased vertical and lateral flow as a result of decreased transpiration. Although post-harvest denitrification rates were substantially greater than old-growth values, these gaseous N losses were insufficient to significantly counteract the much larger increases in soil NO_3 pool and losses the stream. Finally, the post-harvest changes in dissolved C and N losses to the stream and atmosphere simulated by VELMA were consistent with previously published studies of biogeochemical dynamics in recently clearcut old-growth forest [e.g. *Cairns and Latjtha* 2005; *Grant et al.,* 2007; *Griffiths and Swanson* 2001; *Sollins and McCorison*, 1981; *Fredriksen* 1975].

5.6.2. Harvest Location Simulations

Results for the harvest location simulations indicate that forest harvest location is important in reducing nutrient losses to the stream (Figure 5.7). Specifically, dissolved C and N losses from the terrestrial system to the stream and atmosphere were sensitive to variations in the location of a 20% harvest of WS10 (Figure 5.5, Scenarios A - T). In particular, the relative location of harvested and unharvested areas with respect to the stream had major effects on the suite of hydro-biogeochemical processes discussed in

section 5.6.1 and, consequently, on dissolved and gaseous losses of NH_4, NO_3, DON and DOC. Figure 5.7 shows that simulated annual NH_4 and NO_3 losses to the stream increased exponentially with decreasing harvest area distance to the stream channel. Specifically, a 20% clearcut area in the uplands (at an average distance of 152m to the nearest stream channel, based on flow direction) resulted in an average annual increase in NH_4 and NO_3 losses of 0.8 and 0.6 $mgNm^{-2}yr^{-1}$ (4% and 10% higher than old-growth values). By contrast, a 20% clearcut in the lowlands (at an average distance of 53m from the nearest stream channel) increased average annual NH_4 and NO_3 losses to the stream by 35 and 326 $mgNm^{-2}yr^{-1}$ (~180% and 54-fold higher than old-growth values). These results suggest that large riparian buffers (i.e. the vegetated area near the stream downslope of the clearcut area) can considerably reduce the amounts of NO_3 and NH_4 that reach the stream. The sensitivity of dissolved inorganic nitrogen losses to harvest location stems from the fact that subsurface flow and nutrient losses generated from an upland clearcut area, as opposed to a lowland clearcut area, have a relatively longer flowpath through downslope vegetated areas. Within this vegetated area, subsurface flow and dissolved inorganic nitrogen are subjected to plant transpiration, plant N uptake, soil nitrification and soil denitrification, all of which reduce the amount of water and nutrients that reach the stream. These results support previous reports about the importance of riparian forest buffers in reducing nutrient loads to the stream [*Martin et al.*, 1984]. *Bernhardt et al.,* [2005] argues that riparian forest buffers, with their associated root and microbial populations, act as natural filters limiting the movement of nitrogen from the soil into the stream. Similarly, *Hubbard and Lowrance* [1992] found that nitrate losses are considerably reduced after passing through a 7 m forest buffer. *Hubbard and Lowrance* [1992] attributed this reduction in NO_3 loss to the stream to a combination of denitrification and plant uptake. *Castelle et al.,* [1994] found that the capacity of riparian forest buffers to reduce N losses to streams generally increases with increasing buffer width.

In contrast to the large exponential increases in dissolved inorganic nitrogen losses, simulated annual dissolved organic C and N losses to the stream increased linearly and at a modest rate as a function of decreasing harvest area distance to the stream channel (Figure 5.7). Specifically, a 20% clearcut area in the uplands resulted in an

average annual increase in DON and DOC losses of 3.6mgNm^{-2}yr^{-1} and 87gCm^{-2}yr^{-1} (2.6% and 3% higher than old-growth values), whereas a 20% clearcut in the lowlands resulted in an average annual increase in DON and DOC losses of 6.4mgNm^{-2}yr^{-1} and 119gCm^{-2}yr^{-1} (~5% and 4% higher than old-growth values). This linear increase in dissolved organic C and N to the stream is the result of (1) the near-linear negative relationship between streamflow and harvest distance to the stream [*Abdelnour et al.,* 2011], (2) the high correlation between dissolved organic C and N to the stream and streamflow [*Hope et al.*, 1994; *Vanderbilt et al.*, 2003], and (3) the model assumption that dissolved organic C and N are not appreciably reduced through decomposition or plant N uptake [*Abdelnour et al.,* in review].

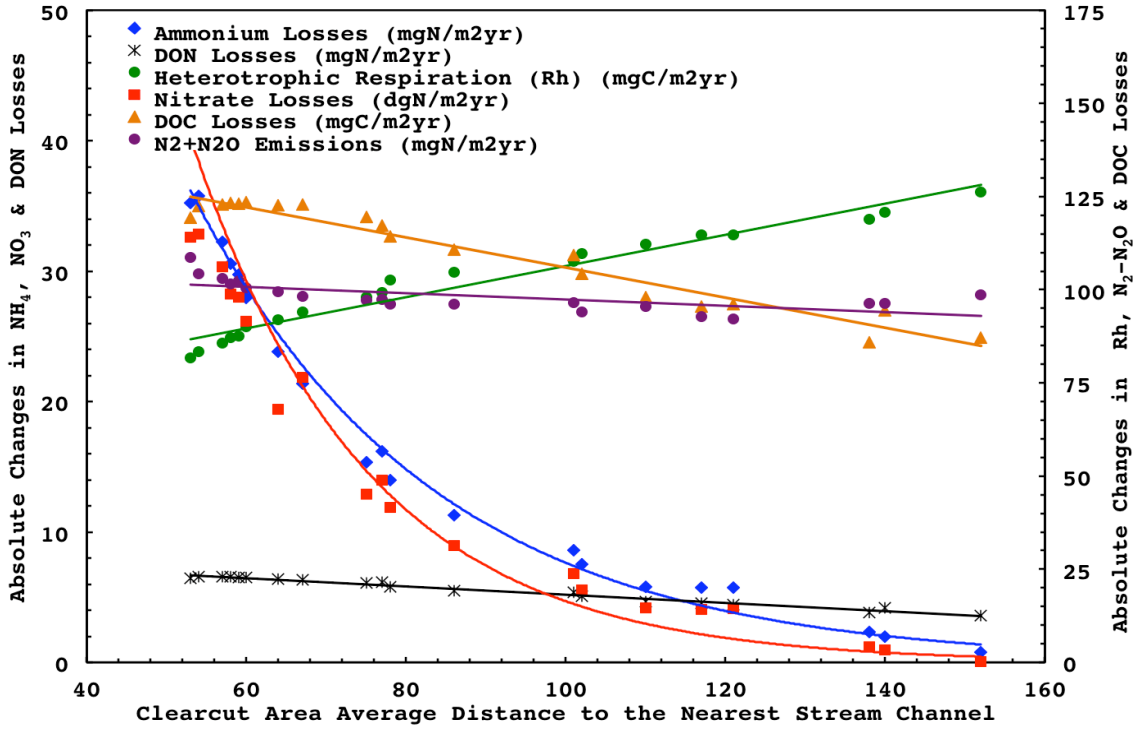

Figure 5.7: *Absolute annual changes in heterotrophic respiration (R_h; green dots; mgCm^{-2}yr^{-1}), denitrification (N_2-N_2O emissions; purple dots; mgNm^{-2}yr^{-1}), ammonium (blue diamonds; mgNm^{-2}yr^{-1}), nitrate (red squares; dgNm^{-2}yr^{-1}), DON (black stars; mgNm^{-2}yr^{-1}), and DOC (orange triangles; mgCm^{-2}yr^{-1}) losses for a 20% clearcut as a function of the average flow path distance in meters between the harvest area and the nearest stream channel. Ammonium and nitrate losses are fitted with an exponential trendline (blue (R^2=0.97) and red (R^2=0.88) solid line, respectively). R_h, N_2-N_2O emissions, DON, and DOC losses are fitted with a linear trendline (green (R^2=0.96), purple (R^2=0.46), black (R^2=0.98), and orange (R^2=0.95) solid line, respectively).*

Figure 5.7 also shows that the simulated annual soil N_2 and N_2O emissions increased with decreasing harvest area distance to the stream channel. Specifically, a 20% clearcut area in the uplands resulted in an average annual increase in N_2-N_2O emissions of 99 $mgNm^{-2}yr^{-1}$ (164% higher than old-growth values), whereas a 20% clearcut in the lowlands resulted in an average annual increase in N_2-N_2O emissions of 109 $mgNm^{-2}yr^{-1}$ (180% higher than old-growth values). This result is consistent with the processes that govern soil denitrification rates. Soil denitrification is an anaerobic process controlled by environmental factors such as soil nitrate level, soil oxygen availability and soil labile carbon availability [*Weier et al.*, 1993]. As a result, soil denitrification rates are generally higher in the wet lowlands and lower in the dry uplands [*Zak and Grigal*, 1991]. Therefore, harvested lowland areas tend to increase soil saturation (through lower transpiration) and soil nitrate availability (through higher ammonium availability and nitrification in surface layers), which in turn enhances denitrification (typically in surface layers after rainfall, or in saturated deep soil layers). Although upland clearcuts also led to increased amounts of soil water and denitrification, the increases in denitrification were ~20% lower than the levels simulated for the lowland clearcut.

It is also important to examine the effects of harvest location on SOC decomposition, given the importance of soil heterotrophs in regulating the production and consumption of dissolved forms of C and N. Simulated annual soil heterotrophic respiration decreased linearly with decreasing harvest area distance to the stream channel (Figure 5.7). Specifically, a 20% clearcut area in the uplands resulted in an average annual increase in soil heterotrophic respiration of 36 $mgCm^{-2}yr^{-1}$ (7% higher than old-growth values), whereas a 20% clearcut in the lowlands resulted in an average annual increase of 23 $mgCm^{-2}yr^{-1}$ (4% higher than old-growth values). This result is consistent with the processes that govern soil heterotrophic respiration. Soil heterotrophic respiration varies with environmental factors such as soil temperature [*Davidson et al*., 2000; *Davidson et al*., 1993; *Raich and Potter,* 1995] and soil moisture [*Bowden et al.*, 1998]. Soil moisture affects heterotrophic respiration by limiting decomposition in low and high moisture conditions, with peak respiration occurring at ~ 40% saturation [*Alexander*, 1977]. In our upland harvest simulations, soil moisture conditions were

more favorable for decomposition than the lowland harvests, where frequently saturated conditions limited decomposition.

5.6.3. Harvest Amount Simulations

Model results for the harvest amount simulations consisted of two sets of simulations results pertaining to the ridge-to-valley and valley-to-ridge scenarios described in section 5.5.3.2. We first present the results of the ridge-to-valley simulations, then the results of the valley-to-ridge simulations, and finally, we combine these two sets of simulations to draw insights into the relationship between harvest amount and nutrient losses, irrespective of location.

For the ridge-to-valley simulations, simulated annual NH_4 and NO_3 losses to the stream increased exponentially with increasing harvest area and exhibited a threshold behavior (Figure 5.8A and 5.9A). Specifically, over the first five years after clearcut, the annual increases in NH_4 and NO_3 losses were less than 3 and 17 $mgNm^{-2}yr^{-1}$ (12% and 210% higher than old-growth values), respectively, for harvest amounts less than 40%. For harvest amounts greater than 40% of the total catchment area, NH_4 and NO_3 losses increased exponentially with percent harvest area, reaching an average of 80 and 900 $mgNm^{-2}yr^{-1}$ (4-fold and 150-fold higher than old-growth values) over the first five year after a 100% clearcut. By contrast, simulated annual DON and DOC losses and N_2-N_2O emissions increased nearly linearly (correlation coefficient R^2=0.97, 0.99 and 0.98, respectively) with increasing harvest amount, and exhibited a slight convex curvature (Figure 5.10). Specifically, average annual DON losses, DOC losses and N_2-N_2O emissions increased by 0.2 $mgNm^{-2}yr^{-1}$, 4.3 $mgCm^{-2}yr^{-1}$, and 8.7 $mgNm^{-2}yr^{-1}$, respectively for each 1% of catchment area harvested near the ridge, but by 0.25 $mgNm^{-2}yr^{-1}$, 5 $mgCm^{-2}yr^{-1}$, and 11.8 $mgNm^{-2}yr^{-1}$, respectively for each 1% of catchment area harvested near the valley. Simulated annual rates of soil heterotrophic respiration increased nearly linearly (correlation coefficient R^2=0.97) with increasing harvest amount, exhibiting a slight concave curvature in the rate of increase (Figure 5.10D). Average annual soil heterotrophic respiration increased by 1.6 $gCm^{-2}yr^{-1}$ for each 1% harvest amount located near the ridge, and by 0.8 $gCm^{-2}yr^{-1}$ for each 1% harvest amount located near the valley.

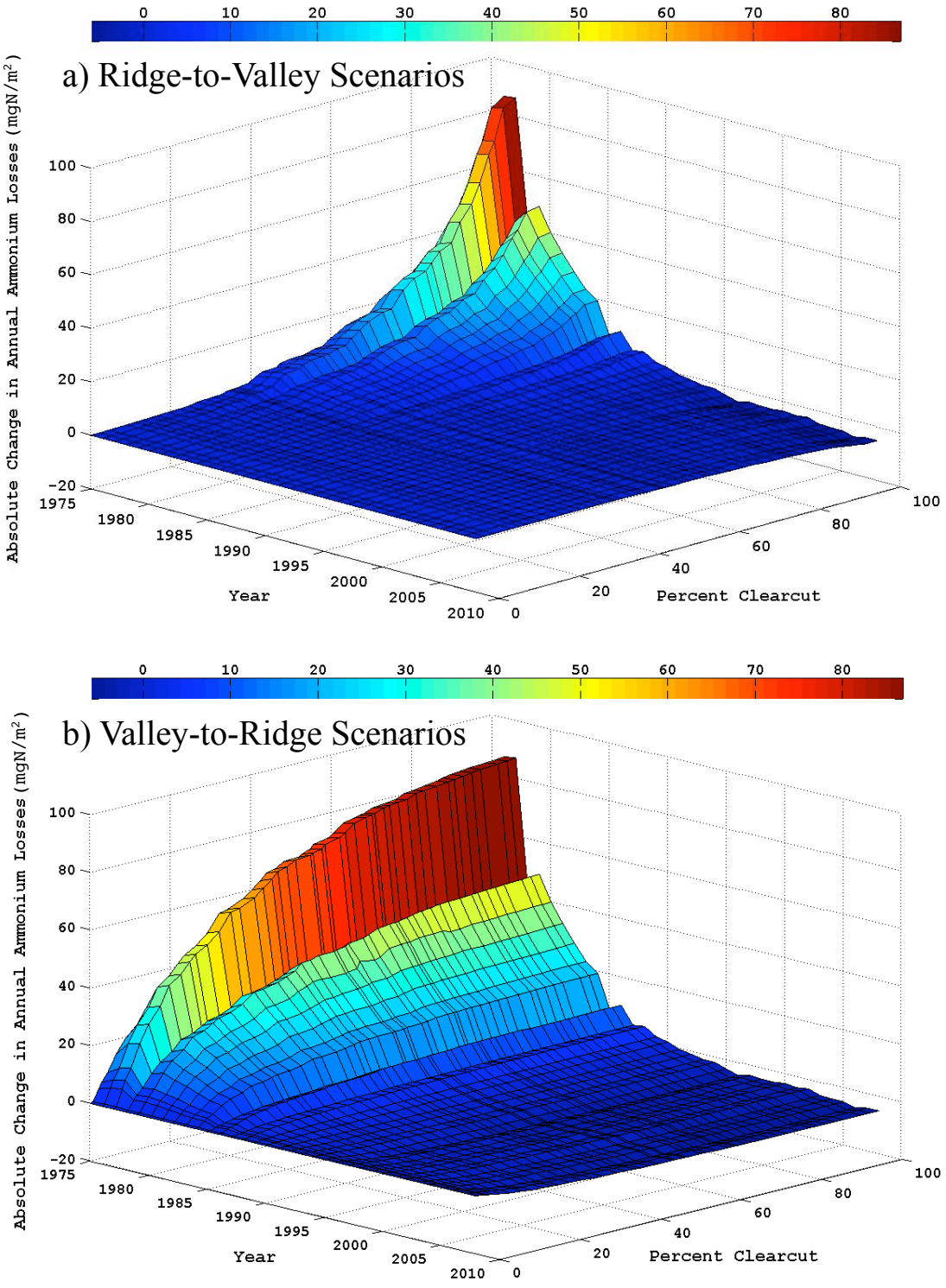

Figure 5.8: *The absolute change (compared to old-growth values) in simulated annual ammonium ($mgNm^{-2}yr^{-1}$) losses to the stream with respect to harvest area for the a) ridge-to-valley and b) valley-to-ridge set of scenarios. The x-axis represents the 1975-2008 period of available precipitation and temperature data. The y-axis represents the harvest amount as the percentage of the watershed area that is clearcut.*

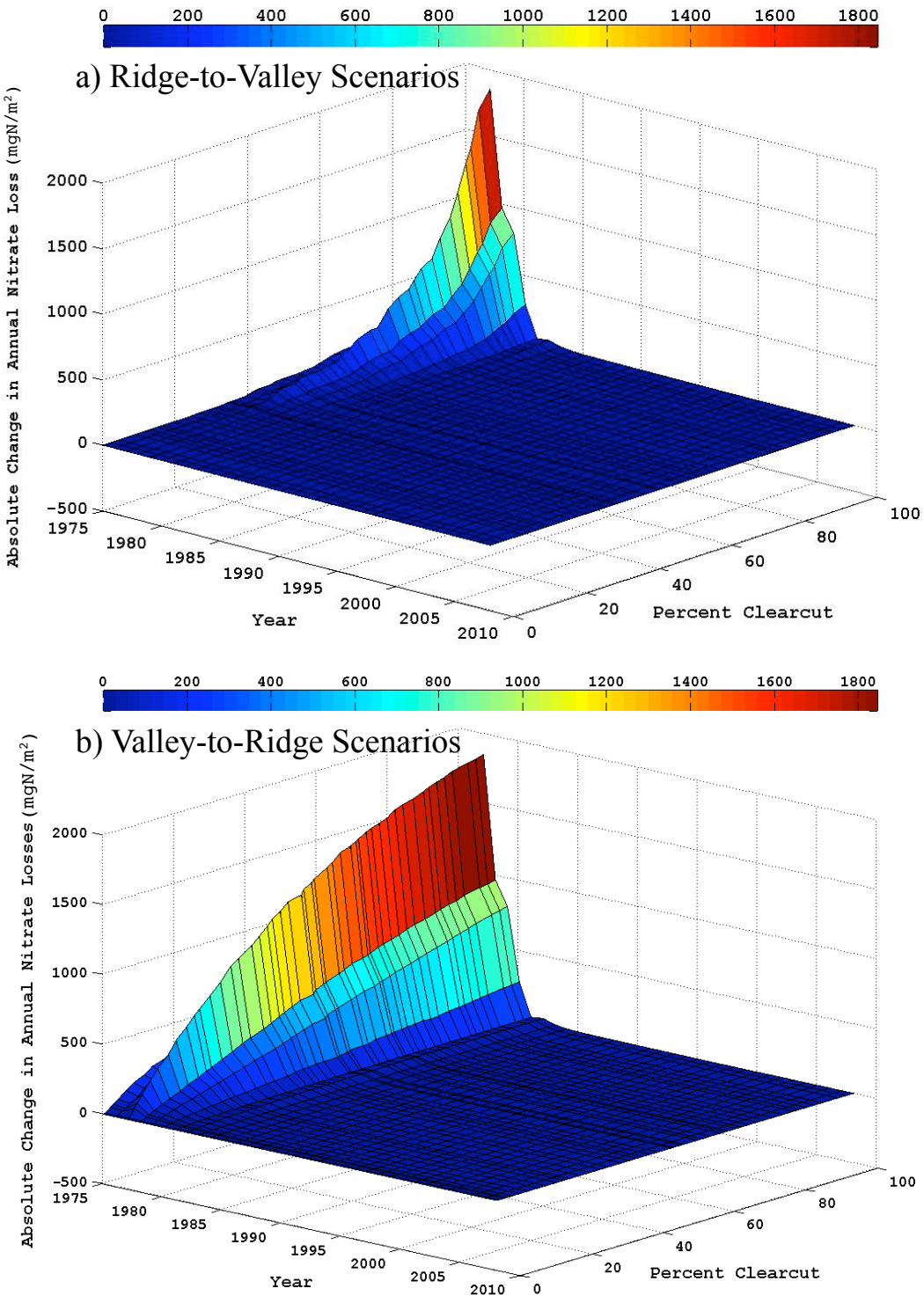

Figure 5.9: *The absolute change (compared to old-growth values) in simulated annual nitrate NO_3 ($mgNm^{-2}yr^{-1}$) losses to the stream with respect to harvest area for the a) ridge-to-valley and b) valley-to-ridge set of scenarios. The x-axis represents the 1975-2008 period of available precipitation and temperature data. The y-axis represents the harvest amount as the percentage of the watershed area that is clearcut.*

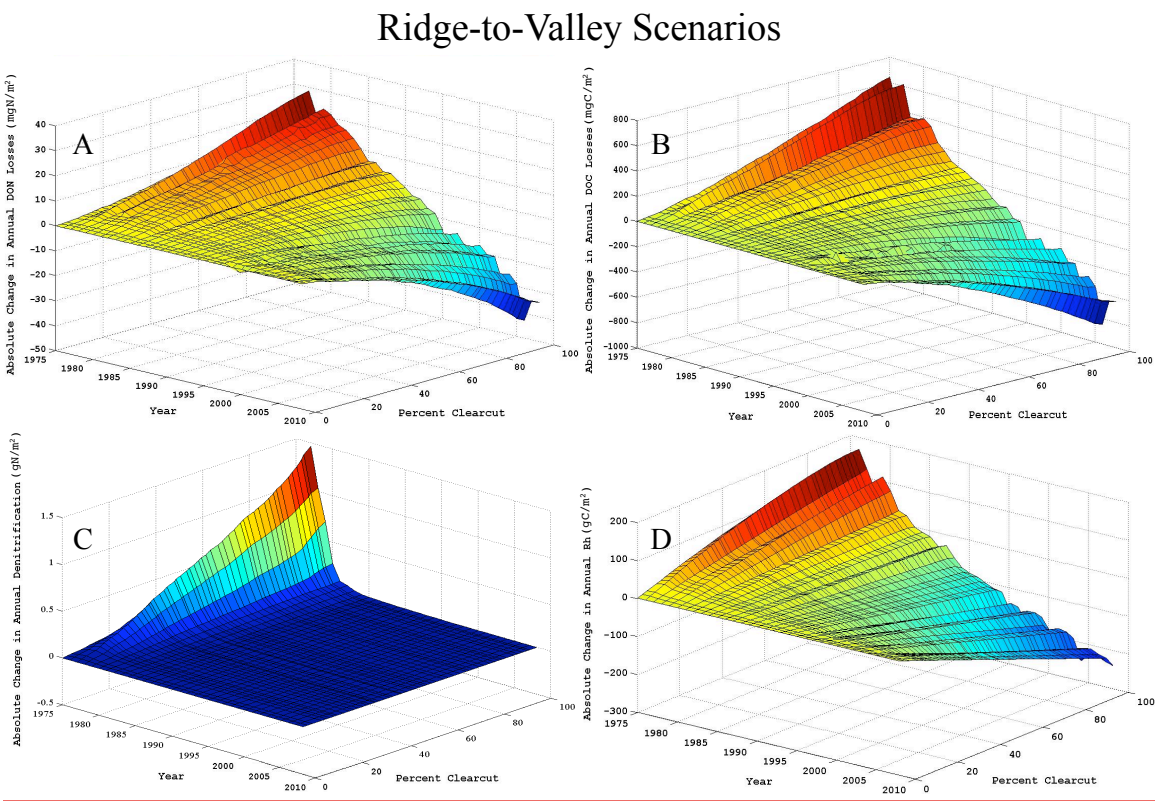

Figure 5.10: *The absolute change (compared to old-growth values) in simulated annual DON losses ($mgNm^{-2}yr^{-1}$;subplot A), DOC losses ($mgCm^{-2}yr^{-1}$; subplot B), N_2-N_2O emission ($gNm^{-2}yr^{-1}$; subplot C) and R_h ($gCm^{-2}yr^{-1}$; subplot D) with respect to harvest area for the ridge-to-valley set of scenarios. The x-axis represents the 1975-2008 period of available precipitation and temperature data. The y-axis represents the harvest amount as the percentage of the watershed area that is clearcut.*

For the valley-to-ridge simulations, simulated annual NH_4 and NO_3 losses to the stream increased logarithmically with increasing harvest area (Figure 5.8B and 5.9B). Specifically, average annual NH_4 and NO_3 losses increased by 1.8 $mgNm^{-2}yr^{-1}$ and 15 $mgNm^{-2}yr^{-1}$, respectively, for each 1% of catchment area harvested near the valley, but by 0.1 $mgNm^{-2}yr^{-1}$ and 5.5 $mgNm^{-2}yr^{-1}$, respectively, for each 1% of catchment area harvested near the ridge. By contrast, simulated annual increases in DON and DOC losses and N_2-N_2O emissions increased nearly linearly (correlation coefficient R^2=0.97, 0.99 and 0.99, respectively) with increasing harvest amount, and exhibited a slight concave curvature (Figure 5.11). In particular, average annual DON losses, DOC losses and N_2-N_2O emissions increased by 0.3 $mgNm^{-2}yr^{-1}$, 6 $mgCm^{-2}yr^{-1}$, and 10.2 $mgNm^{-2}yr^{-1}$,

respectively for each 1% of catchment area harvested near the valley, but by 0.16 $mgNm^{-2}yr^{-1}$, 4 $mgCm^{-2}yr^{-1}$, and 9.5 $mgNm^{-2}yr^{-1}$, respectively for each 1% of catchment area harvested near the ridge. Simulated annual rates of soil heterotrophic respiration increased nearly linearly (correlation coefficient R^2=0.99) with increasing harvest amount, and exhibited a slight concave curvature (Figure 5.11D). Average annual soil heterotrophic respiration increased by 1.4 $gCm^{-2}yr^{-1}$ for each 1% harvest amount located near the ridge, and by 1.5 $gCm^{-2}yr^{-1}$ for each 1% harvest amount located near the valley.

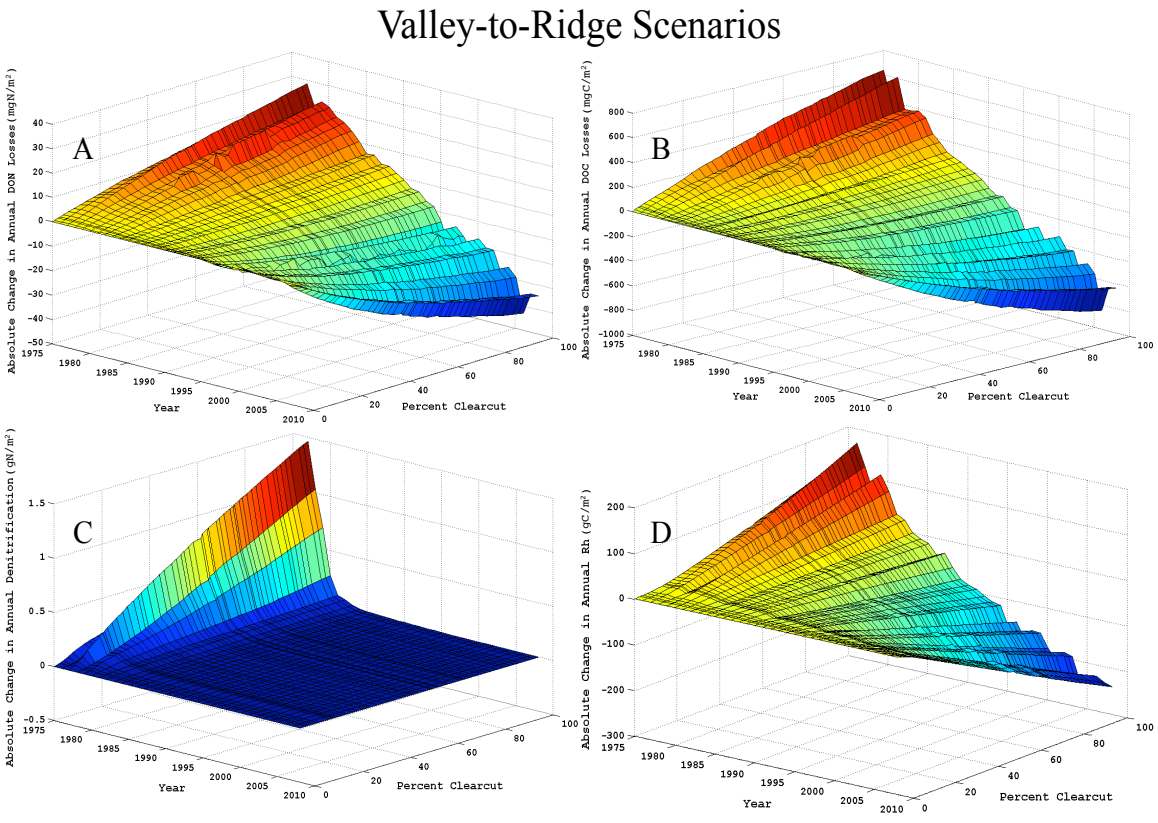

Figure 5.11: *The absolute change (compared to old-growth values) in simulated annual DON losses ($mgNm^{-2}yr^{-1}$;subplot A), DOC losses ($mgCm^{-2}yr^{-1}$; subplot B), N_2-N_2O emission ($gNm^{-2}yr^{-1}$; subplot C) and R_h ($gCm^{-2}yr^{-1}$; subplot D) with respect to harvest area for the valley-to-ridge set of scenarios. The x-axis represents the 1975-2008 period of available precipitation and temperature data. The y-axis represents the harvest amount as the percentage of the watershed area that is clearcut.*

A clear difference between the ridge-to-valley and the valley-to-ridge simulations is reflected in the shapes of the response curves described above. This difference is most

apparent in the relationship between NH_4 and NO_3 losses and harvest amount. The threshold behavior of NH_4 and NO_3 losses observed in the ridge-to-valley simulations is essentially caused by the riparian buffer dynamics. Riparian buffers reduce nitrogen losses to the stream through nitrogen uptake by plants, microbial immobilization, soil storage, ground water mixing and denitrification [*Lowrance et al.*, 1997]. Figure 5.8A and 5.9A show that NH_4 and NO_3 losses sharply increased after a clearcut of 40%. Buffer areas of 60% or more in WS10 strongly limited NH_4 and NO_3 losses to the stream (i.e. NH_4 and NO_3 losses to the stream were less than 7% and 2% of their maximum values). However, riparian buffer area or width is site specific and governed by soil type, vegetation type, subsurface flowpath, subsurface biogeochemistry and climate [*Mayer et al.*, 2007]. For example, in contrast to our result, *Martin et al.,* [1984] reported the effects of forest harvest on water quality from 38 watersheds within New England, and found that forest harvest amount had to exceed 70% of the watershed in order to have an increase in streamwater nitrate concentration.

While harvest location clearly affected the magnitude and the shapes of the response curves described above, taken together (Figure 5.12; solid black line), the ridge-to-valley and valley-to-ridge simulations suggested that average annual DON and DOC losses, N_2-N_2O emissions and soil heterotrophic respiration increase linearly (correlation coefficient R^2=0.95, 0.98, 0.98, and 0.96, respectively) at a rate of 0.2 $mgNm^{-2}yr^{-1}$, 5 $mgCm^{-2}yr^{-1}$, 9 $mgNm^{-2}yr^{-1}$, and 1.3 $gCm^{-2}yr^{-1}$ for each 1% of catchment area harvested, respectively. A comparison of our results with observed data is difficult, given that few catchment-scale studies have monitored the impact of different harvest types and intensities on carbon and nitrogen losses. The empirical studies that have been conducted have generally found that the effect of forest harvest on stream water chemistry and gaseous C and N emissions increases with increasing harvest area [*Fowler et al.*, 1988; *Stark*, 1979; *Tiedemann et al.*, 1988]. *Grier et al.,* [1989] reported that in forest harvesting or thinning, nutrient losses tend to be proportional to the amount of timber removed. *Feller et al.,* [2000] monitored nutrient fluxes from 74 sampling sites in the MASS study site located in British Columbia and consisting of four different forest harvest treatments and an undisturbed old-growth forest. *Feller et al.,* [2000] found that the amount of nutrients (NO_3^-, K^+, SO_4^{2-}) in the stream and in solution beneath an old-

growth forest increased with the percentage of forest that was harvested. *Londo et al.,* [1999] examined the impact of harvest intensity on in situ and laboratory mineral soil respiration in an East Texas hardwood forest, and found that the mean rate of CO_2 efflux in the clearcuts was significantly higher than that in the partial cuts, which in turn was significantly higher than that in the old-growth.

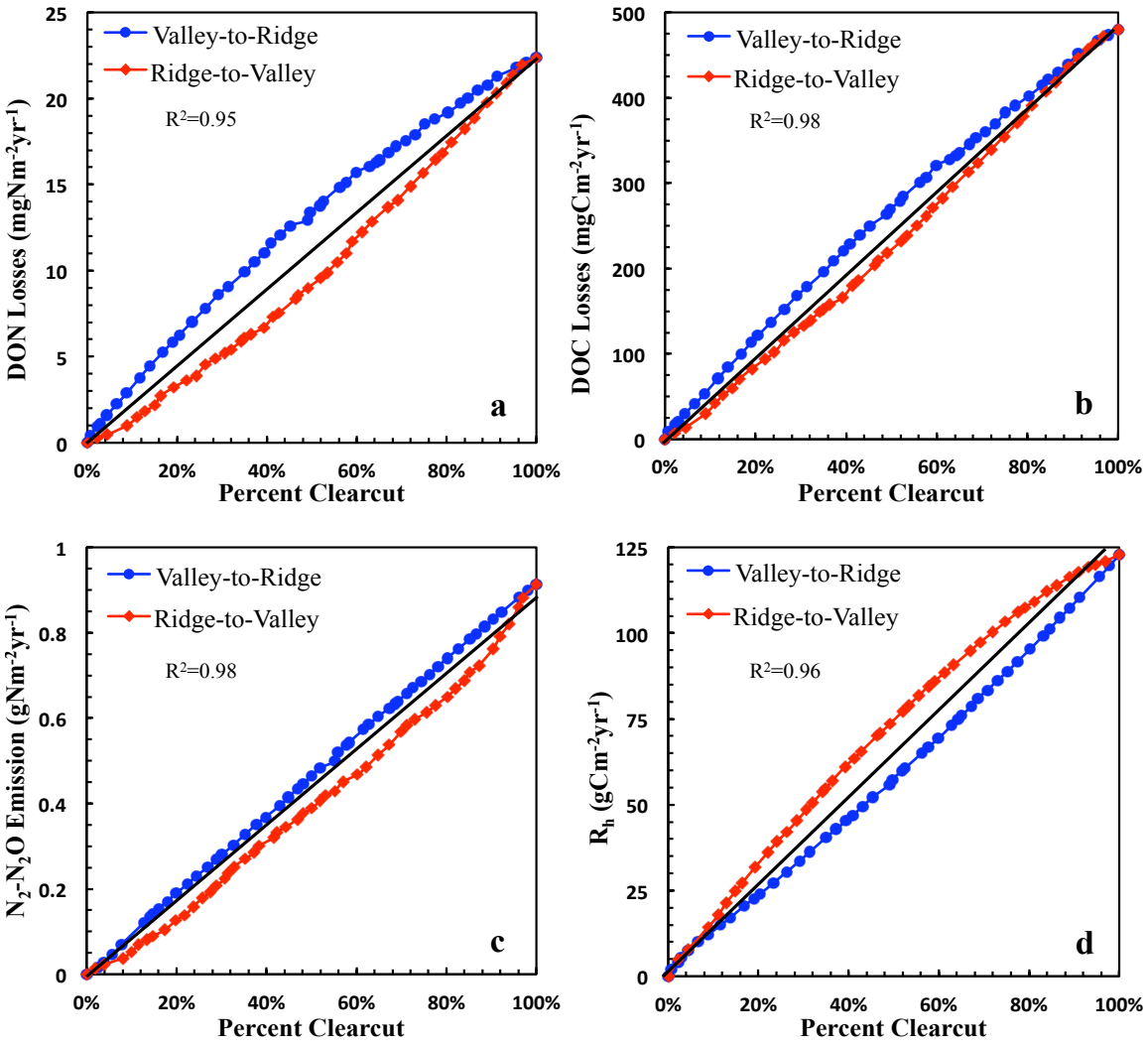

Figure 5.12: *The average absolute change (compared to old-growth values) in simulated annual DON losses ($mgNm^{-2}yr^{-1}$; subplot a), DOC losses ($mgCm^{-2}yr^{-1}$; subplot b), N_2-N_2O emission ($gNm^{-2}yr^{-1}$; subplot c) and R_h ($gCm^{-2}yr^{-1}$; subplot d) with respect to harvest amount, over the first five years after clearcut (1975-1980) for (1) the valley-to-ridge scenarios (blue dots and line), and (2) for the ridge-to-valley scenarios (red dots and line). The black solid line is the fitted linear trendline for both valley-to-ridge and ridge-to-valley scenarios. The x-axis represents harvest amount as the percentage of the watershed area that is clearcut.*

5.7. Conclusion

A spatially-distributed ecohydrologic model, VELMA, was used to explore the impact of harvest location and amount on catchment C and N dynamics at a small intensively studied watershed (WS10) in the Pacific Northwest – details that would be difficult or impossible to capture through experimentation or observation alone. Specifically, three main sets of simulations were conducted: (1) a whole catchment clearcut simulation, from 1975 to 2008, used to describe how the interaction of hydrological and biogeochemical processes within the terrestrial ecosystem mediate post-clearcut temporal dynamics of C and N fluxes, (2) twenty harvest location simulations, from 1975 to 2008, used to assess the impact of harvest location on C and N fluxes, and (3) one-hundred harvest amount simulations, from 1975 to 2008, used to explore the impact of harvest amount, irrespective of location, on nutrient fluxes. These simulations provided a framework to assess the effectiveness of forested riparian buffers in limiting the losses of dissolved C and N from the terrestrial system to the stream and to the atmosphere. Moreover, the interaction of hydrological and biogeochemical processes represented in VELMA provide additional insight into how feedbacks among the cycles of C, N and water regulate N supplies, and therefore, responses to disturbance across a wide range of spatial and temporal scales – stands to hillslopes to catchment, and days to centuries. The main insights from this exercise included the following: (1) Dissolved inorganic nitrogen losses to the stream increased exponentially when unharvested riparian buffer zones fell below 60% of total catchment area. These results suggest that forested riparian buffers effectively reduce the amount of inorganic nitrogen that reaches the stream through nitrogen uptake by plants, soil storage, nitrification and denitrification; (2) Dissolved C and N losses from the terrestrial system to the stream and atmosphere were strongly sensitive to the location of harvest as a result of the spatial variation in soil water content, plant N uptake, SOC decomposition, nitrification, and denitrification. For example, harvesting forest vegetation near the steam promoted greater losses of NH_4 and NO_3 to the stream by increasing soil nitrogen pools (via decreased plant uptake), and by increasing soil moisture levels (via decreased evapotranspiration) and, consequently, the potential for vertical and lateral flow within the hillslope; and (3) Post-clearcut increases in dissolved C and N losses from the terrestrial system to the stream and atmosphere are

primarily driven by the amount of vegetation removed. Specifically, NO_3 and NH_4 losses to the stream increase exponentially with increasing harvest area, whereas DON and DOC losses, soil heterotrophic respiration, and N_2-N_2O emissions increase near linearly with increasing harvest area.

5.8. Acknowledgements

The information in this document has been funded in part by the US Environmental Protection Agency. It has been subjected to the Agency's peer and administrative review, and it has been approved for publication as an EPA document. Mention of trade names or commercial products does not constitute endorsement or recommendation for use. This research was additionally supported in part by the following NSF Grants 0439620, 0436118, and 0922100. We thank Sherri Johnson, Barbara Bond, Suzanne Remillard, Theresa Valentine and Don Henshaw for invaluable assistance in accessing and interpreting various H.J. Andrews LTER data sets used in this study. Sherri Johnson also provided helpful comments on an earlier draft. Data for streamflow, stream chemistry and climate were provided by the H.J. Andrews Experimental Forest research program, funded by the National Science Foundation's Long-Term Ecological Research Program (DEB 08-23380), US Forest Service Pacific Northwest Research Station, and Oregon State University.

5.9. References

Abdelnour, A., M. Stieglitz, F. Pan, and R. McKane (2011), Catchment Hydrological Responses to Forest Harvest Amount and Spatial Pattern, Water Resour. Res., doi:10.1029/2010WR010165, in press.

Abdelnour, A., M. Stieglitz, F. Pan, R. McKane, and Y. Cheng (In review), Effects of Fire and Harvest on Carbon and Nitrogen Dynamics in a Pacific Northwest Forest Catchment.

Aber, J., S. Ollinger, C. Driscoll, G. Likens, R. Holmes, R. Freuder, and C. Goodale (2002), Inorganic Nitrogen Losses from a Forested Ecosystem in Responseto Physical, Chemical, Biotic, and Climatic Perturbations, Ecosystems, 5(7), 648-658.

Aber, J. D., S. V. Ollinger, and C. T. Driscoll (1997), Modeling nitrogen saturation in forest ecosystems in response to land use and atmospheric deposition, Ecological Modelling, 101(1), 61-78.

Arheimer, B., and M. Brandt (1998), Modelling nitrogen transport and retention in the catchments of southern Sweden, Ambio, 27(6), 471-480.

Arheimer, B., J. Andreasson, S. Fogelberg, H. Johnsson, C. B. Pers, and K. Persson (2005), Climate change impact on water quality: model results from southern Sweden, Ambio, 559-566.

Arnold, J. G., R. Srinivasan, R. S. Muttiah, and J. Williams (1998), Large Area Hydrologic Modeling and Assessment Part I: Model Development, JAWRA Journal of the American Water Resources Association, 34(1), 73-89.

Aust, W. M., and C. R. Blinn (2004), Forestry best management practices for timber harvesting and site preparation in the eastern United States: an overview of water quality and productivity research during the past 20 years (1982ñ2002), Water, Air, & Soil Pollution: Focus, 4(1), 5-36.

Band, L., C. Tague, P. Groffman, and K. Belt (2001), Forest ecosystem processes at the watershed scale: hydrological and ecological controls of nitrogen export, Hydrological Processes, 15(10), 2013-2028.

Band, L. E., P. Patterson, R. Nemani, and S. W. Running (1993), Forest ecosystem processes at the watershed scale: incorporating hillslope hydrology, Agricultural and Forest Meteorology, 63(1-2), 93-126.

Bernhardt, E., M. Palmer, J. Allan, G. Alexander, K. Barnas, S. Brooks, J. Carr, S. Clayton, C. Dahm, and J. Follstad-Shah (2005), Ecology: synthesizing US river restoration efforts, Science, 308(5722), 636.

Binkley, D., and T. Brown (1993), Forest practices as nonpoint sources of pollution in North America, Water Resources Bulletin, 29(5), 729-740.

Bormann, F., G. Likens, D. Fisher, and R. Pierce (1968), Nutrient loss accelerated by clear-cutting of a forest ecosystem, Science, 159(3817), 882.

Bormann, F., G. Likens, T. Siccama, R. Pierce, and J. Eaton (1974), The export of nutrients and recovery of stable conditions following deforestation at Hubbard Brook, Ecological Monographs, 44(3), 255-277.

Bowden, R. D., K. M. Newkirk, and G. M. Rullo (1998), Carbon dioxide and methane fluxes by a forest soil under laboratory-controlled moisture and temperature conditions, Soil Biology and Biochemistry, 30(12), 1591-1597.

Castelle, A., A. Johnson, and C. Conolly (1994), Wetland and stream buffer size requirements--a review, Journal of Environmental Quality, 23(5), 878-882.

Cheng, Y., M. Stieglitz, and F. Pan (2010), A Simple Method to Evolve Daily Ground Temperatures From Surface Air Temperatures in Snow Dominated Regions, Journal of Hydrometeorology.

Daly, C., and W. McKee (2011), Meteorological data from benchmark stations at the Andrews Experimental Forest. Long-Term Ecological Research. Forest Science Data Bank, Corvallis, OR. [Database]. Available: http://andrewsforest.oregonstate.edu/data/abstract.cfm?dbcode=MS001 (16 July 2011).

Davidson, E., L. Verchot, J. Catt,nio, I. Ackerman, and J. Carvalho (2000), Effects of soil water content on soil respiration in forests and cattle pastures of eastern Amazonia, Biogeochemistry, 48(1), 53-69.

Davidson, E., P. Matson, P. Vitousek, R. Riley, K. Dunkin, G. Garcia-Mendez, and J. Maass (1993), Processes regulating soil emissions of NO and N20 in a seasonally dry tropical forest, Ecology, 74(1), 130-139.

Del Grosso, S., W. Parton, A. Mosier, D. Ojima, A. Kulmala, and S. Phongpan (2000), General model for N2O and N2 gas emissions from soils due to dentrification, Global Biogeochemical Cycles, 14(4).

Dingman, S. (1994), Physical hydrology, Prentice Hall Upper Saddle River, NJ.

Dyrness, C. (1973), Early stages of plant succession following logging and burning in the western Cascades of Oregon, Ecology, 54(1), 57-69.

Feller, M., R. Lehmann, and P. Olanski (2000), Influence of forest harvesting intensity on nutrient leaching through soil in southwestern British Columbia, CRC.

Fowler, W., T. Anderson, and J. Helvey (1988), Changes in water quality and climate after forest harvest in central Washington State, USDA Forest Service research paper PNW-RP-United States, Pacific Northwest Research Station (USA).

Fredriksen, R. (1975), Nitrogen, phosphorus and particulate matter budgets of five coniferous forest ecosystems in the western Cascades Range, Oregon, Doctoral thesis, 71 pp, Oregon State University, Corvallis.

Freeman, T. (1991), Calculating catchment area with divergent flow based on a regular grid, Computers & Geosciences, 17(3), 413-422.

Gholz, H. L., G. M. Hawk, A. Campbell, K. Cromack Jr, and A. T. Brown (1985), Early vegetation recovery and element cycles on a clear-cut watershed in western Oregon, Canadian Journal of Forest Research, 15(2), 400-409.

Golding, D. L. (1987), Changes in streamflow peaks following timber harvest of a coastal British Columbia watershed, paper presented at Forest Hydrology and Watershed Management, IAHS, Vancouver.

Grant, R., T. Black, E. Humphreys, and K. Morgenstern (2007), Changes in net ecosystem productivity with forest age following clearcutting of a coastal Douglas-fir forest: testing a mathematical model with eddy covariance measurements along a forest chronosequence, Tree Physiology, 27(1), 115.

Grier, C., and R. Logan (1977), Old-growth Pseudotsuga menziesii communities of a western Oregon watershed: biomass distribution and production budgets, Ecological Monographs, 47(4), 373-400.

Grier, C., K. Lee, N. Nadkarni, G. Klock, and P. Edgerton (1989), Productivity of forests of the United States and its relation to soil and site factors and management practices: a review, Gen. Tech. Rep. PNW-GTR-222. Portland, OR: Pacific Northwest Research Station, Forest Service, US Department of Agriculture, 51.

Harmon, M. E., W. K. Ferrell, and J. F. Franklin (1990), Effects on carbon storage of conversion of old-growth forests to young forests, Science, 247(4943), 699-701.

Harr, R. (1976), Forest practices and streamflow in western Oregon, Gen. Tech. Report PNW-GTR-049. Portland, OR: US Department of Agriculture, Forest Service, Pacific Northwest Research Station. 23 p.

Harr, R., and F. M. McCorison (1979), Initial effects of clearcut logging on size and timing of peak flows in a small watershed in western Oregon, Water Resources Research, 15(1), 90-94, doi:10.1029/WR1015i1001p00090.

Harr, R., A. Levno, and R. Mersereau (1982), Streamflow changes after logging 130-year-old Douglas fir in two small watersheds, Water Resources Research, 18(3), 637-644, doi:610.1029/WR1018i1003p00637.

Hibbert, A. (1966), Forest treatment effects on water yield, in Proceedings of a National Science Foundation advanced science seminar, International symposium on forest hydrology. Pergamon Press, USA, edited by W.E. Sopper and H.W. Lull, pp. 527-543, Pergamon Press, New York,.

Hicks, B., R. Beschta, and R. Harr (1991), Long-term changes in streamflow following logging in western Oregon and associated fisheries implications, Water Resources Bulletin, 27(2), 217-226.

Hope, D., M. Billett, and M. Cresser (1994), A review of the export of carbon in river water: fluxes and processes, Environmental Pollution, 84(3), 301-324.

Hubbard, R., G. Vellidis, and R. Lowrance (1992), Wetland restoration for filtering nutrients from an animal waste application site.

Johnson, S., and J. Rothacher (2009), Stream discharge in gaged watersheds at the Andrews Experimental Forest. Long-Term Ecological Research. Forest Science Data Bank, Corvallis, OR. [Database]. Available:

http://andrewsforest.oregonstate.edu/data/abstract.cfm?dbcode=HF004 (16 July 2011).

Johnson, S., and R. Fredriksen (2011), Long-term stream chemistry concentrations and fluxes: Small watershed proportional samples in the Andrews Experimental Forest. Long-Term Ecological Research. Forest Science Data Bank, Corvallis, OR. [Database]. Available: http://andrewsforest.oregonstate.edu/data/abstract.cfm?dbcode=CF002 (18 July 2011).

Jones, J. A. (2000), Hydrologic processes and peak discharge response to forest removal, regrowth, and roads in 10 small experimental basins, western Cascades, Oregon, Water Resources Research, 36(9), 2621-2642, doi:2610.1029/2000WR900105.

Jones, J. A., and G. E. Grant (1996), Peak flow responses to clear-cutting and roads in small and large basins, western Cascades, Oregon, Water Resources Research, 32(4), 959-974.

Jones, J. A., and D. A. Post (2004), Seasonal and successional streamflow response to forest cutting and regrowth in the northwest and eastern United States, Water Resources Research, 40(5), W05203, doi:05210.01029/02003WR002952.

Keppeler, E. T., and R. R. Ziemer (1990), Logging effects on streamflow: water yield and summer low flows at Caspar Creek in northwestern California, Water Resources Research, 26(7), 1669-1679.

Krysanova, V., and U. Haberlandt (2002), Assessment of nitrogen leaching from arable land in large river basins:: Part I. Simulation experiments using a process-based model, Ecological Modelling, 150(3), 255-275.

Krysanova, V., D. I. Muller-Wohlfeil, and A. Becker (1998), Development and test of a spatially distributed hydrological/water quality model for mesoscale watersheds, Ecological Modelling, 106(2-3), 261-289.

Lam, Q., B. Schmalz, and N. Fohrer (2009), Ecohydrological modelling of water discharge and nitrate loads in a mesoscale lowland catchment, Germany, Advances in Geosciences, 21, 49-55.

Likens, G., and F. Bormann (1995), Biogeochemistry of a forested ecosystem, Springer Science & Business.

Likens, G., F. Bormann, R. Pierce, and W. Reiners (1978), Recovery of a deforested ecosystem, Science, 199(4328), 492-496.

Londo, A., M. Messina, and S. Schoenholtz (1999), Forest harvesting effects on soil temperature, moisture, and respiration in a bottomland hardwood forest, Soil Science Society of America Journal, 63(3), 637.

Lowrance, R., L. Altier, J. Newbold, R. Schnabel, P. Groffman, J. Denver, D. Correll, J. Gilliam, J. Robinson, and R. Brinsfield (1997), Water quality functions of riparian forest buffers in Chesapeake Bay watersheds, Environmental Management, 21(5), 687-712.

Marks, P., and F. Bormann (1972), Revegetation following forest cutting: mechanisms for return to steady-state nutrient cycling, Science, 176(4037), 914.

Martin, C., D. Noel, and C. Federer (1984), Effects of forest clearcutting in New England on stream chemistry, Journal of Environmental Quality, 13(2), 204.

Mayer, P. M. R., S. K. McCutchen, M. D. Canfield, and J. Timothy (2007), Meta-analysis of nitrogen removal in riparian buffers, Journal of Environmental Quality, 36(4), 1172.

McKane, R., E. Rastetter, G. Shaver, K. Nadelhoffer, A. Giblin, J. Laundre, and F. Chapin III (1997), Climatic effects on tundra carbon storage inferred from experimental data and a model, Ecology, 78(4), 1170-1187.

Parton, W., A. Mosier, D. Ojima, D. Valentine, D. Schimel, K. Weier, and A. Kulmala (1996), Generalized model for N2 and N2O production from nitrification and denitrification, Global Biogeochemical Cycles, 10(3).

Parton, W., E. Holland, S. Del Grosso, M. Hartman, R. Martin, A. Mosier, D. Ojima, and D. Schimel (2001), Generalized model for NO x and N2O emissions from soils, Journal of Geophysical Research-Atmospheres, 106(D15).

Quinn, P., K. Beven, P. Chevallier, and O. Planchon (1991), Prediction of hillslope flow paths for distributed hydrological modelling using digital terrain models, Hydrological Processes, 5(1), 59-79.

Raich, J., E. Rastetter, J. Melillo, D. Kicklighter, P. Steudler, B. Peterson, A. Grace, B. Moore Iii, and C. Vorosmarty (1991), Potential net primary productivity in South America: application of a global model, Ecological Applications, 1(4), 399-429.

Raich, J. W., and C. S. Potter (1995), Global patterns of carbon dioxide emissions from soils, Global Biogeochemical Cycles, 9(1), 23-36.

Ranken, D. W. (1974), Hydrologic properties of soil and subsoil on a steep, forested slope, Master's thesis, 117 pp, Oregon State University, Corvallis.

Rothacher, J. (1965), Streamflow from small watersheds on the western slope of the Cascade Range of Oregon, Water Resources Research, 1, 125-134, doi:110.1029/WR1001i1001p00125.

Rothacher, J. (1970), Increases in water yield following clear-cut logging in the Pacific Northwest, Water Resources Research, 6(2), 653-658, doi:610.1029/WR1006i1002p00653.

Santantonio, D., R. Hermann, and W. Overton (1977), Root biomass studies in forest ecosystems. Pedobiologia, Bd. 17, S. 1-31. Paper 957, Forest Research Laboratory, School of Forestry Oregon State University, Corvallis, Oregon.

Sollins, P., and F. M. McCorison (1981), Nitrogen and carbon solution chemistry of an old-growth coniferous forest watershed before and after cutting, Water Resources Research, 17(5), 1409–1418, doi:1410.1029/WR1017i1005p01409. .

Sollins, P., K. Cromack Jr, F. Mc Corison, R. Waring, and R. Harr (1981), Changes in nitrogen cycling at an old-growth Douglas-fir site after disturbance, Journal of Environmental Quality, 10(1), 37.

Stark, N. (1979), Nutrient losses from timber harvesting in a Larch/Douglas fir forest [Montana], United States. Intermountain Forest and Range Experiment Station. USDA Forest Service research paper INT (USA).

Stednick, J. (1996), Monitoring the effects of timber harvest on annual water yield, Journal of Hydrology, 176(1-4), 79-95.

Stednick, J. (2008), Long-term Water Quality Changes Following Timber Harvesting, ECOLOGICAL STUDIES, 199, 157.

Swank, W., J. Vose, and K. Elliott (2001), Long-term hydrologic and water quality responses following commercial clearcutting of mixed hardwoods on a southern Appalachian catchment, Forest Ecology and Management, 143(1-3), 163-178.

Tiedemann, A., T. Quigley, and T. Anderson (1988), Effects of timber harvest on stream chemistry and dissolved nutrient losses in northeast Oregon, Forest Science, 34(2), 344-358.

Valentine, T., and G. Lienkaemper (2005), 30 meter digital elevation model (DEM) clipped to the Andrews Experimental Forest. Long-Term Ecological Research. Forest Science Data Bank, Corvallis, OR. [Database]. Available: http://andrewsforest.oregonstate.edu/data/abstract.cfm?dbcode=GI002 (16 July 2011).

Vanderbilt, K., K. Lajtha, and F. Swanson (2003), Biogeochemistry of unpolluted forested watersheds in the Oregon Cascades: temporal patterns of precipitation and stream nitrogen fluxes, Biogeochemistry, 62(1), 87-117.

Vitousek, P., and W. Reiners (1975), Ecosystem succession and nutrient retention: a hypothesis, BioScience, 25(6), 376-381.

Vitousek, P., J. Gosz, C. Grier, J. Melillo, W. Reiners, and R. Todd (1979), Nitrate losses from disturbed ecosystems, Science, 204(4392), 469-474.

Waichler, S. R., B. C. Wemple, and M. S. Wigmosta (2005), Simulation of water balance and forest treatment effects at the HJ Andrews Experimental Forest, Hydrological Processes, 19(16), 3177-3199.

Weier, K., J. Doran, J. Power, D. Walters, and A. USDA (1993), Denitrification and the dinitrogen/nitrous oxide ratio as affected by soil water, available carbon, and nitrate.

Zak, D. R., and D. F. Grigal (1991), Nitrogen mineralization, nitrification and denitrification in upland and wetland ecosystems, Oecologia, 88(2), 189-196.

CHAPTER 6

CLIMATE CHANGE IMPACT ON CATCHMENT HYDROLOGICAL AND BIOGEOCHEMICAL PROCESSES

Alex Abdelnour[1], Sopan Patil[1], Marc Stieglitz[1,2], Robert McKane[3], Feifei Pan[1,4]

[1] Department of Civil and Environmental Engineering, Georgia Institute of Technology, Atlanta, GA, USA.
[3]School of Earth Atmospheric Sciences, Georgia Institute of Technology, Atlanta, GA, USA.
[2]US Environmental Protection Agency, Corvallis, OR, USA
[4]Department of Geography, University of North Texas, Denton, TX, USA.

6.1. Abstract

The goal of this study is to provide process level insight into the impact of climate change on ecosystem processes at high spatial resolution relevant to formulating management decision. To this end, a new eco-hydrological model, Visualizing Ecosystems for Land Management Assessments (VELMA) is used to simulate the impact of future climate change on watershed hydrology and carbon (C) and nitrogen (N) dynamics. VELMA is applied to the H.J. Andrews Experimental Forest, a Long Term Ecological Research site in the Pacific Northwest. Daily projected temperature and precipitation for upper, lower and middle of the road climate change scenarios are used to force the model. Simulation results suggest that the combined effects of warmer and wetter winters as well as drier and hotter summers will result in lower winter snow accumulation, earlier spring snowmelt, higher winter streamflow, and lower summer streamflow and soil moisture. Simulation results also suggest that warmer air temperatures will enhance soil microbial activity and lengthen the growing season, which results in higher plant and soil carbon accumulation and increased dissolved C and N losses from the terrestrial system to the stream and atmosphere.

6.2. Introduction

The Pacific Northwest region of the United States is rich in natural resources such as water, forest product, wildlife and salmon [*Barten et al.*, 2008], which generate a wide range of economic, social and cultural benefits [*Knudsen*, 2000]. However, these resources may be at risk due to changes in air temperature and precipitation. Over the course of the 20th century, the Pacific Northwest has experienced an increase in annual temperature and precipitation of 0.8°C and 13%, respectively [*Mote*, 2003]. The largest warming rates have been in the winter and spring and the largest increase in precipitation has been in winter [*Cayan et al*., 2001; *Folland et al*., 2001; *Mote et al*., 2003; *Regonda et al*., 2005]. As a result, the hydrological and ecological regime of the region changed [*Mote et al.,* 2003]. These changes include reduced snow accumulation depth [*Knowles et al*., 2006; *Mote et al*., 2005; *Mote et al*., 2003], earlier spring snowmelt [*Regonda et al.*, 2005], reduced summer streamflow [*Stewart et al.*, 2005], increased forest productivity [*Boisvenue and Running*, 2006], and a shift in species distribution [*Walther et al.*, 2002], amongst others. Moreover, these changes to the ecosystem dynamics may be further exacerbated with the continued projected change in climate in the 21th century [*Elsner et al*., 2010; *Mote et al*., 2003]. Based on the 2007 Intergovernmental Panel on Climate Change (IPCC) Fourth Assessment Report (AR4), the average annual temperature and precipitation in the Pacific Northwest are projected to increase by 3°C (1.6 to 9.4°C), and 2% (-10 to +20%), respectively, by 2100. Moreover, most climate models used in the IPCC report project an enhanced seasonal cycle with warmer and drier summers, wetter falls and winters, and an increase in extreme precipitation events for this region. How these future changes in climate will impact ecosystem hydrological and biogeochemical response in the Pacific Northwest is still uncertain [*Barten et al.*, 2008].

A number of modeling studies have explored the potential impact of the projected changes in temperature and precipitation on the hydrological regime of the Pacific Northwest. *Elsner et al.,* [2010] applied the DHSVM hydrological model at a spatial resolution of 150m over the Puget Sound watershed to assess the impact of the projected change in climate on streamflow, soil moisture and snowdepth. *Hamlet and Lettenmaier* [1999] applied the VIC hydrological model at 1/8 degree over the Columbia River basin

to explore the impact of climate change on basin hydrology. *Chang and Jung* [2010] applied the Precipitation-Runoff Modeling system model at 1/16 resolution over 218 sub-basin of the Willamette River basin to explore the impact of changes in temperature and precipitation on seasonal runoff. *Tague et al.,* [2008] applied the RHESSys (Regional Hydro-Ecologic Simulation System; [*Tague and Band*, 2004]) eco-hydrological model to the HJA watershed to test the impact of a 1.5°C increase in temperature on watershed hydrology. These and other studies indicate that the 21th century projected change in Pacific Northwest air temperature and precipitation will result in smaller snowpack accumulation [*Casola et al.*, 2009; *Graves and Chang*, 2007; *Minder*, 2010; *Tague et al.*, 2008], earlier melt [*Elsner et al.*, 2010; *Pike et al.*, 2008; *Rauscher et al.*, 2008; *Stewart et al.*, 2005], and higher winter runoff as more precipitation is projected to fall as rain rather than snow [e.g. *Elsner et al.* 2010; *Graves and Chang,* 2007; *Hamlet and Lettenmaier* 1999; *Loukas et al.,* 2002; *Mote et al.,* 2003]. In turn, these changes result in a decrease in spring and summer streamflow [*Lettenmaier et al.*, 1999; *Leung and Wigmosta*, 1999; *Mastin et al.*, 2008], a decrease in summer soil moisture [*Elsner et al.*, 2010; *Hamlet and Lettenmaier*, 1999], and a general increase in annual evapotranspiration [*Spittlehouse*, 2007; *Spittlehouse and Stewart*, 2003].

While there have been a number of modeling studies that explored the potential impact of the projected climate change on water quality and ecology in places such as eastern U.S. [e.g. *Aber et al*., 1993; *Chang et al*., 2001; *Sebestyen et al*., 2009], California [e.g. *Lenihan et al.*, 2003; *Tague et al.,* 2009], Alaska [e.g. *Epstein et al.,* 2000; *Stieglitz et al*., 2000], and Europe [e.g. *Arheimer et al*., 2005; *Kesik et al*., 2006; *Varanou et al*., 2002; *Zweimuller et al*., 2008], few studies have modeled the impact of climate change on ecosystem biogeochemical processes in the Pacific Northwest [e.g. *Boisvenue and Running,* 2006] . Nevertheless, a number of generalizations have emerged from existing climate change impact analysis performed in Europe, Alaska, California and eastern U.S. amongst others. Specifically, these studies found that, irrespective of location, a projected increase in cool and warm seasons air temperatures result in higher soil microbial decomposition [*Boisvenue and Running*, 2006; *Clair and Ehrman*, 1996; *McClain et al.*, 1998], higher ecosystem growth rates when water is not a limiting factor [*Boisvenue and Running,* 2006; *Spittlehouse and Stewart,* 2003; *Boisvenue and Running,*

2006], and longer growing season period [*Feng and Hu*, 2004; *Graumlich et al.*, 1989; *Sebestyen et al.*, 2009]. In turn, these changes increase nutrients concentration in the stream [*Arheimer et al.*, 2005; *Baron et al.*, 2009; *Chang et al.*, 2001], enhance greenhouse gas emissions [*Kesik et al.*, 2006; *Lenihan et al.*, 2003], reduce the total carbon storage in the soil [*Franklin*, 1992; *McClain et al.*, 1998], and increase ecosystem net primary production due to the effects of higher temperature on soil nitrogen mineralization [*Boisvenue and Running*, 2006; *Melillo et al.*, 1993; *Sun et al.*, 2000].

In this paper, we use a spatially distributed, eco-hydrological model VELMA (Visualizing Ecosystems for Land Management Assessment) [*Abdelnour et al.*, 2011], that is both computationally efficient and relatively easy to implement for analyzing the effects of changes in climate, land-use, and land cover, on watershed hydrological and biogeochemical processes. We apply this model to the H.J. Andrews Experimental Forest in western Oregon, USA, to simulate the impact of future climate change on watershed hydrology and C and N dynamics. Daily projected temperature and precipitation for three climate change scenarios that cover the range of projected 21th century changes in Pacific Northwest climate are used to force the model. We first explore the impact of climate change on catchment hydrological processes such as the seasonal evolution of snow accumulation and melt, streamflow, and evapotranspiration. We then turn our attention to ecosystem C and N dynamics and fluxes such as ecosystem growth, dissolved C and N losses to the stream, greenhouse gas emissions and site productivity.

A description of the study area and history is provided in section 6.3. Model description and data description are provided in section 6.4 and 6.5, respectively. Simulation methods are provided in section 6.6. Simulation results are provided in section 6.7. Discussion and conclusion are presented in section 6.8 and 6.9, respectively.

6.3. Site Description:

The H.J. Andrews (HJA) Experimental Forest is a Long Term Ecological Research (LTER) site located at latitude 44°12′N, longitude 122°15′W, in the western Cascades Ranges of Oregon (Figure 6.1). This LTER has been the site of intensive research and

manipulation by the U.S. forest Service since the 1950's, mainly to study the effects of forest harvest on hydrology, sediment transport, and nutrient loss [*Dyrness*, 1973; *Fredriksen*, 1975; *Harmon et al*., 1990; *Harr and Yee*, 1975; *Harr and McCorison*, 1979; *Jones and Grant*, 1996; *Rothacher*, 1965; *Sollins and McCorison*, 1981; *Sollins et al*., 1981].

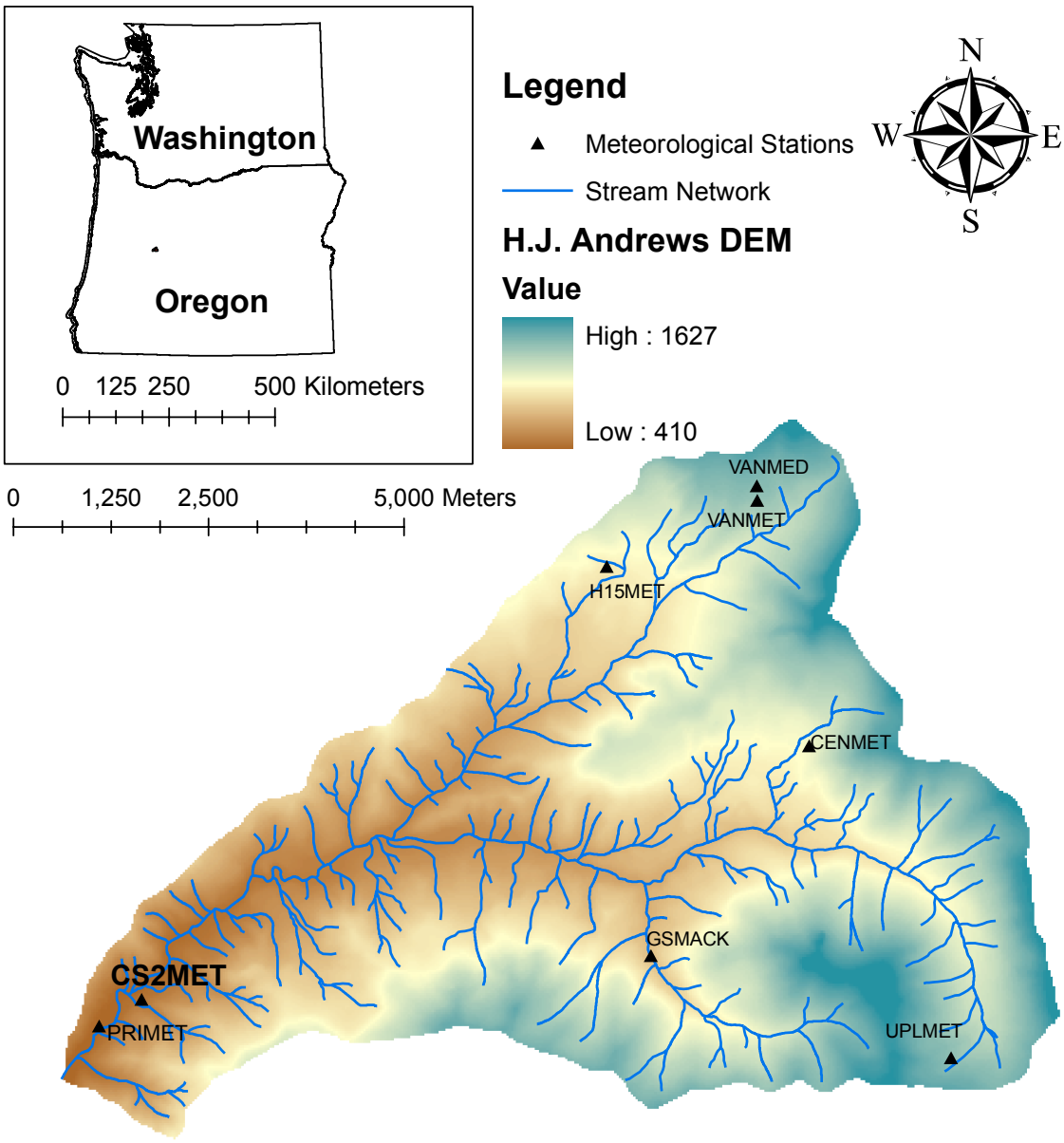

Figure 6.1: *The study site is the 64 km^2 H. J. Andrew Experimental Forest located in the western Cascade Range of Oregon. The black triangles represent the locations of the meteorological stations. CS2MET is the meteorological station used in this study.*

The HJA forest occupies the 64km^2 drainage basin of Lookout Creek, a tributary of Blue River and the McKenzie River. Elevation ranges from 410m at the south west corner to 1627m at the highest elevation of Lookout Mountain. The climate is relatively mild with wet winters and dry summers [*Grier and Logan*, 1977]. Mean annual temperature varies between 8.5°C at low elevation and 3.5°C at high elevation. Mean monthly temperatures vary from a low of 1°C in January to a high of 18°C in July. Mean annual precipitation ranges from 2300mm at the base station to 3500mm at upper elevations [*Daly*, 2005] and falls primarily between October and April [*Grier and Logan*, 1977]. Precipitation falls primarily as rain at low elevation and as snow above 1000m. Snow depth often reaches 5 meters in depth at the highest elevation [*Waring et al.*, 1978]. Annual streamflow averages 1800mm. Peak streamflows occur in the winter season (November-February) during warm rain-on snow events.

Soils are of the Frissel series, which are classified as Typic Dystrochrepts with fine loamy to loamy-skeletal texture [*Sollins et al.*, 1981; *Vanderbilt et al.*, 2003] and are generally deep and well drained [*Grier and Logan*, 1977]. Before timber cutting began in 1950, 65% of the H.J. Andrews Forest was covered by old-growth stands (400-500 years old) with the rest consisting of regenerating trees after the wildfires that occurred in the 1800's. Currently, old-growth stands constitute 40% of the total area. Lower elevation (below 1000m) forests are dominated by Douglas-fir (*Pseudotsuga menziesii*), western hemlock (*Tsuga heterophylla*), and western red cedar (*Thuja plicata)*, whereas noble fir (*Abies procera*), Pacific silver fir (*Abies Amabilis*), and mountain hemlock (*Tsuga mertensiana*) are common at upper elevations.

6.4. Model Description

VELMA (Visualizing Ecosystems for Land Management Assessment) is a spatially distributed ecohydrological model used to simulate changes in soil water infiltration and redistribution, evapotranspiration, surface and subsurface runoff, carbon (C) and nitrogen (N) cycling in plants and soils, and the transport of dissolved forms of carbon and nitrogen from the terrestrial landscape to streams. The model is designed to simulate the integrated responses of watershed hydrology, ecology, and biogeochemistry to multiple forcing variables, e.g., changes in climate, land-use and land cover. It is intended to be

broadly applicable to a variety of ecosystems (forest, grassland, agricultural, tundra, etc.) and to provide a computationally efficient means for scaling up eco-hydrological responses across multiple spatial and temporal scales – hillslopes to basins, and days to centuries.

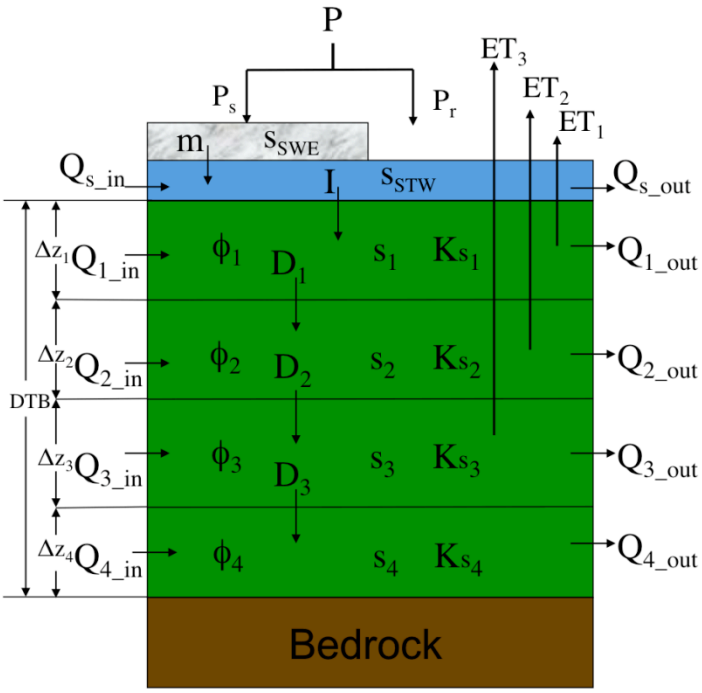

Figure 6.2: *The soil column hydrological framework consists of 4-layer soil column, a standing water layer, and a snow layer. DTB is the soil column depth to bedrock. Δz_i, Ks_i, $\phi_{i,}$, and s_i, are the thickness, the saturated hydraulic conductivity, the soil porosity, and the soil water storage of layer i, respectively; P, P_s and P_r, are the precipitation, snow, and rain, respectively; m is the snowmelt and s_{SWE} is the snow water equivalent depth; I is the infiltration and s_{STW} is the standing water amount; Q_s is the surface runoff; Q_i, D_i and ET_i, are the subsurface runoff, the drainage and the evapotranspiration of layer i, respectively.*

The model uses a distributed soil column framework to simulate the movement of water and nutrients (organically bound carbon (C) and nitrogen (N) in plants and soils; dissolved inorganic nitrogen (DIN), dissolved organic nitrogen (DON) and dissolved organic carbon (DOC); and gaseous forms of C and N including CO_2, N_2O and N_2) within the soil, between the soil and the vegetation, and from the soil surface and vegetation to the atmosphere. The soil column model consists of three coupled sub-

models:

(1) A *hydrological model* (Figure 6.2) that simulates vertical and lateral movement of water within soil, losses of water from soil and vegetation to the atmosphere, and the growth and ablation of the seasonal snowpack – a detailed description of the hydrological model is provided in Appendix A of *Abdelnour et al.,* [2011] (Chapter 3).

(2) A *soil temperature model* [*Cheng et al.*, 2010] that simulates daily soil layer temperatures from surface air temperature and snow depth by propagating the air temperature first through the snowpack and then through the ground using the analytical solution of the one-dimensional thermal diffusion equation.

(3) A *plant-soil model* (Figure 6.3) that simulates ecosystem carbon storage and the cycling of C and N between a plant biomass layer and the active soil pools [*Abdelnour et al.*, In review] (Chapter 4). Specifically, the plant-soil model simulates the interaction between aboveground plant biomass, soil organic carbon (SOC), soil nitrogen including dissolved nitrate (NO_3), ammonium (NH_4), and organic nitrogen (DON), as well as dissolved organic carbon (DOC). Daily atmospheric inputs of wet and dry nitrogen deposition are accounted for in the ammonium pool of the shallow soil layer. Uptake of ammonium and nitrate by plants is modeled using a Type II Michaelis-Menton function. Loss of plant biomass is simulated through a density dependent mortality. The mortality and the nitrogen uptake rate mimic the exponential increase in biomass mortality and the accelerated growth rate, respectively, as plants go through succession and reach equilibrium. Nitrification and denitrification rates were simulated using the equations from the generalized model of N_2 and N_2O production of *Parton et al.,* [1996; 2001] and *Del Grosso et al.,* [2000]. Decomposition of soil organic carbon follows first order kinetics controlled by soil temperature and moisture content as described in the TEM model (Terrestrial Ecosystem Model) of *Raich et al.,* [1991]. Vertical transport of nutrients from one layer to another in a soil column is function of water drainage.

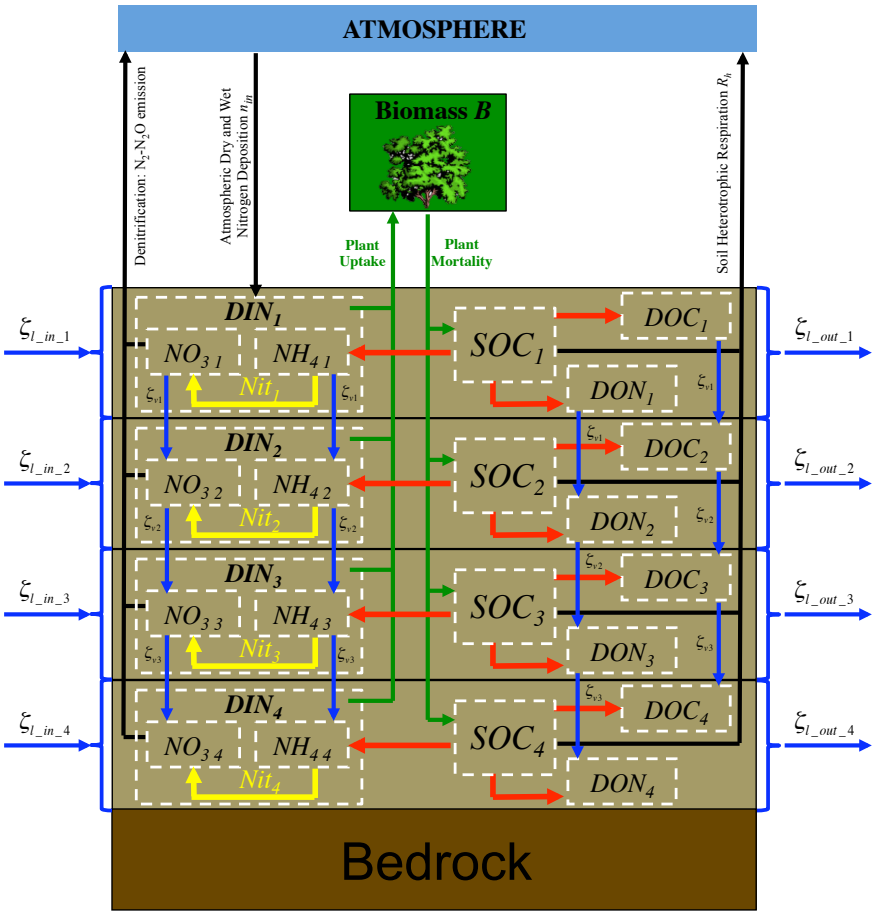

Figure 6.3: *The soil column biogeochemical framework simulates ecosystem carbon storage and the cycling of carbon and nitrogen between a plant biomass layer and a 4-layer soil column.*

The soil column model is placed within a catchment framework to create a spatially distributed model applicable to watersheds and landscapes (Figure 6.4). Adjacent soil columns interact with each other through the downslope lateral transport of water and nutrients. Surface and subsurface lateral flow are routed using a multiple flow direction method [*Freeman*, 1991; *Quinn et al.*, 1991]. As with vertical drainage of soil water, lateral subsurface downslope flow is modeled using a simple logistic function and corrected for the local slope angle. Lateral transport of nutrients from one soil column to the subsequent soil column or towards the stream is simulated as a function of subsurface flow and nutrient-specific loss rates. Nutrients transported downslope from one soil column to another can be processed through the different C and N cycling sub-models in

that downslope soil column, or continue to flow downslope, interacting with other soil columns, or ultimately discharging water and nutrients to the stream.

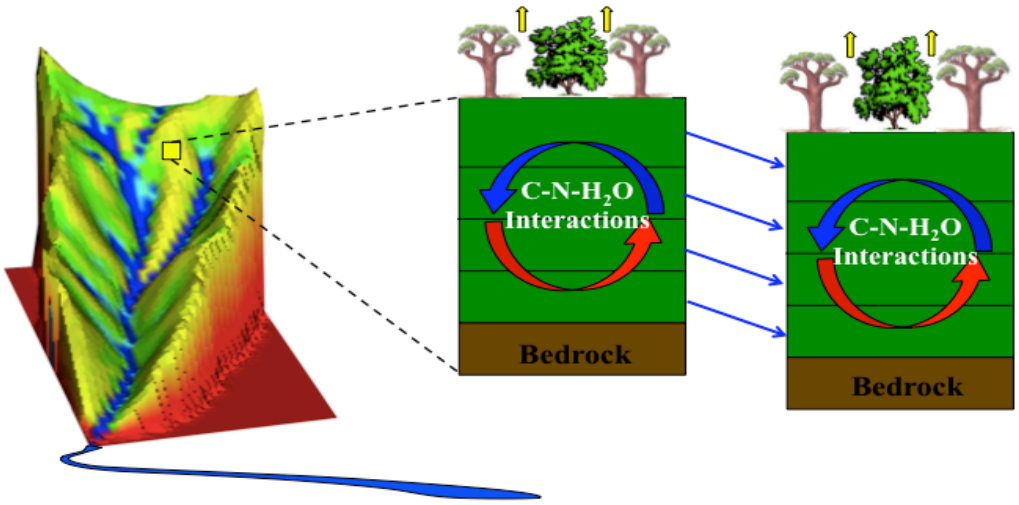

Figure 6.4: *Conceptual catchment modeling framework using multi-layered soil columns.*

A 30-m resolution Digital Elevation Model (DEM) of the H.J. Andrews [*Valentine and Lienkaemper*, 2005] is used to compute flow direction, delineate watershed boundaries, and generate a channel network. Each soil column is divided into 4 layers and is assumed to have an average depth to bedrock of 2m [*Ranken*, 1974]. The dominant soil texture is specified as loam [*Ranken*, 1974]. Porosity, field capacity and wilting point values are obtained accordingly [*Dingman*, 1994].

6.5. Climate Forcing and Validation Data Descriptions

6.5.1. *Climate Forcing Data*

The model is forced with daily air temperature, precipitation and atmospheric nitrogen deposition. Observed daily air temperature and precipitation data are available from the H.J. Andrews LTER CS2MET meteorological station for the period January 1 1959 to December 31 2008 [*Daly and McKee*, 2011] (see Figure 6.1). Daily downscaled (1/8 of a degree) air temperature and precipitation data, for the period January 1 2009 to December 31 2100, were obtained for three global climate simulation models (GCM) and

emission scenarios from the Climate Impact Group website (http://cses.washington.edu/data/ipccar4/). These three climate simulations were chosen by *Salathe et al.,* [2007] and provide upper (IPSLCM4_A2), lower (GISS_ER_B1) and middle of the road (ECHAM5_A2) climate projections for the Pacific Northwest. A detailed description of the models used to obtain the upper bound (UB), lower bound (LB), and middle of the road (MR) scenarios as well as the selection criteria used by *Salathe et al.,* [2007] is presented in Appendix B.

For the purpose of our simulations, we will use the average annual value of the total wet and dry nitrogen deposition found by *Sollins et al*., [1980]. *Sollins et al*., [1980] measured the average wet and dry nitrogen deposition in WS10 for the period 1973 to 1975 and found that annual N input in precipitation and dust averaged $0.2 gNm^{-2}yr^{-1}$. This average annual value is then partitioned based on the ratio of daily precipitation to the historical (1959-1999) average annual precipitation. Thus, annual wet and dry nitrogen deposition, for any given year, is assumed to change consistently with the projected changes in precipitation (i.e. if precipitation increases, N deposition increases and vice-versa).

6.5.2. *Climate Projection Data (2009-2100):*

Daily downscaled air temperature and precipitation data for the period January 1, 2009 to December 31, 2100 are available from the Climate Impact Group website (http://cses.washington.edu/data/ipccar4/) at a resolution of $1/8^{th}$ degree. However, at this resolution the downscaled data will not capture the observed (1) air temperature and precipitation frequency distribution, and (2) spatial distribution of air temperature and precipitation throughout the 64 km^2 catchment. Therefore, we use a cumulative distribution function (CDF) technique [*Ines and Hansen*, 2006; *Salathe et al.*, 2007; *Wood et al.*, 2002] to bias correct for the offset of the future downscaled climate data to the historical observed climate data, and to match the frequency distribution of the historical daily observed air temperature and precipitation at the CS2MET meteorological station (see Appendix C for details). After bias and frequency correcting the downscaled 2009 to 2100 climate data, we then spatially interpolated the future air temperature and precipitation data across our 64 km^2 watershed using existing spatial maps of monthly

average air temperature [*Daly and Smith*, 2005] and precipitation [*Daly*, 2005] following the procedures set forth in Appendix D. It should be noted that for all simulations conducted in this study air temperature and precipitation data taken from CS2MET was spatially interpolated across the catchment.

The corrected daily climate data for the period January 1, 2009 to December 31, 2100, is shown in Figures 6.5 and 6.6. Specifically, by the end of the century, annual air temperature is projected to increase by 1°C (LB) to 4.3°C (UB), and annual precipitation is projected to either decrease by 87mm (LB) or increase by 535 mm (UB). At the seasonal scale, all three climate change scenarios predict warmer and wetter cool seasons (winter and fall), as well as hotter and drier warm seasons (spring and summer). Specifically, for winter and fall, air temperature is projected to increase by 1.9°C (MR) and 2.1°C (MR), and precipitation is projected to increase by 201 mm (MR) and 80 mm (MR), for the period 2070-2089 (Figures 6.5 and 6.6). By contrast, for spring and summer, all climate change scenarios predict an end of the century increase in air temperature of 2.8°C (MR) and 3.9°C (MR), and a decrease in precipitation of 18mm (MR) and 27mm (MR) (Figures 6.5 and 6.6).

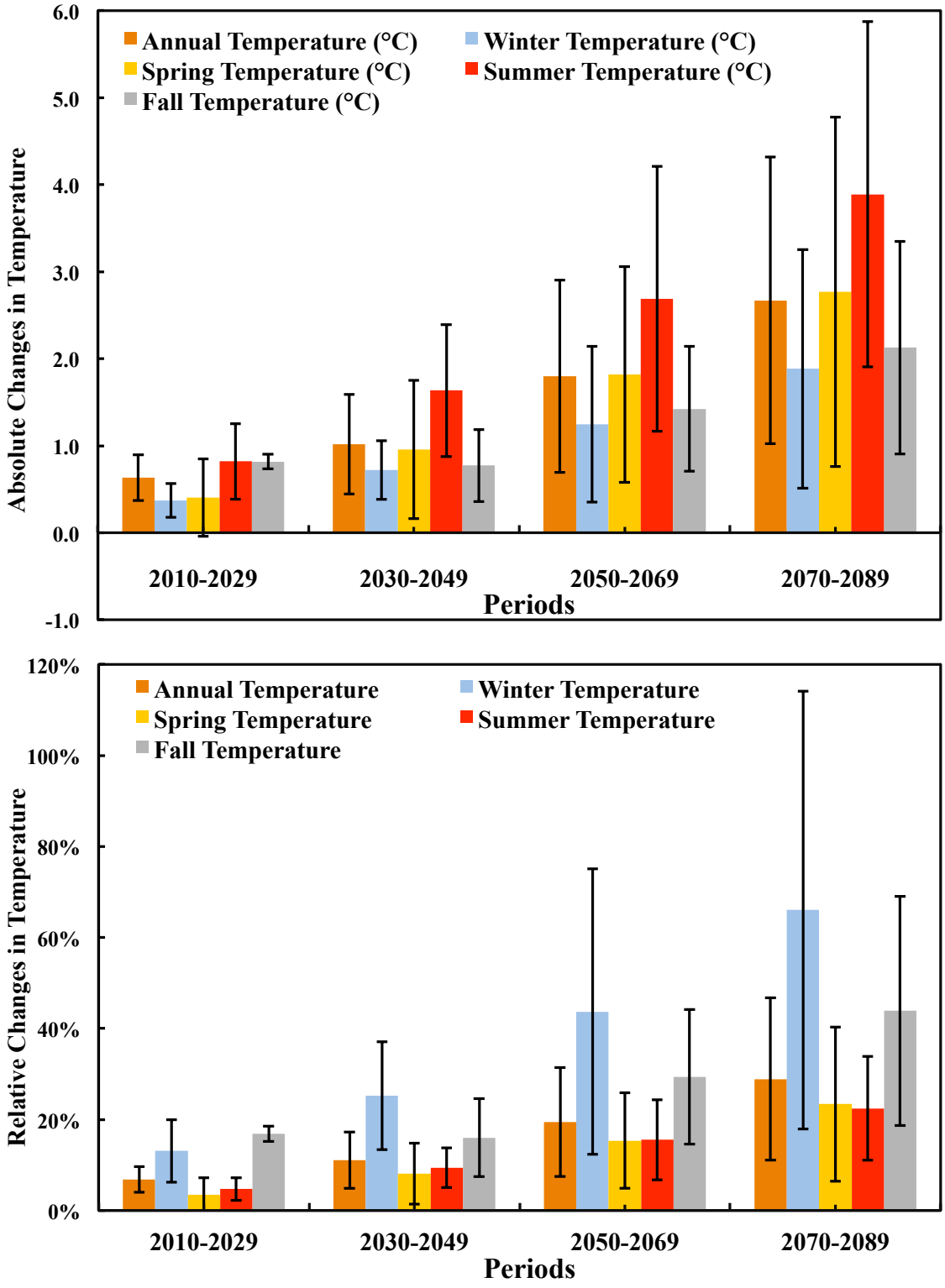

Figure 6.5: *Absolute and relative changes in average annual and seasonal temperature for the periods 2010-2029, 2030-2049, 2050-2069, and 2070-2089. The black bars represent the upper-bound and lower-bound projected values.*

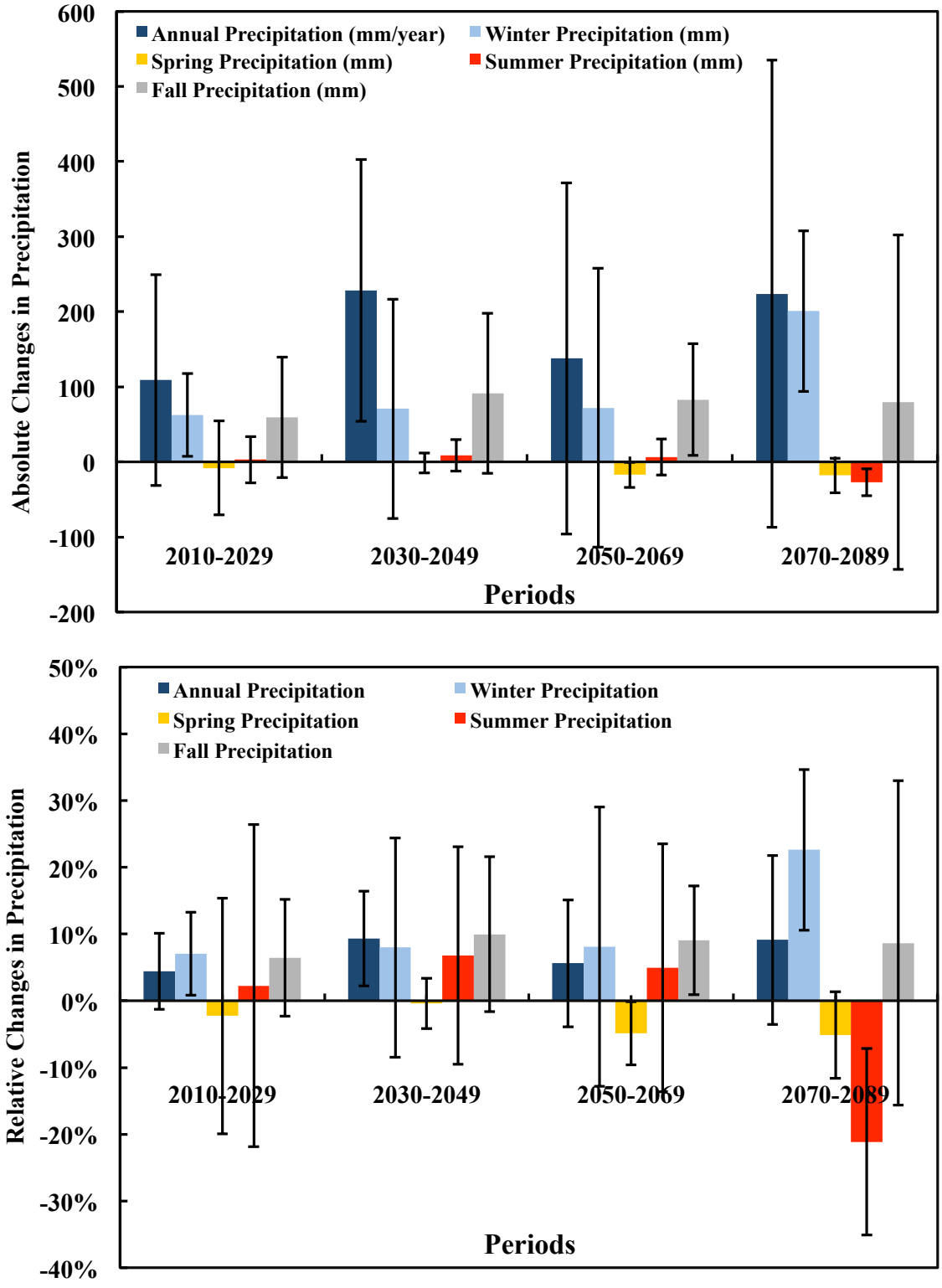

Figure 6.6: *Absolute and relative changes in average annual and seasonal precipitation for the periods 2010-2029, 2030-2049, 2050-2069, and 2070-2089. The black bars represent the upper-bound and lower-bound projected values.*

6.5.3. *Model Calibration-Validation Data*

Daily observed streamflow measurements at H.J. Andrews are available for the period 1994 to 2008 [*Johnson and Rothacher*, 2009] and were used to calibrate and validate the model hydrological parameters. Observed annual data of nutrients losses as well as net primary production (NPP), net ecosystem production (NEP), above- and below-ground biomass, soil organic carbon and heterotrophic respiration for HJA, in combination with published chronosequence data from other Pacific Northwest forest ecosystems, are used to validate model biogeochemical parameters [*D Binkley and Brown*, 1993; *Grier and Logan*, 1977; *Harmon et al.*, 2004a; *Smithwick et al.*, 2002; *P Sollins and F M McCorison*, 1981; *Sollins et al.*, 1980].

6.6. Simulation Methods

A number of HJA simulations were conducted. First, a simulation was conducted, for the period 1994 to 1998, to calibrate model parameters. Then a validation simulation was conducted, for the period 1999 to 2008, to validate the model against observed hydrological and biogeochemical measurements. Finally, climate change simulations were conducted for the period 2009 to 2100, to explore the impact of the projected changes in air temperature and precipitation on catchment hydrological and biogeochemical processes.

6.6.1. Calibration Simulation (1994-1998)

To calibrate model parameters, a simulation was conducted for the period 1994 to 1998. VELMA was forced with daily spatially-distributed air temperature and precipitation data from the historical meteorological station CS2MET. To initialize the model, an existing vegetation stand-age map [*O'Connell*, 2005] was used to represent the biomass stand age distribution at the time of the simulation (see Appendix C for details). This simulation addressed calibration of the model hydrological parameters such as the surface soil hydraulic conductivity (*Ks*), layer thickness, *ET* shape factor, and snowmelt parameters, among others. These hydrological parameters were calibrated to yield the highest statistical coefficient of efficiency between simulated and observed daily

streamflow for the period 1994-1998. Due to the lack of observed biogeochemical fluxes from the HJA watershed, the model biogeochemical parameters were assumed similar to the calibrated parameters used to simulate the biogeochemical fluxes in a small watershed within the H.J. Andrews Experimental Forest (Watershed 10). Specifically, VELMA biogeochemical parameters have been previously calibrated to simulate (1) the accumulation of ecosystem C and N stocks from a stand-replacing fire that occurred in 1525 A.D. [*Wright et al.*, 2002] to present day, (2) old-growth biogeochemical dynamics, and (3) forest recovery after clearcut [*Abdelnour et al.,* in review]. The single set of hydrological and biogeochemical parameters obtained from our calibration simulation are fixed (i.e. held constant) for all subsequent simulations to (1) ensure that the simulated changes in the catchment hydro-biogeochemical response to climate change is entirely due to differences in treatments/climate, not to differences in parameters, and (2) to provide a self-consistent framework for the analysis and the interpretation of the simulations results [*McKane et al.*, 1997]. Model calibrated parameters and values are provided in Appendix A.

6.6.2. Model Validation Simulation (1999-2008).

A validation simulation based on site hydro-meteorological data was conducted, for the period 1999 to 2008, in order to validate the model against measured hydrological and biogeochemical data. Similar to the calibration simulation, VELMA was forced with daily spatially-distributed climate data from CS2MET, and initialized using the existing stand age vegetation map which defines the stand age of vegetation, the biomass value, and the soil organic carbon value at every grid within the watershed (Appendix E). The model was able to capture the seasonal and annual dynamics of streamflow (Figure 6.7) with a Nash-Sutcliffe coefficient of 0.7 [*Nash and Sutcliffe,* 1970], a correlation coefficient of 0.87, and an index of agreement of 0.8 [*Willmott*, 1981] (Table 6.1.b). Simulated annual values of NO_3, NH_4, DON and DOC losses, net ecosystem productivity (NEP), net primary production (NPP), soil heterotrophic respiration as well as N_2 and N_2O emissions to the atmosphere were within the range of measured values for Pacific Northwest forests (see Table 6.2).

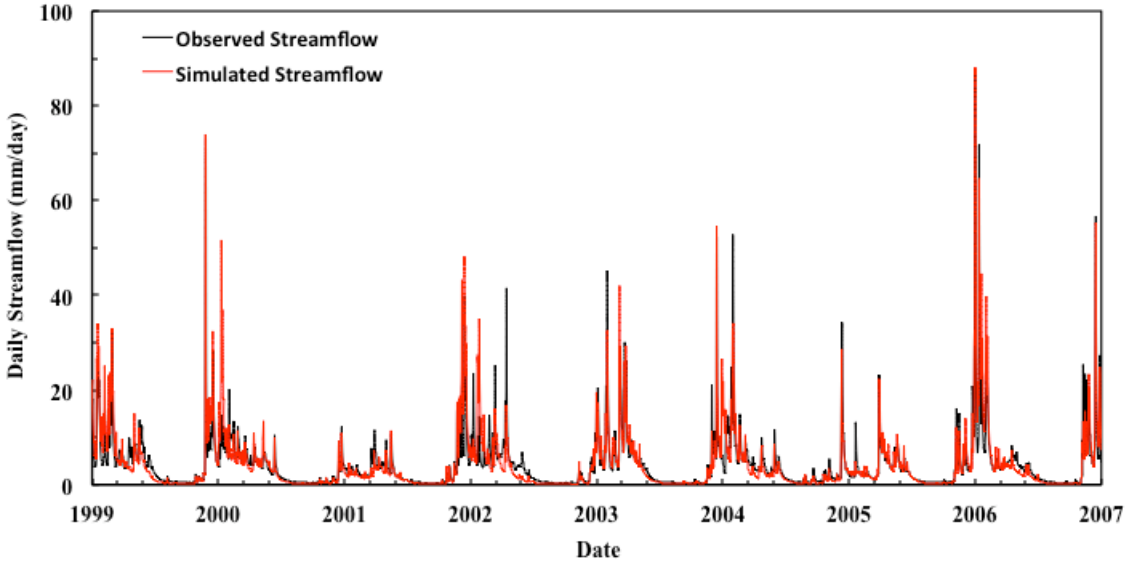

Figure 6.7: *Simulated and observed stream discharge for the validation period of 1999 to 2008.*

Table 6.1: Daily, monthly and annual streamflow modeling performance for: a) the calibration period (1992-1998), and b) the validation period (1999-2008).

Period	Streamflow Modeling Skills for Daily, Monthly and Yearly Time Period					
	Correlation Coefficient R^2	Nash-Sutcliffe Efficiency E_2	First degree Efficiency E'_1	Baseline adjusted Index of agreement d'_1	Root Mean Square Error RMSE	Water Balance Error (%)
a- Calibration Period (1994-1998)						
Daily Flow	0.89	0.79	0.67	0.83	4.48	1.34
Monthly Flow	0.96	0.89	0.74	0.88	46.87	0.23
Annual Flow	0.98	0.95	0.74	0.88	102.34	1.34
b- Validation Period (1999-2008)						
Daily Flow	0.88	0.76	0.61	0.81	3.74	0.40
Monthly Flow	0.95	0.79	0.67	0.85	53.03	1.49
Annual Flow	0.93	0.75	0.51	0.79	143.57	1.49

Nash and Sutcliffe [1970] *defined the coefficient of efficiency E_2, which ranges from minus infinity to 1.0, with higher values indicating better agreement. Values of E_2 are always less than R^2. Willmott* [1981] *developed the index of agreement d'_1, to overcome the insensitivity of correlation-based measures to differences in the observed and simulated means and variances. The index of agreement varies from 0.0 to 1.0, with higher values indicating better agreement. Garrick et al.,* [1978] *defined the baseline–adjusted first-degree coefficient of efficiency E'_1, which varies from minus infinity to 1.0, with higher values indicating better agreement. Hogue et al.,* [2006] *defined the water balance error percentage as a measure of the bias in the simulated flow from the observed flow. A detailed description of these coefficients can be found in the papers by Legates and McCabe Jr.,*[1999], *Waichler et al.,* [2005], and *Hogue et al.,* [2006].

Table 6.2: Comparison between the validation simulation results (i.e. 40% old-growth, 20% mature, 40% post-clearcut between the age of 5 and 25 year-old) and the observed Pacific Northwest mature/old-growth ecosystem average values.

Output Parameter	Simulated Mean Value	Simulated Range of Values	Observed Mean Value	Observed Range of Values	Reference
NH_4 Losses ($gNm^{-2}yr^{-1}$)	0.035	(0.022-0.05)	0.04	0.01-0.05	*Vanderbilt et al.,* [2003]; *Sollins et al.,* [1980]
NO3 losses ($gNm^{-2}yr^{-1}$)	0.014	0.011-0.02	0.01	0.009-0.06	*Sollins et al.,* [1980]; *Martin and Harr* [1989]
DON Losses ($gNm^{-2}yr^{-1}$)	0.08	0.06-0.11	0.089	0.0745-0.1043	*Sollins and McCorison* [1981]
DOC Losses ($gCm^{-2}yr^{-1}$)	1.51	1.15-2.1	3.178	2.015-4.34	*Sollins and McCorison* [1981]
			3.000	1.0-10.0	*Grier and Logan* [1977]
Plant Biomass (gC/m^2)	32,400	31,600-33,000	39,807	34,800-44,800	*Harmon et al.,* [2004a]
			45,500	14,700-60,600	*Smithwick et al.,*[2002]
			43,500	---	*Grier and Logan* [1977]
Soil Organic Carbon (gC/m^2)	24,540	24,200-24,900	22,092	20,600-23,600	*Harmon et al.,* [2004a]
			19,000	---	*Grier and Logan* [1977]
			39,600	---	*Means et al.,* [1992]
			27,500	7,500-50,000	*Smithwick et al.,*[2002]
Total Carbon Storage (gC/m^2)	56,940	55,800-57,900	61,899	56,600-67,700	*Harmon et al.,* [2004a]
			62,400	---	*Grier and Logan* [1977]
Heterotrophic Soil Respiration ($gCm^{-2}yr^{-1}$)	440	409-512	577	479 to 675	*Harmon et al.,* [2004a]
Denitrification Rate ($gNm^{-2}yr^{-1}$)	0.04	0.026-0.053	0.04	0.03-0.09	*Schmidt et al.,* [1988]
			0.013	0.008-0.021	*Binkley et al.,* [1992]
NPP ($gCm^{-2}yr^{-1}$)	451	424-518	597	453 to 741	*Harmon et al.,* [2004a]
			544	---	*Grier and Logan* [1977]
NEP ($gCm^{-2}yr^{-1}$)	9	3-17	20	(-116) to (+156)	*Harmon et al.,* [2004a]
			44	---	*Grier and Logan* [1977]

6.6.3. Climate Change Simulations (2009-2100)

We conducted a total of 4 simulations, three climate change simulation and one control simulation, to explore the impact of the 21th century climate on streamflow, soil moisture, snowpack, nutrient losses, net primary production (NPP), net ecosystem production (NEP) and soil CO_2 and N_2-N_2O emissions. The three climate change simulation were conducted, for the period 2009 to 2100, using the projected daily spatially-distributed air temperature and precipitation data for the upper, lower and middle of the road climate change scenarios defined in section 4.1. The three climate change simulations were then compared to a control simulation to estimate the changes in

hydrological and biogeochemical processes due to the projected change in climate. The control simulation was conducted, for the period 1959 to 1999, using daily spatially-distributed air temperature and precipitation data from the CS2MET station within H.J. Andrews. For all simulations in this section, we assume that the initial hydrological and biogeochemical conditions at H.J. Andrews are at steady state and correspond to old-growth condition. This simplification is acceptable as more than 60% of the watershed is mature/old-growth forest. The goal of the steady-state condition is to allow the analysis of ecosystem response to climate change, irrespective of land-use.

6.7. Simulation Results

Results are presented as follows: We first explore the impact of climate change on catchment hydrological processes such as snow growth and ablation, streamflow, and evapotranspiration. We then present the impact of climate change on catchment C and N dynamics such as biomass and soil organic carbon, dissolved organic and inorganic C and N losses to the stream, gaseous losses of C and N to the atmosphere, and ecosystem productivity (i.e. NPP and NEP).

6.7.1. Catchment Hydrological Response to Climate Change

Simulation results show that the projected increase in winter and spring air temperature reduced winter snowpack and shifted snowmelt to earlier in the season (Figure 6.8). Figure 6.8 shows that end of the century (2070-2089) snowpack melted approximately 20 to 80 days earlier, and that the average winter accumulation was 100mm or 74% lower than control values. These changes in snowpack accumulation and ablation impacted seasonal streamflow (Figure 6.9). Specifically, the combination of lower winter snowpack, earlier snowmelt, lower spring and summer precipitation, and higher spring evapotranspiration reduced spring and summer streamflow (Figure 6.9). End of the century simulated spring and summer streamflow were 14% and 35% lower than control values. By contrast, higher winter air temperature and precipitation contributed to an increase in winter streamflow as more precipitation fell as rain rather than snow. Simulated winter streamflow, for the period 2070-2089, was on average 187mm or 24% higher than control values (figure 6.9). Simulated changes in fall

streamflow were less important than winter and summer changes in streamflow, and primarily driven by the projected higher fall precipitation. Simulated fall streamflow, for the period 2070-2089, was 20mm or 4% higher than control values (Figure 6.9). Simulated seasonal changes in ET further exacerbated the changes in seasonal streamflow by decreasing spring and summer streamflow. In general, simulated seasonal changes in ET were high in the winter, spring, and fall when soil moisture was not a limiting factor and low in the summer due to soil moisture deficits. Specifically, simulated end of the century average winter, spring and fall ET were 26mm (17%), 47mm (18%), and 28mm (16%) higher than control values, respectively. By contrast, end of the century summer ET were on average 10mm (4%) lower than control values. At the annual scale, all climate change simulations projected an end of the century average increase in annual streamflow and ET of 155mm or 9% and 81mm or 9%, respectively (Figure 6.10).

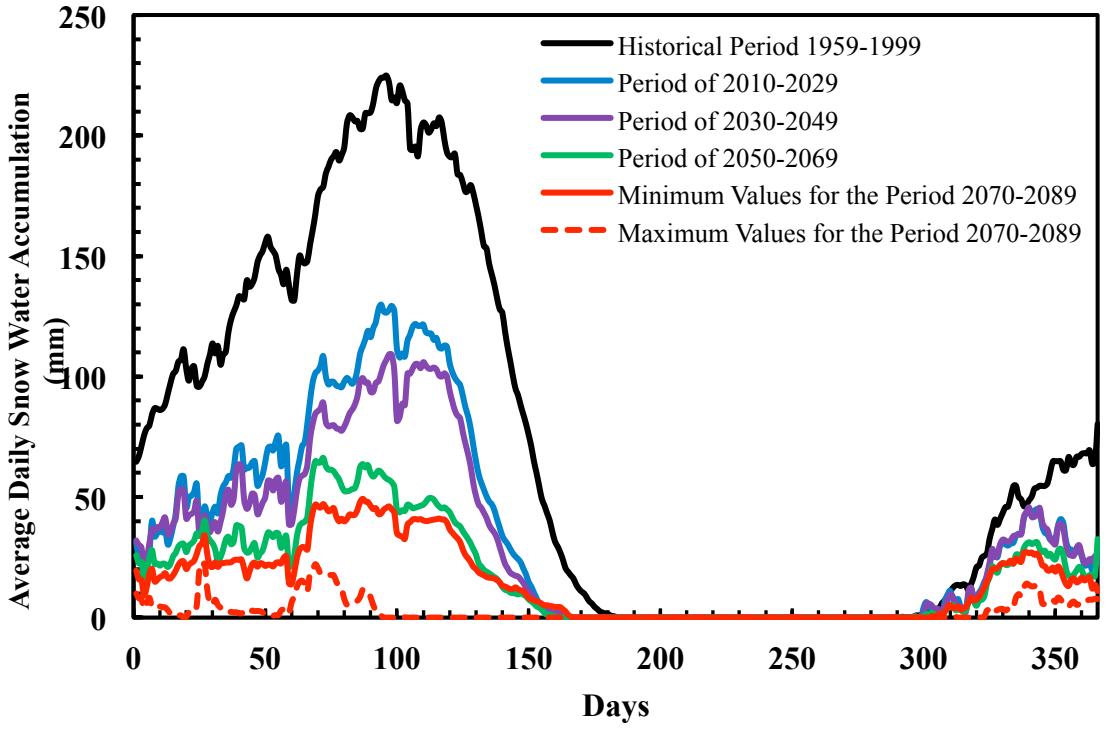

Figure 6.8: *Simulated daily changes in control (historical period of 1959-1999) and future basin average snow water equivalent (mm). The projected 2010-2029 (blue line), 2030-2049 (purple line), 2050-2069 (green line), 2070-2089 (red line) daily changes in snow water equivalent correspond to the average value of the upper, lower, and middle of the road climate change scenarios.*

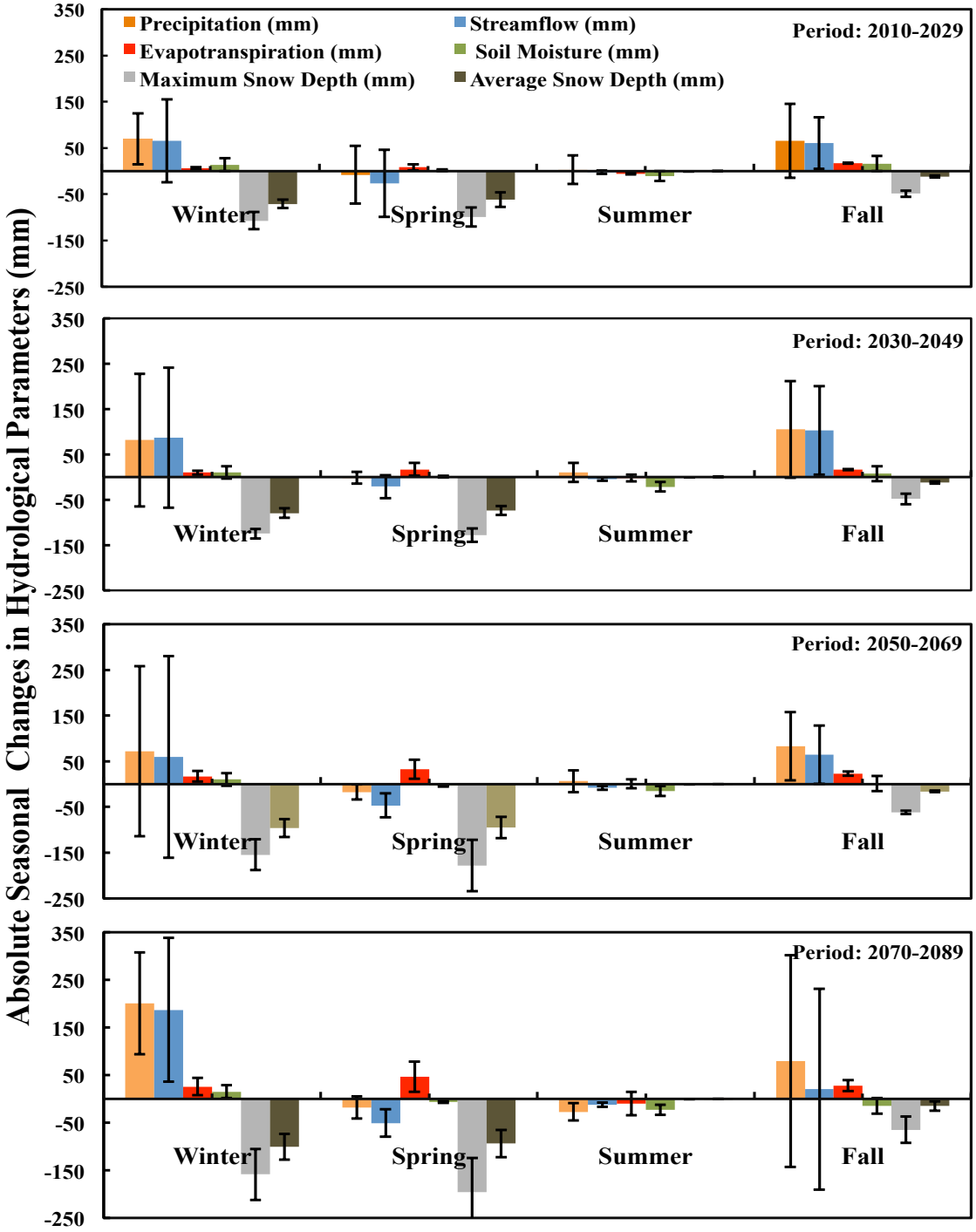

Figure 6.9: *Absolute and relative changes in average seasonal precipitation (orange), streamflow (blue), evapotranspiration (red), soil moisture (green), maximum snow water equivalent depth (gray) and average snow water equivalent depth (brown) for the periods 2010-2029, 2030-2049, 2050-2069, and 2070-2089. The black bars represent the simulated upper-bound and lower-bound as a result of the variability in the projected GCM values of air temperature and precipitation.*

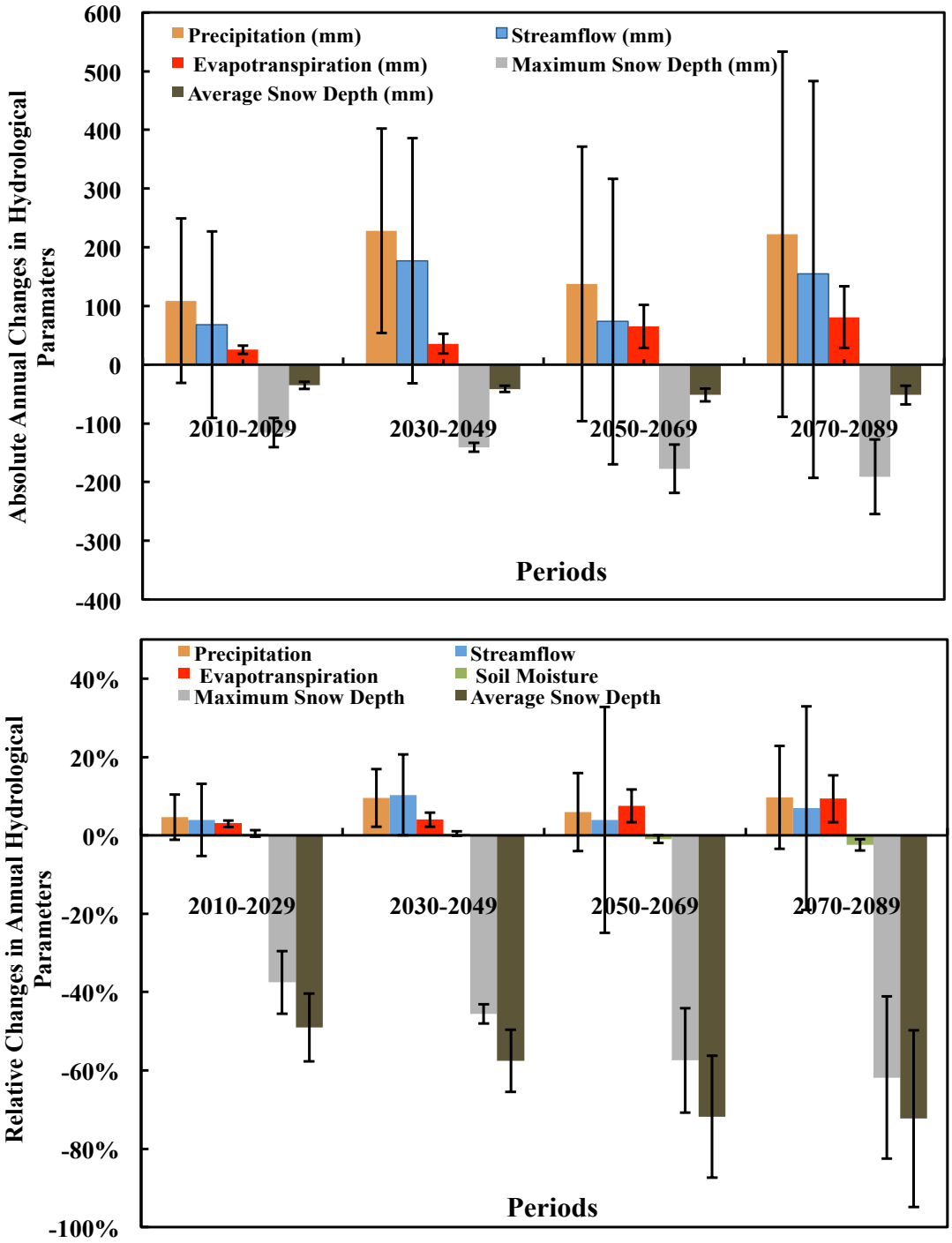

Figure 6.10: *Absolute and relative changes in average annual precipitation (orange), streamflow (blue), evapotranspiration (red), soil moisture (green), maximum snow water equivalent depth (gray) and average snow water equivalent depth (brown) for the periods 2010-2029, 2030-2049, 2050-2069, and 2070-2089. The black bars represent the simulated upper-bound and lower-bound as a result of the variability in the projected GCM values of air temperature and precipitation.*

6.7.2. Catchment Biogeochemical response to Climate Change

Simulated annual plant biomass and soil organic carbon increased at the beginning of the century with increasing air temperature and soil water content, and were 4% and 1% higher than control values, respectively, for the period 2030-2049. This beginning of the century projected increase in plant biomass was primarily driven by the increase in the growing season and nitrogen availability as a result of higher precipitation and soil organic carbon decomposition. Figure 6.11A shows that net biomass growth (Net Primary Productivity, NPP) in the H.J. Andrews increased by approximately 10% and shifted from late spring to mid-spring and from early fall to mid-fall as a result of higher spring and fall air temperatures and soil water content. Specifically, simulated spring and fall biomass growth were ~ 5% and 20% higher than control values, whereas summer biomass growth was 3% lower than control value. This increase in the growing season length was responsible for the increase in plant biomass, which in turn provided higher amounts of detritus input into the soil, thereby increasing the soil carbon pool. However, at the end of the century, higher air temperatures and increased soil moisture deficits reduced the growth rate of biomass and reduced the soil organic carbon pool. Specifically, simulated plant biomass and soil organic carbon pool, for the period 2070-2089, were 4% and 0.7% higher than control values.

Simulated annual changes in gaseous losses of C and N were primarily driven by the changes in air temperature, soil organic carbon decomposition and soil water content (Figures 6.12 and 6.13). At the seasonal scale, end of the century soil heterotrophic respiration increased in spring and fall as a result of higher air temperatures and higher soil organic carbon, but decreased in the summer as a result of high soil moisture deficits (Figure 6.11B). At the annual scale, all climate change simulations projected an increase in soil heterotrophic respiration and nitrification rates as a result of higher air temperature and soil organic carbon decomposition (Figures 6.12 and 6.13). Specifically, simulated end of the century soil heterotrophic respiration and nitrification rates were 21$gCm^{-2}yr^{-1}$ (4%) and 0.10$gNm^{-2}yr^{-1}$ (8%) higher than control values, respectively. By contrast, the projected simulated changes in denitrification rates were negative as a result of spring, summer and fall soil water deficit (Figure 6.12). Specifically, end of the century

simulated average annual denitrification rates were 38mgNm^{-2}yr^{-1} or 46% lower than control values. Although, soil nitrification and denitrification rates were both strongly driven by temperature, the projected end of the century soil moisture deficit strongly limited the anaerobic denitrification process and enhanced the aerobic nitrification process.

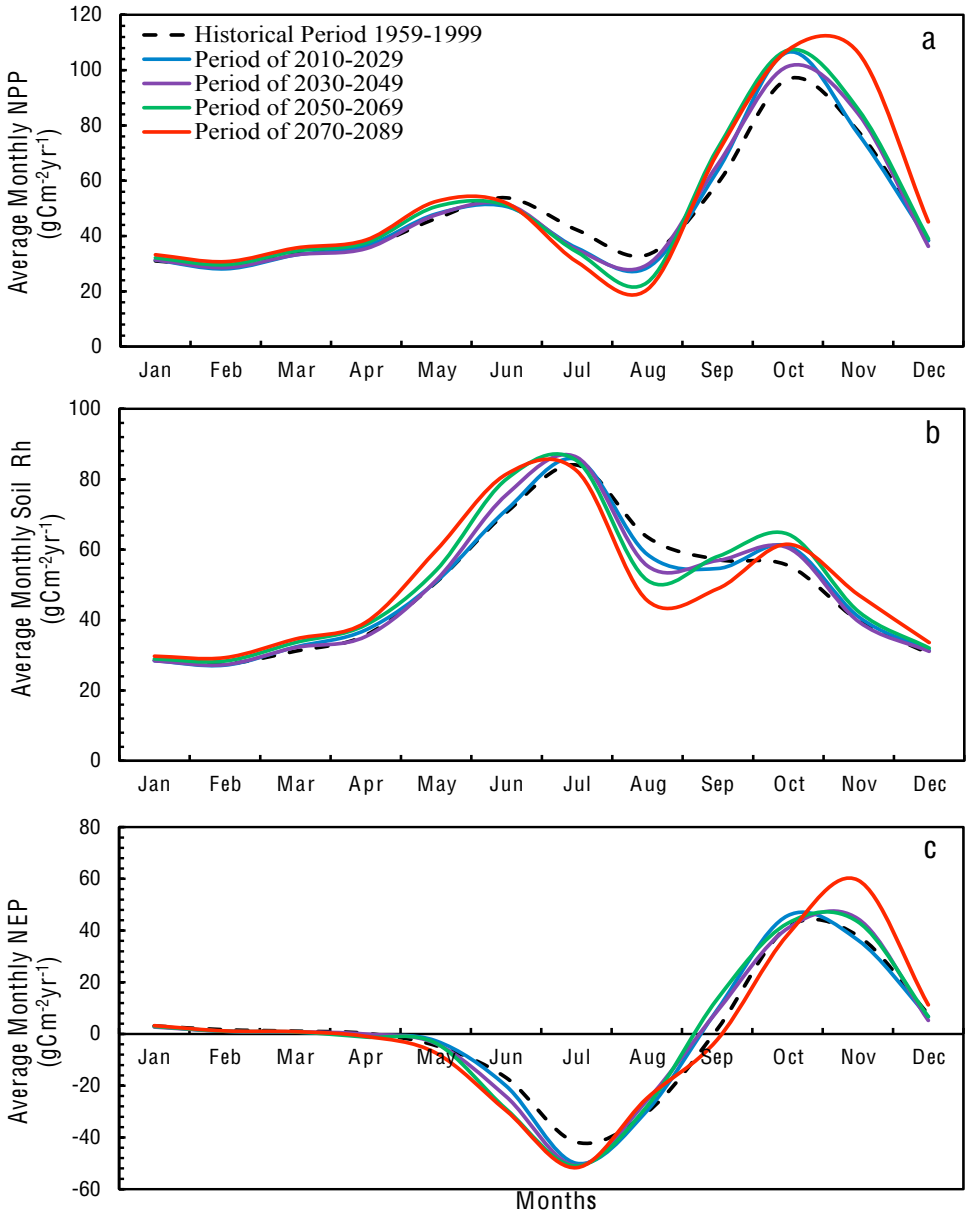

Figure 6.11: *Simulated historical and future monthly changes in net primary production (NPP; sub-plot a), soil heterotrophic respiration (Rh; sub-plot b), and net ecosystem production (NEP; sub-plot c). The projected 2010-2029 (blue line), 2030-2049 (purple line), 2050-2069 (green line), 2070-2089 (red line) monthly correspond to the average value of the upper, lower, and middle of the road climate change scenarios.*

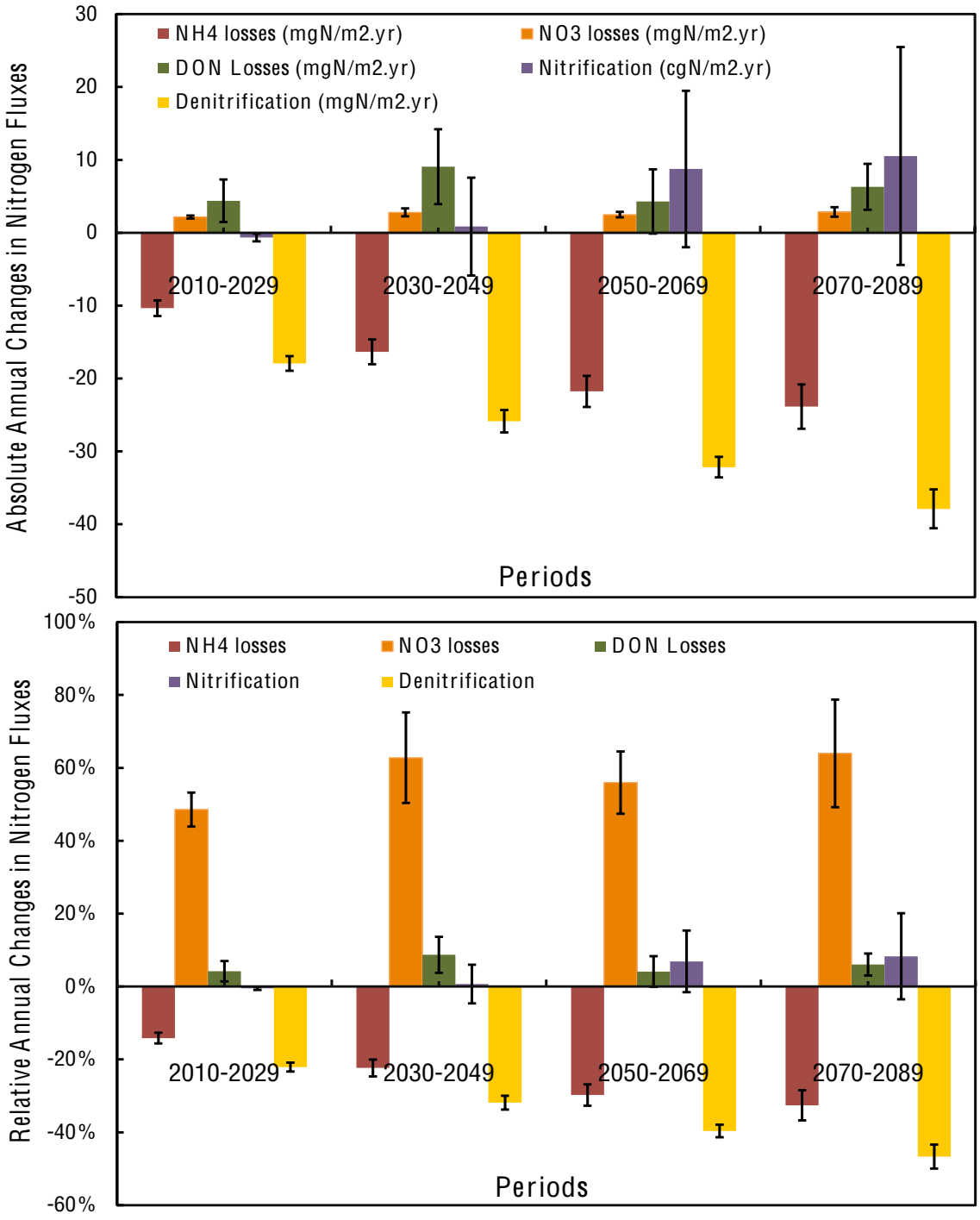

Figure 6.12: *Absolute and relative changes in average annual ammonium NH_4 losses (red; $mgNm^{-2}yr^{-1}$), nitrate NO_3 losses (orange; $mgNm^{-2}yr^{-1}$), DON losses (green; $mgNm^{-2}yr^{-1}$), nitrification rates (purple; $gNm^{-2}yr^{-1}$), and denitrification rates (yellow; $mgNm^{-2}yr^{-1}$) for the periods 2010-2029, 2030-2049, 2050-2069, and 2070-2089. The black bars represent the simulated upper-bound and lower-bound as a result of the variability in the projected GCM values of air temperature and precipitation.*

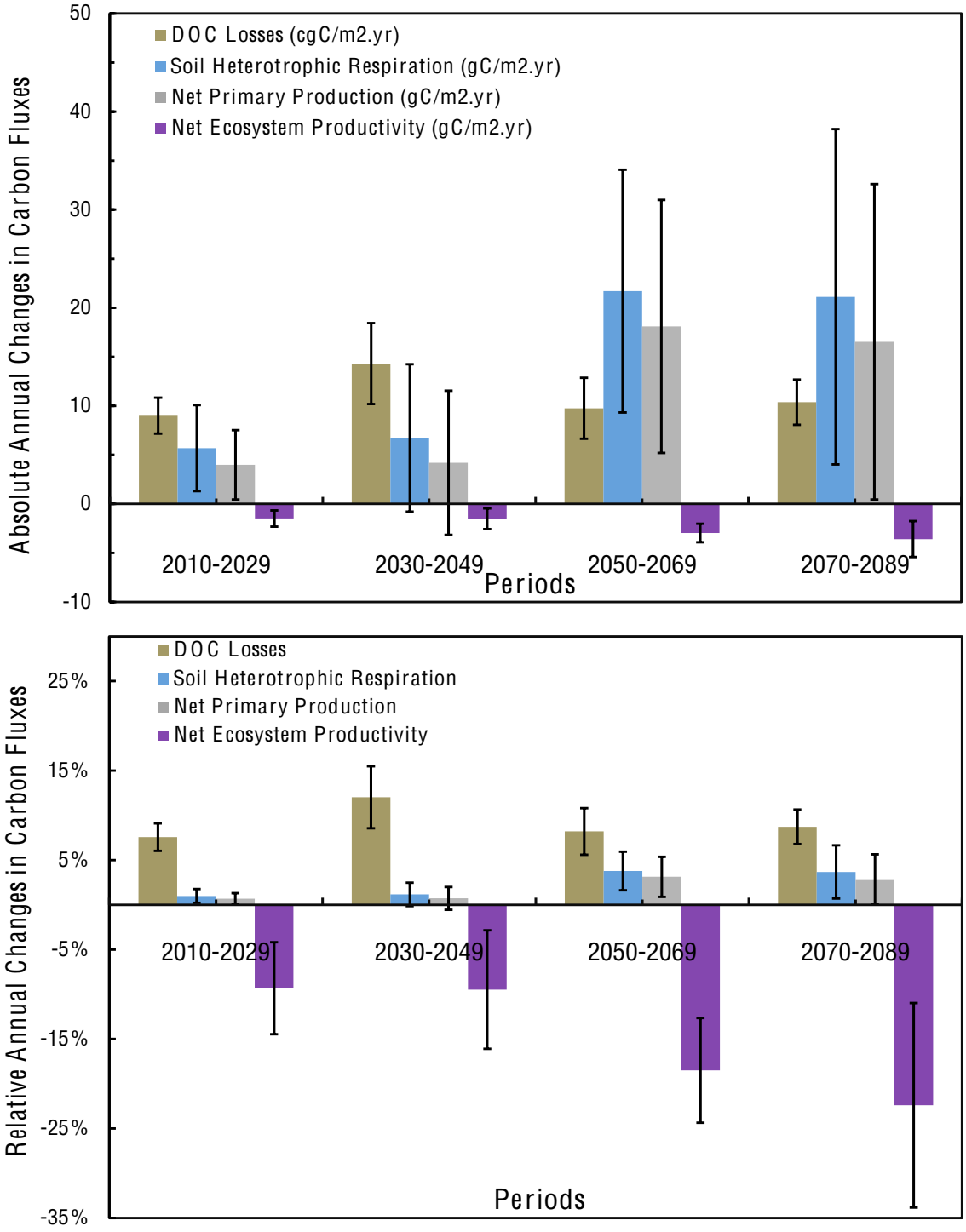

Figure 6.13: *Absolute and relative changes in average annual DOC losses (brown; $mgCm^{-2}yr^{-1}$), soil heterotrophic respiration (blue; $gCm^{-2}yr^{-1}$), net primary production (light purple; $gCm^{-2}yr^{-1}$), and net ecosystem production (gay; $gCm^{-2}yr^{-1}$) for the periods 2010-2029, 2030-2049, 2050-2069, and 2070-2089. The black bars represent the simulated upper-bound and lower-bound as a result of the variability in the projected GCM values of air temperature and precipitation.*

Simulated dissolved inorganic nitrogen (NH_4 and NO_3) was primarily driven by high N uptake by plants and high soil organic carbon decomposition (Figure 6.12). Specifically, end of the century annual NH_4 losses to the stream were on average 2.6 $mgNm^{-2}yr^{-1}$ (33%) lower than control values as a result of high NH_4 uptake by plant, and high nitrification rates of NH_4 into NO_3. Consequently, end of the century annual NO_3 losses to the stream were on average 2.8$mgNm^{-2}yr^{-1}$ (64%) higher than control values as a result of high nitrification rates of NH_4 into NO_3 and low denitrification rates of NO_3 into N_2-N_2O. Simulated dissolved organic nitrogen and carbon increased as a result of high soil organic carbon decomposition and high annual streamflow (Figures 6.12 and 6.13). End of the century annual DON and DOC losses to the stream were on average 6.3$mgNm^{-2}yr^{-1}$ (6%) and 100$mgCm^{-2}yr^{-1}$ (9%) higher than control values, respectively. The projected increase in DON losses might be in part due to a model assumption that plant nitrogen uptake impacts the nitrate and ammonium pool only. As such, the magnitude of DON losses would be reduced in places where DON pool contributes a substantial amount of nitrogen to the growing plants.

Finally, simulated annual changes in NEP and NPP were primarily driven by plant growth and ecosystem C losses as CO_2 to the atmosphere and as DOC to the stream (Figure 6.13). Specifically, simulated annual NPP increased with increasing nitrogen availability and was on average 17$gCm^{-2}yr^{-1}$ or 3% higher than control values at the end of the century. Although simulated NPP was projected to increase, NEP–defined as the net gain or loss of carbon from the ecosystem, calculated as NPP minus heterotrophic respiration and DOC losses – was projected to decrease as a result of the projected increase in soil heterotrophic respiration and DOC losses. At the seasonal scale, simulated end of the century fall NEP was positive and 30% higher than control values, whereas simulated summer NEP was negative and ~10% lower than control values (Figure 6.11C). At the annual scale, for the period 2010-2029, simulated annual NEP averaged 0.6$gCm^{-2}yr^{-1}$ but was 70% lower than control values. However, with increasing soil heterotrophic respiration and DOC losses to the stream, as well as a decreasing SOC pool, NEP over the last twenty years of the simulation turns negative at -3.6$gCm^{-2}yr^{-1}$.

6.8. Discussion

A spatially distributed eco-hydrologic model, VELMA, was used to explore the impact of climate change on catchment hydrological and biogeochemical processes at the H.J. Andrews Experimental Forest in the Pacific Northwest. . Daily projected air temperature and precipitation from an upper, lower and middle of the road climate change scenarios were used to force VELMA. These bounding climate change scenarios were chosen to span a large range of potential future air temperature and precipitation for the Pacific Northwest [*Salathe et al.,* 2007]. Bias corrected air temperature and precipitation data were spatially interpolated across the HJA using a climate analysis model PRISM in order to capture the effects of elevation, topography, and orographic lifting on air temperature and precipitation [*Daly*, 1996; *Daly et al.*, 1994; *Daly et al.*, 2002]. Simulation results show that climate change strongly impacts catchment hydrological and biogeochemical processes. Specifically, our main hydrological insights suggest an end of the century shift from snow dominated to rain dominated precipitation with a ~ 72% decrease in average snow water equivalent and a shift in snowmelt from early July to mid-April. We also found that these changes in snow accumulation and ablation resulted in higher winter streamflow and lower summer low flow. Similar results were found by *Elsner et al.,* [2010], *Tague et al.,* [2008], and *Graves and Chang,* [2007], amongst others. *Elsner et al.,* [2010] applied the DHSVM hydrological model to the Puget Sound catchment in Washington State to assess the impact of climate change on snow accumulation, and found that April 1 winter SWE decreased by 53 to 65% and snowmelt occurred earlier as a result of the projected increase in winter air temperatures. *Tague et al.,* [2008] applied the RHESSys eco-hydrological model to the same 64km^2 HJA watershed used in this study to test the impact of a 1.5°C increase in air temperature on hydrology and found that there was a significant loss of snow accumulation, a 25% to 50% decrease in the number of days with snow cover, and a ~ 60% decrease in peak snowpack. Although, *Tague et al.,* [2008] assumed that future precipitation do not change in the future, their results were well within the ranges of values simulated by VELMA. *Graves and Chang,* [2007] applied a GIS based distributed hydrological model at a monthly time scale to the Upper Clackamas River basin in Oregon and found that the

mean peak snowpack decreased by 83 to 88%, whereas winter streamflow increased by 13.7% to 46.4% in the period 2070-2099. By contrast, the simulation results obtained by *Hamlet and Lettenmaier* [1999] were higher than the values simulated by VELMA for the HJA. *Hamlet and Lettenmaier* [1999] applied the VIC hydrological model at 1/8 degree over the Columbia River basin to explore the impact of climate change on hydrology, and found that cool season streamflow increased by up to 89%, whereas summer season streamflow decreased by up to 20% at the end of the century. This large difference in result may owe in part to the difference in forcing data. *Hamlet and Lettenmaier* [1999] used the projected air temperature and precipitation from the Hadley center simulation, which projected an end of century 4.5°C increase in temperature and 20% increase in precipitation which is at the upper bound of the projected climate used in our simulations.

In addition to the changes in the hydrological regime of the H.J. Andrews, climate change simulations suggest that the HJA forest will experience a moderate increase in vegetation growth due to longer growing season and higher ecosystem net primary production. Moreover, higher air temperatures and soil organic carbon decomposition enhances greenhouse gas emissions (i.e. soil CO_2 respiration and N_2 emissions from nitrification) and increases the amount of nutrients that reach the stream. These projected changes in catchment C and N dynamics are generally consistent with the results of other climate change impact studies conducted around the world. For example, *Tague et al*., [2009] used the RHESSys ecohydrological model to investigate the potential response of vegetation to a hypothetical range of changes in air temperature (0°C, 2°C and 4°C) and precipitation (-30%, -10%, 0%, +10%, +30%) in a chaparral ecosystem of south California, and found a similar trend of increasing plant biomass and net ecosystem productivity. Similarly, *VEMAP Members* [1995] used three biogeochemistry models (Biome-GBC, Century, and TEM) to test the impact of the projected changes in local climate on total ecosystem carbon storage and net primary production in forested areas of the United States and also found that the changes in total carbon storage range from -33% to+16% and changes in NPP range from 0% to +40%. *Cramer et al.,* [1999] used seventeen global models of terrestrial biogeochemistry to simulate the impact of a standardized climate change scenario on ecosystem processes and found that global NEP

generally decreased with the projected climate warming as soil respiration exceeds ecosystem carbon uptake. *Sebestyen et al*., [2009] used a statistical model to assess how stream nutrient loading respond to higher precipitation and longer growing season in the Sleepers River research watershed in Vermont. Their results were similar to ours and suggested that, for the period 2070-2099, DOC loading would increase by 9% as a result of higher streamflow whereas nitrogen load would decrease by 2% as a result of longer growing season and higher N uptakes. *Kesik et al.,* [2006] used a GIS coupled biogeochemical model PnET-N-DNDC to investigate the potential impact of future climate change on forest soil N_2O and NO emissions in Europe and found that in regions where future climate change conditions results in lower soil water content, denitrification rates decreased and nitrification rates increased. Finally, several climate change impact studies suggest that future soil heterotrophic respiration will increase as a result of higher temperature and precipitation [*Lenihan et al.*, 2003; *McGlinchy*, 2011].

The simulated future changes in the H.J. Andrews hydrological, ecological and biogeochemical processes are likely to represent the range of potential changes that will affect the Pacific Northwest. Such future impacts are likely to have implications for forest and water resources management. Specifically, higher winter streamflow is expected to increase the probability of floods, landslides and debris flow activity [*Spittlehouse and Stewart*, 2003], whereas lower summer streamflow and soil moisture will reduce the ability to supply water to all users, increase competition for water supply between municipalities, farmers and hydropower production [*Payne et al.*, 2004], limit vegetation survival [*Breshears et al*., 2005; *Spittlehouse*, 1996; *Spittlehouse and Stewart*, 2003], and negatively affect freshwater fisheries habitat [*Mantua et al.*, 2010]. Moreover, higher greenhouse gas emissions and lower net ecosystem productivity are likely to enhance climate change and reduce forest carbon sequestration, whereas higher C and N losses to the stream will decrease water quality and negatively impact freshwater fisheries habitat [*Mantua et al.*, 2010].

Finally, the impact of climate change on ecosystem processes simulated in this study did not account for the indirect effects of climate change on C and N dynamics, water quality and quantity. The indirect effects of climate change include (1) a shift in vegetation distribution towards drought tolerant species [*Dale and Franklin*, 1989;

Hamann and Wang, 2006; *Shafer et al.*, 2001], (2) an increase in fire frequency and severity due to the projected increase in spring-summer air temperatures as well as a decrease in precipitation, soil moisture and fuel moisture conditions [*Brown et al.*, 2004; *Lettenmaier et al.*, 2008; *McKenzie et al.*, 2004; *Westerling et al.*, 2006], (3) an increase in insect and pathogen outbreak partially caused by the lack of low winter minimum air temperatures, which would normally kill the larvae [*Beukema et al.*, 2007; *Carroll et al.*, 2003; *Logan et al.*, 2001; *Powell et al.*, 2000], and (4) an increase in tree mortality due to changes in air temperature and precipitation [*Breshears et al.*, 2005; *Lutz and Halpern*, 2006] as well as higher susceptibility to attack by insects such as bark beetles and spruce budworm. These indirect disturbances associated with climate change are not currently simulated in VELMA, but are likely to be significant agents of changes in forest structure and composition than climate change alone. *Little et al*., [2010] argues that the future changes in forest structure, composition and productivity in response to climate change will likely be driven by the projected increase in disturbances rather than the gradual change in climate. The combined effects of water stress, increase fire frequency and severity, and increase insect outbreak suggest that climate change is likely to impact site productivity, C and N losses and water quantity and quality to a degree not currently simulated in this study.

6.9. Conclusion

The ecohydrological model VELMA, presented in this study, provides resource managers with critical insights on the potential extend of impact climate change will have on forest C and N dynamics, site productivity and water quality and quantity. Land managers and policy makers can use VELMA as a tool to explore how their management decisions impact future water resources, species preservation and salmon industry, amongst others. VELMA can also be used to test the efficiency of adaptation strategies in making the ecosystem more resilient to the impact of climate change. Management strategies could include (1) reducing fuel load to decrease the risk of fire, (2) thinning in the summer to decrease the amount of water lost through transpiration and increase summer low flow, and (3) developing draught tolerant and insect outbreak resistant species in order to reduce large scale tree mortality due to insect outbreak.

6.10. Acknowledgements

The information in this document has been funded in part by the US Environmental Protection Agency. It has been subjected to the Agency's peer and administrative review, and it has been approved for publication as an EPA document. Mention of trade names or commercial products does not constitute endorsement or recommendation for use. This research was additionally supported in part by the following NSF Grants 0439620, 0436118, and 0922100. We thank Sherri Johnson, Barbara Bond, Suzanne Remillard, Theresa Valentine and Don Henshaw for invaluable assistance in accessing and interpreting various H.J. Andrews LTER data sets used in this study. Data for streamflow, stream chemistry and climate were provided by the H.J. Andrews Experimental Forest research program, funded by the National Science Foundation's Long-Term Ecological Research Program (DEB 08-23380), US Forest Service Pacific Northwest Research Station, and Oregon State University.

6.11. Appendix A: Model Parameters and Calibration Values

The model parameters values presented in the tables below are specific to the 64 km^2 H.J. Andrews watershed. Model hydrological parameters were either chosen from observed values in the field (e.g. soil texture, soil depth, root depth, etc.) or calibrated to yield the highest statistical coefficient of efficiency between simulated and observed daily streamflow for the period 1994-1998 (e.g. hydraulic conductivity, snow parameters, etc.), and are provided in Table 6.A.1. Model biogeochemical parameters were either chosen from observed values in the field (e.g. soil texture, soil depth, root depth, etc.) or based on the previously calibrated parameters used to simulate carbon and nitrogen dynamics in Watershed 10 (a small watershed within H.J. Andrews). Specifically, to simulate (1) the accumulation of ecosystem C and N stocks from a stand-replacing fire that occurred in 1525 A.D. [*Wright et al.*, 2002] to present day, (2) old-growth biogeochemical dynamics, and (3) forest recovery after clearcut [*Abdelnour et al.,* in review] (Refer to Chapter 4). Table 6.A.2 provides the parameters calibration values and references pertaining to the soil temperature and plant-soil model.

Table 6.A.1: Hydrological Model Parameters and Calibration Values

Parameters	Value	References	Parameters	Value	References
Soil Texture	Loam*	*Ranken,* 1974	d_r	3	*Santantonio et al.* 1977
θ_i^{fc}	0.27	*Clapp and Hornberger*, 1978	$W_{E,deep}$	0.2	Calibrated
ϕ_i	0.463	*Clapp and Hornberger*, 1978	c_{ET}	5	Calibrated
θ_i^{w}	0.117	*Clapp and Hornberger*, 1978	K_{PET}	2	Calibrated
Δz_1	300	Calibrated	α	5	Calibrated
Δz_2	750	Calibrated	T_{th}	-1	Calibrated
Δz_3	750	Calibrated	T_m	2	Calibrated
Δz_4	200	Calibrated	σ	0.5	Calibrated
Ks	950	Calibrated	r_{ET}	0.3	Calibrated
f_v	1.3	Calibrated	r_T	3000	Calibrated
f_l	1.55	Calibrated	Ω	10	Calibrated

Table 6.A.2: Soil Temperature and Plant-Soil Model Parameters and Calibration Values

Parameters	Value	References	Parameters	Value	References
kn	0.1	Calibrated	$W_{\lambda 2}$	0.85	Fixed *a priori*
δ_{NO3}	0.3	[*Rygiewz and Bledsoe.,* 1986; *Kamminga-Van Wijik and Prins.,* 1993]	WS_{min}	40	Fixed *a priori*
δ_{NH4}	0.7	[*Rygiewz and Bledsoe.,* 1986; *Kamminga-Van Wijik and Prins.,* 1993]	WS_{max}	80	Fixed *a priori*
α_{CN}	50	[*P Sollins and F McCorison*, 1981]	k_c	0.45	Calibrated
c_d	0.004	Calibrated	M_{sat}	0.25	[*Raich et al.*, 1991]
n_{in}	0.4	[*Sollins et al.*, 1980]	ma_1	0.14	[*Raich et al.*, 1991]
β	0.976	[*Jackson et al.*, 1996]	$(s_i/s_i^{max})_{opt}$	50%	[*Alexander*, 1977]
q	0.015	Calibrated	pH	4.5	[*Chaer et al.*, 2009]
m_{st}	0.0125	[*Lutz and Halpern.,* 2006]	$K_N^{\max}$	0.15	[*Parton et al.,* 2001]
B_{st}	42350	[*Harmon et al.*, 2004b; *Sollins et al.*, 1980]	N_a	0.4	[*Parton et al.*, 1996]
m_a	1.55	Fixed *a priori*	N_b	1.7	[*Parton et al.*, 1996]
m_b	4	Fixed *a priori*	N_c	3.22	[*Parton et al.*, 1996]
m_c	1.E-14	Fixed *a priori*	N_d	0.007	[*Parton et al.*, 1996]
μ_{min}	0.20	Fixed *a priori*	D_a	5.0	[*Del Grosso et al.*, 2000]
μ_{st}	0.25	Fixed *a priori*	qf_{NH_4}	0.12	Calibrated
Wt_{max}	35	[*Luyssaert et al.*, 2008]	qf_{NO_3}	0.04	Calibrated
W_{k1}	1.60	Fixed *a priori*	qf_{DON}	0.02	Calibrated
$W_{\lambda 1}$	1.70	Fixed *a priori*	qf_{DOC}	0.06	Calibrated
W_{k2}	0.95	Fixed *a priori*	λ_{snow}	670	*Hillel*, 1998

6.12. Appendix B: Future Meteorological Data Selection:

A large collection of global climate simulation models and emission scenarios were performed for the International Panel on Climate Change (IPCC) Fourth Assessment Report (AR4) [*Alley et al.*, 2007]. These models and emissions scenario project a wide variety of changes in air temperature and precipitation for the Pacific Northwest [*Mote et Salathe,* 2010]. As a result, most climate change impact studies either use a large ensemble of climate models and scenarios referred to as reliability ensemble averaging "REA" approach [*Giorgi and Mearns*, 2003] or a few bounding (upper and lower bound) climate models and scenarios. However, *Salathe et al.,* [2007] argues that the choice of these bounding scenarios has to be done carefully to span a large range of future climate and precipitation as the REA approach. *Salathe et al.,* [2007] analyzed a selection of global climate simulation models, evaluated their skills at capturing the 20th century climate of the Pacific Northwest, and identified the best performing (i.e. lowest air temperature and precipitation biases) climate models for the Pacific Northwest. Thereafter, *Salathe et al.,* [2007] examined the 21th century projected changes in air temperature and precipitation simulated by these climate models forced with the A2 (higher end of the emission scenarios with aggressive increase in greenhouse gases) and B1 (lowest emission scenario with moderate increase in greenhouse gases) emission scenarios and clustered these climate models and emissions scenarios into three categories: (1) high rate of warming and large increase in precipitation, (2) moderate rate of warming and moderate increase in precipitation, and (3) low rate of warming and small increase in precipitation. Three global climate simulation models and emission scenarios have been then identified in each of these categories based on their 20th century performance: IPSLCM4_A2 [*IPSL*, 2005] (upper bound scenario; Institut Pierre Simon Laplace), ECHAM5_A2 [*Jungclaus*, 2006; *Roeckner et al.*, 2003] (middle of the road scenario; Max-Planck-Institute for Meteorology), and GISS_ER_B1 [*Russell et al.*, 2000] (lower bound scenario; Goddard Institute for Space Studies) [*Salathe et al.,* 2007].

Daily air temperature and precipitation data for the upper bound, lower bound and middle of the road scenarios have been statistically downscaled to 1/8 of a degree over

the Pacific Northwest by the Joint Institute for the Study of Atmosphere and Oceans Climate Impacts Group (CIG) at the University of Washington. The statistical downscaling method used by the CIG is based on methods described by *Wood et al.,* [2002], *Widmann et al.,* [2010] and *Salathe*, [2005]. In this paper, daily downscaled (1/8 of a degree or 0.125 x 0.125 degrees) air temperature and precipitation data for the period 2008-2100 were obtained for the upper bound (IPSLCM4_A2), lower bound (GISS_ER_B1) and middle of the road (ECHAM5_A2) scenarios from the Climate Impact Group website (see Center For Science in the Earth System; http://cses.washington.edu/data/ipccar4/).

[Note: a detailed description of the greenhouse gas emission scenario can be found in the IPCC's Special Report on Emissions Scenarios (SRES) [*Nakicenovic et al.*, 2000] and are beyond the scope of this paper. In short, the A2 scenario is at the higher end of the SRES emissions scenarios and entails an aggressive increase in greenhouse gas emissions, a heterogeneous world, and high population growth, whereas the B1 emission scenario is the lowest SRES emission scenario and entails a small increase in greenhouse gas emissions, an integrated and ecologically friendly world, and a declining population at the end of the 21th century].

6.13. Appendix C: Mapping Future Climate Data to CS2MET:

The statistically downscaled daily air temperature and precipitation data has a resolution of 0.125 x 0.125 degrees. As a result, the climate at the scale of our watershed may not be correctly represented by the downscaled data due to site-specific properties such as elevation and land-use [*Salathe et al.,* 2007]. Therefore, mapping of the projected climate data (extracted from the grid cell encompassing the H.J. Andrews watershed) to a meteorological station within HJA is required. To this end, a cumulative distribution function (CDF) technique for bias correction [*Wood et al.*, 2002; *Ines and Hansen*, 2006; *Salathe et al.*, 2008] is used. This technique calibrates the downscaled air temperature and precipitation so that their frequency distribution matches that of the historical observed air temperature and precipitation within the watershed. Below, we describe step-by step the method used in this paper to bias correct the daily GCM air temperature (T) and precipitation (P) data.

Step 1: Daily simulated T and P data, for the period 1959 to 2000, are first obtained from the GCM and the meteorological station within HJA, and then converted into monthly data (i.e. sum of daily values in the month for P and average of daily values in the month for T).

Step 2: Empirical cumulative distribution functions (CDFs) are calculated for the GCM (F_{GCM}) and the observed (F_{obs}) monthly data. These empirical CDFs of T and P are then fit with a Gaussian distribution.

Step 3: Transformation relationships are first defined for each month of the year by comparing the empirical CDFs of the observed meteorological data (period 1959 to 2000) to the empirical CDFs of the downscaled simulated historical climate data (over the same period) from the global climate models of interested. The bias corrected monthly value is calculated using the following formula:

$$x_i' = F_{obs}^{-1}(F_{GCM}(x_i)) \tag{6.C.1}$$

Where, x_i is the P or T value in GCM data for month i, and x_i' is the corresponding bias corrected value. Thereafter, the future downscaled monthly climate data, for the period 2000 to 2100, are mapped to the historical station location using these transformations.

Step 4: The statistically downscaled daily T and P are scaled (addition for T and ratio for P) to yield the bias corrected mean monthly values. Specifically, daily T and P data are modified so that their monthly values are the same as monthly bias corrected data. The formulae for modifying daily data are as follows:

$$p_i' = p_i \cdot \frac{P_{bc}}{P_{raw}} \tag{6.C.2}$$

and

$$t_i' = t_i + (T_{bc} - T_{raw}) \tag{6.C.3}$$

where, T_{raw} and P_{raw} are the original raw statistically downscaled temperature and precipitation, respectively; T_{bc} and P_{bc} are the new bias corrected temperature and precipitation (from step 3), respectively; t_i and p_i are the original daily raw temperature

and precipitation values from the GCM data for day i, respectively; and t_i' and p_i' are the daily bias corrected temperature and precipitation values used as input into VELMA.

6.14. Appendix D: Spatial Distribution of Temperature and Precipitation:

Spatial interpolation of the historical (CS2MET) and the projected future (21th century) air temperature and precipitation data to the HJA 64km^2 watershed is based on PRISM (Parameter-elevation Regressions on Independent Slopes Model). PRISM is a climate analysis model that uses point meteorological data, surface topography and other spatial data sets to generate continuous gridded estimates of annual and monthly climate variables [*Daly*, 1996; *Daly et al.*, 1994; *Daly et al.*, 2002]. PRISM is well suited for climate mapping in mountainous terrain and includes for the effects of elevation, forest canopy, cloudiness, topographic shading, orographic lifting, and temperature inversion on air temperature and precipitation [*Daly*, 1996; *Smith et al.*, 2005].

Spatial maps (i.e. cartographic representation of gridded data) of monthly average air temperature [*Daly and Smith*, 2005] and precipitation [*Daly*, 2005] have been developed for the HJA using the PRISM model. These maps were based on historical average monthly air temperature (1971-2000) and precipitation (1980-1990) time series at different climate stations within the watershed [*Daly and Smith*, 2005; *Daly*, 2005]. These maps are first re-sampled to the 30m resolution of the current study [*Valentine and Lienkaemper*, 2005] from their native 100m resolutions. Then, a set of monthly differences (temperature) and ratios (precipitation) are calculated for every grid cell (i.e. soil column) within the watershed, relative to the location of the climate station CS2MET. These sets of modifiers (differences, ratios) are then applied to the historical and the projected future daily air temperature and precipitation time series to derive daily climate data at each grid cell within the watershed (Figure 6.D.14).

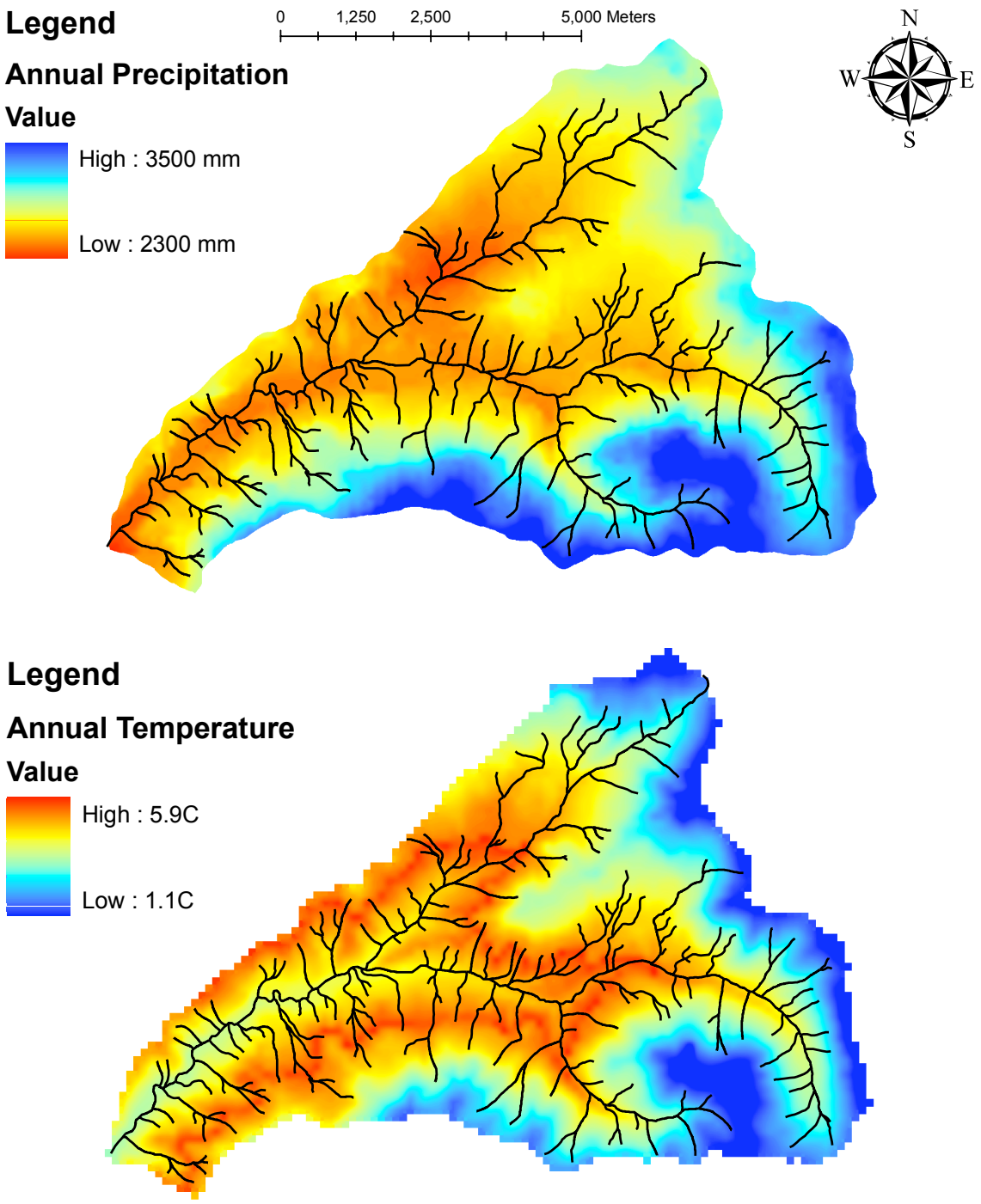

Figure 6.D.14: *Spatial maps at 30m resolution of annual average air temperature and precipitation developed for the HJA using the PRISM model. These maps were based on historical average temperature (1971-2000) and precipitation (1980-1990) time series at different climate stations within the watershed [Daly and Smith, 2005; Daly, 2005].*

6.15. Appendix E: Stand Age Map:

The H.J. Andrews Experimental Forest has been the site of numerous natural and anthropogenic disturbances. Wildfires in the mid-1800's to early 1900's as well as forest harvest experiments reduced the old-growth forest coverage. Currently, old-growth forest stands (i.e. 400-500 years old) cover about 40% of the total watershed, mature stand (i.e. 100-140 years old) originating from last century wildfire cover 20% of the total area, and young post-clearcut stands cover the rest. As a result, stand age, biomass, and plant transpiration (Note: transpiration in VELMA is simulated as a function of stand age) distribution across the watershed is highly heterogeneous. Therefore, a stand age map for the HJA watershed is needed to accurately simulate present day forest distribution and its impact on catchment processes.

A land cover map has been previously developed for the HJA watershed [*Cohen et al.*, 2001; *Cohen et al.*, 1998; *Cohen et al.*, 2002]. Landsat satellite imagery taken in the year 1988 were used to estimate and map forest age structure over western Oregon [*Cohen et al.*, 1995]. These images were first transformed into Tasseled Cap brightness, greenness, and wetness indices following the method by *Crist et al.,* [1986]. The Tasseled Cap transformation is a series of three indices (i.e. brightness, greenness, and wetness) used with Landsat images to enhance the vegetation components of imagery. In short, brightness is associated with soil and litter color [*Cohen et al.,* 1995], greenness is associated with vegetation cover (similar to NDVI) [*Cohen et al.,* 2001], and wetness is associated with forest structure in closed canopy stands [*Collins and Woodcock*, 1996]. Thereafter, an iterative unsupervised classification was used to define several forest classes such as open cover, closed cover and conifer cover [*Cohen et al*., 2001]. Five forest cover classes were defined for the HJA watershed:

1. Open (total cover <30%);
2. Semi-Open (30 %< total cover <70%);
3. Closed mixed forest (30 %< total cover <70%);
4. Young Conifer (30-100 years old);
5. Mature Conifer (101-200 years old);
6. Old-growth Conifer (above 200 years old).

Each of these classes was associated with a representative stand age [*Turner et al.,* 2000; *Cohen et al.,* 1995]. This 1988 land cover map is publicly available at the HJA website (http://andrewsforest.oregonstate.edu/). It was first resampled to the 30m resolution of the current study from its native 25m resolution, and then used to define biomass age distribution in the watershed (Figure 6.E.15).

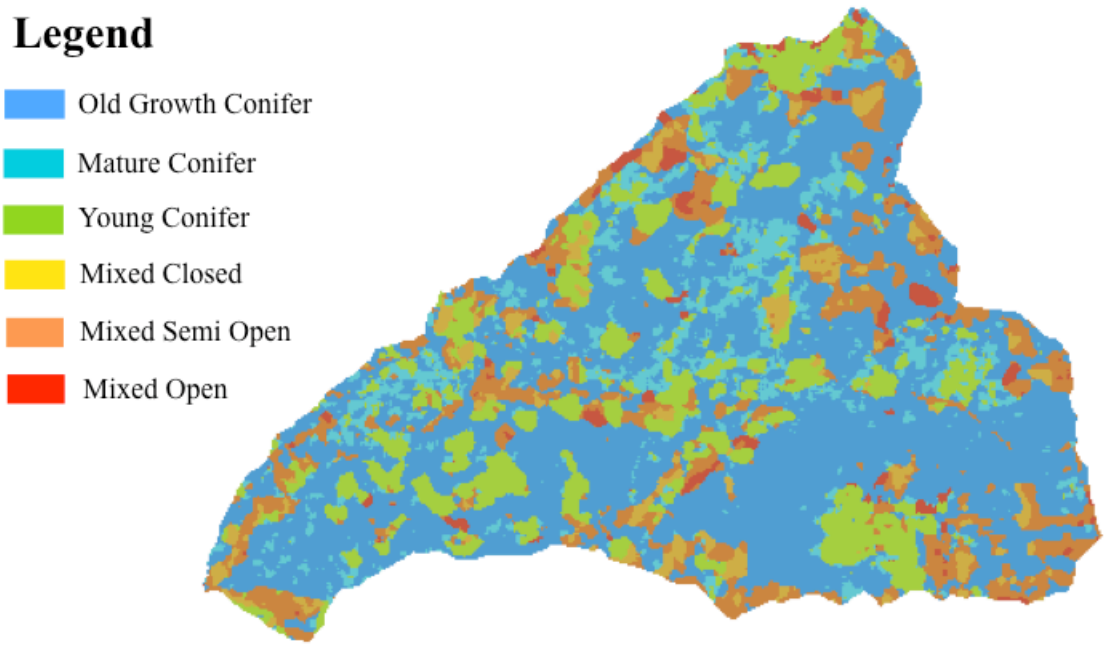

Figure 6.E.15: *The 1988 land cover map for the H.J. Andrews Experimental forest. Five forest cover classes are defined: Mixed Open (~5 year-old stand), Mixed Semi-Open (~15 year-old stand), Mixed Closed (~25 year-old stand), Young Conifer (~55 year-old stand); Mature Conifer (~140 year-old stand), and Old-growth Conifer (~300 year-old Stand).*

6.16. References:

Abdelnour, A., M. Stieglitz, F. Pan, and R. McKane (2011), Catchment Hydrological Responses to Forest Harvest Amount and Spatial Pattern, *Water Resour. Res., doi:10.1029/2010WR010165, in press.*

Abdelnour, A., M. Stieglitz, F. Pan, R. McKane, and Y. Cheng (In review), Effects of Fire and Harvest on Carbon and Nitrogen Dynamics in a Pacific Northwest Forest Catchment.

Aber, J. D., C. Driscoll, C. A. Federer, R. Lathrop, G. Lovett, J. M. Melillo, P. Steudler, and J. Vogelmann (1993), A strategy for the regional analysis of the effects of

physical and chemical climate change on biogeochemical cycles in northeastern (US) forests, *Ecological Modelling*, *67*(1), 37-47.

Alexander, M. (1977), Introduction to soil microbiology , 467 pp. New York, the United States, edited, Wiley & Sons.

Alley, R., T. Berntsen, N. L. Bindoff, Z. Chen, A. Chidthaisong, P. Friedlingstein, J. Gregory, G. Hegerl, M. Heimann, and B. Hewitson (2007), Climate change 2007: The physical science basis--summary for policymakers. Intergovernmental Panel on Climate Change, Geneva, CH.

Arheimer, B., J. Andreasson, S. Fogelberg, H. Johnsson, C. B. Pers, and K. Persson (2005), Climate change impact on water quality: model results from southern Sweden, *Ambio*, 559-566.

Baron, J. S., T. M. Schmidt, and M. D. Hartman (2009), Climate induced changes in high elevation stream nitrate dynamics, *Global Change Biology*, *15*(7), 1777-1789.

Barten, K., A. Jone, and L. Achterman (2008), Hydrologic Effects of a Changing Forest Landscape. Committee on Hydrologic Impacts of Forest Management, *Water Science and Technology Board. The National Academies Press: Washington, DC*.

Beukema, S., D. Robinson, and L. Greig (2007), Forests Insects & Pathogens and Climate,, *Workshop Report*.

Binkley, D., and T. Brown (1993), Forest practices as nonpoint sources of pollution in North America, *Water Resources Bulletin*, *29*(5), 729-740.

Binkley, D., P. Sollins, R. Bell, D. Sachs, and D. Myrold (1992), Biogeochemistry of adjacent conifer and alder-conifer stands, *Ecology*, 2022-2033.

Boisvenue, C. L., and S. W. Running (2006), Impacts of climate change on natural forest productivity evidence since the middle of the 20th century, *Global Change Biology*, *12*(5), 862-882.

Breshears, D. D., N. S. Cobb, P. M. Rich, K. P. Price, C. D. Allen, R. G. Balice, W. H. Romme, J. H. Kastens, M. L. Floyd, and J. Belnap (2005), Regional vegetation die-off in response to global-change-type drought, *Proceedings of the National Academy of Sciences of the United States of America*, *102*(42), 15144.

Brown, T. J., B. L. Hall, and A. L. Westerling (2004), The impact of twenty-first century climate change on wildland fire danger in the western United States: an applications perspective, *Climatic Change*, *62*(1), 365-388.

Carroll, A. L., S. W. Taylor, J. Regniere, and L. Safranyik (2003), Effect of climate change on range expansion by the mountain pine beetle in British Columbia.

Casola, J. H., L. Cuo, B. Livneh, D. P. Lettenmaier, M. T. Stoelinga, P. W. Mote, and J. M. Wallace (2009), Assessing the Impacts of Global Warming on Snowpack in the Washington Cascades, *Journal of Climate*, *22*(10), 2758-2772.

Cayan, D. R., S. A. Kammerdiener, M. D. Dettinger, J. M. Caprio, and D. H. Peterson (2001), Changes in the onset of spring in the western United States, *BULLETIN-AMERICAN METEOROLOGICAL SOCIETY*, *82*(3), 399-416.

Chaer, G., D. Myrold, and P. Bottomley (2009), A soil quality index based on the equilibrium between soil organic matter and biochemical properties of undisturbed coniferous forest soils of the Pacific Northwest, *Soil Biology and Biochemistry*, *41*(4), 822-830.

Chang, H., and I. W. Jung (2010), Spatial and temporal changes in runoff caused by climate change in a complex large river basin in Oregon, *Journal of Hydrology*, *388*(3-4), 186-207.

Chang, H., B. M. Evans, and D. R. Easterling (2001), The Effects of Climate Change on Streamflow and Nutrient Loading *JAWRA Journal of the American Water Resources Association*, *37*(4), 973-985.

Cheng, Y., M. Stieglitz, and F. Pan (2010), A Simple Method to Evolve Daily Ground Temperatures From Surface Air Temperatures in Snow Dominated Regions, *Journal of Hydrometeorology*.

Clair, T. A., and J. M. Ehrman (1996), Variations in discharge and dissolved organic carbon and nitrogen export from terrestrial basins with changes in climate: a neural network approach, *Limnology and Oceanography*, 921-927.

Clapp, R. B., and G. M. Hornberger (1978), Empirical equations for some soil hydraulic properties, *Water Resources Research*, *14*(4), 601-604, doi:610.1029/WR1014i1004p00601.

Cohen, W. B., T. A. Spies, and M. Fiorella (1995), Estimating the age and structure of forests in a multi-ownership landscape of western Oregon, USA, *International Journal of Remote Sensing*, *16*(4), 721-746.

Cohen, W. B., T. K. Maiersperger, T. A. Spies, and D. R. Oetter (2001), Modelling forest cover attributes as continuous variables in a regional context with Thematic Mapper data, *International Journal of Remote Sensing*, *22*(12), 2279-2310.

Cohen, W. B., M. Fiorella, J. Gray, E. Helmer, and K. Anderson (1998), An efficient and accurate method for mapping forest clearcuts in the Pacific Northwest using Landsat imagery, *Photogrammetric engineering and remote sensing*, *64*(4), 293-299.

Cohen, W. B., T. A. Spies, R. J. Alig, D. R. Oetter, T. K. Maiersperger, and M. Fiorella (2002), Characterizing 23 years (1972-95) of stand replacement disturbance in western Oregon forests with Landsat imagery, *Ecosystems*, *5*(2), 122-137.

Collins, J. B., and C. E. Woodcock (1996), An assessment of several linear change detection techniques for mapping forest mortality using multitemporal Landsat TM data, *Remote Sensing of Environment*, *56*(1), 66-77.

Cramer, W., D. Kicklighter, A. Bondeau, B. M. Iii, G. Churkina, B. Nemry, A. Ruimy, and A. Schloss (1999), Comparing global models of terrestrial net primary productivity (NPP): overview and key results, *Global Change Biology*, *5*(S1), 1-15.

Crist, E. P., R. Laurin, and R. C. Cicone (1986), Vegetation and soils information contained in transformed Thematic Mapper data, paper presented at Proceedings, IGARSS "86 Symposium Ziirich, Switzerland, 8-11 September 1986, ESA Publ. Division, SP-254, pp. 1465-1470.

Dale, V. H., and J. F. Franklin (1989), Potential effects of climate change on stand development in the Pacific Northwest, *Canadian Journal of Forest Research*, *19*(12), 1581-1590.

Daly, C. (1996), Overview of the PRISM Model, *PRISM Climate Mapping Program: accessed March*, *18*, 1999.

Daly, C. (2005), Average monthly and annual precipitation spatial grids (1980-1989), Andrews Experimental Forest. Long-Term Ecological Research. Forest Science Data Bank, Corvallis, OR. [Database]. Available: http://andrewsforest.oregonstate.edu/data/abstract.cfm?dbcode=MS027 (29 August 2011).

Daly, C., and J. Smith (2005), Mean monthly maximum and minimum air temperature spatial grids (1971-2000), Andrews Experimental Forest. Long-Term Ecological Research. Forest Science Data Bank, Corvallis, OR. [Database]. Available: http://andrewsforest.oregonstate.edu/data/abstract.cfm?dbcode=MS029 (4 September 2011).

Daly, C., and W. McKee (2011), Meteorological data from benchmark stations at the Andrews Experimental Forest. Long-Term Ecological Research. Forest Science Data Bank, Corvallis, OR. [Database]. Available: http://andrewsforest.oregonstate.edu/data/abstract.cfm?dbcode=MS001 (16 July 2011).

Daly, C., R. P. Neilson, and D. L. Phillips (1994), A statistical-topographic model for mapping climatological precipitation over mountainous terrain, *Journal of applied meteorology*, *33*(2), 140-158.

Daly, C., W. P. Gibson, G. H. Taylor, G. L. Johnson, and P. Pasteris (2002), A knowledge-based approach to the statistical mapping of climate, *Climate Research*, *22*(2), 99-113.

Del Grosso, S., W. Parton, A. Mosier, D. Ojima, A. Kulmala, and S. Phongpan (2000), General model for N2O and N2 gas emissions from soils due to dentrification, *Global Biogeochemical Cycles*, *14*(4).

Dingman, S. (1994), *Physical hydrology*, Prentice Hall Upper Saddle River, NJ.

Elsner, M. M., L. Cuo, N. Voisin, J. S. Deems, A. F. Hamlet, J. A. Vano, K. E. B. Mickelson, S. Y. Lee, and D. P. Lettenmaier (2010), Implications of 21st century climate change for the hydrology of Washington State, *Climatic Change*, *102*(1), 225-260.

Epstein, H. E., M. D. Walker, F. S. Chapin III, and A. M. Starfield (2000), A transient, nutrient-based model of arctic plant community response to climatic warming, *Ecological Applications*, *10*(3), 824-841.

Feng, S., and Q. Hu (2004), Changes in agro-meteorological indicators in the contiguous United States: 1951 to 2000, *Theoretical and Applied Climatology*, *78*(4), 247-264.

Folland, C., T. Karl, R. Christy, R. Clarke, G. Gruza, J. Jouzel, M. Mann, J. Oerlermans, M. Salinger, and S. Wang (2001), Climate change 2001: the scientific basis, *Contribution of Working Group I to the IPCC Third Assessment Report, Cambridge University Press, Cambridge*, 99-181.

Franklin, J. (1992), New Forestry Principles From Ecosystem Analysis of Pacific Northwest Forests 1,2 *Ecological Applications*, *2*(3), 262-214.

Freeman, T. (1991), Calculating catchment area with divergent flow based on a regular grid, *Computers & Geosciences*, *17*(3), 413-422.

Garrick, M., C. Cunnane, and J. Nash (1978), A criterion of efficiency for rainfall-runoff models, *Journal of Hydrology*, *36*(3-4), 375-381.

Giorgi, F., and L. Mearns (2003), Probability of regional climate change based on the Reliability Ensemble Averaging (REA) method, *Geophysical Research Letters*, *30*(12), 1629.

Graumlich, L. J., L. B. Brubaker, and C. C. Grier (1989), Long-term trends in forest net primary productivity: Cascade Mountains, Washington, *Ecology*, 405-410.

Graves, D., and H. Chang (2007), Hydrologic impacts of climate change in the Upper Clackamas River Basin, Oregon, USA, *Climate Research*, *33*(2), 143-158.

Grier, C., and R. Logan (1977), Old-growth Pseudotsuga menziesii communities of a western Oregon watershed: biomass distribution and production budgets, *Ecological Monographs*, *47*(4), 373-400.

Hamann, A., and T. Wang (2006), Potential effects of climate change on ecosystem and tree species distribution in British Columbia, *Ecology*, *87*(11), 2773-2786.

Hamlet, A. F., and D. P. Lettenmaier (1999), Effects of Climate Change on Hydrology and Water Resources in the Columbia River Basin, *JAWRA Journal of the American Water Resources Association*, *35*(6), 1597-1623.

Harmon, M., K. Bible, M. Ryan, D. Shaw, H. Chen, J. Klopatek, and X. Li (2004a), Production, respiration, and overall carbon balance in an old-growth Pseudotsuga-Tsuga forest ecosystem, *Ecosystems*, *7*(5), 498-512.

Harmon, M., J. Franklin, F. Swanson, P. Sollins, S. Gregory, J. Lattin, N. Anderson, S. Cline, N. Aumen, and J. Sedell (2004b), Ecology of coarse woody debris in temperate ecosystems, *Classic Papers*, 59.

Hillel, D. (1998), *Environmental soil physics*, Academic Pr.

Hogue, T. S., H. Gupta, and S. Sorooshian (2006), A User-Friendly approach to parameter estimation in hydrologic models, *Journal of Hydrology*, *320*(1-2), 202-217.

Ines, A. V. M., and J. W. Hansen (2006), Bias correction of daily GCM rainfall for crop simulation studies, *Agricultural and forest meteorology*, *138*(1-4), 44-53.

IPSL (2005), Coauthors, 2005: The new IPSL climate system model: IPSL-CM4, *Note du Pole de Modelisation*, *26*, 86.

Jackson, R., J. Canadell, J. Ehleringer, H. Mooney, O. Sala, and E. Schulze (1996), A global analysis of root distributions for terrestrial biomes, *Oecologia*, *108*(3), 389-411.

Johnson, S., and J. Rothacher (2009), Stream discharge in gaged watersheds at the Andrews Experimental Forest. Long-Term Ecological Research. Forest Science Data Bank, Corvallis, OR. [Database]. Available: http://andrewsforest.oregonstate.edu/data/abstract.cfm?dbcode=HF004 (16 July 2011).

Johnson, S., and R. Fredriksen (2010), Long-term precipitation and dry deposition chemistry concentrations and fluxes: Andrews Experimental Forest rain collector samples. Long-Term Ecological Research. Forest Science Data Bank, Corvallis, OR. [Database]. Available: http://andrewsforest.oregonstate.edu/data/abstract.cfm?dbcode=CP002 (31 August 2011). .

Jungclaus, J. (2006), Coauthors, 2006: Ocean circulation and tropical variability in the coupled model ECHAM5/MPI-OM, *J. Climate*, *19*, 3952-3972.

Kamminga-Van Wijk, C., and H. B. A. Prins (1993), The kinetics of NH 4+ and NO 3- uptake by Douglas fir from single N-solutions and from solutions containing both NH 4+ and NO 3, *Plant and soil*, *151*(1), 91-96.

Kesik, M., N. Br¸ggemann, R. Forkel, R. Kiese, R. Knoche, C. Li, G. Seufert, D. Simpson, and K. Butterbach-Bahl (2006), Future scenarios of N2O and NO emissions from European forest soils, *Journal of Geophysical Research*, *111*(G2), G02018.

Knowles, N., M. D. Dettinger, and D. R. Cayan (2006), Trends in snowfall versus rainfall in the western United States, *Journal of Climate*, *19*(18), 4545-4559.

Knudsen, E. E. (2000), *Sustainable fisheries management: Pacific salmon*, CRC.

Legates, D. R., and G. J. McCabe Jr (1999), Evaluating the use of "goodness-of-fit" measures in hydrologic and hydroclimatic model validation, *Water Resources Research*, *35*(1), 233-241.

Lenihan, J. M., R. Drapek, D. Bachelet, and R. P. Neilson (2003), Climate change effects on vegetation distribution, carbon, and fire in California, *Ecological Applications*, *13*(6), 1667-1681.

Lettenmaier, D. P., D. Major, L. Poff, and S. Running (2008), The Effects of Climate Change on Agriculture, Land Resources, Water Resources, and Biodiversity in the United States. Chapter 4: Water Resources, *Report by the US Climate Change Sciences Program and the Subcommittee on Global Change Research, Synthesis and Assessment Product*, *4*.

Lettenmaier, D. P., A. W. Wood, R. N. Palmer, E. F. Wood, and E. Z. Stakhiv (1999), Water resources implications of global warming: A US regional perspective, *Climatic Change*, *43*(3), 537-579.

Leung, L. R., and M. S. Wigmosta (1999), Potential Climate Change Impacts on Mountain Watersheds in the Pacific Northwest, *JAWRA Journal of the American Water Resources Association*, *35*(6), 1463-1471.

Littell, J. S., E. E. Oneil, D. McKenzie, J. A. Hicke, J. A. Lutz, R. A. Norheim, and M. M. Elsner (2010), Forest ecosystems, disturbance, and climatic change in Washington State, USA, *Climatic Change*, *102*(1), 129-158.

Logan, J., B. Bentz, and J. Powell (2001), Ghost forests, global warming, and the mountain pine beetle, *BOREAL ODYSSEY*, 27.

Loukas, A., L. Vasiliades, and N. R. Dalezios (2002), Climatic impacts on the runoff generation processes in British Columbia, Canada, *Hydrology and Earth System Sciences*, *6*(2), 211-228.

Lutz, J. A., and C. B. Halpern (2006), Tree mortality during early forest development: a long-term study of rates, causes, and consequences, *Ecological Monographs*, *76*(2), 257-275.

Luyssaert, S., E. Schulze, A. Borner, A. Knohl, D. Hessenmoller, B. Law, P. Ciais, and J. Grace (2008), Old-growth forests as global carbon sinks, *Nature*, *455*(7210), 213-215.

Mantua, N., I. Tohver, and A. Hamlet (2010), Climate change impacts on streamflow extremes and summertime stream temperature and their possible consequences for freshwater salmon habitat in Washington State, *Climatic Change*, *102*(1), 187-223.

Martin, W. C., and H. Dennis (1989), Logging of mature Douglas-fir in western Oregon has little effect on nutrient output budgets, *Canadian Journal of Forest Research*, *19*(1), 35-43.

Mastin, M. C., U. S. B. o. Reclamation, and G. Survey (2008), *Effects of potential future warming on runoff in the Yakima River Basin, Washington*, US Dept. of the Interior, US Geological Survey.

McClain, M. E., R. E. Bilby, and F. J. Triska (1998), Nutrient cycles and responses to disturbance, *River ecology and management: lessons from the Pacific coastal ecoregion*, 347-372.

McGlinchy, M. C. (2011), Simulated response of ecosystem processes to climate change in northern California and western Nevada, Master's thesis, Oregon State University, Corvallis.

McKenzie, D., Z. Gedalof, D. L. Peterson, and P. Mote (2004), Climatic change, wildfire, and conservation, *Conservation Biology*, *18*(4), 890-902.

Means, J., P. MacMillan, and K. CROMACK (1992), Biomass and nutrient content of Douglas-fir logs and other detrital pools in an old-growth forest, Oregon, U. S. A, *Canadian journal of forest research(Print)*, *22*(10), 1536-1546.

Melillo, J. M., A. D. McGuire, D. W. Kicklighter, B. Moore, C. J. Vorosmarty, and A. L. Schloss (1993), Global climate change and terrestrial net primary production, *Nature*, *363*(6426), 234-240.

Members, V. (1995), Vegetation/Ecosystem Modeling and Analysis Project (VEMAP): Comparing biogeography and biogeochemistry models in a continental-scale

study of terrestrial ecosystem responses to climate change and CO 2 doubling, *Global Biogeochemical Cycles*, *9*(4), 407-437.

Minder, J. R. (2010), The sensitivity of mountain snowpack accumulation to climate warming, *Journal of Climate*, *23*(10), 2634-2650.

Mote, P. (2003), Trends in snow water equivalent in the Pacific Northwest and their climatic causes, *Geophysical Research Letters*, *30*(12), 1601.

Mote, P. W., and E. P. Salathe (2010), Future climate in the Pacific Northwest, *Climatic Change*, *102*(1), 29-50.

Mote, P. W., A. F. Hamlet, M. P. Clark, and D. P. Lettenmaier (2005), Declining mountain snowpack in western North America, *Bulletin of the American Meteorological Society*, *86*(1), 39-44.

Mote, P. W., E. A. Parson, A. F. Hamlet, W. S. Keeton, D. Lettenmaier, N. Mantua, E. L. Miles, D. W. Peterson, D. L. Peterson, and R. Slaughter (2003), Preparing for climatic change: the water, salmon, and forests of the Pacific Northwest, *Climatic Change*, *61*(1), 45-88.

Nakicenovic, N., J. Alcamo, G. Davis, B. de Vries, J. Fenhann, S. Gaffin, K. Gregory, A. Grubler, T. Y. Jung, and T. Kram (2000), Special report on emissions scenarios: a special report of Working Group III of the Intergovernmental Panel on Climate Change*Rep.*, Pacific Northwest National Laboratory, Richland, WA (US), Environmental Molecular Sciences Laboratory (US).

Nash, J., and J. Sutcliffe (1970), River flow forecasting through conceptual models part I--A discussion of principles, *Journal of Hydrology*, *10*(3), 282-290.

O'Connell, K. (2005), Vegetation classification, Andrews Experimental Forest and vicinity. Long-Term Ecological Research. Forest Science Data Bank, Corvallis, OR. [Database]. Available: http://andrewsforest.oregonstate.edu/data/abstract.cfm?dbcode=TV061 (6 September 2011). .

Parton, W., A. Mosier, D. Ojima, D. Valentine, D. Schimel, K. Weier, and A. Kulmala (1996), Generalized model for N2 and N2O production from nitrification and denitrification, *Global Biogeochemical Cycles*, *10*(3).

Parton, W., E. Holland, S. Del Grosso, M. Hartman, R. Martin, A. Mosier, D. Ojima, and D. Schimel (2001), Generalized model for NO x and N2O emissions from soils, *Journal of Geophysical Research-Atmospheres*, *106*(D15).

Payne, J. T., A. W. Wood, A. F. Hamlet, R. N. Palmer, and D. P. Lettenmaier (2004), Mitigating the effects of climate change on the water resources of the Columbia River basin, *Climatic Change*, *62*(1), 233-256.

Pike, R., D. Spittlehouse, K. Bennett, V. Egginton, P. Tschaplinski, T. Murdock, and A. Werner (2008), Climate change and watershed hydrology: part in recent and projected changes in British Columbia, *Streamline Watershed Management Bulletin*, *11*(2), 1-8.

Powell, A., J. Rodda, and L. Ubertini (2000), *Will ecology provide the next major advance in freshwater science?*, International Association of Hydrological Sciences, IAHS Press Centre for Ecology and Hydrology Wallingford Oxfordshire OX 10 8 BB UK.

Quinn, P., K. Beven, P. Chevallier, and O. Planchon (1991), Prediction of hillslope flow paths for distributed hydrological modelling using digital terrain models, *Hydrological Processes*, *5*(1), 59-79.

Raich, J., E. Rastetter, J. Melillo, D. Kicklighter, P. Steudler, B. Peterson, A. Grace, B. Moore Iii, and C. Vorosmarty (1991), Potential net primary productivity in South America: application of a global model, *Ecological Applications*, *1*(4), 399-429.

Ranken, D. W. (1974), Hydrologic properties of soil and subsoil on a steep, forested slope, Master's thesis, 117 pp, Oregon State University, Corvallis.

Rauscher, S. A., J. S. Pal, N. S. Diffenbaugh, and M. M. Benedetti (2008), Future changes in snowmelt-driven runoff timing over the western US, *Geophysical Research Letters*, *35*(5).

Regonda, S. K., B. Rajagopalan, M. Clark, and J. Pitlick (2005), Seasonal cycle shifts in hydroclimatology over the western United States, *Journal of Climate*, *18*(2), 372-384.

Roeckner, E., G. Bauml, L. Bonaventura, R. Brokopf, M. Esch, M. Giorgetta, S. Hagemann, I. Kirchner, L. Kornblueh, and E. Manzini (2003), The atmospheric general circulation model ECHAM5. Part I: Model description, *Max Planck Institute for Meteorology Report*, *349*, 127.

Russell, G., V. Gornitz, and J. Miller (2000), Regional sea level changes projected by the NASA/GISS atmosphere-ocean model, *Climate Dynamics*, *16*(10), 789-797.

Rygiewicz, P., and C. Bledsoe (1986), Effects of pretreatment conditions on ammonium and nitrate uptake by Douglas-fir seedlings, *Tree Physiology*, *1*(2), 145.

Salathe, E. P. (2005), Downscaling simulations of future global climate with application to hydrologic modelling, *International Journal of Climatology*, *25*(4), 419-436.

Salathe, E. P., P. W. Mote, and M. W. Wiley (2007), Review of scenario selection and downscaling methods for the assessment of climate change impacts on hydrology in the United States pacific northwest, *International Journal of Climatology*, *27*(12), 1611-1621.

Schmidt, J., W. Seiler, and R. Conrad (1988), Emission of nitrous oxide from temperate forest soils into the atmosphere, *Journal of atmospheric chemistry*, *6*(1), 95-115.

Sebestyen, S. D., E. W. Boyer, and J. B. Shanley (2009), Responses of stream nitrate and DOC loadings to hydrological forcing and climate change in an upland forest of the northeastern United States, *Journal of Geophysical Research*, *114*(G2), G02002.

Shafer, S. L., P. J. Bartlein, and R. S. Thompson (2001), Potential changes in the distributions of western North America tree and shrub taxa under future climate scenarios, *Ecosystems*, *4*(3), 200-215.

Smith, R. B., I. Barstad, and L. Bonneau (2005), Orographic precipitation and Oregon's climate transition, *Journal of the atmospheric sciences*, *62*(1), 177-191.

Smithwick, E., M. Harmon, S. Remillard, S. Acker, and J. Franklin (2002), Potential upper bounds of carbon stores in forests of the Pacific Northwest, *Ecological Applications*, *12*(5), 1303-1317.

Sollins, P., and F. McCorison (1981), Nitrogen and carbon solution chemistry of an old growth coniferous forest watershed before and after cutting, *Water Resources Research*, *17*(5).

Sollins, P., and F. M. McCorison (1981), Nitrogen and carbon solution chemistry of an old growth coniferous forest watershed before and after cutting, *Water Resources Research*, *17*(5), 1409–1418, doi:1410.1029/WR1017i1005p01409. .

Sollins, P., K. Cromack Jr, F. Mc Corison, R. Waring, and R. Harr (1981), Changes in nitrogen cycling at an old-growth Douglas-fir site after disturbance, *Journal of Environmental Quality*, *10*(1), 37.

Sollins, P., C. Grier, F. McCorison, K. Cromack Jr, R. Fogel, and R. Fredriksen (1980), The internal element cycles of an old-growth Douglas-fir ecosystem in western Oregon, *Ecological Monographs*, *50*(3), 261-285.

Solomon, S., D. Qin, M. Manning, Z. Chen, M. Marquis, K. Averyt, M. Tignor, and H. Miller (2007), IPCC, 2007: Climate change 2007: The physical science basis. Contribution of Working Group I to the fourth assessment report of the Intergovernmental Panel on Climate Change, edited, New York: Cambridge University Press.

Spittlehouse, D. (2007), Climate change, impacts and adaptation scenarios, *BC Ministry of Forests and Range, Victoria, BC URL:* http://www. *for. gov. bc. ca/hts/Future_Fore sts/Scenarios. pdf*.

Spittlehouse, D. L. (1996), 15. Assessing and Responding to the Effects of Climate Change on Forest Ecosystems, *High-latitude rainforests and associated*

ecosystems of the West Coast of the Americas: climate, hydrology, ecology, and conservation, *116*, 306.

Spittlehouse, D. L., and R. B. Stewart (2003), Adaptation to climate change in forest management, *BC Journal of Ecosystems and Management*, *4*(1), 1-11.

Stewart, I., D. Cayan, and M. Dettinger (2005), Changes towards earlier streamflow timing across North America, *Journal of Climate*, *18*, 1136-1155.

Stieglitz, M., A. Giblin, J. Hobbie, M. Williams, and G. Kling (2000), Simulating the effects of climate change and climate variability on carbon dynamics in Arctic tundra, *Global Biogeochemical Cycles*, *14*(4), 1123-1136.

Sun, G., D. M. Amatya, S. G. McNulty, R. W. Skaggs, and J. H. Hughes (2000), Climate Change Impacts on the Hydrology and Productivity of a Pine Plantation *JAWRA Journal of the American Water Resources Association*, *36*(2), 367-374.

Tague, C., L. Seaby, and A. Hope (2009), Modeling the eco-hydrologic response of a Mediterranean type ecosystem to the combined impacts of projected climate change and altered fire frequencies, *Climatic Change*, *93*(1), 137-155.

Tague, C., G. Grant, M. Farrell, J. Choate, and A. Jefferson (2008), Deep groundwater mediates streamflow response to climate warming in the Oregon Cascades, *Climatic Change*, *86*(1), 189-210.

Turner, D. P., W. B. Cohen, and R. E. Kennedy (2000), Alternative spatial resolutions and estimation of carbon flux over a managed forest landscape in western Oregon, *Landscape Ecology*, *15*(5), 441-452.

Valentine, T., and G. Lienkaemper (2005), 30 meter digital elevation model (DEM) clipped to the Andrews Experimental Forest. Long-Term Ecological Research. Forest Science Data Bank, Corvallis, OR. [Database]. Available: http://andrewsforest.oregonstate.edu/data/abstract.cfm?dbcode=GI002 (16 July 2011).

Vanderbilt, K., K. Lajtha, and F. Swanson (2003), Biogeochemistry of unpolluted forested watersheds in the Oregon Cascades: temporal patterns of precipitation and stream nitrogen fluxes, *Biogeochemistry*, *62*(1), 87-117.

Varanou, E., E. Gkouvatsou, E. Baltas, and M. Mimikou (2002), Quantity and quality integrated catchment modeling under climate change with use of soil and water assessment tool model, *Journal of Hydrologic Engineering*, *7*, 228.

Waichler, S. R., B. C. Wemple, and M. S. Wigmosta (2005), Simulation of water balance and forest treatment effects at the HJ Andrews Experimental Forest, *Hydrological Processes*, *19*(16), 3177-3199.

Walther, G. R., E. Post, P. Convey, A. Menzel, C. Parmesan, T. J. C. Beebee, J. M. Fromentin, O. Hoegh-Guldberg, and F. Bairlein (2002), Ecological responses to recent climate change, *Nature*, *416*(6879), 389-395.

Waring, R., H. Holbo, R. Bueb, and R. Fredriksen (1978), Documentation of meteorological data from the coniferous forest biome primary station in Oregon. Gen. Tech. Rep. PNW-GTR-073. Portland, OR: U.S. Department of Agriculture, Forest Service, Pacific Northwest Research Station: 1-23.

Westerling, A. L., H. G. Hidalgo, D. R. Cayan, and T. W. Swetnam (2006), Warming and earlier spring increase western US forest wildfire activity, *Science*, *313*(5789), 940.

Widmann, M., C. S. Bretherton, and E. P. SalathÈ Jr (2010), Statistical Precipitation Downscaling over the Northwestern United States Using Numerically Simulated Precipitation as a Predictor*.

Willmott, C. J. (1981), On the validation of models, *Physical geography*, *2*(2), 184-194.

Wood, A. W., E. P. Maurer, A. Kumar, and D. P. Lettenmaier (2002), Long range experimental hydrologic forecasting for the eastern US, *J. Geophys. Res*, *107*(D20), 4429.

Wright, P., M. Harmon, and F. Swanson (2002), Assessing the effect of fire regime on coarse woody debris.

Zweimuller, I., M. Zessner, and T. Hein (2008), Effects of climate change on nitrate loads in a large river: the Austrian Danube as example, *Hydrological Processes*, *22*(7), 1022-1036.

CHAPTER 7

CONCLUSIONS AND FUTURE RESEARCH

7.1. Conclusions

The ecohydrological model presented in this study, VELMA, provides a relatively simple, spatially distributed framework for assessing the effects of changes in climate, land-use (harvest, fire, etc.) and land cover on ecohydrological processes within watersheds. VELMA was used to provide process-level insights into the impact of forest fire, clearcut, harvest location, harvest amount and climate change on catchment hydrological and biogeochemical fluxes such as streamflow, evapotranspiration, soil moisture, plant biomass, soil organic carbon, dissolved C and N losses to the stream, gaseous C and N losses to the atmosphere and site productivity–details that would be difficult or impossible to capture through experimentation or observation alone.

A number of simulations scenarios were designed to address the research questions presented in Chapter 1. Specifically, (1) twenty scenarios, where harvest amount was fixed at 20% but harvest location varied, were simulated to explore the impact of harvest location on water quality and quantity (Chapter 3 and 5); (2) one hundred scenarios, where harvest amounts ranged from 2% to 100%, irrespective of location, were conducted to first explore the relationship between harvest amount and hydro-biogeochemical fluxes (i.e. streamflow, soil moisture, evapotranspiration, dissolved C and N losses from the terrestrial system to the stream and atmosphere) and then test for the existence of hydrological and biogeochemical thresholds (Chapter 3 and 5); (3) A number of WS10 simulations were conducted to reconstruct and analyze the impact of two historical disturbances on vegetation growth, and C and N dynamics: a stand-replacing fire in *circa* 1525 A.D. and a man-made clearcut in 1975 A.D. (Chapter 4); and (4) An upper bound, lower bound and middle of the road climate change scenarios were used to drive the model and simulate the impact of a wide range of projected changes in air temperature and precipitation on catchment hydrological and biogeochemical fluxes at high spatial resolution relevant to land-managers (Chapter 6).

These simulations provided a framework for understanding how (1) harvest location within a watershed strongly impact water and nutrient losses from the terrestrial system to the stream, (2) harvest amount increases streamflow generation and reduces water quality, (3) riparian buffers effectively reduce the amount of inorganic nitrogen that reaches the stream, (4) limited supplies of available N tightly constrains ecosystem responses (production and accumulation of biomass, net ecosystem production, etc.) to major disturbances, (5) climate change strongly impact the magnitude and seasonality of the hydrological regime, increase greenhouse gaz emissions and reduce ecosystem productivity. Moreover, the interaction of hydrological and biogeochemical processes represented in VELMA provide additional insight into how feedbacks among the cycles of C, N and water regulate C and N supplies, and therefore, responses to disturbance across a wide range of spatial and temporal scales – stands to hillslopes to catchment, and days to centuries. The main insights from this study include the following:

1) Forest clearcut strongly impacts catchment hydrological processes. Specifically, following a 100% harvest in WS10, plant transpiration decreased and evapotranspiration was reduced by 43% or 370mm/year compared to pre-disturbance value. Consequently, stream discharge increased by ~ 29% or 345 mm as a result of vegetation removal but returned to pre-clearcut levels within 50 years.

2) Harvest amount and streamflow relationship was found to be near linear. Specifically, annual streamflow increased at a near linear rate of 3.5mm/year for each percent of catchment harvested in WS10, irrespective of location.

3) Streamflow response is strongly sensitive to harvest distance from the stream channel. This streamflow sensitivity to harvest location stems from the fact that subsurface flow generated from an upland clearcut area, as opposed to a lowland clearcut area, has a relatively longer flowpath. This longer flowpath subjects subsurface flow to downslope plant water uptake, which reduces the amount of water that reaches the stream channel.

4) Following fire and harvest, losses of N from the terrestrial system to the stream were tightly constrained by the hydrological cycle, particularly at the hillslope scale. Losses of ammonium and DON (and DOC) to the stream were driven mainly by wet-

season rain events large enough to generate hydrologic connectivity and flushing of nutrients along hillslopes. In contrast, losses of nitrate to the stream were less predictable, owing to complex spatial and temporal patterns of nitrification and denitrification within soil columns, hillslopes and riparian areas. Furthermore, the combined effects of increased runoff, decreased N uptake by plants prior to significant plant regrowth, and large pulse of detritus to the soil led to sharp increases in dissolved losses of N following fire and harvest.

5) Gaseous losses of C and N to the atmosphere, following disturbance, were primarily driven by water availability, high soil organic carbon decomposition, and the sharp increase in soil nitrate as a result of ammonium nitrification into nitrate and low N uptake. Specifically, post-disturbance increase in soil moisture and nitrate availability enhanced the anaerobic process of soil denitrification and substantially increased N_2-N_2O emissions to the atmosphere, whereas post-disturbance increase in soil organic carbon decomposition enhanced soil heterotrophic respiration and increased CO_2 emission to the atmosphere.

6) Beyond the short-term loss of N after fire, the supply of available N for vegetation regrowth was enhanced by the decades-long release of N from the large pulse of decomposing bole wood killed by the fire. In contrast, the regrowth of plant biomass following the 1975 A.D. clearcut in WS10 was about 30% lower than the rate of regrowth after fire, owing to the large loss of N in harvested bolewood, into the stream and to the atmosphere, as well as a rather small increase in detritus N from decomposing roots.

7) Ammonium and nitrate losses to the stream increased exponentially with increasing harvest area and exhibited a threshold behavior. This threshold behavior of NH_4 and NO_3 losses is essentially caused by riparian buffer dynamics. Riparian buffers reduce nitrogen losses to the stream through nitrogen uptake by plants, nitrification, and denitrification. Simulations results showed that buffer areas of 60% or more in WS10 strongly limited NH_4 and NO_3 losses to the stream (i.e. NH_4 and NO_3 losses to the stream were less than 7% and 2% of their maximum values).

8) Climate Change will strongly impact the seasonality of the hydrological processes in the H.J. Andrews Watershed and more generally in the Pacific Northwest. Specifically, the projected end of the 21th century effects of warmer and wetter winters as well as drier and hotter summers will result in lower winter snow accumulation, earlier spring snowmelt, higher winter streamflow, and lower summer streamflow and soil moisture. Such future impacts on the Pacific Northwest hydrological regime are likely to have implications for forest and water resources management. In particular, higher winter streamflow is expected to increase the probability of floods, landslides and debris flow activity, whereas lower summer streamflow and soil moisture will reduce the ability to supply water to all users, increase competition for water supply between municipalities, farmers and hydropower production, limit vegetation survival, and negatively affect freshwater fisheries habitat.

9) Climate Change will also impact catchment C and N dynamics at WS10 and more generally across the Pacific Northwest. Specifically, the projected end of the 21th century warmer winter and spring enhance soil microbial activity and biomass growth, which results in higher gaseous C and N fluxes and higher DON and DOC losses to the stream, but lower dissolved inorganic C and N losses to the stream and lower amount of carbon sequestration.

7.2 Future Research

The results presented in this study suggest that models such as VELMA that include for the changes in watershed hydrology, C and N dynamics, greenhouse gas emissions, and water quality can help inform land managers and policymakers interested in exploring the impact of alternative land-use scenarios and future climate change on water quantity, nitrogen and carbon losses to surface waters and the atmosphere as well as address issues of ecosystem services delineated in the recent Millennium Ecosystem Assessment report. VELMA can link effects to causes, identify processes controlling ecosystem service tradeoffs, map “bundles” of ecosystem services across a wide range of spatial and temporal scales, and provide a user-friendly decision support framework to assess outcomes of alternative policies and management decisions. Specifically, VELMA can be used by land managers and policymakers as a tool to understand how

management decisions alter ecosystem services such as food, water amount and quality, timber production, floods, droughts, and nutrient cycling, amongst others, to assess the tradeoffs between interconnected services such as timber production and water quality, and to design scenarios that captures positive impacts and minimizes negative ones.

An extension of this work is to use VELMA to answer questions relevant to the research community and to forest managers and to draw insight into the processes that govern catchment processes. VELMA represent a state of the art real-time visualization tool that shows temporal and spatial patterns of state and flux variables, which allows decision makers to view how alternative future scenarios of population growth, land use and climate may affect changes in carbon and nitrogen storage, water quality and other ecosystem services across large landscapes. For example, VELMA can be used to:

1) Test for the effectiveness of riparian buffers cover type in reducing stream nutrient loads as a result of timber harvest, fire, fertilization or road construction.

2) Identify best management practices for agriculture such as tradeoffs between corn production and water quality.

3) Explore the impact of the seasonal controlled burning of Konza Tallgrass prairies on vegetation structure and growth, cattle grazing potential, water quality, and air quality.

4) Simulate the fate and transport of mercury in the ecosystem and investigate the impact of mercury pollution on wildlife, stream ecosystems, fish food sources, public health, and ultimately economic opportunities.

5) Identify potential hotspots for fire based on moisture index and fuel loads with the goal to prevent undesired wildfires.

6) Test the efficiency of climate change adaptation strategies such as reducing fuel load to decrease the risk of fire, thinning in the summer to decrease the amount of water lost through transpiration and increase summer low flow, and developing draught tolerant and insect outbreak resistant species in order to reduce large scale tree mortality due to insect outbreak.

Other areas of research can be related to the model development. VELMA can ultimately be linked to a decision support tool that allows examination of the nature and

properties of coupled human and natural environmental systems and their impacts on ecosystem services and tradeoffs. Moreover, VELMA uses a simplified modeling approach with comparatively few parameters and data input requirements. A list of processes not explicitly treated in VELMA was provided in Chapter 3 and 4. These processes can potentially be incorporated into the model to answer specific questions. For example, (1) multiple species dynamics can be added to analyze species competition throughout succession, as well as to test shift in species under disturbances or changes in climate, (2) In-stream processes such as adsorption mechanisms, algae uptake, benthic release, denitrification, and decomposition can be added in order to explore N export from large watersheds at short time scales, and to analyze the effects of catchment nutrient losses on stream ecosystem (i.e. algae, fishery, etc.), and (3) a spatial map of soil depth can be used to test the sensitivity of streamflow to the depth to bedrock. However, it should be recognized that adding unnecessary processes (i.e. not useful to the questions asked) comes at the cost of computational efficiency, model complexity, and applicability to larger spatial and temporal scales of interest. These are important tradeoffs to consider, given that data needed to implement complex models are not generally available.

CURRICULUM VITAE

ALEX GABRIEL ABDELNOUR

RESEARCH INTERESTS

Watershed dynamics with emphasis on the interactions between climate, climate variability, hydrology, and terrestrial biology, terrestrial carbon and nitrogen cycling. Impacts of natural and anthropogenic disturbances such as clear-cutting, fire and climate change.

EDUCATION

Georgia Institute of Technology,
School of Civil & Environmental Engineering — Atlanta, GA
PhD in Environmental Fluid Mechanics and Water Resources — Dec 2012
Overall GPA: 3.86/4.0
Research includes: Hydrology, Ecology, Fire, Climate Change, Forest Harvest, Forest Management and Modeling.

Georgia Institute of Technology,
School of Earth and Atmospheric Science — Atlanta, GA
Master of Science in Earth and Atmospheric Science — Dec 2009
Overall GPA: 4.0/4.0
Coursework includes: Climate Change, Thermodynamics of Atmosphere and Oceans, Large-Scale Atmospheric Circulations, Fluid Dynamics and Synoptic Meteorology, Resources, Energy and the Environment.

Georgia Institute of Technology,
School of Civil & Environmental Engineering — Atlanta, GA
Master of Science in Civil & Environmental Engineering — Dec 2006
Overall GPA: 3.8/4.0
Coursework includes: Fluid Mechanics, Physical Hydrology, Open Channel Flow, Environmental Fluid Mechanics, Flow through Porous Media, Probability and Statistics, and Water Resource Management.

Université Saint Joseph,
Ecole Supérieur des Ingénieurs de Beyrouth (ESIB) — Beirut, Lebanon
***Diplôme d'Ingénieur* in Civil & Environmental Engineering** — June 2005
Relevant GPA: 4.0/4.0
***Classes Préparatoires Math Sup et Spé*, Minor in Math and Physics** — June 2002

AWARDS AND SKILLS

- Bill Schutz Graduate Teaching Assistant Award 2009.
- Fluent in English, French and Arabic.
- Proficient in Mathematica, Processing, GIS, HECRAS, AutoCAD, WaterCAD.
- Math and physics background with strong analytical and problem solving skills.
- Strong statistical analysis of data and technical writing.

EXPERIENCE

Georgia Institute of Technology Atlanta, GA
Research Assistant Jan 2006 – Present

- Developed, for EPA, a spatially explicit eco-hydrological model (VELMA) to address the effects of changes in climate, land-use and other interacting stressors on multiple ecosystem services such as the production of food and fiber, carbon sequestration, regulation of water quality and quantity, reduction of greenhouse gases (CO_2, N_2O, NO_x), and regulation of sources and sinks of reactive nitrogen (N_r) within watersheds.
- Simulated the effects of climate change, forest fire, and forest harvest on water quantity, water quality (nutrient losses to the stream) and greenhouse gas emissions.
- Performed a sensitivity study to assess the hydrological and biogeochemical response of a catchment to harvest Intensity and spatial patterns.

Georgia Institute of Technology Atlanta, GA
Teaching Assistant for Professor Marc Stieglitz:
Hydrology for Undergraduates (up to 55-student classroom) Fall 2006, 2007, 2008
Physical Hydrology for Graduates (8-student classroom) Spring 2007, 2008, 2009

- Conceived and organized class material, prepared and delivered lectures, guided students through research projects, held office hours, assigned and graded homeworks, quizzes and exams.

STUCKY ENGINEERING LTD France & Switzerland
Hydrologist Intern Summer 2004

- Designed and calculated a retaining wall of the fluids spillways of Thurgat embankment dam (Libya).
- Elaborated a 3-D representation of water seepage in the dam of Wadi Megenin (Libya).
- Conceived and calculated sheet piles to widen navigation in the Lot river (Lock of Gregols) (France).

Bureau d'étude Hydraulic et Technique, B.E.H.T Beirut, Lebanon
Hydrologist Intern Summer 2003

- Supervised the construction of ductile iron main pressure line in Jeita (Lebanon).
- Oversaw the installation of electro-mechanical equipments related to the Zouk Mosbeh and Shaileh pumping stations (Lebanon).

JOURNAL PUBLICATIONS

- Abdelnour, A., M. Stieglitz, F. Pan, and R. B. McKane, (2011) Catchment Hydrological Responses to Forest Harvest Intensity and Spatial Pattern, In press, Water Resources Research doi:10.1029/2010WR010165.
- Abdelnour, A., R. B. McKane, M. Stieglitz, F. Pan, and Y. Cheng, (In review) Effects of Fire and Harvest on Carbon and Nitrogen Dynamics in a Pacific Northwest Forest Catchment, Water Resources Research.
- Abdelnour, A., M. Stieglitz, F. Pan, and R. B. McKane, (In review) Catchment Biogeochemical Responses to Forest Harvest Intensity and Spatial Pattern, Water Resources Research.
- Abdelnour, A., M. Stieglitz, F. Pan, and R. B. McKane, (In preparation) Catchment Hydro-biogeochemical Response to Climate Change and Future Land-use.

CONFERENCE PROCEEDINGS

- McKane, R., A. Abdelnour, A. Brookes, K. Djang, T. Jordan, B. Kwiatkowski, F. Pan, B. Peterjohn, M. Stieglitz, A. Skibbe and D. Weller (2011) Riparian Forest Effects on Nitrogen Export to an Agricultural Stream Inferred from Experimental Data and a Model, AGU Fall Meeting 2011, San Francisco, USA.
- Davis, G., C.D. Knightes, A. Abdelnour, M. Stieglitz, (2011) Biogeochemical Cycling of Mercury in Watersheds: VELMA (Visualizing Ecosystems for Land Management Assessment), International Conference on Mercury as a Global Pollutant, Halifax, Nova Scotia.
- Osborne-Gowey, J., D. Bachelet, A. Hamlet, E. Garcia, C. Tague, R. McKane, A. Abdelnour, M. Stieglitz, and F. Pan, (2011) Assessing the skill of hydrology models at simulating the water cycle in the HJ Andrews LTER: assumptions, strengths and weaknesses, National American Fisheries Society 2011, Seattle, USA
- Abdelnour, A., M. Stieglitz, R. McKane and F. Pan, (2010) An Integrated Eco-hydrologic Modeling Framework for Assessing the Effects of Interacting Stressors on Multiple Ecosystem Services updated, (2011), University of Pennsylvania, Philadelphia, USA.
- Bond, B., K. Peterson, R. McKane, K. Lajtha, D. Quandt, S. Allen, S. Sell, C. Daly, M. Harmon, S. Johnson, T. Spies, P. Sollins, A. Abdelnour, and M. Stieglitz, (2010) How does complex terrain influence responses of carbon and water cycle processes to

climate variability and climate change?, AGU Fall Meeting 2010, San Francisco, USA.

- Peterson K., B. Bond, R. McKane, A. Abdelnour, and M. Stieglitz, (2010) Scaling Issues and Spatio-Temporal Variability in Ecohydrological Modeling on Mountain Topography: Methods and Future of the VELMA Model, AGU Fall Meeting 2010, San Francisco, USA.
- Abdelnour, A., M. Stieglitz, F. Pan, and R. B. McKane, (2010) Catchment Hydro-biogeochemical Response to Climate Change and Future Land-use, AGU Fall Meeting 2010, San Francisco, USA.
- McKane, R. B., A. Abdelnour, M. Stieglitz, F. Pan, B. Bond, and S. Johnson (2010) An Integrated Eco-hydrologic Modeling Framework for Assessing the Effects of Interacting Stressors on Multiple Ecosystem Services, ESA Annual Meeting 2010, Pittsburgh, USA
- Abdelnour, A., M. Stieglitz, F. Pan, and R. B. McKane, (2010) Catchment Hydro-Biogeochemical Threshold Response to Different Harvest Area and Location, Georgia Tech Research and Innovation Conference 2010, Atlanta, USA.
- Cheng, Y., M. Stieglitz, A. Abdelnour, and F. Pan, (2010) Simulating Watershed Scale Hydrologic Characteristics from Fine Scale Processes, Arctic LTER Meeting, Woods Hole, MA, USA.
- Abdelnour, A., M. Stieglitz, F. Pan, and R. B. McKane, (2009) Catchment Hydrological and Biogeochemical Response to Forest Harvest Intensity and Spatial Pattern, AGU Fall Meeting 2009, San Francisco, USA.
- McKane, R. B., M. Stieglitz, A. Abdelnour, and F. Pan, (2009) An Integrated Eco-hydrologic Modeling Framework for Assessing the Effects of Interacting Stressors on Multiple Ecosystem Services, ESRP Modeling Workshop, 2009, Athens, GA.
- Abdelnour, A., M. Stieglitz, F. Pan and R. B. McKane, (2008) Catchment Hydrologic Threshold Response to Forest Harvest Intensity, Georgia Tech Research and Innovation Conference 2008, Atlanta, USA.
- Abdelnour, A., M. Stieglitz, F. Pan, and R. B. McKane, (2006) The Hydrological Response of a Small Catchment to Clear-Cutting, AGU Fall Meeting 2006, San Francisco, USA.

PROFESSIONAL MEMBERSHIPS

- Member of the American Geophysical Union
- Member of the Union of Concerned Scientists.
- Member of the Lebanese Order of Engineers.
- Member of the H.J. Andrews Forest LTER.
- Member of the Georgia Tech Consulting Club.

ACTIVITIES AND INTERESTS

- Co-founder and first president (Elected) of the Lebanese Club at Georgia Tech (2006-2007).
- Held numerous offices (Vice-president, treasurer) in the Lebanese Club at Georgia Tech (2008-2009).
- Led a cooking team to compete for the Lebanese Club in the International Food Festival-Won second place in 2009 and third place in 2007 out of 29 clubs.
- Ex-member of the Ecole Supérieur des Ingénieurs de Beyrouth basketball team (2000-2003).
- Enjoys basketball, racquetball, soccer, swimming, cooking, movies, travel and reading current affairs books and novels.